School of Engineering & Design
Electronic & Computer Engineering

Convex Optimization-based Resource Scheduling for Multi-User Wireless Systems

by

Charilaos C. Zarakovitis

A Thesis submitted for the degree of
Doctor of Philosophy

Brunel University
London, United Kingdom
October 2011

Στα χρόνια που δεν με συντρόφευσα…

Abstract

In the past decades, the growth of mobile communications has impelled the research and industry societies to innovation and development. The interactions between transmitting, computing and scheduling have introduced many interesting yet difficult issues for investigation. Channel and link access, capacity planning, energy consumption, fairness provision, Quality-of-Service (QoS) guarantee and low implementation complexity are recognized as the most increasingly important topics in the field of modern networking.

This Thesis approaches the abovementioned issues by introducing convex optimization solutions for resource management in multi-user frequency-selective fading environments. The basic idea lays on the effective distribution of the wireless resources at the downlink phase of orthogonal frequency division multiple access networks by exploiting knowledge of imperfect channel state information and traffic characteristics. The objective of this Thesis is to develop new theoretical frameworks from the cross-layer perspective to advocate joint strategies of dynamic mechanisms at physical and medium access control layers.

In particular, we initially propose optimal network operation under imperfect channel and heterogeneous QoS considerations by introducing a power-efficient cross-layer design that incorporates an innovative approach of minimizing the overall transmitting power. Our methodology considers independent-bit encoding to define a power-bit-loading process that induces notably smaller throughput degradation and power ascents at the presence of channel uncertainty than commonly used capacity-based approaches.

Secondly, we investigate the trade-off between power efficiency, QoS guarantee and fairness provision in networks employing real-time resource scheduling under the asymmetric-Nash-Bargaining-Solution (NBS) property with channel imperfections. We propose the first NBS-oriented and iteration-independent optimal cross-layer policy for joint channel and transmitting power allocation by means of final formulas, with significantly lower complexity than relevant approaches.

Thirdly, we focus on intelligent spectrum sharing technologies to present the first symmetric-NBS oriented cross-layer framework for cognitive radio networks with channel

uncertainties. Our developments achieve optimal scheduling of the dynamically available resources guaranteeing rapid convergence to Pareto optimal equilibriums and also increase the reliability of the network by means of interference cancelation between primary and secondary users.

Extensive simulations are conducted for various practical scenarios to demonstrate the superior performance of our proposals against rival studies in the literature. Thanks to their environmental-friendly character, practicality and low complexity, the introduced frameworks can be used in candidate protocols for next generation broadband wireless communication systems.

Περίληψη

Τις τελευταίες δεκαετίες, η αυξημένη αναγκαιότητα για προηγμένη κινητή επικοινωνία έχει ωθήσει τον ερευνητικό και βιομηχανικό κλάδο σε καινοτομία και ανάπτυξη. Οι αλληλεπιδράσεις μεταξύ της διαβίβασης της πληροφορίας, της υπολογιστικής δυνατότητας και του σχεδιασμού συστημάτων έχουν εισαγάγει πολλά ενδιαφέροντα συνάμα δύσκολα θέματα προς έρευνα. Η πρόσβαση σε τηλεπικοινωνιακά κανάλια και συνδέσεις, η εκμετάλλευση της χωρητικότητας των συστημάτων, η κατανάλωση την παρεχόμενης ισχύος, η δίκαιη κατανομή των πόρων, η εγγύηση ποιότητας παροχής υπηρεσιών (QoS) και η πολυπλοκότητα κεντρικών μηχανισμών ελέγχου, αναγνωρίζονται ως τα όλο και περισσότερο σημαντικά θέματα στον τομέα της σύγχρονης δικτύωσης.

Η διδακτορική αυτή διατριβή δρομολογεί τα προαναφερθέντα ζητήματα προτείνοντας αναλυτικές λύσεις περί της διαχείρισης των πόρων σε ασύρματα συστήματα πολλών χρηστών με επιλεκτικά στη συχνότητα διαλειπτικά κανάλια ασθενούς σκίασης. Η βασική ιδέα βασίζεται στην αποτελεσματική διανομή των πόρων σε κατιούσες συνδέσεις ορθογωνιακής συχνότητας και πολλαπλής πρόσβασης καναλιού εκμεταλλευόμενη τις πληροφορίες που προσδιορίζουν την κατάσταση του καναλιού και του φόρτου πληροφορίας του δικτύου. Ο στόχος της διδακτορική διατριβής είναι να αναπτυχθούν θεωρητικά μοντέλα που αναφέρονται σε διαστρωματικές (cross-layer) τεχνικές συστημάτων και που βασίζονται σε στρατηγικές δυναμικών μηχανισμών ελέγχου πρόσβασης τόσο του φυσικού όσο και των υψηλότερων στρωμάτων.

Αρχικά προτείνουμε βέλτιστη λειτουργία ασύρματου συστήματος με ατελή κανάλια και χρήστες με ετερογενείς απαιτήσεις παροχής υπηρεσιών, εισάγοντας ένα αποδοτικότατο μοντέλο κατανομής πόρων, αναφερόμενο στο επίπεδο διαστρωμάτωσης, που ενσωματώνει μια καινοτόμο προσέγγιση ελαχιστοποίησης της συνολικής εκπεμπόμενης ισχύος. Η προτεινόμενη μεθοδολογία βασίζεται σε ανεξάρτητη κωδικοποίηση πληροφοριών, για τον προσδιορισμό μιας βασικής συνάρτησης που περιγράφει τον τρόπο διαχείρισης ισχύος και πληροφοριών του συστήματος. Η συνιστώμενη συνάρτηση αποδίδει μικρότερες υποβαθμίσεις του ρυθμού απόδοσης και αναβαθμίσεις της ισχύος (PBL), σε σχέση τις υπάρχουσες προσεγγίσεις, ειδικότερα για τις περιπτώσεις καναλιών με υψηλή αβεβαιότητα.

Αφετέρου, διερευνούμε την συσχέτιση μεταξύ της απόδοσης ισχύος, της εγγύησης παροχής υπηρεσιών και της δίκαιης κατανομής των πόρων για λειτουργία δικτύων σε πραγματικό χρόνο με τη χρήση ασυμμετρικής λύσης διαπραγμάτευσης του Nash (A-NBS) για παίγνια δικτύων με ατελή κανάλια. Προτείνουμε την πρώτη πολιτική βελτιστοποίησης της απόδοσης του συστήματος, σε μορφή τελικών εξισώσεων, η οποία αναφέρεται στο επίπεδο διαστρωμάτωσης και βασίζεται στο NBS ελέγχου ισχύος και κατανομής υποκαναλιών. Η προτεινόμενη πολιτική είναι ανεξάρτητη από μηχανισμούς αναζήτησης των πολλαπλασιαστών Lagrange μειώνοντας έτσι σημαντικά την πολυπλοκότητα του συστήματος σε σύγκριση με τις υπάρχουσες προσεγγίσεις.

Τρίτον, εστιάζουμε σε ευφυείς κατανομές φάσματος γνωσιακών δικτύων (Cognitive Radio) (CR) για να παρουσιάσουμε το πρώτο διαστρωματικό μοντέλο συμμετρικής λύσης διαπραγμάτευσης του Nash (S-NBS) για παιγνιοθεωρητικά CR δίκτυα με ατελή κανάλια. Η πρότασή μας εγγυάται αποδοτική και δίκαιη κατά S-NBS κατανομή των δυναμικά διαθέσιμων πόρων στο CR δίκτυο με γρήγορη σύγκλιση των αποτελεσμάτων σε Pareto βέλτιστα ισοζύγια. Επίσης, επιτυγχάνουμε αυξημένη αξιοπιστία παροχής υπηρεσιών περιλαμβάνοντας κανόνες για την απαλοιφή παρεμβολών μεταξύ πρωτευόντων και δευτερευόντων χρηστών.

Η διδακτορική διατριβή παρουσιάζει επίσης εκτενείς προσομοιώσεις αναφερόμενες σε ποικίλα πρακτικά σενάρια τα οποία καταδεικνύουν την ανώτερη απόδοση των προτάσεών μας έναντι σχετικών μελετών. Χάρη στο φιλικό προς το περιβάλλον τους χαρακτήρα, την πρακτικότητα και τη χαμηλή τους πολυπλοκότητά, τα προτεινόμενα μοντέλα μπορούν να ενσωματωθούν σε καινούργια πρωτόκολλα που είναι υποψηφία για να χρησιμοποιηθούν σε δίκτυα επόμενης γενεάς.

Acknowledgments

I am indebted to many people who both directly and indirectly contributed to this Thesis. First, I would like to thank those collaborators who directly contributed. Most of all, I'm grateful for the help and friendship of Prof. Ioannis C. Spiliotis from the National Technical University of Athens, Greece. Prof. Spiliotis was my advisor on several matters for the past five years - his influence is evident throughout this document and also on my perception about life. I'm also grateful for my collaboration with Dionysios E. Skordoulis, who performed many of the experiments included in Chapter 3. Finally, this work has been jointly funded by the United Kingdom Engineering and Physical Sciences Research Council (EPSRC) and Motorola Ltd. under the Grant No 07000486 and EP/G070350/1. I would like to thank the financial support from my sponsors and particularly Mr. Oliver Tyce.

Most importantly, I am indebted to Dr. Qiang Ni and Dr. Marios G. Hadjinicolaou, my supervisors, whose guidance and support was unwavering these past five years. Dr. Ni and Dr. Hadjinicolaou were always positive in the face of my many failures along the way. They gave me the freedom to pursue projects of my own choosing, which contributed greatly to my academic independence, if not the selection of wise projects.

There are numerous people who contributed indirectly to this Thesis. First among these is my intelligent, lovely and vivacious girlfriend Eirini Saranti-Papasaranti, whose light made me feel strong and happy. Next, my beloved parents Krystallia A. Charla and Christos C. Zarakovitis, who tenderly showed me the essence of creation and the gist of evolution. Also, my grandmother Sophia G. Zarakoviti and my aunt Alexandra G. Viltanioti, who wisely taught me the values of encouragement and insistence. Lastly but not least, my dear brother Athanasios C. Zarakovitis - without his love I would had lost myself in the lapse of my recent years.

Table of Contents

List of Figures

List of Tables

Chapter 1

Introduction

Ubiquitous internet has produced a plurality of strong demands for advanced telecommunications engineering. Future wireless access is visualized as broadband and high-speed in network structures tailored to support reliable Quality of Service (QoS) for numerous multimedia applications. Given that current technologies [1], [2], [3], [4], [5] could only partially satisfy such prospects [6] the research community is called to deliver solid solutions in alliance with the environmental-friendly character of our days.

1.1 Significance of the Thesis

The reliability of a network is perceived via its provided QoS support to various mobile users. A challenge is posted since multimedia applications of individual users have diverse characteristics in terms of Physical (PHY) measures such as target bandwidth, delay, and packet loss rate [7]. Given that limited energy resources are becoming serious concern worldwide, modern networking also seeks for better power efficiency; reducing the transmitting power saves electrical energy of mobile devices and decreases the level of radiation offering healthy environments to users. Several studies [8], [9], [10] recognize that the trade-off between QoS support and power efficiency can be addressed by opportunistic scheduling of the wireless resources using effective *multiple access technologies* such as Orthogonal Frequency Division Multiple Access (OFDMA) [11], [12]. Although current research efforts, there are several open issues to be investigated.

Resource management in OFDMA systems is essentially a Medium Access Control (MAC) layer problem. This feature encourages performing optimal scheduling on a *per-layer* basis considering only PHY layer dynamics [13], [14], [15], [16], [17]. However, without knowing the Queue State Information (QSI) from transport and network layers, each user's specific QoS cannot be always guaranteed [18]. To bypass such issues, the *cross-layer* architecting [19] can be adopted to involve both PHY and higher-layer parameters in the resource scheduling process. Nevertheless, most recent efforts in cross-layer design undertake that *homogeneous* QSI and *perfect channel* conditions are available [20], [21], [22], [23], [24], [25], [26]. Such considerations are far from reality, where users are instead *heterogeneous* and channel is *imperfect*. In fact, wireless transmissions are often quite damaged [27], [28] due to noisy channels with sophisticated time-varying dynamic effects such as imperfect *Channel State Information* (CSI), multipath delay spread, deep fading, Inter Symbol Interference (ISI) and Doppler spread. Accounting such channel imperfections in new proposals contributes more convenient designs with actual improvements of the transmitting power. Furthermore, new research topics focus on the efficient exploitation of *diversity* phenomena in *multi-user multi-carrier* systems to further enhance systems' performance.

Along this research direction, we initially propose a centralized power-efficient scheme to provide heterogeneous QoS support for *opportunistic OFDMA* downlink networks. We approach the problem from the cross-layer perspective utilizing both *information* [29] and *queuing* [30] theories to adjust the PHY and MAC layer dynamics. The significances of this research part lay on an estimation process for imperfect multipath channels and on an innovative methodology that delivers an energy-effective *Power-Bit-Loading* (PBL) process with high resilience to channel uncertainties. To describe the heterogeneous QoS requirements of each user at the cross-layer, we also introduce an advanced optimal strategy that expresses the traffic rate of each user at the higher-layers into equivalent rate at the PHY layer. We demonstrate that our scheme has high resilience to channel errors and it significantly outperforms relevant proposals in terms of power consumption and QoS provision.

Another technically challenging topic in modern networking is the *trade-off* between *fairness* and throughput/power efficiency. Simply optimizing the resource scheduling efficiency may tend to over-allocate resources to some users with good channel conditions, but starve some other users with bad channel conditions leading to disadvantageous *unfairness*. In addition, with limited available radio resources, increasing system's throughput efficiency and maintaining fairness are usually conflicting with each other [31], [32] leading to a natural trade-off between these two performance measures. The challenge lies on the balance between resource scheduling efficiency, QoS guarantee and fairness provision. A tangible metric is offered in *utility theory* [33], where such trade-offs can be mapped onto different shapes of *utility functions*. Based on either *non-cooperative* [34], [35], [36] or *cooperative game-theoretic* strategies [37], [38], [39] utility theory provides a means to formulate the gain of a quality measurement when certain resources are assigned to a user [33]. In non-cooperative strategies fairness is concerned in conjunction with efficiency frequently causing *Nash equilibrium* [40] issues that lower the system's performance as compared to cooperative game-theoretical approaches [37], [41]. Therefore, recent viewpoints believe that cooperative game theory is more suitable for cross-layer resource allocation, where *Nash Bargaining Solution* (NBS) [40] is one promising candidate. However, current research on NBS for cross-layer systems is still at very early stage providing solutions using graphic and numerical methods [37], [39], [42], [43] mainly due to the *recursive* origin of the NBS problem [44].

Besides fair and efficient resource scheduling, *real-time* QoS provision is essential to be considered as fundamental demand in modern networking. Real-time service occurs when the resource allocation process operates successfully in less time than the transmission's cycle duration. Exceeding the time limits causes major delays to the system users. Hence, major concern must be given to the implementation complexity of the scheduling policies that can be categorised to *iteration-dependent* and *iteration-independent*. Iteration-dependent schemes operate by computing their *online* policies on the primary definition of any extra optimization variables, e.g., *Lagrangian multipliers*. Calculating these variables involves *offline* mechanisms that solve non-linear equations using *root-finding* methods [45], [46]. Therefore, the ability for real-time service in such schemes is depended on the effectiveness and convergence of their root-finding algorithms. Several iteration-dependent proposals [20]-

[26], [34] - [43] often report linear complexity, which is only seemingly correct since offline parts have been disregarded. In contrary, iteration-independent schemes are tailored to compute their online policies concurrent with the extra optimization variables promising more convenient real-time operation. Nevertheless, developments in this direction are particularly narrow since ordinary cross-layer design scopes do not favour iteration-independent policies. Especially when NBS is adopted, transformations of *Non-deterministic Polynomial-time* (NP) problems into *convex* are either infeasible or imprecise obliging to only numerical solutions.

In the second research part of this Thesis, we aim to inspect the above issues and to suggest solid analytical solutions. We utilize information [29], queuing [30], *number* [44] and *game* [41], [47] theories to propose a game theoretical and iteration-independent cross-layer scheme for OFDMA networks. Our design considers pragmatic conditions in terms of imperfect channel, packet outage, heterogeneous QoS demands and various users' payoffs. The first significance of this research part is our new scope on the design of PBL objectives that fully comply with the *Symmetric-NBS* (S-NBS) and the *Asymmetric-NBS* (A-NBS) *fairness Axioms* [40], [41] in terms of both power and channel allocation. A second impact of this research part is our technique that transforms game-theoretic NP-hard cross-layer problems into equivalent convex optimization problems, making feasible to derive iteration-independent solutions via analysis. The third significance of this research part is our innovative methodology that provides analytical solutions by means of final formulas, to the *transcendental algebraic equations* tailed by the *recursive* origin of the NBS problem [44]. Our proposals address several issues on the trade-off between scheduling efficiency, QoS guarantee and weighted fairness provision by also guaranteeing rapid convergence to *Pareto optimal equilibriums*.

We have not so far considered in our designs the enabling *Cognitive Radio* (CR) technology, which promises to overcome the problem of spectrum scarcity caused by the current way of fixed spectrum allocation [12], [48], [49]. In CRs, users are able to intelligently detect and utilize spectrum holes, so-called *white spaces*, that are temporarily unused by licensed Primary Users (PUs). One key issue is the effective scheduling of these dynamically available resources without interfering potential communications from PUs and with simultaneous QoS provision to CR users, so-called Secondary Users (SUs). In particular, interference elimination can be achieved through considering Signal-to-Interference-plus-Noise Ratio (SINR) rules on predefined power thresholds for both SUs and PUs. Nevertheless, bearing such SINR rules usually results into reduction of the spectrum's white spaces due to large power thresholds or increased QoS requirements of some PUs. Hence, the QoS of SUs could be tremendously degraded and a critical topic arises regarding resource fairness regulations between SUs and PUs. Although CR systems have recently received great attention [37], [38], [39], [42], [43], [50], [51], [52], [53], [54], [55] only few research efforts propose analytical solutions on the NBS allocation of power [37], [42], [43], while numerical proposals dominate. However, power control itself cannot definitely meet the full QoS and fairness requirements, where those diverse requirements are needed to be considered in the optimization problem formulation. Our viewpoint is that analytical NBS-based strategies of both power and channel assignments can address several fairness and performance issues in CR networks.

In the third part of this Thesis, we utilize information [29], number [45] queuing [30] and game [41], [47] theories to address the above issues by proposing a NBS-based cross-layer scheme for CR systems. The significance of this research part is that we introduce the first analytical and joint channel and transmitting power allocation policy for CR networks in fully compliance to the S-NBS Axioms. Our policy boosts the overall system efficiency by exploiting multi-user diversity [14], [23] and it is implemented with iteration-independent algorithms thanks to our previously mentioned research efforts.

1.2 Contributions & Novelties of the Thesis

This Thesis solves four resource allocation problems by introducing intelligent schemes to enhance system performance with minimal complexities. We theoretically discuss the contributions and highlight the novelties of our proposals as follows.

- ***Power-Efficient Cross-Layer Design*** **-** As modern networking aims to guarantee various QoS characteristics with low power consumption, we propose an opportunistic *power-efficient* resource scheduler to provide heterogeneous QoS support for OFDMA downlink networks. In particular, we firstly describe the structure of the imperfect channel and introduce a robust Minimum Mean Square Error (MMSE) *channel estimation process*. A notable contribution is that in our MMSE estimation the channel error covariance matrix is not a scalar multiple of the identity matrix, in contrary to the mean feedback model adopted by the related work in [17], [24], [56], [57], [58]. In other words, our MMSE estimation does not satisfy the assumptions of sphericity [59] but it estimates based on a non-sphericity pattern meaning that the estimation errors among each user's OFDMA sub-channels, so-called subcarriers, are independent but not identically distributed; as shown in the single-user OFDM case studied in [16], such estimation patterns can provide decent resilience performance to CSI errors. In addition, when being applied to our multi-user scenario our estimation process results in asymptotically efficient performance, which also contributes to increase power efficiency.

  Furthermore, we rely on *independent bit-encoding* and introduce a methodology to express the effective *throughput* of each user under potential packet outage and estimated CSI. Another significant contribution is that our methodology substantially improves the power consumption due to a key theoretical difference from existing approaches [13], [14], [17], [20], [23], [24], [56], [57], [58], [60]; accounting that the estimated *channel gain* is Circularly Symmetric Complex Gaussian (CSCG) distributed and that the actual absolute channel gain squared is a chi-squared non-central variable, we firstly express the Probability Density Function (PDF) of the *maximum capacity* to define the throughput policy in terms of estimated CSI and channel outage. Then we compute the throughput policy through a series expansion and observe that it can be approximated by a Gaussian PDF. Based on this PDF,

we define a PBL function that signifies the maximum achievable throughput for error-free transmissions. A key advantage of our PBL function is that its utility dynamics have low-pace growth ratio to variations of the outage probability and the MMSE variance meaning that our function induces slow throughput degradations with notably small decay rate. In contrary, the methodologies followed in [13], [14], [17], [20], [23], [24], [56], [57], [58], [60] deliver the so-called *goodput*-rate. As we discuss later, the goodput-rate dynamics are highly sensitive to escalations of the outage probability and the MMSE variance inducing rapid goodput-rate degradations. Also, goodput-rate is always less than the actual capacity since the amount of packet overhead depends on the application protocol stack hence, some resources are wasted.

In continue we use our PBL function as optimization objective to formulate an NP-hard cross-layer problem, aiming to minimize the system's transmitting power subject to heterogeneous QoS, packet outage, channel and transmitting power allocation rules. A major contribution is that it is the first work that considers minimizing the system's transmitting power under such constraints. We then transform the QoS rules into equivalent cross-layer throughput constraints by developing a Memoryless/General/Single-Server (*M/G/1*) [59] queuing system. In our queuing system the service provided by all subcarriers of each user is a server with service rate according to the system's dynamics at the PHY and higher layers and to the user's buffer status. Different from approaches with simple delay-optimal policies [27], [61], [62], [63], [64], [65], [66], [67] we contribute by proposing an advanced cross-layer strategy to account heterogeneous delay and arrival rate requirements of each of the various users.

Furthermore, we introduce variable relaxation in terms of *time-sharing* subcarrier factors that indicate the fractions of time where a user occupies the subcarriers. Through this feature, we can transform the NP-hard problem into a *convex optimization* problem determined over a feasible convex set that satisfies the equivalent cross-layer constraints. We utilize convex optimization and derive the *optimal solutions* via *explicit analysis* based on the *Lagrangian technique*. Another important contribution of this research part is that our solution attains significantly improved power-efficiency from low to high channel imperfectness, by achieving similar throughput gains due to multi-user and multi-carrier diversities phenomena with the same computational complexity to relevant approaches. Finally, we experimentally address the impact of opportunistic scheduling on heterogeneous

QoS provision in terms of average system throughput, resilience to imperfect channel in the PHY and packet average throughput, packet maximum delay and packet arrival rate in the MAC layers.

The key novelties of the first research part of this Thesis are summarised as follows.

– *Design of MMSE estimation process*: We propose a MMSE estimator that performs estimations relying on a non-sphericity pattern. In contrary to the mean feedback model adopted by the related work in [17], [24], [56], [57], [58] our estimation approach provides decent resilience performance to CSI errors and results in asymptotically efficient performance to the multi-user system.

– *Design of power-efficient cross-layer framework*: This is the first approach by introducing power minimization as optimization objective into the cross-layer OFDMA design with heterogeneous QoS requirements and packet outage. To the best of our knowledge, cross-layer power minimization problems have not been introduced yet.

– *Methodology on the formation of power-efficient PBL process with respect to CSIT errors and packet outage*: It is the first work that introduces a novel methodology on the design of a PBL function that induces notably smaller throughput degradation and/or power ascents than commonly used capacity-based approaches. This new feature brings significant improvements to systems' power efficiency due to its increased resilience to CSIT errors.

– *Methodology on the support of users' heterogeneity*: In this study, the simple delay-optimal policies are extended to an advanced optimal strategy, which accounts both users' heterogeneous delays and arrival rates. To the best of our knowledge, relevant approaches in the literature either consider homogeneous QoS, i.e., [10], [21], [23], [27] [61] or develop queuing models that express the heterogeneous QoS parameters less accurate than our proposal in terms of convex cross-layer constraints [19], [24], [56].

- ***Game-Theoretic Cross-Layer Design -*** As the trade-off between resource efficiency, real-time QoS guarantee and fairness provision is still in early stage, we focus on designing cross-layer scheme that converges rapidly to Pareto optimal solutions. In particular, we propose iteration-independent and NBS oriented optimal network operation under packet outage, imperfect channel and heterogeneous QoS considerations with price rules for users' various payoffs. We initially contribute by proposing a new PBL function to represent the users' satisfaction accounting the exact effective throughput of each user based on the A-NBS as perceived by the cross-layer of the OFDMA system according to PHY and MAC layer parameters. We prove that our new PBL process is in fully compliance with the A-NBS of both power and subcarrier allocation and also meets the metric of weighted proportional fairness of resource sharing.

It is widely admitted that one significant advantage of NBS over other fairness concepts, such as Max-Min (M-M), is that NBS is a natural framework that allows defining fair resource assignments between applications with different concave utilities. Based on that fact, we track time-sharing variable transformations and adopt our M/G/1 queuing model to formulate a convex cross-layer problem constrained over packet outage, channel, power, heterogeneous QoS and payoff rules. We contribute by introducing a new approach for solving such cross-layer problems on a completely different basis than existing methodologies [18], [23], [24], [25], [37], [42], [43], [56], [68], [69]. The rational of our scope is that upon applying time-sharing among subcarriers, the optimal A-NBS-based subcarrier time-sharing factors would be real numbers that indicate the faction of time each subcarrier requires to transmit the amount of information. Hence, we initially perform uniform transmitting power allocation assigning that way an even amount of information on each subcarrier time-sharing factor. We then apply convex optimization to define each subcarrier's optimal time-sharing factor that clarifies each subcarrier's conditions. For example, subcarriers in good conditions would require less time to transfer the same amount of information of each user (small optimal subcarrier time-sharing factor) than subcarriers in bad conditions (large optimal subcarrier time-sharing factor). At the same time we derive the optimal transmitting powers of the corresponding optimal subcarrier time-sharing factors. At this point, instead of performing resource allocation based on the subcarrier with the best channel conditions as in the traditional approach, we have to opportunity to further improve system's power efficiency

by allocating the resources relying on the subcarriers with the minimum optimal power. With that way, we can finally define a joint optimal subcarrier and transmitting power allocation policy, which is not only independent of iterative mechanisms but also power efficient. We show that our introduced methodology reduces system's complexity from phenomenal linear to actually linear meaning that the proposed scheme literally supports real-time service provision in the OFDMA network.

A significant difficulty of this research part is that upon utilizing convex optimization the logarithmic origin of the NBS involves equations with recursive relations between their optimization variables. In other words, the optimal solutions cannot be straightforward defined as transcendental algebraic equations intervene in many phases of the optimization process. It is well-known that deriving the exact roots of transcendental algebraic equations is a difficult generalised problem, which frequently is not solved analytically. Especially in NBS oriented cross-layer optimization all the proposed methods derive graphic or numerical solutions of such equations. Nevertheless, we contribute by proposing an innovative and intelligent technique to derive the analytical solutions for transcendental algebraic equations entailed by the NBS-oriented optimization cross-layer problems.

In sum, this research part proposes the first NBS-based iteration-independent scheduling policy by means of final formulas and in fully compliance with the A-NBS of both power and subcarrier allocation. We study the accuracy of our policy demonstrating that we achieve high optimality level in contrary to many other approaches that derive solutions far from the actual ones. In addition, for the clarifications of our comparisons we solve the A-NBS problem via the dual decomposition method [59] to further demonstrate the accuracy and reduced complexity of our solution.

The key novelties of the second research part of this Thesis are summarised as follows.

– *Methodology on power-efficient designs for iteration-independent cross-layer scheduling schemes*: It is the first work that proposes a novel methodology to derive optimal power-efficient scheduling operation for joint power and subcarrier cross-layer allocation. Our policy has factually linear complexity and converges rapidly to Pareto optimal equilibriums without requiring iterative mechanisms. The ordinary methodology, literally adopted by all

relevant approaches, result to iteration-dependent strategies without improving the system's power efficiency [18], [23], [24], [25], [37], [42], [43], [56], [68], [69].

− *Design of convex NBS oriented cross-layer schemes with channel uncertainty*: This is the first cross-layer design to introduce the A-NBS rules into convex optimization problems along with imperfect channel and packet outage considerations. To the best of our knowledge, relevant game-theoretic studies consider perfect CSI available at the BS or have been developed on single-layer architectures [69], [70], [71], [72], [73], [74], [75], [76], [68], [77], [78], [70], [79], [80], [81], [82], [83].

− *Methodology on the formulation of actual A-NBS rules in PBL functions:* It is the first work that introduces PBL functions to represent users' satisfaction relying on the effective throughput of each user, which is in fully compliance with the A-NBS of both power and subcarrier allocation. To the best of our knowledge, the only relevant work is our study in [84] that embraces the S-NBS property, while all other approaches describe the effective throughput of each user under the S-NBS of transmitting power allocation only.

− *Methodology on optimal solutions by means of final formulas for game-theoretic schemes:* It is the first solution methodology to consider closed-form analysis in terms of convex optimization involving new techniques for the solution transcendental algebraic equations entailed by A-NBS-oriented optimization problems. Relevant studies are far from supporting sufficient analysis proposing either graphic or numerical solutions [71], [72], [73], [74], [75], [76], [68], [77], [78], [70], [79], [80], [81], [82], [83].

- ***Game Theoretic Cross-Layer Design for Cognitive Radios*** - As NBS-based scenarios in CR systems can mitigate the impending spectrum scarcity problem by maintaining fair and opportunistic access to white spaces, we introduce the first game-theoretical cross-layer scheme with joint channel and transmitting power allocation optimal policy for CR networks. More precisely, we consider a prototype OFDMA system with imperfect channel to establish the primary policies on channel, power and throughput allocation. We maintain the communication quality of SUs and protect the potential transmissions of PUs, by denoting QoS and interference elimination regulations based on the SINR of each SU and PU. We firstly contribute by expressing our CR regulations in relation with the primary policies of the OFDMA system by means of power thresholds. In addition, apart from other CR studies where such regulations are expressed via power-unrelated utilities [52], [53], we contribute by coupling the control decisions of all users in QoS and interference power constraints and properly transforming them into pricing terms in SINR and QoS-based utility functions. We will see later that such expressions facilitate the transformation and convexity of the optimization problem as well as the global convergence of our optimal solutions.

Furthermore, we rely on the S-NBS theorem to define a PBL utility function that maintains the throughput of the CR network as perceived by the MAC layer of the OFDMA system according to PHY layer parameters. Although relevant works propose capacity-related expressions for the utility function for Non-cooperative Power Control Games (NPCGs) [52], [53], [54], [55] or cooperative games for power control [37], [42], [43], we contribute further by proposing a proper PBL utility function that not only reflects the network spectrum utilization efficiency but also facilitates the implementation of joint power and channel control algorithms. Our utility PBL function describes the actual CR throughput in fully compliance with the Axioms of S-NBS of both power and channel allocation employing a capacity-related expression that comforts the optimization problem in terms of convexity and global convergence.

Moreover, we describe our modelling through a mixed combinatorial problem that targets to maximize CR system's throughput subject to several system constraints. Adopting time-sharing variable transformation we then formulate an equivalent convex optimization problem and derive analytical optimal policies via our power-efficient solution methodology for NBS games. In contrary with all other relative studies, we examine the validity of our

solutions as there may be instances, where the determined convex set may be zero. The reason is that the cross-layer constraints for transmission interference are power-driven and frequently contradict each other. Hence, we contribute by introducing a feasibility condition that shows the region, where CR-based optimization problems are valid. The major contribution of this research part is that not only our CR optimal resource allocation is the first that embraces the NBS Axioms but also it is iteration-independent and guarantees convergence to Pareto optimal equilibriums. In contrary some few resent cooperative game-theoretical studies [37], [42] [52], [53], [54], [55] provide analytical solutions regardless NBS or propose NBS-based solutions by only concerning optimal power control and not channel assignment [43]. Simulation results reveal the superiority of the proposed optimal scheduling over relevant approaches in terms of throughput performance, power consumption, fairness provision, computational complexity and optimality level.

The key novelties of the fourth research part of this Thesis are summarised as follows.

– *Adaptation of CR and OFDMA regulations into equivalent convex constraints*: In this work, we express the CR and OFDMA system rules by means of power-related utilities that can be transformed into pricing terms in a SINR and QoS-based utility function. In contrary to relevant studies, where such regulations are expressed via power-unrelated utilities [52], [53], [54], [55] we achieve convexity of the optimization problem and ensure global convergence of our optimal solutions.

– *Design on cross-layer S-NBS-based game-theoretic schemes for CR systems*: It is the first work that introduces joint channel and transmitting power allocation designs for CR systems in fully compliance with the Nash bargaining Axioms. As discussed previously, relevant approaches in CR networks have only considered single-layer structures with cooperative game-theoretical allocation of power [37], [42], [43], [52], [53], [54], [55].

– *Methodology on analytical and iteration-dependent solutions for S-NBS based resource scheduling in CR systems*: It is the first work that proposes closed-form analytical solutions for joint optimal resource allocation in game-theoretic CR systems. To the best of our knowledge, many studies in the CR literature [38], [39], [50], [51], [52], [53], [54], [55]

propose numerical or graphical solutions, while very few resent works [37], [42], [43] provide analytical iteration-dependent cooperative game-theoretical solutions in partial compliment with the S-NBS Axioms of channel allocation. In contrary, not only we introduce analytical optimal solutions for joint power and channel allocation through convex optimization but also our solutions are iteration-independent guaranteeing real-time QoS provision to the SUs and contributing to increase the reliability of CR network.

1.3 Author's Publications

The following is the complete list of publications.

1) **C. C. Zarakovitis** and Q. Ni**,** "Nash Bargaining Game Theoretic Scheduling for Joint Channel & Power Allocation in Cognitive Radio System", *IEEE Journal on Selected Areas in Communications (JSAC)*, 10.1109/JSAC.2012.120107, vol 30, Issue 1, pp 70-81, 2012.
2) **C. C. Zarakovitis**, Q. Ni, D. Skordoulis and M. G. Hadjinicolaou, "Power-Efficient Cross-Layer Design for OFDMA Systems with Heterogeneous QoS, Imperfect CSI and Outage Considerations", *IEEE Transactions on Vehicular Technology (TVT)*, 10.1109/TVT.2011.2179817, 2011.
3) **C. C. Zarakovitis** and Q. Ni, "A Performance Comparative Study on the Implementation Methods for OFDMA Cross-Layer Optimization", *Elsevier Journal of Future Generation Computer Systems (FGCS)*, 10.1016/j.future.2011.10.008, Nov. 2011 (Selected Paper from CIT 2010).
4) **C. C. Zarakovitis,** I. G. Nikolaros, D. Skordoulis, M. G. Hadjinicolaou and Q. Ni, "A Comparative Study on Iterative Methods Regarding Cross-Layer Optimization for OFDMA Systems," *IEEE International Conference on Computer and Information Technology (CIT)*, 10.1109/CIT.2010.98, pp.420-425, July 2010.
5) **C. C. Zarakovitis,** Q. Ni, I. G. Nikolaros and O. Tyce, "A Novel Game-Theoretic Cross-Layer Design for OFDMA Broadband Wireless Networks," *IEEE International Conference on Communications (ICC)*, 10.1109/ICC.2010.5502203, pp.2649-2654, 23-27, May, 2010.

6) **C. C. Zarakovitis,** Q. Ni and D. Skordoulis, "Cross-Layer Design for Single-Cell OFDMA Systems with Heterogeneous QoS and Partial CSIT," *IEEE Wireless Communications and Networking Conference (WCNC)*, 10.1109/WCNC.2009. 4917652, pp.1-6, April, 2009.
7) I. G. Nikolaros, **C. C. Zarakovitis**, D. Skordoulis, M. G. Hadjinicolaou and Q. Ni, "Cross-layer Design for Multiuser OFDMA Systems with Cooperative Game and MMPP Queuing Considerations," *IEEE International Conference on Scalable Computing and Communications (ScalCom)*, 10.1109/CIT.2010.446, pp.2649-2654, June-July, 2010.
8) D. Skordoulis, Q. Ni and **C. C. Zarakovitis,** "A Selective Delayed Channel Access (SDCA) for the High-Throughput IEEE 802.11n," *IEEE Wireless Communications and Networking Conference (WCNC)*, 10.1109/WCNC.2009.4917544, pp.1-6, April, 2009.
9) **C. C. Zarakovitis** and Q. Ni, "Novel Cross-Layer Scheduling for Single-Cell OFDMA Systems with Heterogeneous QoS and Partial CSIT", *SED Research Conference*, p.p. 86-92, June 2009.
10) **C. C. Zarakovitis** and Q. Ni, "Novel Game-Theoretic Cross-Layer Scheduling for Single-Cell OFDMA Systems with Heterogeneous QoS and Partial CSIT", *SED Research Conference*, p.p. 425-431, June 2010.
11) **C. C. Zarakovitis,** I.G. Nikolaros, Q. Ni and M. G. Hadjinicolaou, "Game Theoretic Cross-Layer Design for Resource Allocation in Heterogeneous OFDMA Network", *IET Journal on Communications*, under review.

1.4 Outline of the Thesis

In Chapter 1 we introduced the significance of the Thesis among related studies in the literature. In addition, we overviewed the contributions and novelties of our proposals by also providing the author's publications list.

The rest of the Thesis is organized as follows.

- Chapter 2 presents background knowledge regarding contemporary methodologies for resource allocation architectures, spectrum-sharing technologies and game theoretic strategies as well as on convex optimization in engineering accounting recent material in the literature.

- Chapter 3 introduces the design of a power-efficient cross-layer scheme for resource scheduling in OFDMA systems. The chapter includes system modelling, imperfect channel modelling, channel estimation modelling and analysis, formulation of the PBL process with specifications, transformation of system constraints into cross-layer constraints, formulation of cross-layer convex optimization problem, optimal solutions with detailed analysis, specifications on the functionality of the optimal policy, extended simulation results and Appendix A.

- Chapter 4 proposes a game theoretic cross-layer design for A-NBS-based resource allocation scheduling in OFDMA systems. The chapter includes system modelling, imperfect channel modelling, formulation of the PBL process with specifications, transformation of system constraints into cross-layer constraints, formulation of cross-layer convex optimization problem, analytical methodology for iteration-independent and power efficient cross-layer designs, optimal solutions, specifications on the functionality of the optimal policy, extended simulations and Appendix B.

- Chapter 5 presents a game theoretic cross-layer design for S-NBS-based resource scheduling in CR systems with OFDMA spectrum-sharing. The chapter includes system modelling, imperfect channel modelling, definition of power-driven transmission cancelation CR regulations, formulation of the PBL process with specifications, transformation of system constraints into cross-layer constraints, formulation of cross-layer convex optimization problem, methodology for iteration-independent and power efficient cross-layer designs, optimal solutions with detailed analysis, specifications on the functionality of the optimal policy, extended simulation results and Appendix C.

Chapter 2

Background Knowledge

Before presenting our proposals, we shall firstly inspect some basic background knowledge on protocol architectures, spectrum-sharing technologies and game theoretic strategies as well as on convex optimization in engineering problems accounting recent material in the literature. Such inspection helps for appropriate presenting the features of our proposals.

2.1 Protocol Architectures

In contrary to wire-line technology, wireless systems have restricted physical resources since the frequency spectrum, so-called bandwidth, is limited. This major constraint creates an increasingly critical aspect on the network's performance optimization, which is substantially depended on the considered architecture of the resource allocation scheme.

The Open System Interconnection (OSI) [59] network model defines a hierarchy of functionalities and services provision by dividing the overall networking task into seven individual layers. The provided services are realized through protocol designs, so-called schemes, for the different layers. Schemes can involve either per-layer or cross-layer optimization. In per-layer optimization, higher-layer schemes ensure the services at the lower layers with no concern about the way these services are being provided. In cross-layer optimization, the OSI structure is violated implicating that direct communication between schemes is allowed at non-adjacent layers or sharing variables between layers.

The presence of wireless links in the network motivates the researcher to focus on scheme architectures involving cross-layer optimization for three main reasons. The first reason is that wireless links create several new problems for scheme designs that cannot be handled well in the framework of the layered architectures, e.g., valuing the packet error rate

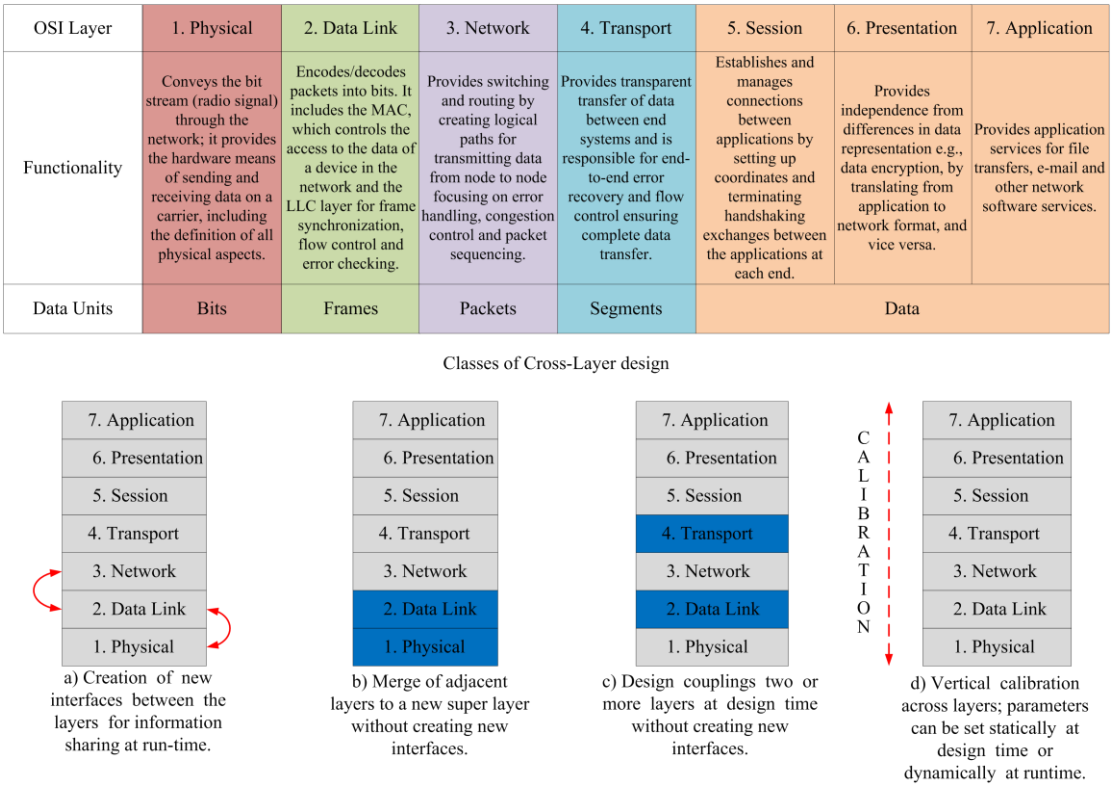

Figure 2.1 - The classes of cross-layer design in relation with the OSI layer model.

on a wireless link [85]. The second reason is that wireless networks offer several avenues for opportunistic communication that cannot be exploited sufficiently in a strictly layered design.

For example, the time-varying link quality allows opportunistic usage of the channel, whereby the transmission parameters can be dynamically adjusted according to the variations in the channel quality [86]. The third reason is that wireless medium offers some new modalities of communication the layered architectures do not accommodate, e.g., the physical layer can be made capable of simultaneous reception of multiple packets [87].

However, breaking up the layered structure of the networking stack may also have negative consequences in terms of compatibility issues and resulting performance. In particular, cross-layer coordination schemes can introduce dependency relations and unintended interactions [88]. In some situations, adaption mechanisms in different layers start working in contradiction of each other, leading to worse practical performance than in a

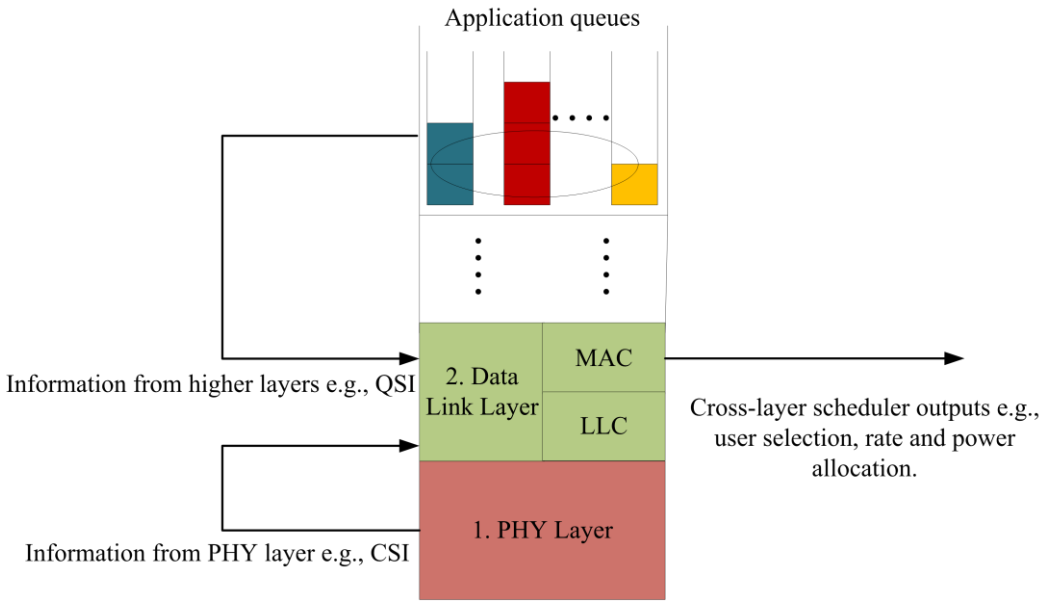

Figure 2.2 - Generic cross-layer scheduling model.

layered network. Such malfunctions can be avoided by choosing an effective and stable method of cross-layer scheme architecture [19], [89].

Cross-layer architecture methods can rely on the creation of new interfaces utilized for information sharing between the layers at runtime [85] or by involving coupling between two or more layers at design time without creating any extra interfaces for information sharing at runtime [87]. In the latter case, new interfaces are absent and the architectural cost lays on the possibility of replacing one layer without making corresponding changes to another layer. Another way in which cross-layer scheme design proposals in the literature fit is with vertical calibration across layers, where the performance seen at the level of the application is a function of the parameters at all the layers below it [69]. The most promising so far unexplored [19] method among all relies on the design of two or more adjacent layers together such that the service provided by the new so-called super-layer is the union of the services provided by the constituent layers. To the best of our knowledge, proposal that explicitly creates a super-layer cannot be found in the literature. The classes of cross-layer design in relation with the OSI model are depicted and described in Figure 2.1.

Yet it has recently been recognized that the collaborative design between the network, PHY and MAC layers tends to blur the boundary between these adjacent layers [19]. Improvements on the lifetime as well as the power consumption of the network system are also achieved by adjusting those layers in a cross-layer design. To explore the potential on the performance of contemporary resource allocation and packet scheduling, this Thesis focuses on the design of cross-layer schemes advocating the joint strategy of resource allocation mechanisms in network, PHY and MAC layers. The generic cross-layer scheduling model adopted in this Thesis is shown in Figure 2.2.

2.2 Random Access Technologies

Guaranteeing some form of diversity in time, frequency, space or coding, the performance of wireless communications over fading channels can be extensively improved. Leveraging on these carrier-multiplexing concepts, several random access technologies have been designed to control the users' access to the radio resources. Such technologies are classified in contention-based and conflict-free MAC schemes [90]. In contention-based MAC schemes, competition between users occurs for the access of a common resource, resulting in possible conflicts that the schemes handle via static and dynamic contention resolution techniques, e.g., Aloha [91], Carrier Sense Multiple Access (CSMA) [92]. In conflict-free MAC schemes, a variety of access techniques is utilized ensuring the collision avoidance during transmissions and allowing to users the occupancy of a portion of the communications resource. Conflict-free schemes are based on Time Division Multiplexing (TDM), Frequency Division Multiplexing (FDM), Space Division Multiplexing (SDM) and Code Division Multiplexing (CDM) that define the concepts of dividing the wireless spectrum among the active users [93]. The corresponding to TDM, FDM, SDM and CDM random access technologies are known as Time Division Multiple Access (TDMA), Frequency Division Multiple Access (FDMA), Spatial Division Multiple Access (SDMA) and Spread-Spectrum (SS) based technologies, such as Code Division Multiple Access (CDMA), respectively.

The idea of separating the channels into multiple subcarriers in FDM [93] makes FDMA the most straightforward random access technique among the aforementioned. The last decades have been formulated the principles of a more advanced multiple carrier

technology known as Orthogonal Frequency Division Multiplexing (OFDM) [93]. OFDM has been developed by the European Telecommunication Standards Institute Broadband Radio Access Network (ETSI BRAN) and the Multimedia Mobile Access Communications (MMAC). The comparative advantages of OFDM have been just recently evaluated and exploited. Random access technologies based on OFDM are known as OFDM-TDMA, OFDM-CDMA and OFDM-FDMA. From resource allocation point of view, OFDM-FDMA, so-called OFDMA, outperforms OFDM-TDMA and OFDM-CDMA in the un-coded and coded Bit-Error-Rate (BER) performance [14], [94]. This is because multiple channels in OFDMA systems naturally have the potential for more efficient MAC since subcarriers can be assigned to different users [95] and because OFDMA systems performance is improved by applying adaptive transmitting power allocation [14]. Today, OFDMA is the global standard for the band of 5 GHz and has been adopted in the standards of Digital Audio Broadcasting (DAB) [96], Digital Video Broadcasting (DVB) [97], Asymmetric Digital Subscriber Line (ADSL) [98], IEEE802.11a/g Wireless Fidelity (WiFi) [2], HIPERLAN/2 [3], 3G Long-Term Evolution (3G LTE) [4] and IEEE802.16 knows as Worldwide Interoperability for Microwave Access (WiMAX) [5].

Accounting the characteristics of pioneering random access technologies, this Thesis embraces the OFDMA technique for the design of resource allocation and packet scheduling schemes between MAC and PHY layers. To further validate the benefits of OFDMA technology and to keep consistency of the system model analysis introduced in this Thesis, we provide a microscopic view on the fundamental principles of OFDM in anachronism with other challenging technologies.

2.2.1 Fundamental Principles of OFDM

The primary advantage of OFDM over TDM, FDM, SDM and CDM is the combination of adaptive spectrum modulation and multiple accesses. OFDM is a special case of multi-carrier transmission, where the overall flow of information data is transmitted through a number of subcarriers each one having different transmission rate. Some of the subcarriers carry pilot symbols for measurement of the channel conditions. So, one main reason of using OFDM

modulation is the effective way of managing the dissemination of information through multiple paths, which increases the resistance of the system against frequency selective fading and interference phenomena between neighbouring subcarriers transmission [99].

Multi-carrier modulation superimposes the single-carrier modulated waveforms that represent a sequence of bits. The transmitted signal is the summation of all the independent subcarriers of identical amplitude and central frequency. The number of bits on each subcarrier can be modulated based on *encoding techniques* as Quadrature Amplitude Modulation (QAM) or Phase Shift Keying (PSK). The conversion of the binary bits into, e.g., QAM values is achieved through applying *interleaving*. In contrast to FDM, the bit encoding in multi-carrier modulation can differ at every time slot. With this way, subcarriers abide minor attenuation and are less prone to noise hence, they transfer more bits of information maximizing system's performance. In band-pass multipath communication channels, as Local Loop (LL) channels, occurs wide variation regarding signal attenuation and variable phase shift in frequency. In such channel configurations, multi-carrier modulation is optimal when the number of subcarriers is large.

However, most initial efforts to implement such channel configurations did not have the desired results mainly because of the difficulty in maintaining equal spacing between subcarriers. Most recent efforts are successful due to the progress of the Digital Signal Processor (DSP), which can accurately synthesize the sum of modulated waveforms utilizing Fast Fourier Transform (FFT) and Inverse-FFT (IFFT) [100] for efficient calculation of the sum for large number of carriers at the signal modulation and demodulation process, respectively. To exploit the very low computational complexity of FFT, the number of subcarriers is used in the power of two. The number of subcarriers required to achieve maximum performance depends on the abruption of the channel transfer function in relation with the frequency.

In a single-carrier system, a simple attenuation or interference can lead to failure of the entire transmission network. Conversely, in a multi-carrier system, only a small percentage of subcarriers will be affected. In a traditional parallel system, the frequency spectrum is divided into a number of non-overlapping fields, each one representing a subcarrier, which broadcasts a special symbol. These subcarriers are multiplexed in the frequency domain. By choosing non-overlapping spectrum fields, interference phenomena

between subcarriers transmission are avoided, however, the available spectrum is inefficiently exploited.

To address this problem, several multi-carrier technologies have been introduced, combining the parallel data stream and the FDM with overlapping subcarrier transmissions. In such cases, the data transmitted at the high transmission rate channel, are broadcasted on separate subcarriers with lower transmission rates. The data can be then multiplexed with appropriate methods to achieve more efficient use of the available bandwidth. In such multi-carrier technologies, the overlapping subcarriers are placed in series so that using appropriate demodulator filters they can be easily distinguished by the receivers. However, such receivers use chronic controls, co-called guard-times, between different subcarriers in the frequency domain, which results in the available spectrum reduction. Spectrum is additionally reduced by interferences among the overlapping subcarriers.

The solution to the above problems is given by originating the *orthogonality principle* between subcarriers in OFDM technology. The term orthogonality implies that there is a precise mathematical relationship between frequencies of different subcarriers in the system. Orthogonality implies that the placement of subcarriers is performed in such a way that band overlapping is achieved with simultaneous elimination of interference phenomena. Since OFDM exhibits these advantages, it has become subject of extensive research.

In OFDM systems with parallel transmission, Discrete Fourier Transformation (DFT) is utilized as part of the modulation and demodulation process. As the central frequency of each subcarrier is not affected, the associated values based on the central frequency are calculated at the receiver via DFT hence, data are retrieved with no Inter Symbol Interference (ISI). ISI is also avoided for the reason that the receiver evaluates the OFDM signal at the points, where subcarriers have peak amplitude hence, demodulation is achieved without interference. At the peak amplitude of each subcarrier, the spectrum of all the other subcarriers is equal with zero. In addition, the spectrum of the OFDM signal matches the *Nyquist* criterion [101] for a free shape pulses with ISI cancelation. Therefore, when the maximum spectrum of a subcarrier interbreeds with the zeros of other subcarriers, Inter Carrier Interference (ICI) is also avoided. In case of imperfect channel, ICI, ISI as well as Inter Frame Interference (IFI) are totally suppressed through adding Cyclic Prefix (CP) ahead of each OFDM symbol. The CP length should be greater than expected delay spread, so that

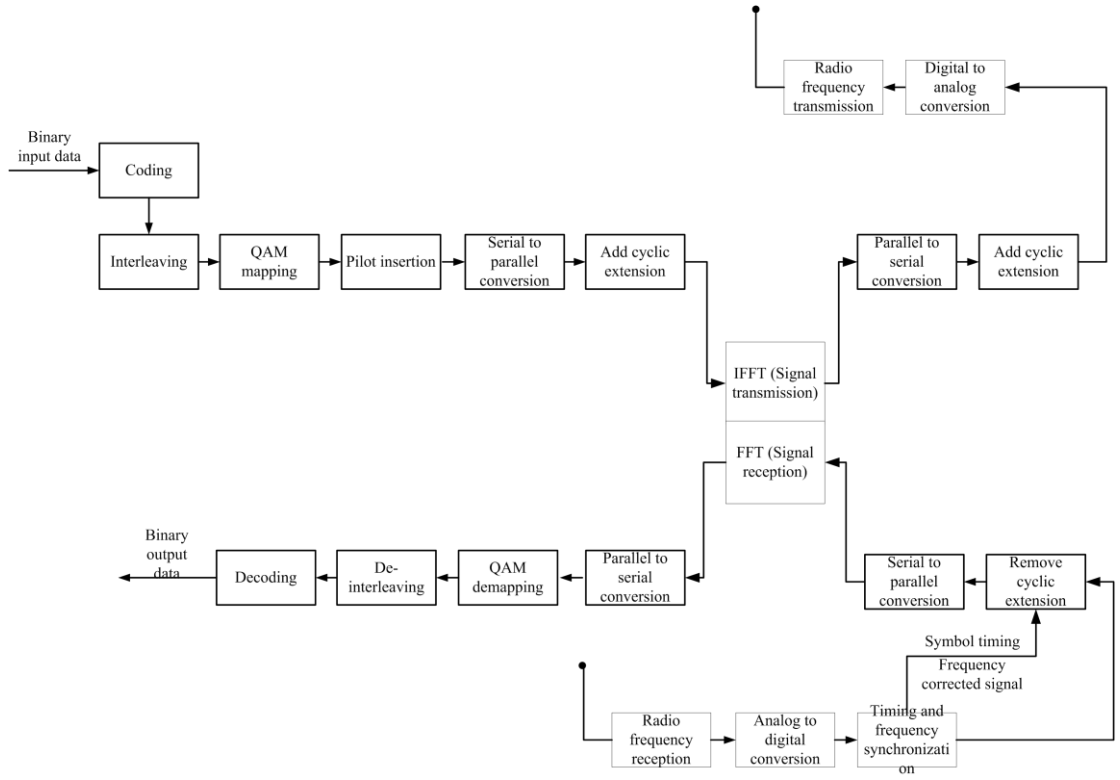

Figure 2.3 - Block diagram of a typical OFDM transceiver.

the component of a frame of symbols transmitted from a subcarrier cannot interfere with the next frame. In case where multiple channel paths are involved during the reception or transmission each path has often time delays. To correct time delays low pass filters are used at the receiver. In addition, upon conversion from analogue to digital signal the digital signal process starts with a pilot process that helps to define and synchronize any frequency shift.

The implementation of DFT so-called FFT [100] further enhances OFDM system performance. Low-cost, high-speed FFT chips are implemented through Very Large Scale Integration (VLSI) systems. In this way, both the transmitter and receiver use FFT and IFFT techniques by reducing the computational complexity of OFDM modulation and demodulation, respectively, from exponential to linear [101]. Figure 2.3 depicts a typical OFDM transceiver.

2.3 Resource Allocation for OFDMA Wireless Systems

In an OFDMA wireless network, the channel is divided into orthogonal narrowband subcarriers so, different subcarriers can be allocated to different users to provide a flexible multi-user access scheme and exploit multi-user diversity [95], [102]. The specific subset of subcarriers assigned to each of the system users and the powers transmitted on these subcarriers can be properly selected such that some performance metric of the OFDMA system is optimized. The abovementioned parameters, i.e., the subcarriers subsets and the transmitting powers are commonly called as the *resource allocation parameters*. The process of determining these parameters in order to optimize a certain performance metric is referred to as *resource allocation*.

There are many ways to exploit the high degree of flexibility of radio resource management in the context of OFDMA. Since channel frequency responses are different at different frequencies and for different users, *data rate adaptation* over each subcarrier, *Dynamic Subcarrier Assignment* (DSA) and *Adaptive Transmitting power allocation* (APA) can significantly improve the performance of OFDMA networks. Using data rate adaptation [103], [104] the transmitter can send higher transmission rates over the subcarriers with better conditions so as to improve throughput and simultaneously to ensure an acceptable BER at each subcarrier. Despite the use of data rate adaptation, deep fading on some subcarriers still leads to low channel capacity. On the other hand, channel characteristics for different users are almost mutually independent in multi-user environments, e.g., subcarriers experiencing deep fading for one user may not be in a deep fade for other users. Therefore, each subcarrier could be in a good condition for some users in a multi-user OFDMA wireless network. Resource allocation issues and the achievable regions for multiple access and broadcast channels are investigated in [105] and [106], respectively, which prove that the largest data rate region is achieved when the same frequency range is shared with overlap by multiple users in broadcast channels. However, when optimal DSA with data rate adaptation is used, there is only a small range of frequency with overlapping power sharing [107]. Yet it has been shown that the combination of APA, DSA and data rate adaptation in joint optimal algorithms can achieve data transmission rates close to the channel capacity boundary [14], [108], [109], [110].

Within this Thesis we focus on such joint optimal schemes over *non-deterministic channels*. Many works in the literature assume that channel coefficients are instead *deterministic*; from an information-theoretic perspective, this means that perfect CSI is considered to be available at the transmitter (CSIT). In practice, the latter assumption only holds if there is an error-free feedback link from each user to the Base Station (BS). Under the deterministic channels assumption, several performance metrics are used in the literature to optimize the selection of the resource allocation parameters, e.g., maximization of the sum rate, maximization of a weighted sum rate and minimization of the total transmitting power needed to satisfy all users' rate requirements. For most of the aforementioned resource allocation problems, there is no simple way to find their respective optimal solution. Most of the existing works [14], [110], [111], [112] resorted to numerical approaches in order to compute suboptimal solution to the above resource allocation problems.

Furthermore, many proposals are either based on *ergodic* or *non-ergodic* channel capacities. In ergodic channels the sequence of the channel coefficients for each user and each subcarrier is a random ergodic process meaning that the randomness of the channel gains can be averaged out (removed) over time. These models best fit the case of *fast fading channels*, i.e., channels whose coherence time is much smaller than the code-word duration [113], [105], [114]. On the other hand, very few works [115], [116] addressed the resource allocation problem in the case where the sequence of channel coefficients is modelled as a non-ergodic process. This model is best adapted to the case of *slow fading channels*, i.e., channels whose coherence time is much larger than the code-word duration.

2.4 Game Theoretic Resource Allocation

Game theory [41], [47], [117] is a discipline aimed at modelling situations in which decision makers have to make specific actions that have mutual, possibly conflicting, consequences. It has been used primarily in economics and adopted in politics, biology and engineering. The first notion of game theory was made in [118], while the NBS introduction brought significant additional contributions [40], the cornerstone of which is the famous Nash equilibrium.

Recently, game theory has been also applied in networking and communications, where there exist a number of decision makers, called *players* who have potentially

conflicting interests. In the wireless networking context, game theory is the analysis of conflict and cooperation among *intelligent rational* players. A player can be either a user or network operator and is said to be rational if it makes decisions consistently in a pursuit of its own objectives. In a multi-player game, individuals make decisions that influence each other expected *utility*. The objective of game theory is how players can appropriate adjust their objectives to maximize their utilities and act according to their *game strategies* such as *prisoner's dilemma, matching pennies, joint packet forwarding games* and *multiple access games* [41], [47].

In wireless networking, there are many *types of game strategies*; a game can be *symmetric*, where payoffs of players depend on the other strategies employed or *asymmetric*, meaning that payoffs depend on the requirements of each player. In addition, games can be either *nonzero-sum*, where players cooperate each other to increase their payoffs, e.g., prisoner's dilemma, joint packet forwarding games and multiple access games, or *zero-sum* meaning that the gain of one player represents the loss of the other player, e.g., matching pennies games. Other types of game strategies can be considered either as *static*, where players have only a *single move* in an one time-step strategy, either as *dynamic*, where players have a set of moves during multiple time steps making their moves simultaneously without knowing what the other players do, or *repeated*, which is a subset of dynamic games, where players interact several times using a repeated strategy. Moreover, if all players know all the utility functions, then the game type is said to be with *complete information*, while if there is some information concerning the game that is not common knowledge, then the game is said to be with *incomplete information*, represented by *Bayesian* games [41]. In addition, when players aim to maximize their own utility then the game is said *non-cooperative*, while when players are allowed to form coalitions the game is said to be *cooperative*.

Any game type can be defined in *strategic form* with the set of game strategies to constitute a *strategic profile*. Once the game is expressed in strategic form it can be solved by many *solution concepts*, which are predictions about what rational intelligent players should play in the game. There are two possible ways to analyse such games: the *dominant* and *Nash equilibrium* [41], [47]. The dominant analysis is the simplest way of solving game strategies and is distinguished into *strict dominant*, or *iterated dominant*. A strict dominant strategy is a fixed strategy a player follows regardless the strategies of other players and other strategies of

its own that might be more dominant. However, strict dominant solutions are not resilient to system changes, frequently leading to high unfairness. On the other hand, in iterated dominant strategies are more convenient, where a player recognizes that other players have strictly dominated strategies acts accordingly. In addition, a broad class of games are characterized by the Nash equilibrium solution, which is a profile of strategies such that each player strategy is an optimal response to the other players' strategies. Although any solution derived by iterated strict dominance is a Nash equilibrium [41], iterated dominant solutions cannot solve many problems in resource allocation mainly due to the increased complexity, e.g., in multiple access game types. Fortunately, using the concept of Nash equilibrium, we can identify solutions to such strategy profiles using the concept of *Pareto-optimality*. In a Pareto-optimal multiple access game strategy, the payoff of a player cannot be increased without decreasing the payoff of at least one other player. The concept of Pareto-optimality eliminates the Nash equilibriums that can be improved by changing to a more efficient, i.e., *Pareto-superior*, or less efficient, i.e., *Pareto-inferior*, strategy profiles.

In this Thesis we focus on cooperative, nonzero-sum, multiple access game type strategies in dynamic games with complete information. Our game analysis is based on Pareto-optimal Nash equilibriums for symmetric and asymmetric Nash bargaining game structures.

2.5 Utility Theory in Nash Bargaining Multiple Access Games

The concept of utility functions is of outmost importance in game theory. A utility function f_j of a player $j = 1,...,K$, where K is the total number of players, quantifies the outcome of the game for a player given the strategy type. A utility function is a twice-differentiable function of *objective* $U\left(f_j\right)$ defined for $f_j > 0$, having properties of *non-satiation*, e.g., the first derivative is positive $\partial U\left(f_j\right)/\partial f_j > 0$ and *risk aversion*, e.g., the second derivative is negative $\partial^2 U\left(f_j\right)/\partial\left(f_j\right)^2 < 0$. The non-satiation property states that utility increases with objective, while the risk aversion property states that the utility function is concave or, in other words, that the marginal utility of objective decreases as objective increases.

Let us suppose that $u_j^0 \in f_j$ is the initial minimum utility of each user to join the multiple access game, e.g., its minimum QoS requirements in terms of data rate. Then a *bargaining problem* is the pair of $\left(f_j, u_j^0\right)$, where f_j is defined as a close convex subset of $\Im^K = \{\Psi\}$, e.g., $f_j \subseteq \Im^K$, with $\Im^K$ to represent the set of game strategies of the K players and Ψ the space of the utility vectors, and there exists $\psi \in \Psi$ with $f_j(\psi) >> u_j^0$. Assuming that the minimum utility u_j^0 can be achieved for each player, then there exists at least one feasible sub-space Ψ_0 in Ψ for which the utility vector $\mathbf{f} = \left[f_1(\psi), ..., f_K(\psi)\right]$ is larger or equal to the initial utility vector $\mathbf{u^0} = \left[u_1^0, ..., u_K^0\right]$, e.g., $\mathbf{f} \geq \mathbf{u^0}$, allowing the sub-set $\Psi_0 \in \Psi$ to be defined as $\Psi_0 = \left\{\psi \in \Psi \middle| f_j(\psi) \geq u_j^0\right\}$. Moreover, let $U = \left\{f_j(\psi) \middle| \psi \in \Psi\right\}$ to denote the set of achievable utility and $G = \left[U\left(f_j(\psi)\right), u_j^0 \middle| U\left(f_j(\psi)\right) \subset \Im^K\right]$ to represent the set of all bargaining problems or, in other words, the class of sets of individual intelligent rational utility measures satisfying the minimum utility bound $\mathbf{u^0}$. A utility-based *bargaining solution* is a set-valued function $S: G \to \Im^K \neq \varnothing$ such that for every utility-based bargaining problem $G = \left(U\left(f_j(\psi)\right), u_j^0\right)$ it is $S(G) \subseteq U\left(f_j(\psi)\right)$. In the bargaining problem $\left(U\left(f_j(\psi)\right), u_j^0\right)$ we say that $\psi \in U\left(f_j(\psi)\right)$ is *individually intelligent rational* if $f_j(\psi) \geq u_j^0$. Also, that $\psi \in U\left(f_j(\psi)\right)$ is *weakly efficient* if there is no $\psi' \in U\left(f_j(\psi)_j\right)$ such that $\psi' >> \psi$ and that ψ is *efficient* if there is no $\psi' \in U\left(f_j(\psi)\right)$, $\psi' \neq \psi$ such that $\psi' \geq \psi$.

A *Nash bargaining solution* is the solution $S^{NBS}: G \to \Im^K \neq \varnothing$ that for each utility-based bargaining problem $\left(U\left(f_j(\psi)\right), u_j^0\right)$ selects the set $\left\{\psi_1^*, \psi_2^*\right\} \subseteq U\left(f_j(\psi)\right)$ that contains the only point in $G\left(U\left(f_j(\psi)\right), u_j^0\right)$, which satisfies $\left(\psi_1^* - u_1^0\right), ..., \left(\psi_j^* - u_j^0\right), ..., \left(\psi_K^* - u_K^0\right) \geq \left(\psi_1 - u_1^0\right), ..., \left(\psi_j^* - u_j^0\right), ..., \left(\psi_K - u_K^0\right)$ for all $\left(\psi_1, ..., \psi_j, ..., \psi_K\right) \in G\left(U\left(f_j(\psi)\right), u_j^0\right)$. A bargaining problem is *symmetric* if $u_1^0 = ... = u_j^0 = ... = u_K^0$ and $\left(\psi_1, ..., \psi_j, ..., \psi_K\right) \in$

$G\left(U\left(f_j(\psi)\right),u_j^0\right)$ implies that $\left(\psi_K,...,\psi_j,...,\psi_1\right)\in G\left(U\left(f_j(\psi)\right),u_j^0\right)$. A *symmetric NBS* S^{SNBS} follows the following Axioms.

- $S^{SNBS}\left(U\left(f_j(\psi)\right),u_j^0\right)$ is Pareto optimal meaning that there exists no other allocation $S^{SNBS\prime}\left(U\left(f_j(\psi)\right),u_j^0\right)$ that leads to superior performance for some users without inferior performance for some other users, i.e., $S^{SNBS}\left(U\left(f_j(\psi)\right),u_j^0\right)>S^{SNBS\prime}\left(U\left(f_j(\psi)\right),u_j^0\right),\ \exists j$ and $S^{SNBS}\left(U\left(f_j(\psi)\right),u_j^0\right)\geq S^{SNBS\prime}\left(U\left(f_j(\psi)\right),u_j^0\right),\ \forall j$.
- $S^{SNBS}\left(U\left(f_j(\psi)\right),u_j^0\right)$ guarantees the minimum utility for every player, e.g., $S^{SNBS}\left(U\left(f_j(\psi)\right),u_j^0\right)\in U^0$, where U^0 is the set of minimum utilities given by $U^0=\left\{u^{0\prime}\in U\left(f_j(\psi)\right)\middle| u^{0\prime}\geq u^0\right\},\ \forall j$.
- $S^{SNBS}\left(U\left(f_j(\psi)\right),u_j^0\right)$ provides fairness by being independent of irrelevant alternatives, e.g., if the feasible set shrinks but the solution remains feasible, then the solution for the smaller feasible set is the same point. This can be written as $U'\left(f_j(\psi)\right)\subset U\left(f_j(\psi)\right)$, $\left(U'\left(f_j(\psi)\right),u^0\right)\in G$ and $S^{SNBS}\left(U\left(f_j(\psi)\right),u_j^0\right)\in G$ then $S^{SNBS}\left(U\left(f_j(\psi)\right),u_j^0\right)=S^{SNBS}\left(U'\left(f_j(\psi)\right),u^0\right),\ \forall j$.
- $S^{SNBS}\left(U\left(f_j(\psi)\right),u_j^0\right)$ provides symmetry, meaning that all users have the same priorities, e.g., assuming that $U\left(f_j(\psi)\right)$ is symmetric with respect to a subset of indices of users who are able to achieve a performance strictly superior to their initial performance, e.g., $J\subseteq\{1,...,j,...,K\}$ and $u_j^0\in U\left(f_j(\psi)\right),\ u_{j'}^0\in U\left(f_j(\psi)\right),\ j,j'\in J$ then if $u_j^0=u_{j'}^0$ it stands that $S^{SNBS}\left(U\left(f_j(\psi)\right),u^0\right)_j=S^{SNBS}\left(U\left(f_j(\psi)\right),u^0\right)_{j'},\ j\neq j'$.

An *asymmetric bargaining problem* is the pair $\left(U\left(w_j f_j(\psi)\right),u_j^0\right)$, where players have different weights $w_1\neq...\neq w_j\neq...\neq w_K$ and various minimum *payoffs*

$u_1^0 \neq ... \neq u_j^0 \neq ... \neq u_K^0$. An *asymmetric NBS* $S^{ANBS} : G \to \Im^K \neq \varnothing$, with $G' = \left[U\left(w_j f_j(\psi)\right), u^0 \middle| U\left(w_j f_j(\psi)\right) \subset \Im^K \right]$ follows the abovementioned Axiom's properties except the latter's one, e.g., it does not provide symmetry. The asymmetrical bargains are due to various players' utilities, which must reflect the players' different preferences in terms of their weights meaning that $S^{ANBS}\left(U\left(w_j f_j(\psi)\right), u^0\right)_j \neq S^{ANBS}\left(U\left(w_j f_j(\psi)\right), u^0\right)_{j'}$, $j \neq j'$.

In utility theory the *principle of expected utility maximization* [33], [41] states that an intelligent rational player, when faced with a choice among a set of competing feasible strategy alternatives, acts to select a strategy, which maximizes his expected utility function. Based on this principle, we can express the *S-NBS property* as unconstrained utility maximization problem as follows.

Lemma 2.1 - If a utility function f_j is convex upper-bounded defined on Ψ and Ψ is convex and subset of $\Im^K$, then there exists a symmetric Nash bargaining point ψ^{sym} that verifies $f_j\left(\psi^{sym}\right) \geq u_j^0$, $j \in J$ and comprises the unique solution of the maximization problem

$$\max \prod_{j \in J} \left(f_j\left(\psi^{sym}\right) - u_j^0 \right), \ \psi^{sym} \in \Psi_0. \tag{2.1}$$

Proof - The proof of *Lemma 2.1* is similar to the proof of the S-NBS property presented in [40] and has been omitted from this Thesis due to space limitations. ■

Similarly, the *A-NBS property* can be denoted as unconstrained utility maximization problem as below.

Lemma 2.2 - For each weight $w_j \in (0,1]$, an asymmetric Nash bargaining point $\psi^{asym} \in \Psi$ is a convex function $f_j : \Psi \to \Im^K$, $j \in J$, defined as $f_j\left(\psi^{asym}\right) \geq u_j^0$, $\forall \psi^{asym} \in \Psi$ that gives the unique solution to the maximization problem

$$\max \prod_{j \in J} \left(f_j\left(\psi^{asym}\right) - u_j^0 \right)^{w_j}, \ \psi^{asym} \in \Psi_0 . \tag{2.2}$$

Proof - The proof of *Lemma 2.2* is similar to the proof of the A-NBS property presented in [40] and has been omitted from this Thesis due to space limitations. ■

2.6 Convex Optimization Problems

Convex optimization can be described as a fusion of three disciplines: *optimization* [59], [119], [120], [121], [122], *convex analysis* [121], [123], [124], [125], [126], and *numerical computation* [127], [128], [129], [130]. In recent years, convex optimization has become a computational tool of central importance in engineering, thanks to its ability to solve very large, practical problems reliably and efficiently. A vast number of design problems in resource allocation can be posed as constrained combinatorial optimization problems, which, accounting our notations in (2.1), have the standard form

$$\max U\left(\psi^{sym}\right) \tag{2.3}$$

subject to:

$$U_i\left(\psi^{sym}\right) \leq 0, \quad i = 1,...,N_F, \tag{2.4}$$

$$U_j'\left(\psi^{sym}\right) = 0, \quad j = 1,...,K. \tag{2.5}$$

In the maximization problem (2.3) - (2.5) the S-NBS point ψ^{sym} is an *optimization variable*, U is an *objective or cost function*, $U_i\left(\psi^{sym}\right) \leq 0$ are *inequality constraints* and $U_j'\left(\psi^{sym}\right) = 0$ are *equality constraints*. $U_i\left(\psi^{sym}\right)$ are usually related with subcarrier or channel allocation constraints, where i is the subcarrier or channel index and N_F the maximum number of subcarriers or channels, while $U_j'\left(\psi^{sym}\right)$ frequently express power or data rate allocation rules. However, such problems can be very hard to solve in general,

especially when the number of decision variables in ψ^{sym} is large. There are several reasons for this difficulty; first, the problem "terrain" may be riddled with local optima. Second, it might be very hard to find a feasible point, i.e., a ψ^{sym}, which satisfies all the equalities and inequalities, in fact the feasible set, which needn't even be fully connected, could be empty. Third, stopping criteria used in general optimization algorithms are often arbitrary. Forth, optimization algorithms might have very poor convergence rates. Fifth, numerical problems could cause the minimization algorithm to stop all together or wander.

Nevertheless, it has been known [59], [121], [125], [126] that if U_i are all *convex* and U_j' are *affine* then the first three problems disappear, e.g., any local optimum is a global optimum, feasibility of convex optimization problems can be determined unambiguously and very precise stopping criteria are available using *duality*. However, convergence rate and numerical sensitivity issues still remained a potential problem. Geometrically, the above problem corresponds to the minimization of U, over a set described by as the intersection of 0-sublevel sets of the U_i s with surfaces described by the 0-solution sets of the U_j' s. A point ψ^{sym} is *feasible* if it satisfies the constraints; the feasible set Ψ_0 is the set of all feasible points; and the problem is feasible if there are feasible points. The problem is said to be *unconstrained* if $N_F = K = 0$. The *optimal value* is denoted by $U^* = \inf_{\psi^{sym} \in \Psi_0} U\left(\psi^{sym}\right)$, and we adopt the convention that $U^* = +\infty$ if the problem is infeasible. A point $\psi^{sym} \in \Psi_0$ is an *optimal point* if $U\left(\psi^{sym}\right) = U^*$ and the *optimal set* is $\Psi^* = \left\{\psi^{sym} \in \Psi_0 \middle| U\left(\psi^{sym}\right) = U^*\right\}$. Moreover, in the standard problem above, the *explicit* constraints are given by $U_i\left(\psi^{sym}\right) \le 0$, $U_j'\left(\psi^{sym}\right) = 0$. However, there are also the *implicit* constraints $\psi^{sym} \in \mathbf{dom} U_i$, $\psi^{sym} \in \mathbf{dom} U_j'$, i.e., ψ^{sym} must lie in the set $\mathbf{dom} U_1 \cap ... \cap \mathbf{dom} U_{N_F} \cap ... \cap \mathbf{dom} U_1' \cap ... \cap \mathbf{dom} U_K'$, which is called the *domain of the problem*. A *feasibility problem* is a special case of the standard problem, where we are interested merely in finding any feasible point. Thus, problem is really to either find $\psi^{sym} \in \Psi_0$ or determine that Ψ_0 is non-empty, e.g.,

$\Psi_0 = \varnothing$. Equivalently, the feasibility problem requires that we either solve the inequality / equality system

$$\begin{cases} U_i\left(\psi^{sym}\right) \le 0,\ i = 1,...,N_F \\ U_j{}'\left(\psi^{sym}\right) = 0,\ j = 1,...,K \end{cases} \tag{2.6}$$

or determine that it is inconsistent. An optimization problem in standard form is a *convex optimization problem* if U_0, $U_1,\ldots,U_{N_F}$ are all convex, and $U_j{}'$ are all affine. This is often written as

$$\begin{aligned} & \max U\left(\psi^{sym}\right) \\ \textit{subject to:} \quad & U_i\left(\psi^{sym}\right) \le 0, \quad i = 1,...,N_F, \\ & \alpha \cdot \psi^{sym} = \beta, \quad j = 1,...,K, \end{aligned}$$

where $\alpha \in \mathbb{R}^{N_F \times K}$ and $\beta \in \mathbb{R}^K$. Convex optimization problems have three crucial properties that make them fundamentally more tractable than generic non-convex optimization problems; they have no local optimum, e.g., any local optimum is necessarily a global optimum, using duality theory they have track infeasibility detection and the derived algorithms are easy to initialize efficient numerical solution methods that can handle very large problems. To understand global optimality in convex problems, recall that $\psi^{sym} \in \Psi_0$ is locally optimal if for $\psi^{sym\prime} \in \Psi_0$ it satisfies $\left\|\psi^{sym\prime} - \psi^{sym}\right\| \le \delta \Rightarrow U\left(\psi^{sym\prime}\right) \ge U\left(\psi^{sym}\right)$, where δ is a positive number, e.g., $\delta > 0$. A point $\psi^{sym} \in \Psi_0$ is global optima means that $\psi^{sym\prime} \in \Psi_0$, $U\left(\psi^{sym\prime}\right) \ge U\left(\psi^{sym}\right)$. For convex optimization problems, any local solution is also global. There is also a *first order condition* that characterizes optimality in convex optimization problems. Suppose U is differentiable, then $\psi^{sym} \in \Psi_0$ is optimal if for $\psi^{sym\prime} \in \Psi_0$ it stands $\nabla U\left(\psi^{sym}\right)^{\mathcal{T}}\left(\psi^{sym\prime} - \psi^{sym}\right) \ge 0$, with $(\cdot)^{\mathcal{T}}$ denoting matrix transpose. So $-\nabla U\left(\psi^{sym}\right)$ defines supporting hyperlane for Ψ_0 at ψ^{sym}, meaning that if we move from ψ^{sym} towards any other feasible $\psi^{sym\prime}$ then U does not decrease. A convex optimization problem in standard form with *generalized inequalities* is written as

$$\max U\left(\psi^{sym}\right)$$

subject to: $U_i\left(\psi^{sym}\right) \underline{\prec} 0,\ i=1,...,L,$

$$\alpha \cdot \psi^{sym} = \beta,$$

where $U:\mathbb{R}$ are all convex, $\underline{\prec}$ are generalized inequalities on $\mathbb{R}^{N_{Fi}}$ and $U_i:\mathbb{R}\to\mathbb{R}^{N_{Fi}}$ are convex.

Moreover, the cost functions in convex optimization problems may also be *quasiconvex*. A function $U:\mathbb{R}$ is quasiconvex if every sub-level set $S_{\delta'}=\left\{\psi^{sym}\in \mathbf{dom}U \middle| U\left(\psi^{sym}\right)\le\delta'\right\}$ is convex. We say that f is *quasiconcave* if $-U$ is quasiconvex. A function which is both quasiconvex and quasiconcave is called *quasilinear*. It is remarked that a function of the form $U\left(\psi^{sym}\right)=\ln\psi^{sym}$ is quasilinear on $\mathbb{R}_+$. Such optimization functions shall detain us in the next Chapters due to NBS's logarithmic origin.

2.7 Queue Structures for Cross-Layer Schemes

A cross-layer problem is usually constrained on channel selection, power distribution, transmission interference elimination and QoS provision rules. Although the first three types of rules can be expressed into convex cross-layer constraints with variable transformation techniques, QoS regulations require more special treatment. The reason is that such regulations include complicated higher-layer Queue State Information (QSI). QSI include characteristics as source statistics, queuing delays and application level requirements of the heterogeneous users, which should be expressed as PHY layer information theoretical models. Therefore, emphasis should be given to properly design the diverse QoS requirements in terms of *queuing rate* or *delay performance* into the cross-layer problem. In queuing theory, which is mainly seen as a branch of applied probability theory, queuing models are *stochastic models* used to approximate real queuing situations or systems. The main purpose of developing such models is to analyse mathematically the queuing behaviour that represents the probability a queuing system to be found in a particular configuration or state.

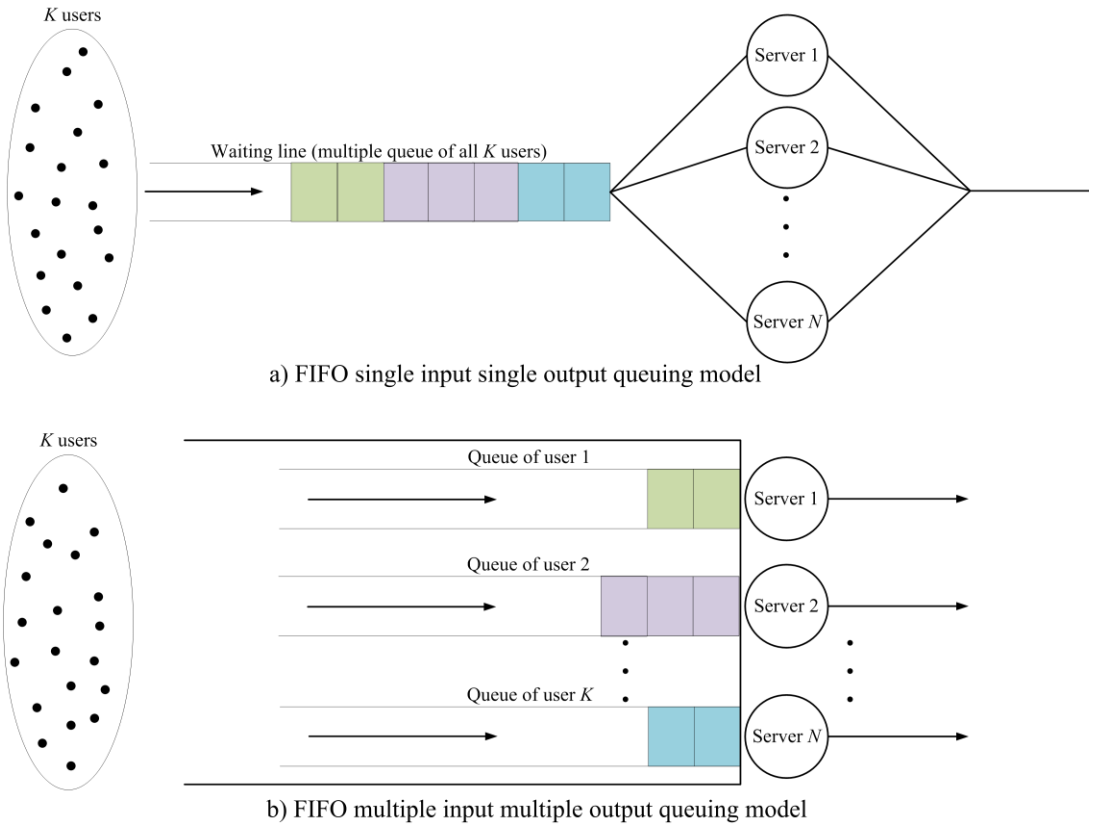

Figure 2.4 - Typical standalone queuing models with N servers and FIFO service mode.

Queuing models allow a number of useful *steady state performance* measures to be determined, including the average number in the queue, the average time spent in the queue (*average delay*), the statistical distribution of those numbers or times, the probability the queue is full, or empty, and the probability of finding the system in a particular state. The importance of such performance measures is significant as issues caused by queuing situations are related to customer dissatisfaction with service. Analysing a queuing model allows the cause of queuing issues to be identified and the impact of proposed changes to be assessed. There are many types of queuing models that can be followed, characterised using *Kendall's notation* [30] such as Memoryless/Markovian/Single-Server (*M/M/1*), Memoryless/Degenerate-distributed/Single-Server (*M/D/1***)**, Markov-Modulated Poisson-Process/General/Single-Server (*MMPP/G/1*) etc. There is a variety of queuing strategies that

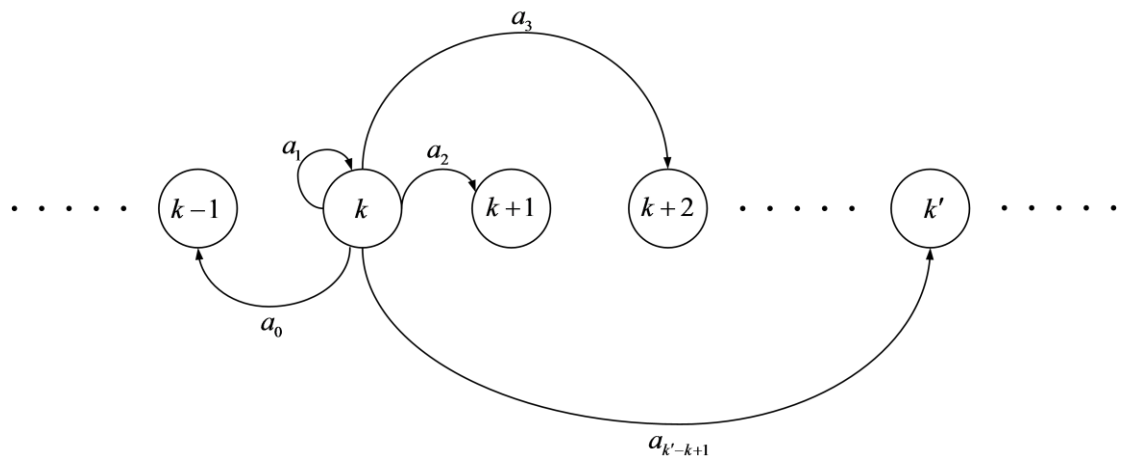

Figure 2.5 - Transition probability diagram for the imbedded Markov chain.

describe the way where service is provided over time such as First-In-First-Out (*FIFO*), Last-In-First-Out (*LIFO*), Service-In-Random-Order (*SIRO*), Shortest-Processing-Time first (*SPT*), Priority (*PR*) etc. In addition, a queuing system with, e.g., N service centres (servers) can be either single input single output or multiple input multiple outputs. An example of two typical standalone queuing models with FIFO service mode is depicted in Figure 2.4.

It is certain that the M/G/1 [30] model with infinite capacity and population, represented by $M/G/1/\infty/\infty$, has been used as a guiding model for performance analysis of widely varying systems. The reason that $M/G/1/\infty/\infty$ is widely adopted is that it can sufficiently describe the system queuing dynamics although the arrival rates and the mean and variance of the service rates are generally complex and difficult to be specified. In $M/G/1/\infty/\infty$ models the arrival rate of each user at the queues, e.g., λ_j is described by a *Poisson process* [30], meaning that the statistical distribution of the inter-arrival times follows the exponential distribution. In addition, the distribution of the service time can follow any general statistical distribution, which is non-exponential. The construction and analysis of every queuing model can be signified by a state transition diagram that represents through a *Markov chain* the possible system states and identifies the rates to enter and leave each state. For example, if a_k denotes the probability that during a service time exactly $k \in K$ users

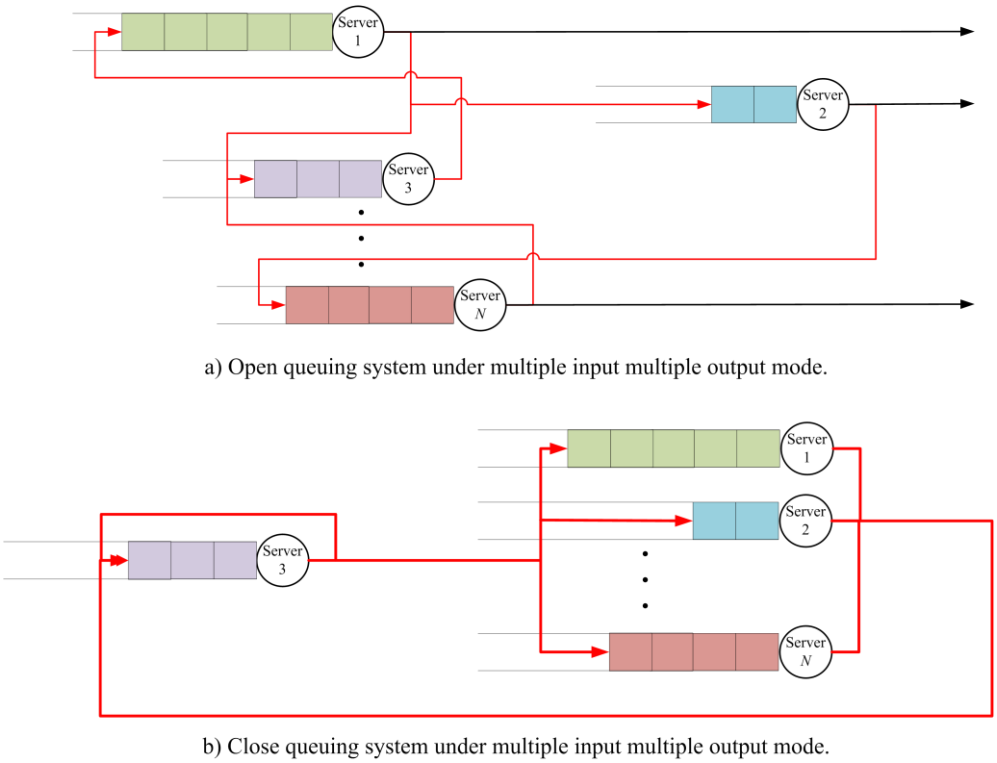

a) Open queuing system under multiple input multiple output mode.

b) Close queuing system under multiple input multiple output mode.

Figure 2.6 - Structures of open and closed queuing system with N servers.

arrive, the transition probability diagram for the $M/G/1/\infty/\infty$ Markov chain can be drawn as depicted in Figure 2.5.

In reality networks are better represented as a system of queues consisted by several single standalone queuing models. An obvious example is the Internet, where each outgoing link of each router is modelled as a single queuing system, and where an end-to-end path traverses a multitude of intermediate routers. One basic classification of queuing systems is the distinction between *open* and *closed* queuing systems. In an arbitrary open queuing system customers may enter the system at any queue and also may leave the system from any queue. The system may contain loopbacks and splitting points, where a customer has several possibilities for selecting the next queue. In closed queuing systems there is a fixed set of tasks and each task alternates between states where it performs some computations using the processor. In closed queuing networks the number of customers is fixed and no user enters or

leaves the system. An example on the architecture of open and closed queuing systems is given in Figure 2.6.

Within this Thesis we develop a queuing model that can be used either in open or closed queuing systems. Our model is based on the $M/G/1/\infty/\infty$ queue and expresses the QoS requirements of system users into equivalent PHY data rate constraints. The proposed modelling account source statistics, queuing delays and application level requirements of the system users and operate according to the FIFO service discipline.

Chapter 3

Power-Efficient Cross-Layer Design

3.1 Introduction

In this Chapter, we propose a Power-Efficient Adaptive Error-Tolerant cross-layer Scheduling (PE-AETS) scheme for OFDMA systems. PE-AETS incorporates an innovative approach of minimizing the average transmitting power of the OFDMA system by considering channel outage and heterogeneous users QoS requirements. To efficiently adjust power and data rates across subcarriers, our scheme is based on a robust PBL process, which asymptotically increases throughput performance retaining high resilience to the imperfect channel conditions. In addition, we introduce a different from the mean feedback model, i.e., [15], [23], [24], [56], channel estimation method, which further contributes to PE-AETS's channel error resilience. In our design, we represent each user's heterogeneous QoS requirements through developing an advanced queuing model that is also different from the one adopted by related studies, i.e., [15], [24], [56]. Finally, we provide extensive simulation results for small and large-scale OFDMA systems, to confirm that PE-AETS significantly outperforms rival cross-layer scheduling approaches. The key contributions and the proposed modelling methodology of this research part have been thoroughly discussed in Section 1.2.

3.2 Literature Review

Initially, resource allocation schemes were designed using only PHY layer PBL processes, e.g., [13], [14], [15], [16] and [131]. In such schemes the data bits and the transmitting powers are adjusted across subcarriers to utilize efficiently the network resources. As shown in [18], although these approaches are simple to implement, without knowing the upper-level packet

arrival characteristics or the queuing conditions the single-layer resource allocation cannot guarantee each user's specific QoS requirements. Hence, recent studies propose cross-layer resource allocation designs to account both the PHY layer channel conditions and the upper layers queuing dynamics, e.g., [17], [20], [21], [22], [23], [24], [27], [56], [60]. Within this direction, most efforts assume that transmissions occur under perfect channel conditions, e.g., [20], [21], [22], [23], [24], [27]. However, in the existence of channel imperfections it is straightforward that this assumption results in power-inefficient cross-layer resource scheduling. Additionally, most of the above studies consider that the QSI is homogeneous, e.g., the same for all users, where in reality it is instead heterogeneous. In actual fact, recent literature is very poor by studies that take under consideration both imperfect channel conditions and heterogeneous QSI in cross-layer scheduling processes, with examples to be given only by the works in [17], [24] and [56]. Nevertheless, the PBL processes developed in [17], [24] and [56] are based on the goodput-rate, which as we will see later, is quite prone to channel errors resulting into infeasible scheduling operation under average to high channel uncertainty. Besides all, the aforementioned works intend to maximize the system's throughput, which potentially increases the system's power consumption, especially when channel uncertainty is high.

In general, the existing literature is based on one or more of the below three unrealistic assumptions. i) The channel outage effects are ignored, ii) the channel is assumed perfect or with low uncertainties and iii) the users' QoS requirements are treated as homogeneous. To deliver effective resource scheduling for pragmatic wireless systems we address the above three issues into a robust cross-layer scheduling scheme. Our first observation is that the BS cannot always perfectly acquire the CSI due to noisy channel conditions, e.g., delayed feedbacks and/or channel outage [132]. Hence, the channel has error, which in fact is usually large, meaning that designing our scheduling scheme targeting small channel error tolerance as, i.e., in [17], [24] and [56], would not result either innovation or contribution. Our second observation is that as CSI is imperfect the BS cannot always identify the channel's maximum capacity, which would be frequently exceeded by the scheduled data rate. Therefore, packets would be systematically corrupted and transmission would fail, resulting in poor network performance. Consequently, we additionally consider the fundamental effect of channel outage into our cross-layer design. Our third observation is that

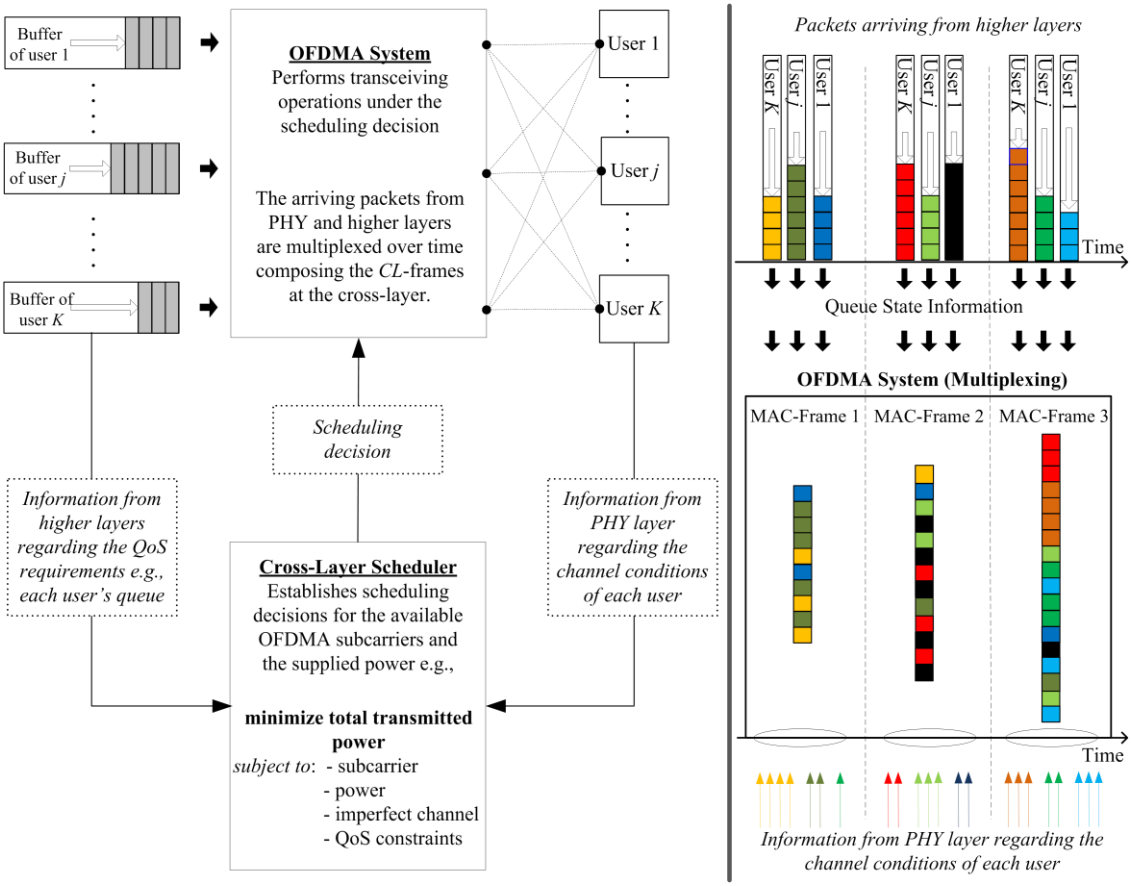

Figure 3.1 - Multi-user DL OFDMA cross-layer scheduler under imperfect channel modelling with heterogeneous users' applications (left). Packet multiplexing process over time for 3 *MAC*-Frames (right).

modern applications have obviously various QoS requirements thus, we provide scheduling policies aiming to satisfy the heterogeneous users' demands.

For the ease of reference, in this Chapter we name the power-inefficient small Error-Considerate cross-layer Scheduler adopted in [17], [24], [56] as ECS, the power-unaware Error-Inconsiderate Opportunistic Scheduler adopted in [14], [20], [21], [22], [23] as EIOS and the power-unaware Error-Inconsiderate Fixed power and subcarrier Assignment Scheduler utilised in [27], [60] as EIFAS.

3.3 System Model

This Section outlines the downlink OFDMA system model, which is the basis of PE-AETS resource allocation problem formulated in Section 3.5. The proposed multi-user downlink OFDMA cross-layer scheduler involves K users and N_F subcarriers as illustrated in Figure 3.1.

Before the scheduling operation is performed, the cross layer resource scheduler first collects the CSI and QSI of all users. In the beginning of each scheduling interval, the resource scheduler obtains the CSI through performing estimation of the imperfect channel in Time Division Duplex (TDD) operation[1] based on UL dedicated sub-channels transmitted by all mobile users. In addition, PE-AETS gathers information for each user's QoS requirements by estimating the QSI according to an incremental update algorithm [133], [134] through observing the current backlogs in each user's independent buffer[2]. The QSI is updated according to how frequently the state of the user's mobility changes. Hence, instead of updating the QSI before each time slot as in [14], [17], [20], [21], [22], [23] [24], [27], [56], [60] we use the incremental update algorithm to reduce PE-AETS's pre-processing process.

In continue, the resource scheduler takes its scheduling decision once every time slot based on the estimated CSI and QSI, and passes the resource allocation result to the OFDMA transmitter. The subcarrier allocation and transmitting power allocation decision made by the BS transmitter is assumed to be announced to individual mobile user through a separate control channel. We further assume perfect CSI available at the receiver (CSIR).

[1] The system can also operate under Frequency Division Duplex (FDD). In this case perfect feedback of DL CSIT from mobile users is required.

[2] To avoid buffer overflow, we assume that users' buffers are sufficiently large enough for storing packets arrived from higher layer. In addition, as we discuss later, we also consider that packets arriving form higher and PHY layers are multiplexed over time comprising *MAC*-frames as shown in Figure 3.1.

3.3.1 Downlink Channel Modelling

We consider an OFDMA system with quasi-static fading channel within a scheduling slot of duration t_s. Due to the orthogonality principle of the OFDMA, the N_F system subcarriers are decoupled. We focus on the downlink OFDMA time varying transmission over a frequency-selective multipath channel of bandwidth BW, consisted by $\Theta = \lfloor BW / \Delta f_c \rfloor$ paths, where $\lfloor \cdot \rfloor$ denotes the floor of a quantity and Δf_c the channel's coherent bandwidth. For simplicity, we assume uniform power delay profile[3], where each path has normalized power of $\frac{1}{\Theta}$. After removing the CP and performing N_F-point DFT, the received OFDM symbol vector for the j-th user at the n-th OFDM block is given by

$$\mathbf{y}_j(n) = \mathbf{H}(n) \cdot \mathbf{x}_j(n) + \mathbf{z}_j(n). \tag{3.1}$$

In (3.1), $\mathbf{y}_j(n) = \left[y_{ij}(n) \right]^{\mathcal{T}}$ is the $N_F \times 1$ DFT complex-valued vector of the received OFDM symbols $y_{ij}(n)$ of user j on the i-th subcarrier at the n-th OFDM block, with the notation $[\cdot]^{\mathcal{T}}$ to denote matrix transpose. Similarly, $\mathbf{x}_j(n) = \left[x_{ij}(n) \right]^{\mathcal{T}}$ is the $N_F \times 1$ Inversed-DFT (IDFT) complex-valued vector of the transmitted OFDM symbols $x_{ij}(n)$ of user j on the i-th subcarrier at the n-th OFDM block. In addition, $\mathbf{H}(n) = diag\left(\mathbf{h}_j(n)\right)$ represents the $N_F \times N_F$ matrix with elements the channel gains $\mathbf{h}_j(n)$, where $diag(\cdot)$ denotes diagonal matrix (more details in Appendix A.1). Finally, the $N_F \times 1$ vector $\mathbf{z}_j(n)$ in (3.1) represents the zero mean CSCG noise at the n-th OFDM block and is given by $\mathbf{z}_j(n) = \left[z_{ij}(n) \right]^{\mathcal{T}}$. The entries $z_{ij}(n)$ signify the channel noise of user j on subcarrier i and are CSCG Independent and Individually Distributed (i.i.d) with zero mean and σ_z^2 variance, e.g., $z_{ij}(n) \sim \mathcal{CN}\left(0, \sigma_z^2\right)$. The noise variance σ_z^2 is given by [59]

[3] The analytical results in this paper can also be applied to non-uniform power delay profiles.

$$\sigma_z^2 = \frac{N_0 \cdot BW}{N_F}, \tag{3.2}$$

where N_0 is the noise density.

The instantaneous transmitting power allocated from the scheduler at the BS to user j through subcarrier i is given by

$$p_{ij} = E\left[\left|x_{ij}\right|^2\right], \tag{3.3}$$

where $\left|\cdot\right|^2$ denotes the absolute value squared of a complex number and it is equal to the number times its complex conjugate transpose symbolized as $\left[\cdot\right]^\dagger$, i.e., $\left|x_{ij}\right|^2 = x_{ij}\left[x_{ij}\right]^\dagger$ [135]. We represent the transmitting power expression in (3.3) in matrix form with the $N_F \times K$ matrix $\mathbf{P} = \left[p_{ij}\right]$, which signifies PE-AETS's transmitting power allocation policy at the PHY layer. In addition, we denote the actual instantaneous data rate allocated from the scheduler at the BS to user j through subcarrier i by r_{ij} and represent it with the $N_F \times K$ matrix $\mathbf{R} = \left[r_{ij}\right]$. More precisely, r_{ij} indicates the number of bits allocated on the i-th subcarrier of user j per time slot and $\mathbf{R}$ is the data rate allocation policy of PE-AETS at the PHY layer[4].

Moreover, we define the $N_F \times K$ matrix $\mathbf{S} = \left[s_{ij}\right]$ that signifies the subcarrier allocation policy of our scheme at the PHY layer. The elements s_{ij} of $\mathbf{S}$ indicate the subcarrier allocation index meaning that $s_{ij} = 1$ when subcarrier i is allocated to user j otherwise $s_{ij} = 0$, e.g., $s_{ij} \in \{0,1\}$. In our system, we do not allow more than one user to occupy the same subcarrier during a timeslot. This subcarrier allocation constraint can be expressed as

[4] We consider information theoretical capacity [146] to simplify the presentation of the introduced PBL process that follows in the next Section. However, although we decouple PE-AETS's modelling from specific implementation of coding and modulation schemes, in our following two scheduling designs we involve an M-QAM modulator to consider bit coding effects.

$$\sum_{j=1}^{K} s_{ij} \leq 1. \quad [5] \tag{3.4}$$

Finally, the transmission is guaranteed when the average transmitting power over all users and subcarriers is smaller or equal than the average total available power at the BS denoted by P_{TOTAL}. This necessary rule can be expressed by the transmitting power allocation condition

$$E\left[\frac{1}{N_F}\sum_{j=1}^{K}\sum_{i=1}^{N_F} s_{ij}\, p_{ij}\right] \leq P_{TOTAL}. \tag{3.5}$$

We remark that the left side of (3.5) is divided by the number of subcarriers N_F as we refer to average quantities. This means that P_{TOTAL} is the total available power at the BS taking into consideration the effects such as Peak-to-Average Power Ratio (PAPR), maximizing that way the utilization of all subcarriers, i.e., we consider both the average transmitting power allowed by the BS and the PAPR of OFDM signals.

3.3.2 Imperfect CSIT and Estimation Modelling

As the imperfect CSIT is estimated at the BS in TDD operation, in the beginning of each OFDM frame the downlink CSIT can be obtained from channel reciprocity through CSIT estimation of UL dedicated pilot symbols ς, sent by all K users. However, the estimated downlink CSIT will be outdated due to unknown subcarrier frequency offset caused by the Doppler effect and inherent instabilities of the transmitter's and receiver's subcarrier frequency oscillators. In our imperfect channel modelling, we signify the $N_F \times 1$ vector

[5] Many studies in the literature, i.e., [17], [24], [56], consider the condition in (3.4) as equality e.g., $\sum_{j=1}^{K} s_{ij} = 1$. However, this expression leads to infeasible allocation in the instance where users have no requirement. In that case, the scheduler would be programmed to select users for transmission even if there would not be any.

$\hat{\mathbf{h}}_j = \left[\hat{h}_{ij}\right]^{\mathcal{T}}$, with entries $\hat{h}_{ij}$ to denote the independent identically distributed (i.i.d) estimated channel gain of user j on subcarrier i, as

$$\hat{\mathbf{h}}_j = \mathbf{h}_j + \Delta\hat{\mathbf{h}}_j . \tag{3.6}$$

In (3.6), $\mathbf{h}_j = \left[h_{ij}\right]^{\mathcal{T}}$ is the $N_F \times 1$ channel feedback vector with entries h_{ij} to represent the i.i.d actual channel gain feedback of user j on subcarrier i and $\Delta\hat{\mathbf{h}}_j = \left[\Delta h_{ij}\right]^{\mathcal{T}}$ is the $N_F \times 1$ channel error vector with entries Δh_{ij} the zero mean CSCG channel error terms of user j on subcarrier i with known PDF.

For channel estimation purposes, we assume that the CSIT is updated every frame comprising Θ_{FR} OFDM symbols. To calculate the channel coefficients, we consider the MMSE estimator $\mathbf{h}\left(\left(\rho+\delta\right)\Theta_{FR}\right)$, $\delta > 0$ with $\rho > \Theta$ to represent the number of observations required for the estimation process [59]. Our target is to define the covariance matrix $\mathbf{M}_{\Delta h}$ of the channel error vectors $\Delta\hat{\mathbf{h}}_j$ and the MMSE variance σ_h^2 in order to describe the correlation of the estimated CSIT errors between the subcarriers of each user.

Theorem 3.1 - The error covariance matrix $\mathbf{M}_{\Delta h}$ of the channel error vectors $\Delta\hat{\mathbf{h}}_j$ is given by

$$\mathbf{M}_{\Delta h} = E\left[\Delta\hat{\mathbf{h}}_j \Delta\hat{\mathbf{h}}_j^{\mathcal{H}}\right] = \frac{N_F \cdot \sigma_h^2}{\Theta}\mathbf{W}_{\Theta}\mathbf{W}_{\Theta}^{\mathcal{H}}, \tag{3.7}$$

with $\mathbf{W}_{\Theta}$ to denote the truncated unit-norm FFT matrix and the MMSE variance σ_h^2 to be depended on adaptive estimation observations, e.g.,

$$\sigma_h^2 = 1 - \mathbf{x}_{\mathbf{M}_\varsigma}^{\mathcal{H}}\left[\frac{\Theta \cdot \sigma_z^2}{N_F \cdot P_\varsigma}\mathbf{I}_\varsigma + \mathbf{M}_\varsigma\right]^{-1}\mathbf{x}_{\mathbf{M}_\varsigma}, \tag{3.8}$$

where the terms P_ς, $\mathbf{M}_\varsigma$ and $\mathbf{x}_{\mathbf{M}_\varsigma}$ are presented in Appendix A.2.

Proof - The proof of *Theorem 3.1* is presented in Appendix A.2. ■

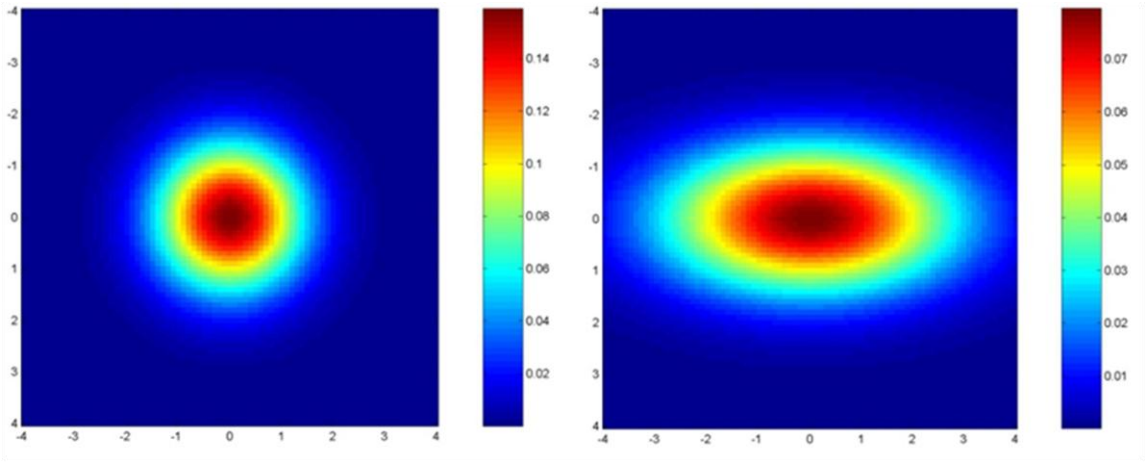

Figure 3.2 - Sphericity - Error covariance is scalar multiple of identity matrix, i.e., $\mathbf{M}_{\Delta h} = \sigma_h^2 \mathbf{I}_{\varsigma}$ (left). Non-sphericity with non-identity – Error covariance is not scalar multiple of identity matrix, i.e., $\mathbf{M}_{\Delta h} = \sigma_h^2 \left(\mathbf{x} + \mathbf{I}_{\varsigma} \right)$ (right).

A first conclusion of the estimation process presented in Appendix A.2 is that the channel error vector $\Delta\hat{\mathbf{h}}_j = \left[\Delta h_{ij} \right]^{\mathcal{T}}$ and the estimated channel gain vector $\hat{\mathbf{h}}_j = \left[\hat{h}_{ij} \right]^{\mathcal{T}}$ are uncorrelated with covariance matrix equal to zero, e.g., $E\left[\Delta\hat{\mathbf{h}}_j \hat{\mathbf{h}}_j \right] = 0$. Another notable conclusion from *Theorem 3.1* and Appendix A.2 is that, due to the implication of the vectors $\mathbf{x}_{\mathbf{M}_{\varsigma}}$ and $\mathbf{x}_{\mathbf{M}_{\varsigma}}^{\mathcal{H}}$, and the matrix $\mathbf{M}_{\varsigma}$ our MMSE variance σ_h^2 in (3.8) is not scalar multiple of the identity matrix of the pilot symbols ς, e.g., $\mathbf{I}_{\varsigma}$. This means that the main diagonal elements of our error covariance matrix $\mathbf{M}_{\Delta h}$ in (3.7) are not equal but differ in respect to each multipath subcarrier's conditions, which are perceived by the estimator through $\left(\rho + \delta \right) \Theta_{FR}$ measurements based on the ς pilot symbols (see example in Appendix A.2). In other words, we perform measurements on independent but not identically distributed errors Δh_{ij}, which signifies that our estimator performs adaptive estimation observations according to each subcarrier's conditions and hence, as shown in Figure 3.2, it does not satisfy the

assumptions of sphericity[6] [59]. In contrary, the mean feedback model[7] adopted by the related work in [24], [56], [18], [58], [57], assumes that the channel errors Δh_{ij} are i.i.d meaning that the conditions of each subcarrier are not taken into consideration individually but identically. This imposes sphericity assumptions, which in practice are frequently violated due to OFDMA channel effects such as Doppler spread, multipath delays, time delay shifting etc. In addition, since in the mean feedback model the channel errors Δh_{ij} are assumed as i.i.d, upon applying sphericity estimation patterns the MMSE variance is imprecisely acquired and obviously any scheduler estimating through the mean feedback model could take its resource allocation decisions based on a wrong prediction (more clarifications in Appendix A.2). In contrary, our non-sphericity estimation pattern is more sensitive[8] attaining the MMSE variance in precision bearing important improvements to system's resilience to channel errors and also performing asymptotically conveying increased throughput or power performance to multi-user OFDMA systems [16]. Finally, the precision of our estimator does not impose complexity increase as both our model and the mean feedback model have the same complexity on the number of subcarriers and multi-paths, e.g., $\mathcal{O}\left(\Theta N_F \times \Theta N_F\right)$, where $\mathcal{O}(\cdot)$ is the big-*O* notation[9] [135].

[6] In general, the sphericity assumption controls the validity of e.g., ΘN_F statistics for inference on receiving data. In sphericity estimation patterns the difference between two measurement sets has equal variance for all pairs of such sets.

[7] We remark that in the mean feedback model, the corresponding to (3.8) MMSE variance σ_h^2 has the form e.g., $\sigma_h^2 = 1 - \left(N_F P_\varsigma / \Theta\sigma_z^2\right)\mathbf{M}_\varsigma \mathbf{I}_\varsigma$. In this case, the error covariance matrix is depended on the correlation between the received symbols based on the time-varying actual channel gain modelling and the ς pilot symbols. In other words, the error covariance matrix is scalar multiple of the identity matrix $\mathbf{I}_\varsigma$ and the mean feedback model features spherical channel error estimations.

[8] The sensitivity of an estimation pattern depends on the precise estimations of the hyper-parameters i.e. high degrees of freedom, which is the number of independent pieces of information available to estimate another piece of information.

[9] The big-*O* notation e.g., $x_K = \mathcal{O}\left(y_K\right)$, is used when $\lim_{K\to\infty} |x_K| / |y_K| < \infty$ and $\lim_{K\to\infty} |y_K| / |x_K| < \infty$.

3.3.3 MAC and Upper Layer Modelling from Cross-Layer Perspective

Without loss of generality, we assume that packets arrive from upper layers to each user j's buffer according to a Poisson arrival process with independent arrival rate denoted by λ_j (in *packets per time slot*). We consider that the applications of each of the K users are heterogeneous in nature in terms of their packets' arrival rates and delay constraints, with the latter ones to be symbolized by $T_j^{\max}$. We characterize the heterogeneous applications of the K users by different packet arrival rates, e.g., $\{\lambda_1,...,\lambda_j,...,\lambda_K\}$, and delay requirements, e.g., $\{T_1^{\max},...,T_j^{\max},...,T_K^{\max}\}$ (in *time slots*). For example, users with heavier traffic load have higher arrival rate λ_j, while uses that are more delay-sensitive have stringent maximum delay tolerance $T_j^{\max}$. We can then describe the QoS parameters of each user j by the characteristic tuple $[F,T_j^{\max},\lambda_j]$, where F denotes the size of each packet in *bits*. We remark that although the size of each packet may vary, for brevity of our queuing analysis we assume that packets have fixed size F.

As all models are characterized by system dynamics, which are mathematical expressions that describe the behaviour of a system over time, so as our scheduler has its own system dynamics denoted by $\hat{\mathbf{H}}$ and $\mathbf{Q}$. PE-AETS's system dynamics at the MAC layer express the perception of our scheme regarding the current system state $(\hat{\mathbf{H}},\mathbf{Q})$, which is depended on the acquired information of the imperfect channel estimation from PHY layer and the QSI from upper layers. We denote those dynamics as $\hat{\mathbf{H}}$ and $\mathbf{Q}$, where $\hat{\mathbf{H}}$ is the $N_F \times K$ matrix of the estimated channel gain given by $\hat{\mathbf{H}} = E\left[\left|\hat{h}_{ij}\right|^2\right]$ with elements the absolute squared estimated channel gains of each user j on subcarrier i, e.g., $\left|\hat{h}_{ij}\right|^2$, and $\mathbf{Q}$ is the $K \times 1$ vector of the QSI given by $\mathbf{Q} = [q_j]$ with its j-th component q_j to denote the number of packets remains in user j's buffer.

As the MAC layer is responsible for the cross-layer scheduling at every fading block, at the beginning of every OFDM frame PE-AETS estimates the channel from dedicated uplink pilot symbols and observes the current backlogs in the buffer according to the incremental update process as described in Section 3.3. Based on the obtained CSIT and QSI, the scheme at the cross-layer determines the subcarrier allocation from the policy $\mathbf{S}\left[\hat{\mathbf{H}},\mathbf{Q}\right]$, the transmitting power allocation from the policy $\mathbf{P}\left[\hat{\mathbf{H}},\mathbf{Q}\right]$ and the throughput allocation from the policy $\mathbf{R}\left[\hat{\mathbf{H}},\mathbf{Q}\right]$, at the MAC layer. The scheduling results are then broadcasted on downlink common channels to all users before subsequent downlink packets transmissions at scheduled rates.

3.4 Effective Data Rate under Imperfect CSIT and Channel Outage - Power-Efficient PBL Process

This Section presents the formulation of a new power-efficient PBL process that defines the effective data rate in OFDMA systems with imperfect channel and outage considerations. Before we present the methodology of the formulation of our PBL process, let us firstly discuss the effect of channel outage.

It is well-known that packet error is contributed by two factors; the channel noise and the channel outage. In the former case, packet error is contributed by the effect of non-ideal channel coding and finite block length of the channel codes. This factor can be reduced by using a strong channel code (e.g., turbo code) and longer OFDM frame length, so that Shannon's capacity [93] can be achieved [136]. However, in the latter case, the effect is systematic and cannot be easily eliminated. The reason is that the actual instantaneous mutual information $W\left(x_{ij};y_{ij}\left|h_{ij}\right.\right)$, signifying the maximum achievable instantaneous actual data rate

r_{ij} for error-free transmissions between the input x_{ij}, e.g., the BS, and the output y_{ij}, e.g., user j, on the i-th subcarrier, is given by[10]

$$W\left(x_{ij};y_{ij}\left|h_{ij}\right.\right)=\log_2\left(1+\frac{p_{ij}h_{ij}}{\sigma_z^2}\right), \tag{3.9}$$

which is a function of actual channel gain h_{ij} (perfect CSIT) that is unknown to the BS as CSIT is imperfect. Hence, packets will be corrupted whenever the actual instantaneous data rate r_{ij} exceeds the instantaneous actual mutual information $W\left(x_{ij};y_{ij}\left|h_{ij}\right.\right)$ and so, the probability of this event is the dominating factor of packet error.

To consider potential packet errors, we express the instantaneous actual data rate r_{ij} under the estimated channel gain $\hat{h}_{ij}$ as follows. Accounting the imperfect channel conditions, the actual instantaneous mutual information $E\left[W\left(x_{ij};y_{ij}\left|\hat{h}_{ij}\right.\right)\right]$ is random [16], [57] and it is written as[11]

$$E_{h_{ij}}\left[W\left(x_{ij};y_{ij}\left|\hat{h}_{ij}\right.\right)\right]=E_{\hat{h}_{ij}}\left[\log_2\left(1+\frac{p_{ij}\left|\hat{h}_{ij}\right|^2}{\sigma_z^2}\right)\right]. \tag{3.10}$$

Let us now define the probability $P_{out,ij}$ as the target data outage probability of user j on subcarrier i. The target data outage probability P_{out} is determined by the probability that the actual instantaneous channel parameters cannot support the actual instantaneous data rate, e.g.,

[10] The actual mutual information can be expressed in matrix form as $W\left(\mathbf{x}_j;\mathbf{y}_j\left|\mathbf{h}_j\right.\right)=\log_2\det\left(\mathbf{I}_{N_F}+\left(\mathbf{h}_j\mathbf{P}\mathbf{h}_j^{\mathcal{H}}/\sigma_z^2\right)\right)$. We remark that the maximum channel capacity is achieved when the input $\mathbf{x}_j$ is CSCG distributed with zero mean and variance the transmitting power allocation matrix $\mathbf{P}$ e.g., $\mathbf{x}_j\sim\mathcal{CN}\left(\mathbf{0},\mathbf{P}\right)$, and it is maximized when $\mathbf{P}$ is diagonal [16].

[11] The expectation operator $E\left[\cdot\right]$ refers to the average of the quantity over the ergodic realizations of the actual and the estimated channel gains e.g., $\left\{h_{ij}\right\}$ and $\left\{\hat{h}_{ij}\right\}$, respectively. To avoid confusion, from this point we shall omit its characterization i.e., "expected" or "averaged".

$$P_{out,ij} = 1 - \Pr\left(E\left[r_{ij} \right] \le E\left[W\left(x_{ij}; y_{ij} \middle| \hat{h}_{ij} \right) \right] \right). \tag{3.11}$$

For simplicity, we can assume that the target data outage probability $P_{out,ij}$ is the same for each user and subcarrier, e.g., $P_{out,ij} = P_{out}$. Hence, the channel outage condition in (3.11) can be also written as

$$\Pr\left(E\left[r_{ij} \right] \le E\left[W\left(x_{ij}; y_{ij} \middle| \hat{h}_{ij} \right) \right] \right) = 1 - P_{out}, \tag{3.12}$$

indicating that given the estimated channel gain realization $\hat{h}_{ij}$, we achieve maximum system's data rate if the probability of the actual instantaneous data rate $E\left[r_{ij} \right]$ to be smaller or equal than the actual instantaneous mutual information $E\left[W\left(x_{ij}; y_{ij} \middle| \hat{h}_{ij} \right) \right]$ is equal to the complementary target data outage probability $1 - P_{out}$. Relying on the target data outage probability P_{out} we can formulate a new power-efficient PBL process as presented in the following Section.

3.4.1 Methodology on the Formulation of the Effective Data Rate for OFDMA Systems under Imperfect Channel Conditions and Outage Considerations

To formulate our PBL process, we rely on independent subcarrier encoding and introduce a novel methodology to describe the actual instantaneous effective data rate satisfying the channel outage condition in (3.12).

Given the estimated channel gain $\hat{h}_{ij}$, the actual channel gain h_{ij} is CSCG distributed with $\hat{h}_{ij}$ mean and σ_h^2 variance, e.g., $h_{ij} \sim \mathcal{CN}\left(\hat{h}_{ij}, \sigma_h^2 \right)$. Then the absolute value of the actual channel gain squared $\left| h_{ij} \right|^2$ is a non-central chi squared variable with PDF $p\left(\left| h_{ij} \right|^2 = x \right)$ given by

$$p\left(\left|h_{ij}\right|^2 = x\right) = \frac{1}{\sigma_h^2}\exp\left(-\frac{\left|\hat{h}_{ij}\right|^2 + x}{\sigma_h^2}\right)\cdot I_0\left(2\sqrt{\frac{\left|\hat{h}_{ij}\right|^2 x}{\sigma_h^4}}\right),\ x\in[0,+\infty). \tag{3.13}$$

The absolute value of the estimated channel gain squared $\left|\hat{h}_{ij}\right|^2$ is also non-central chi squared with two degrees of freedom and non-central parameter $\left|h_{ij}\right|^2$. Hence, from the PDF of $\left|h_{ij}\right|^2$ in (3.13) and given $\left|\hat{h}_{ij}\right|^2$, we can write the PDF of the actual instantaneous mutual information $E\left[W\left(x_{ij};y_{ij}\left|\hat{h}_{ij}\right.\right)\right]$ as

$$p\left(E\left[W\left(x_{ij};y_{ij}\left|\hat{h}_{ij}\right.\right)\right]\right) = \frac{\sigma_z^2}{p_{ij}\sigma_h^2}\exp\left(W\left(x_{ij};y_{ij}\left|\hat{h}_{ij}\right.\right) - \frac{\left|\hat{h}_{ij}\right|}{\sigma_h^2} - \frac{\sigma_z^2\left(\exp\left(W\left(x_{ij};y_{ij}\left|\hat{h}_{ij}\right.\right)\right)-1\right)}{p_{ij}\sigma_h^2}\right) \times I_0\left(2\sqrt{\frac{\left|\hat{h}_{ij}\right|^2\left(\exp\left(W\left(x_{ij};y_{ij}\left|\hat{h}_{ij}\right.\right)\right)-1\right)}{p_{ij}\sigma_h^2}}\right) \tag{3.14}$$

Moreover, from the channel outage condition in (3.12) and the PDF of $E\left[W\left(x_{ij};y_{ij}\left|\hat{h}_{ij}\right.\right)\right]$ in (3.14) we derive the condition that ensures effective transmissions expressed as

$$\int_0^{r_{ij}} p\left(E\left[W\left(x_{ij};y_{ij}\left|\hat{h}_{ij}\right.\right)\right]\right)dW \le 1-P_{out}\ . \tag{3.15}$$

The condition in (3.15) indicates that our objective is to determine the actual instantaneous effective data rate r_{ij} such that the Cumulative Density Function (CDF) of the actual instantaneous mutual information $E\left[W\left(x_{ij};y_{ij}\left|\hat{h}_{ij}\right.\right)\right]$ is equal with the complementary target data outage probability $1-P_{out}$. From the condition in (3.15), we can derive the PBL process that expresses the bit-loading procedure of each user j on the i-th subcarrier in our system.

Theorem 3.2 - Given the estimated channel gain $\hat{h}_{ij}$, and the target data outage probability P_{out}, the actual instantaneous effective data rate r_{ij} in (3.15) can be accurately expressed by the approximated instantaneous effective data rate $\tilde{r}_{ij}$ of user j on subcarrier i as

$$\tilde{r}_{ij} = E\left[\log_2\left(1+\frac{\left|\hat{h}_{ij}\right|^2 p_{ij}}{\sigma_z^2} \right) - \frac{\sqrt{2}\left|\hat{h}_{ij}\right| p_{ij}\sigma_h Q^{-1}\left(1-P_{out}\right)}{\left|\hat{h}_{ij}\right|^2 p_{ij}+\sigma_z^2} \right], \tag{3.16}$$

where $Q(\cdot)$ denotes the complementary Gaussian CDF [59].

Proof - The proof of *Theorem 3.2* is presented in Appendix A.3. ■

In *Theorem 3.2*, we express PE-AETS's PBL process for each user j on subcarrier i with the function in (3.16). We can also denote the approximated effective data rate for user j over all the allocated subcarriers is denoted as $\tilde{r}_j$, which is computed by

$$\tilde{r}_j = E\left[\sum_{i=1}^{N_F} \tilde{r}_{ij} \right]. \tag{3.17}$$

In follow, we provide some details on the performance and behaviour of our proposal.

3.4.2 Specifications on the Introduced PBL Process

In this Section, we demonstrate the key theoretical differences of our PBL process presented in Section 3.4.1 compared with the traditional methodology adopted by several studies in the literature, i.e., [14], [17], [23], [24], [56], [60].

To account channel outage, we firstly define the PDF of the actual instantaneous mutual information $E\left[W\left(x_{ij}; y_{ij} \middle| \hat{h}_{ij} \right) \right]$ in (3.14) in terms of imperfect CSIT realizations, i.e., $\left|\hat{h}_{ij}\right|^2$. Secondly we express the condition that ensures effective transmissions in (3.15) in conjunction with the target data outage probability P_{out}. In continue, we compute the condition in (3.15) by a series expansion and approximate the actual instantaneous effective data rate r_{ij} in (3.15) by the approximated instantaneous effective data rate $\tilde{r}_{ij}$ of user j on

subcarrier i as presented in (3.16) in *Theorem 3.2*. From (3.16), we observe that our function's utility-dynamics[12] has low-pace logarithmic growth ratio, meaning that escalations of the MMSE variance σ_h^2 or the target data outage probability P_{out} or the imperfect CSIT realizations $\left|\hat{h}_{ij}\right|^2$, induce slow degradations of our approximated instantaneous effective data rate $\tilde{r}_{ij}$. In addition, when our function's utility_dynamics increase (the transmission conditions become worst), our approximated instantaneous effective data rate $\tilde{r}_{ij}$ decreases inversely proportionally with notably small decay rate. This can be also translated in terms of instantaneous transmitting power p_{ij}, e.g., when our function's utility-dynamics increase the instantaneous transmitting power p_{ij} increases proportionally with small increase rate.

On the other hand, the traditional methodology firstly expresses the instantaneous outage rate in terms of perfect CSI realizations, i.e., $\left|h_{ij}\right|^2$, and channel outage, i.e., P_{out}. Secondly it relies on the non-central CDF of the perfect CSI realizations, i.e., $\left|h_{ij}\right|^2$ to define its PBL process in conjunction with the imperfect CSI realizations $\left|\hat{h}_{ij}\right|^2$ and channel outage P_{out}. The PBL process resulted by this method is an expression of the effective data rate, widely known as goodput-rate. As we will see later in this Thesis, the advantage of the goodput-rate over our proposal in this research part is that it can be manipulated easier during the optimization procedure for the reason that goodput-rate is entirely a logarithmic function. However, its utility-dynamics are highly sensitive to function-dynamics variations, e.g., σ_h^2, P_{out} and $\left|\hat{h}_{ij}\right|^2$, meaning that goodput-rate is less power-efficient our proposal especially under highly uncertain channel conditions. For example, minor escalations of the MMSE variance

[12] Function-dynamics are defined as the factors that equalize a function, i.e., the function-dynamics of our PBL process in (3.16) are the $\left|\hat{h}_{ij}\right|$, P_{out}, σ_z^2 and σ_h^2. The parts of a function that includes those dynamics are named utility-dynamics i.e., the utility dynamics of our PBL process in (3.16) is $\sqrt{2}\left|\hat{h}_{ij}\right| p_{ij}\sigma_h Q^{-1}\left(1-P_{out}\right)/\left(\left|\hat{h}_{ij}\right|^2 p_{ij}+\sigma_z^2\right)$. Utility-dynamics is an ideal metric to examine the behaviour of a function [59].

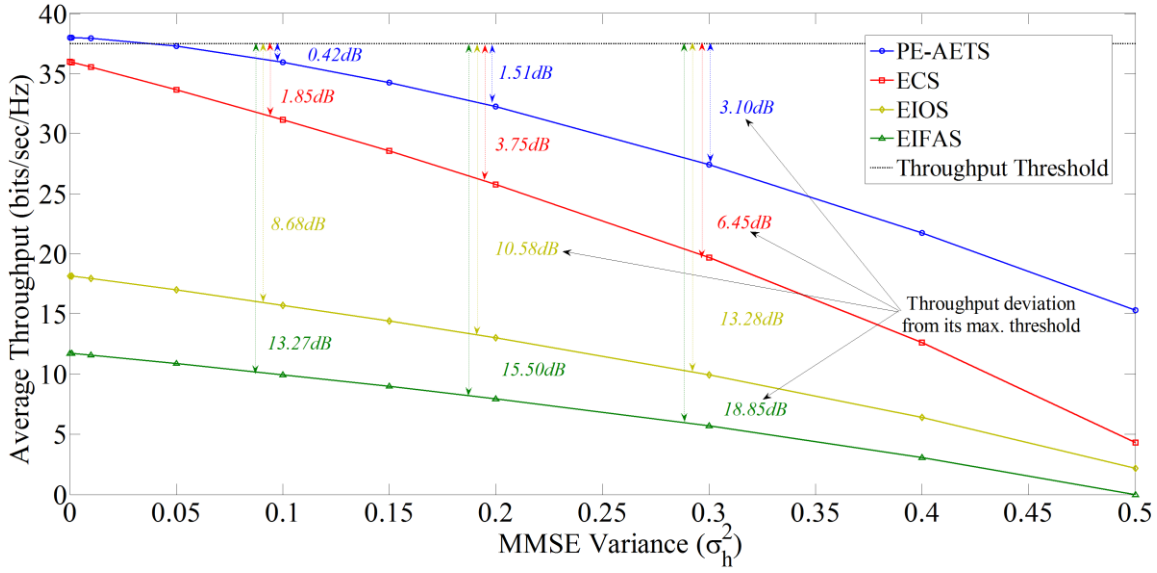

Figure 3.3 - Comparison between the approximated effective data rate in (3.16) and the goodput-rate by means of average throughput versus MMSE variance σ_h^2.

σ_h^2 induce rapid increase to goodput-rate's utility-dynamics and hence, fast rate degradation or, in terms of power, instantaneous transmitting power p_{ij} ascents. Another characteristic that makes goodput-rate less power-efficient than our proposal is that goodput rate is by its origin always less than the actual capacity. The reason is that upon using goodput-rate the amount of overhead depends on the application protocol stack and hence, some resources are wasted.

Except from the theoretical differences, we practically verify the increased rate and power efficiency of our PBL process in (3.16) over goodput rate oriented schemes with comparisons illustrated in Figure 3.3 and Figure 3.4. In particular, from Figure 3.3 we observe that as the MMSE variance σ_h^2 increases, our PBL process provides substantial average throughput enchantment, with significantly lower decay pace over the goodput rate oriented PBL process used in ECS [17], [24], [56], EIOS [14], [20], [21], [22], [23] and EIFAS [27], [60]. In Figure 3.4, for high channel uncertainty, e.g., $\sigma_h^2 > 0.1$, the goodput-rate utility

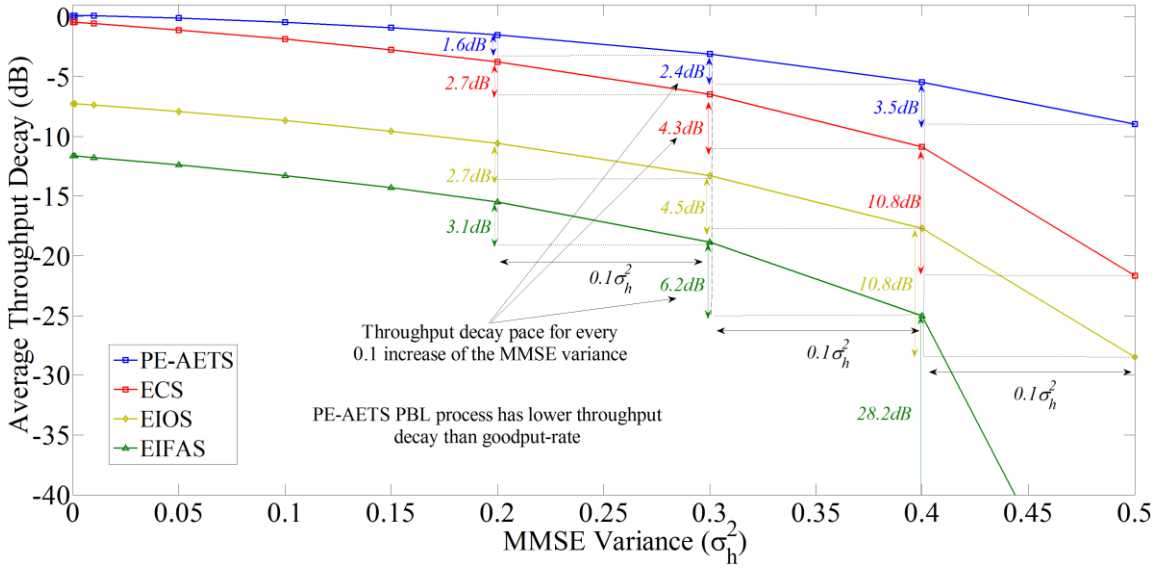

Figure 3.4 - Comparison between the approximated effective data rate in (3.16) and the goodput-rate by means of average throughput decay versus MMSE variance σ_h^2.

dynamics[13] evoke significantly higher rate reduction than our PBL process in (3.16), e.g., ECS's goodput evokes 2.7*dB* rate reduction in average, while PE-AETS's PBL only 1.6 *dBm*. Consequently, our PBL function in (3.16) has also practically higher resistance to channel imperfections compared to the goodput-rate oriented PBL functions. In continue we use our PBL approach in (3.16) to define the QoS constraint in our cross-layer optimization problem.

3.5 Cross-Layer Problem Formulation

In this Section, we formulate the OFDMA cross-layer design for heterogeneous users with imperfect channel and outage considerations as a constrained optimization problem based on the system models in Section 3.3.

[13] We omit details regarding the goodput-rate utility dynamics as they are extensively presented in [56], [60].

3.5.1 Formulation of the Primary Cross-Layer Optimization Problem

We represent the optimal subcarrier allocation policy with the $N_F \times K$ matrix $\mathbf{S}^* = \left[s_{ij}^* \right]$ whose (i, j)-th element is the optimal subcarrier allocation index s_{ij}^* of user j on subcarrier i. In addition, we denote the optimal transmitting power allocation policy with the $N_F \times K$ matrix $\mathbf{P}^* = \left[p_{ij}^* \right]$ whose (i, j)-th element is the optimal instantaneous transmitting power allocation p_{ij}^* of user j on subcarrier i. In continue, we can formulate the primary cross-layer optimization problem as follows[14].

Find optimal subcarrier and transmitting power allocation policies $\mathbf{S}^* \left[\hat{\mathbf{H}}, \mathbf{Q} \right]$ and $\mathbf{P}^* \left[\hat{\mathbf{H}}, \mathbf{Q} \right]$, respectively

such that:
$$\min_{s_{ij}, p_{ij}} E\left[\frac{1}{N_F} \sum_{j=1}^{K} \sum_{i=1}^{N_F} s_{ij} p_{ij} \right] \tag{3.18}$$

subject to:
$$s_{ij} \in \{0,1\}, \quad \forall i, j, \tag{3.19}$$
$$\sum_{j=1}^{K} s_{ij} \le 1, \quad \forall i, \tag{3.20}$$
$$p_{ij} \ge 0, \quad \forall i, j, \tag{3.21}$$
$$E\left[\frac{1}{N_F} \sum_{j=1}^{K} \sum_{i=1}^{N_F} s_{ij} p_{ij} \right] \le P_{TOTAL}, \tag{3.22}$$
$$E\left[D_j \right] \le T_j^{\max}, \quad \forall j, \tag{3.23}$$
$$P_{out} = P_{app}. \tag{3.24}$$

[14] The expectation operator $E[\cdot]$ in (3.18) has been captured over all system states $\left(\hat{\mathbf{H}}_{K \times N_F}, \mathbf{Q}_{K \times 1} \right)$, while in (3.22) and (3.23) it refers to average delay and power over random realizations of the CSIT and QSI realizations, respectively.

The primary cross-layer optimization problem in (3.18) - (3.24) is a power minimization problem over the instantaneous transmitting power p_{ij} and the subcarrier allocation index s_{ij}. The problem is constrained over QoS, channel and packet outage, subcarrier and transmitting power allocation constraints. More precisely, the problem in (3.18) - (3.24) targets to minimize the total power transmitted from the BS to the K heterogeneous users over all the N_F subcarriers. The subcarrier allocation constraints (3.19) and (3.20) are used to certify that only one user j can occupy a subcarrier i at a specific time slot. Moreover, the transmitting power allocation constraints (3.21) and (3.22) ensure that the power cannot take negative values and that the total transmitting power from the BS the K users cannot exceed the average total available power at the BS P_{TOTAL} [15]. Constraint (3.23) is the QoS constraint in terms of average delay of each heterogeneous user j, denoted by $E\left[D_j\right]$ **[16]**, and of the maximum delay tolerance $T_j^{\max}$ specified by user j's queuing characteristics[17]. Finally, the outage constraint (3.24) limits the impact of the imperfect channel by guaranteeing that the target data outage probability P_{out} at the PHY layer, satisfies a target packet outage probability P_{app}. The target packet outage probability P_{app} represents the packet transmission failure and it is usually specified by the application requirements of each user and it is given by $P_{app} = 1 - \Pr\left(E\left[D_j\right] \le T_j^{\max}\right)$.

It is straightforward that the QoS constraint (3.23) and the outage constraint (3.24) have been defined in terms of higher layer parameters meaning that they do not comply with

[15] We remark that although the problem in (3.18) - (3.24) is a power minimization problem, the transmitting power allocation constraint (3.22) is not redundant to the problem. The reason is that (3.22) guarantees the feasibility of the allocated links since there may be instances, where total transmitting power from the BS the K users is greater than P_{TOTAL}. For example in the case where all users are in very bad channel conditions the total transmitted power may be larger than the average total available power at the BS P_{TOTAL} resulting to infeasible resource allocation.

[16] The average delay is adopted in the literature i.e., [18], [24], [56], [27] as a performance measure of the delay performance. In short, it is recognized that average delay is a good characterization of overall delay performance.

[17] In our model, we assume that users have enough traffic waited in the queue, which is ready to be transmitted. Therefore, if a network resource is allocated to a user, that network resource is used up by that user.

the cross-layer structure. For this reason, the primary cross-layer optimization problem in (3.18) - (3.24) cannot be directly solved. To solve the primary cross-layer optimization problem in (3.18) - (3.24) a first step is to express the two constraints (3.23) and (3.24) by means of PHY layer parameters.

3.5.2 Correlation of Outage and QoS constraints in the Cross-Layer Optimization Problem

In this Section, we express the QoS constraint (3.23) and the outage constraint (3.24) of the primary cross-layer optimization problem in (3.18) - (3.24) in terms of optimization variables.

To transform the QoS constraint (3.23), we need to establish a relationship between the approximated effective data rate for user j given in (3.17) and its traffic characteristic tuple $\left[F, T_j^{\max}, \lambda_j\right]$ as described in Section 3.3.3. In our queuing analysis presented in Appendix A.4, we use the following *Lemma*.

Lemma 3.1 - A sufficient condition for the QoS constraint (3.23) of the primary cross-layer optimization problem in (3.18) - (3.24) is

$$\frac{\lambda_j E\left[X_j^{\,2}\right]}{2\left(1-\lambda_j E\left[X_j\right]\right)} \le T_j^{\max}, \tag{3.25}$$

where X_j denotes the service time of the packets of user j.

Proof - The proof of *Lemma 3.1* is presented in Appendix A.4. ■

From *Lemma 3.1* we can transform the QoS constraint (3.23) to an equivalent cross-layer rate constraint that directly relates the approximated effective data rate for user j in (3.17) with the queuing parameters of each user j, e.g., packet size F, maximum delay tolerance $T_j^{\max}$ and Poisson arrival rate λ_j.

Proposition 3.1 - A necessary condition for the QoS constraint (3.23) of the primary cross-layer optimization problem in (3.18) - (3.24) is

$$E\left[\sum_{i=1}^{N_F} s_{ij}\tilde{r}_{ij}\right] \geq \tilde{q}_j\left(F, T_j^{\max}, \lambda_j\right), \tag{3.26}$$

where $\tilde{q}_j\left(F, T_j^{\max}, \lambda_j\right)$ represents the equivalent traffic arrival rate at the user j's queue in *bits/sec/Hz* given by $\tilde{q}_j\left(F, T_j^{\max}, \lambda_j\right) = q_j \cdot \left(\left(1/t_s\right)/\left(BW/N_F\right)\right)$, with q_j to denote the equivalent traffic arrival rate at the user j's queue in *bits* given by

$$q_j = \frac{F}{2T_j^{\max}} \cdot \left(\sqrt{T_j^{\max}\lambda_j\left(T_j^{\max}\lambda_j + 2\right)} + \lambda_j T_j^{\max}\right), \tag{3.27}$$

and BW / N_F to refer to the bandwidth allocated to each subcarrier i.

Proof - The proof of *Proposition 3.1* is presented in Appendix A.4. ■

From *Proposition 3.1*, we correlate the PHY layer with the higher-layer parameters of each user j as the condition in (3.26), expresses the equivalent rate constraint, which indicates that the scheduled approximated effective data rate for user j in (3.17) should be at least the same as the incoming traffic arrival rate to user j's queue $\tilde{q}_j\left(F, T_j^{\max}, \lambda_j\right)$. In addition, we can derive another condition regarding the stability of the queues in our system as follows.

Proposition 3.2 – If the maximum delay tolerance $T_j^{\max}$ of a user j is infinite, e.g., $T_j^{\max} \to \infty$, then a necessary condition for the QoS constraint (3.23) of the primary cross-layer optimization problem in (3.18) - (3.24) is written as

$$E\left[\sum_{i=1}^{N_F} s_{ij} r_{ij}\right] \geq \left(\frac{1}{t_s} / \frac{N_F}{BW}\right) \cdot F\lambda_j, \tag{3.28}$$

which is a condition that guarantees the stability of each user j's queues.

Proof - The proof of *Proposition 3.2* is presented in Appendix A.4. ■

In *Proposition 3.2*, the condition (3.28) guarantees the stability of all the K users' queues in our system by signifying that the system should provide the scheduled

approximated effective data rate even to the delay-insensitive users with no delay constraints[18]. In other words, the condition in (3.28) is a low bound of the condition (3.26) in *Proposition 3.1* indicating that the scheduler must provide an approximated effective data rate of at least the same rate as the bits arrival rate $F\lambda_j$ to user j's buffer.

We remark that several studies in the existing literature on one hand denote the QoS constraint in the form of, e.g., $E\left[\tilde{r}_{ij}\right] \geq q''$, where q'' is the minimum throughput requirement, but on the other hand they do not correlate q'' with the PHY layer parameters. In fact, for simplicity reasons, many authors blur the scheduling process by assuming that the BS has an a priori knowledge of the minimum throughput requirement q''. We bypass these issues with our expressions in *Proposition 3.1* and *Proposition 3.2*, which provide precise correlations between each user's traffic arrival rate and maximum delay tolerance acquired from higher layers, with its approximated effective data rate at the PHY layer.

Furthermore, we focus on the outage constraint (3.24) in the primary cross-layer optimization problem in (3.18) - (3.24). As mentioned in Section 3.5, the outage constraint (3.24) limits the impact of the imperfect CSIT. In other words, by fixing the maximum impact of the imperfect CSIT with the target packet outage probability P_{app}, the solution of the primary cross-layer optimization problem in (3.18) - (3.24) is valid, provided that the CSIT imperfection is fitted in the PBL process (3.16). Hence, we account potential packet outage in the primary cross-layer optimization problem in (3.18) - (3.24) by imposing the outage constraint (3.24) in the PBL process (3.16) to obtain the new expression of the approximated effective data rate as

$$\tilde{r}_{ij} = E\left[\log_2\left(1+\frac{\left|\hat{h}_{ij}\right|^2 p_{ij}}{\sigma_z^2}\right) - \frac{\sqrt{2}\left|\hat{h}_{ij}\right| p_{ij}\sigma_h Q^{-1}\left(1-P_{app}\right)}{\left|\hat{h}_{ij}\right|^2 p_{ij}+\sigma_z^2}\right]. \tag{3.29}$$

[18] It is noted that a queue is stable when there is no infinitely number of backlogged packets in the steady state [27].

3.5.3 Reformulation of the Power-Efficient Cross-Layer Optimization Problem

Considering the new expression of the approximated effective data rate in (3.29) as well as *Proposition 3.1* and *Proposition 3.2*, we are now ready to formulate the power-efficient cross-layer optimization problem as follows.

Find optimal subcarrier and transmitting power allocation policies $\mathbf{S}^*\left[\hat{\mathbf{H}},\mathbf{Q}\right]$ and $\mathbf{P}^*\left[\hat{\mathbf{H}},\mathbf{Q}\right]$, respectively

such that:
$$\min_{s_{ij},p_{ij}} E\left[\frac{1}{N_F}\sum_{j=1}^{K}\sum_{i=1}^{N_F} s_{ij}p_{ij}\right] \tag{3.30}$$

subject to:
$$s_{ij}\in\{0,1\},\quad \forall i,j, \tag{3.31}$$
$$\sum_{j=1}^{K} s_{ij}\le 1,\quad \forall i, \tag{3.32}$$
$$p_{ij}\ge 0,\quad \forall i,j, \tag{3.33}$$
$$E\left[\frac{1}{N_F}\sum_{j=1}^{K}\sum_{i=1}^{N_F} s_{ij}p_{ij}\right]\le P_{TOTAL}, \tag{3.34}$$
$$E\left[\sum_{i=1}^{N_F} s_{ij}\left(\log_2\left(1+\frac{\left|\hat{h}_{ij}\right|^2 p_{ij}}{\sigma_z^2}\right)-\frac{\sqrt{2}\left|\hat{h}_{ij}\right|p_{ij}\sigma_h Q^{-1}\left(1-P_{app}\right)}{\left|\hat{h}_{ij}\right|^2 p_{ij}+\sigma_z^2}\right)\right]\ge \tilde{q}_j\left(F,T_j^{\max},\lambda_j\right),\quad \forall j. \tag{3.35}$$

In the power-efficient cross-layer optimization problem in (3.30) - (3.35), the subcarrier and transmitting power allocation constraints (3.31) - (3.34) are the same with constraints (3.19) - (3.22) of the primary cross-layer optimization problem in (3.18) - (3.24). The new QoS constraint (3.35), is the transformed QoS constraint (3.23) including the outage constraint (3.24) of the primary cross-layer optimization problem in (3.18) - (3.24) and

signifies that the approximated effective data rate of each user j must be larger or equal than the equivalent rate at user j's queue[19].

It is obvious that the power-efficient cross-layer optimization problem in (3.30) - (3.35) is a mixed combinatorial problem as the optimization variable s_{ij} is discrete and the optimization variable p_{ij} is continuous. According to [59] and [135], the power-efficient cross-layer optimization problem can be solved via a combinatorial solution explained as follows. For each possible subcarrier allocation index s_{ij}, we calculate the instantaneous transmitting power allocations p_{ij} and its corresponding approximated effective data rate allocations $\tilde{r}_{ij}$ for a selected user j over a subcarrier i. Then, for all the different cases, we can enumerate all the K^{N_F} possible combinations of the subcarrier allocation indexes s_{ij} s, considering as optimal the one that gives the smallest power. With that way, the combinatorial solution evaluates the total power transmitted from the BS to the K heterogeneous users over all the N_F subcarriers given in (3.30). However, as we perform K^{N_F} searches, the combinatorial solution is highly complex and it is infeasible to be applied in real-time systems, i.e., when $N_F = 2048$ and $K = 200$.

In follow, we make the power-efficient cross-layer optimization problem in (3.30) - (3.35) more tractable and we present low complex and power-efficient optimal solutions.

3.6 Convex Optimization-based Power Efficient Optimal Allocation Strategies

In this Section, we show that the power-efficient cross-layer optimization problem in (3.30) - (3.35) can be transformed into convex optimization problem and we initialize convex optimization to derive its optimal solutions.

[19] In the power-efficient cross-layer optimization problem in (3.30) - (3.35), we use the queuing condition in *Proposition 3.1* instead of the queue stability condition in *Proposition 3.2* for the reason that the queue stability condition in *Proposition 3.2* is straightforward obtained from the queuing condition in *Proposition 3.1* when $T_j^{\max} \to \infty$ (see Appendix A.4).

3.6.1 Convexity of the Power-Efficient Cross-Layer Optimization Problem

With the intention to define new solutions with reduced complexity compared to the combinatorial solution of the power-efficient cross-layer optimization problem in (3.30) - (3.35), we utilize a widely adopted technique in the context of subcarrier assignment in OFDMA systems [109], [137], [138], [139], known as subcarrier time-sharing relaxation [140].

In particularly, we transform the discrete variable s_{ij} into the continues variable $\tilde{s}_{ij} \in (0,1]$, which denotes the subcarrier time-sharing factor. The subcarrier time-sharing factor s_{ij} indicates the portion of time that subcarrier i is assigned to user j during each transmission frame. Hence, we can compute the non-integer fractional part $frac(\cdot)$ of $\tilde{s}_{ij}$ by its fractional function $frac(\tilde{s}_{ij}) = \tilde{s}_{ij} - \lfloor \tilde{s}_{ij} \rfloor$ for $0 < frac(\tilde{s}_{ij}) \leq 1$. To further understand the subcarrier time-sharing relaxation in its full measure, we provide the following example. Let us assume that an OFDM transmission frame is consisted by δ OFDM symbols[20] and that in each frame, user j can use the i-th subcarrier in $\delta \cdot \tilde{s}_{ij}$ symbols. Then, the approximated instantaneous effective data rate $\tilde{r}_{ij}$ and the instantaneous power transmission p_{ij} over the δ symbols are scaled by the same factor $\tilde{s}_{ij}$, e.g., we can write that $\tilde{r}_{ij} = \tilde{s}_{ij} r_{ij}$ and $\tilde{p}_{ij} = \tilde{s}_{ij} p_{ij}$, respectively. Thus, the time-share of each subcarrier i can be taken into account[21].

In continue, we examine the convexity of the power-efficient cross-layer optimization problem in (3.30) - (3.35).

[20] For this example, we consider that the general expression of the positive number δ used in this Thesis, is a very large number.

[21] A notable property of subcarrier time-sharing relaxation lays on the fact that OFDM channels are frequently time-varying hence, they may not remain unchanged long enough for time-sharing to be feasible. However, the authors in [140] show that subcarrier time-sharing is feasible and also more effective in cases where the number of subcarriers or the packet size is large.

Proposition 3.3 - Given the subcarrier time-sharing factor $\tilde{s}_{ij} \in (0,1]$ and the new power transmission variable $\tilde{p}_{ij} = \tilde{s}_{ij} p_{ij}$, the power-efficient cross-layer optimization problem in (3.30) - (3.35) is a convex optimization problem over the non-empty and convex set $\left(\tilde{s}_{ij}, \tilde{p}_{ij}\right)$ if the variables $\tilde{s}_{ij}$ and $\tilde{p}_{ij}$ vary in the region determined by the relationship

$$8\left(Q^{-1}\left(1-P_{app}\right)\right)^2 \leq \frac{\left|\hat{h}_{ij}\right|^2}{\sigma_h^2}\left(1+\frac{\left|\hat{h}_{ij}\right|^2 \tilde{p}_{ij}}{\tilde{s}_{ij}\sigma_z^2}\right)^2 . \tag{3.36}$$

Proof - The proof of *Proposition 3.3* is presented in Appendix A.5. ■

In *Proposition 3.3* we show that the power-efficient cross-layer optimization problem in (3.30) - (3.35) has a unique global optimal solution, which can be obtained in polynomial time if $\tilde{s}_{ij}$ and $\tilde{p}_{ij}$ vary according to condition (3.36). We remark that in [16], where authors propose the single-user version of our PBL process, a similar condition to (3.36) bounds the effectiveness of convexity of the corresponding problem to a region. The physical meaning of these limitations is that the validity of such optimization problems is dependent on the channel's conditions. However, it is extremely rare the convexity conditions to be breached as it only happens upon extremely bad channel conditions, e.g., in our case for $P_{app} = 0.9$, $\sigma_h^2 > 8$ and $\left|\hat{h}_{ij}\right|^2 \to 0$. Considering realistic systems, such transmission conditions are almost impossible to occur due, i.e., to modern networks' infrastructure and mobile devices' technology. Nevertheless, in the case where our convexity condition (3.36) is not satisfied the global optimal solutions can be derived either through utilizing a low complex search as in [24], [17] or, in the worst case, via a combinatorial search similar with the one described in Section 3.5.3. It is also evident that relative schemes [14], [17], [23], [24], [56], [60], which as we will see later provide infeasible allocation even in better transmission conditions, utilize such numerical processes to obtain the global optimum solution. However, to further emphasize the rarity of utilizing such numerical processes, we state that although our simulations tend to match practical conditions, none of the examined schemes required numerical process to derive its optimal solutions.

In the next Section, we provide the optimal solution of the power-efficient cross-layer optimization problem in (3.30) - (3.35).

3.6.2 Convex Optimization-based Optimal Allocation Strategies

As the power-efficient cross-layer optimization problem in (3.30) - (3.35) is a convex optimization problem and also it is a resultant reformulated problem of the primary cross-layer optimization problem in (3.18) - (3.24), we utilize convex optimization to derive the optimal allocation strategies. In particular, after defining the Lagrangian function and the KKT conditions, we derive the optimal transmitting power allocation policy as follows.

Theorem 3.3 - Given the imperfect channel realization $\hat{h}_{ij}$, the optimal transmitting power allocation policy $\mathbf{P}^*\left[\hat{h}_{ij}\right]=\left[\tilde{p}_{ij}^*\right]$ has individual matrix elements the optimal instantaneous transmitting power allocation $\tilde{p}_{ij}^*$ of user j on subcarrier i given by

$$\tilde{p}_{ij}^* = \begin{cases} \left(\dfrac{N_F \xi_j^*}{2\left|\hat{h}_{ij}\right|^2 \left(\mu^* - 1\right)} \left(\beta_{ij} - \left|\hat{h}_{ij}\right|^2 + \dfrac{2\sigma_z^2}{N_F} \dfrac{\left(\mu^* - 1\right)}{\xi_j^*} \right) \right)^+ & , \forall \tilde{s}_{ij}^* = 1 \\ 0 & , \text{otherwise} \end{cases} , \forall i, j , \mu^* \neq 1 , \quad (3.37)$$

where ξ_j^* and μ^* are the optimal Lagrangian Multipliers (LM) related to the QoS constraint (3.35) and the transmitting power allocation constraint (3.34), respectively, the variable β_{ij} is used for notational brevity and it is given by

$$\beta_{ij} = \sqrt{\left|\hat{h}_{ij}\right| \left(\left|\hat{h}_{ij}\right|^3 - \left(\frac{4\sqrt{2}\sigma_h \sigma_z^2 Q^{-1}\left(1 - P_{app}\right)\left(\mu^* - 1\right)}{N_F \xi_j^*} \right) \right)} , \forall i, j , \quad (3.38)$$

while the notation $\left(x\right)^+$ means $\max\left(0, x\right)$.

Proof - The proof of *Theorem 3.3* is presented in Appendix A.6. ■

Relying on *Theorem 3.3* we derive the optimal subcarrier allocation policy as follows.

Theorem 3.4 - Given the imperfect channel realization $\hat{h}_{ij}$, the optimal subcarrier allocation policy $\mathbf{S}^*\left[\hat{h}_{ij}\right]=\left[\tilde{s}_{ij}^*\right]$ has individual matrix elements the optimal subcarrier allocation index $\tilde{s}_{ij}^*$ of user j on subcarrier i given by

$$\tilde{s}_{ij}^* = \begin{cases} 0, \text{ if } \nu_i^* > \xi_j^* \cdot \hat{H}_{ij} \\ 1, \text{ if } \nu_i^* < \xi_j^* \cdot \hat{H}_{ij} \end{cases}, \ \forall i, j, \tag{3.39}$$

where ν_i^* is the optimal LM related with the subcarrier allocation constraint (3.32) and the variable $\hat{H}_{ij}$ is used for notational brevity and it is given by

$$\hat{H}_{ij} = \log_2\left(\left|\hat{h}_{ij}\right|^2 \cdot \left(\beta_{ij}'' + 1\right)\right) - \frac{\beta_{ij}''}{\ln 2 \cdot \left(\beta_{ij}'' + 1\right)} - \frac{\sqrt{2}\left|\hat{h}_{ij}\right| \beta_{ij}''^2 \sigma_h Q^{-1}\left(1 - P_{app}\right)}{\left|\hat{h}_{ij}\right|^2 \beta_{ij}''^2 + \frac{1}{\left|\hat{h}_{ij}\right|^2} + \frac{1}{2\sigma_z^4}\beta_{ij}''}, \ \forall i, j. \tag{3.40}$$

with $\beta_{ij}'' = N_F \xi_j^* \beta_{ij}' - 1$ and $\beta_{ij}' = \beta_{ij} + \left|\hat{h}_{ij}\right|^2$. In addition, the optimal subcarrier allocation policy $\mathbf{S}^*\left[\hat{h}_{ij}\right]$ is decoupled among the N_F OFDM subcarriers to obtain the optimal user denoted by j^* with the following searching process, which is always feasible.

$$\text{For } i = 1 \text{ to } N_F \text{ find } j^* = \arg\max_{j \in [1,K]} \hat{H}_{ij} \text{ and set } \tilde{s}_{ij}^* = \begin{cases} 1, \ j = j^* \\ 0, \ j^* \text{ does not exist} \end{cases}. \tag{3.41}$$

Proof - The proof of *Theorem 3.4* is presented in Appendix A.6. ■

Once we derive the optimal transmitting power allocation policy $\mathbf{P}^*\left[\hat{h}_{ij}\right]$ and the optimal subcarrier allocation policy $\mathbf{S}^*\left[\hat{h}_{ij}\right]$ from *Theorem 3.3* and *Theorem 3.4*, respectively we can define the optimal approximated effective data rate allocation policy $\mathbf{R}^*\left[\hat{h}_{ij}\right]=\left[\tilde{r}_{ij}^*\right]$ as follows.

Theorem 3.5 - Given the imperfect channel realization $\hat{h}_{ij}$, the optimal approximated effective data rate allocation policy $\mathbf{R}^*\left[\hat{h}_{ij}\right]=\left[\tilde{r}_{ij}^*\right]$ has individual matrix elements the optimal approximated effective data rate $\tilde{r}_{ij}^*$ of user j on subcarrier i given by

$$\tilde{r}_{ij}^* = \left(\log_2\left(\frac{\beta_{ij} + \left|\hat{h}_{ij}\right| \xi_j^*}{2\left(1-\mu^*\right)\sigma_z^2} \right) - \frac{\sqrt{2}\sigma_h Q^{-1}\left(1-P_{app}\right)\cdot\left(\beta_{ij} - 2\sigma_z^2\left(1-\mu^*\right) + \left|\hat{h}_{ij}\right|\xi_j^*\right)}{\left|\hat{h}_{ij}\right|\left(\beta_{ij} + \left|\hat{h}_{ij}\right|\xi_j^*\right)} \right)^+ , \ \forall i, j , \ \mu^* \neq 1 . \tag{3.42}$$

Proof - The proof of *Theorem 3.5* is presented in Appendix A.6. ■

In the next Sections, we discuss the implementation process of the optimal allocation policies presented in *Theorem 3.3, Theorem 3.4* and *Theorem 3.5*, and some specifications of PE-AETS.

3.6.3 Implementation Process of the Optimal Allocation Policies

The optimal APA policy in *Theorem 3.3* has the form of multi-user water-filling strategy with power water-level of each user j to be given by $\left(\mu^*-1\right)/\xi_j^*$. This means that the optimal power is allocated according to the CSIT across subcarriers and the QSI of each user j. The optimal LMs μ^* and ξ_j^* can be perceived as the resource scheduling calibrators of the system, e.g., the users with urgent packets to transmit are allocated with a high power water-level $\left(\mu^*-1\right)/\xi_j^*$, while the users with non-urgent packets are assigned with lower water-levels μ^*-1. Moreover, the optimal subcarrier allocation in *Theorem 3.4* can be interpreted as a policy, where a user with high urgency (defined by the LM ξ_j^*, which is depended on the urgency of the delay requirements) has higher chance of being allocated with subcarriers, while users with the same urgency level (the LMs ξ_j^* are the same) have the same chance and subcarriers are allocated to the user with the best CSIT among this user group. As the search for the optimal user j^* in (3.41) of *Theorem 3.4*, is depended on the number of the K users

and the N_F OFDM subcarriers, it has low linear complexity given by $\mathcal{O}\left(N_F \times K\right)$. Nevertheless, to derive the optimal DSA strategies presented in *Theorem 3.3*, *Theorem 3.4* and *Theorem 3.5* we must firstly obtain the optimal LM μ^* and ξ_j^* through solving the following system of non-linear equations.

$$\begin{cases} P\left(\xi_j^*, \mu^*\right) = P_{TOTAL} - E\left[\sum_{i=1}^{N_F}\sum_{j=1}^{K} \tilde{s}_{ij}^* \tilde{p}_{ij}^*\right]^+ = 0 \\ f_j\left(\xi_j^*, \mu^*\right) = \xi_j^*\left(E\left[\sum_{i=1}^{N_F} \tilde{s}_{ij}^* \tilde{r}_{ij}^*\right] - \tilde{q}_j\left(F, T_j^{\max}, \lambda_j\right)\right) = 0, \ \forall j \end{cases}, \tag{3.43}$$

where $P\left(\xi_j^*, \mu^*\right)$ and $f_j\left(\xi_j^*, \mu^*\right)$ are functions that represent the optimal KKT conditions (see Appendix A.6) related with PE-AETS's transmitting power allocation and QoS constraints, respectively. We can obtain the solution of the system in (3.43) via an iterative mechanism that finds the roots of the non-linear equations in (3.43) based on the Secant and bisection methods [135]. For this reason, PE-AETS is an iteration-dependent scheme and its overall complexity is depended on the complexity of the iterative mechanism. For example, considering that the iterative mechanism has stopping criterion the difference between two successive $\left(\xi_j^*, \mu^*\right)$ [59], [135] and assuming that it aims to δ-optimality, PE-AETS's overall complexity is on the order of $\mathcal{O}\left(1/\delta^2\right)$, meaning that its overall complexity increases from $\mathcal{O}\left(N_F \times K\right)$ to $\mathcal{O}\left(N_F \times K/\delta^2\right)$. The value of the term $1/\delta^2$ depends on the number of loops l of the adopted root-finding method that derives the optimal LMs ξ_j^* and μ^*. As shown in Figure 3.5, the first loop begins by fixing μ^* and finding $\left\{\xi_j^*\right\}$, meaning that it has complexity of $\mathcal{O}\left(N_F \times K \times \Delta_{\left\{\xi_j^*\right\}}\right)$, where $\Delta_{\left\{\xi_j^*\right\}}$ is the number of iterations required in one loop to find $\left\{\xi_j^*\right\}$. Then for the derived $\left\{\xi_j^*\right\}$ the second loop starts to search for a new LM μ'^*, meaning that it has complexity of $\mathcal{O}\left(K \times \Delta_{\mu'^*}\right)$, where $\Delta_{\mu'^*}$ is the number of iterations required to find μ'^*. The process continues until the optimal μ^* and $\left\{\xi_j^*\right\}$ are found. Hence,

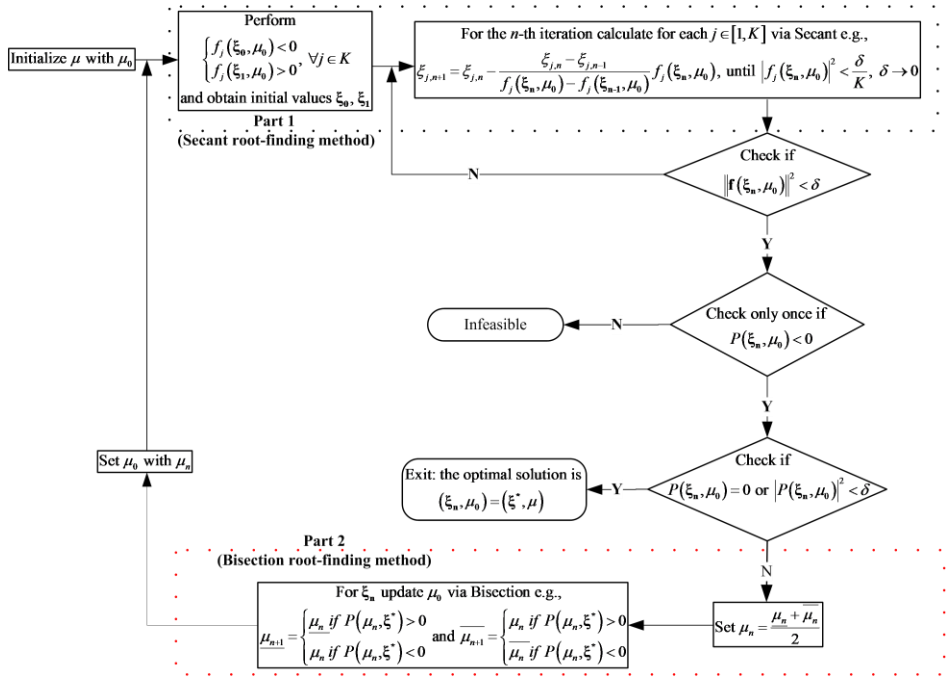

Figure 3.5 - Iterative mechanism of PE-AETS using the Secant and bisection root-finding methods.

the extra complexity is $\mathcal{O}\left(\Delta_{\{\xi_j^*\}} + \Delta_{\mu^*}\right) = \mathcal{O}\left(l\left[N_F \times K \times \Delta_{\{\xi_j^*\}} + \left(K \times \Delta_{\mu^*} - 1\right)\right]\right)$ and hence, the actual total computational complexity is $\mathcal{O}\left(N_F \times K^2 \times l\left[N_F \times \Delta_{\{\xi_j^*\}} + \left(\Delta_{\mu^*} - 1\right)\right]\right)$, where $\Delta_{\{\xi_j^*\}}$, Δ_{μ^*} and l depends on the adopted root-finding method. It is shown in [141] that the most efficient among all the commonly used root-finding methods in terms of computational time and accuracy is the semi-implicit-root finding (SIR) [46] and the Newton's-like [45] method. Nevertheless, considering the overall complexity of several schemes proposed in the relevant literature, i.e., [20], [21], [22], [23], [24], [27], PE-AETS's overall complexity is comparably low.

Let us now examine the convergence of the iterative root-finding mechanism illustrated in Figure 3.5. In Part 1, where the mechanism uses $f_j\left(\xi_j^*, \mu^*\right)$ in (3.43) to find the optimal LMs ξ_j^* for fixed LM μ, the convergence of the iterative mechanism is ensured as a

similar mechanism is used in [140], where its convergence is proven. In addition, as $P\left(\xi_j^*, \mu^*\right)$ in (3.43) is monotonic in μ^*, in Part 2 can we find the optimal LMs μ for fixed optimal LMs ξ_j^* via the bisection root-finding mechanism, which also converges once the initial range gives a bracketing interval. In addition, in the case where the optimal LM μ^* is equal to one, e.g., $\mu^* = 1$ then the proposed allocation policies in *Theorem 3.3*, *Theorem 3.4* and *Theorem 3.5* are infeasible as all subcarriers would be power-off. However, the condition $\mu^* \neq 1$ is a theoretical limitation, which is almost impossible to occur in reality as, e.g., we can exclude it via our implementation mechanism. In addition, we remark that such limitations are unavoidable in such complex modelling, i.e., the allocations in [16], [24], [45], [56], are infeasible under perfect or very high CSI. Consequently, the iterative root-finding mechanism used in PE-AETS always converges to the optimal LMs.

3.6.4 Specifications on PE-AETS Scheduling

To gain insight of the behaviour of PE-AETS's optimal scheduling, in this Section we discuss the asymptotic performance gain due to multi-user diversity, the impact of the imperfect channel on the service time of each packet, the packet multiplexing process and the accuracy of our optimal policy. To avoid confusion, we separate our discussions into four different topics as below.

1) Asymptotic Multi-User Diversity Gain - The optimal approximated effective data rate allocation policy in *Theorem 3.5* performs asymptotically and also it is enhanced throughput exploiting multi-user and multi-carrier diversity. In fact, we show with simulations that PE-AETS attains equivalent throughput gains due to multi-user diversity exploitation to the schedulers in [56] and [23]. Moreover, although we formulate our PBL process in (3.16) relying on independent-bit encoding, PE-AETS does not result in negative leverage of the frequency diversity gain. The reason is that in quasi-static fading channels, either independent or joint subcarrier encoding bring equivalent frequency gain, while in multipath channels, the joint subcarrier encoding technique produces inconsequential gains of maximum 0.3*dBm* over

independent encoding. This effect is shown in [16] and it is also validated in our simulation results.

2) Impact of Channel Imperfectness on Service Time - In the evaluation of the whole transmission-retransmission duration (or the service time of each packet), it is assumed that a packet is re-transmitted immediately whenever outage error occurs. The retransmission is repeated until the packet will be successfully delivered before the transmission of other packets. Hence, considering our discussions in Appendix A.3, for target packet outage probability fixed for all time slots, e.g., $P_{out} = P_{app}$, the mean of the geometric distribution of the service time of each packet represents the average outage slots before each time slot of successful transmission and it is given by $P_{app} / \left(1 - P_{app}\right)$ with parameter $1 - P_{app}$. This means that compared to the packet transmission duration in the perfect CSIT case given by $1/\left(1 - P_{app}\right)$, the transmission duration under imperfect the channel realizations $\hat{h}_{ij}$ is $\left(1 + P_{app}\right)/\left(1 - P_{app}\right)$ times higher. In addition, the average service time $E\left[X_j \right]$ of each user j with imperfect channel, can be calculated by the total service time of all packets averaged over the number of packets served by this user given by $E\left[X_j \right] = F / E\left[\tilde{r}_j \right]$ as in the perfect CSIT case, i.e., [23].

3) Packet Multiplexing - As shown in Figure 3.1, the MAC and PHY layer packets are multiplexed over time composing packet frames at the cross-layer, namely *MAC*-frames. In the presented simulations, the number of packets is calculated in the unit of *MAC*-frames and it is averaged to a finite granularity approximation [142] of the corresponded averaged number of subcarriers N_F allocated to user j. In addition, the approximation assists to calculate the average delay $E\left[D_j \right]$ of user j by $E\left[D_j \right] = N_F / \lambda_j$, which expresses the time-averaged number of packets in the user j's queue. Thus, packets are served and multiplexed through a realistic but exhaustive cross-layer service [143], where only the packets that arrive before or during the current MAC-frame can be served in the present MAC-frame. We omit the presentation of the cross-layer multiplexing procedure between the

packets at the $M/G/1/\infty/\infty$ queues and the arriving packets at the PHY layer, as it is out of the scope of this Thesis.

4) Accuracy of the Optimal Policy - Let us now inspect the effect of the subcarrier time-sharing assumption in PE-AETS. When the optimal subcarrier allocation index $\tilde{s}_{ij}^{*}$ in of *Theorem 3.4* and the optimal transmitting power $\tilde{p}_{ij}^{*}$ in of *Theorem 3.3* are substituted in the modified the power-efficient cross-layer optimization problem in (3.30) - (3.35), we obtain an upper bound of the system's effective throughput, e.g., $\overline{R}^{*}$. Similarly, if $\tilde{s}_{ij}^{*}$ and $\tilde{p}_{ij}^{*}$ are used in the primary cross-layer optimization problem in (3.18) - (3.24), then we determine a lower bound of the system's effective throughput, e.g., $\underline{R}^{*}$. Assuming that R^{*} is the actual system's effective throughout determined through solving the primary cross-layer optimization problem in (3.18) - (3.24) with the exhaustive K^{N_F} combinatorial search presented in Section 3.5.3. Then the correlation between the three throughputs obviously is given as $\underline{R}^{*} \le R^{*} \le \overline{R}^{*}$. The difference between the lower and the upper bound of the system's effective throughput, e.g., $\underline{R}^{*} - \overline{R}^{*}$, shows the accuracy of our proposed solution. We can evaluate experimentally that the proposed optimal policy is accurate as our optimal results deviate only 0.025% in average from the actual system's effective throughpout R^{*}. Similar results are derived by valuations made in [17], [24], [56] where subcarrier time-sharing relaxation has been also considered. However, the accuracy of such proposals is difficult to be precisely classified for the reason that in most of the cases the exhaustive K^{N_F} combinatorial search does not converge to an optimal solution.

3.7 Simulations

In this Section, we present simulations to examine the performance of PE-AETS in comparison with the relative schemes ECS [17], [24], [56], EIOS [14], [20], [21], [22], [23] and EIFAS [27], [60].

	Class 1	Class 2	Class 3	Class 4	Class 5
Poission arrival rate λ_j (*packets/time slot*)	0.8	0.5	0.4	0.15	0.15
Min. delay requirement $T_j^{\max}$ (*time slot*)	2	2	4	8	1000
Min. delay requirement $T_j^{\max}$ (*sec*)	0.004	0.004	0.008	0.016	2
Min. equivalent rate $\tilde{q}_j\left(F, T_j^{\max}, \lambda_j\right)$ (*bits/sec/Hz*)	25.00	17.08	12.50	4.94	3.75

Table 3.1 - Minimum requirements of each heterogeneous class of users, depended on each user's QoS demands.

3.7.1 Simulation Modelling

We consider a prototype single-cell OFDMA system with channel bandwidth of $BW = 80$ *KHz* equally distributed among $N_F = 32$ subcarriers, each one having five independent paths, e.g., $\Theta = 5$. In addition, we specify five different classes of users denoted by $\left(C_1, C_2, C_3, C_4, C_5\right)$, with the QoS requirements of each class to be characterized by the tuple $\left(\boldsymbol{\lambda}, \mathbf{T}, \mathbf{F}\right) = \left(\left(0.8, 2, 125\right), \left(0.5, 3, 125\right), \left(0.4, 4, 125\right), \left(0.15, 8, 125\right), \left(0.15, 1000, 125\right)\right)$. From the tuple structure we clarify in Table 3.1 each user's minimum requirements, depended on its class, in terms of average approximated effective data rate. Furthermore, considering users with pedestrian mobility, where the coherence time of the channel fading is around $20ms$ or more [56], we set the scheduling slot duration to $t_s = 2\,msec$ and we assume that each packet has size of $F = 125\,bits$. To make our simulation model more realistic, we consider that all the heterogeneous users suffer signal path-loss from the BS. The signal path-loss PL_j of user j is computed by [134]

$$PL_j = PL\left(d_0\right) + 10\varpi \log_{10}\left(d_j / d_0\right) + sd_{\sigma_{sd}^2} \text{ (in } dBm\text{)}, \tag{3.44}$$

where $PL\left(d_0\right)$ is the reference path loss at a reference distance d_0, d_j is the distance of user j from the BS, ϖ is the path loss component and $sd_{\sigma_{sd}^2}$ is the Gaussian random variable for shadowing with standard deviation σ_{sd}^2. We remark that we keep consistency among

Channel		**SUI-3**					
Terrain Type	B		Tap 1	Tap 2	Tap 3	Tap 4	Tap 5
Doppler Spread	Low	Delay	0 μs	310 *ns*	710 *ns*	1090 *ns*	1730 *ns*
Spread	Low	Power (omni ant.)	0 *dB*	-1 *dB*	-9 *dB*	-10 *dB*	-15 *dB*
		90% K-factor (omni)	1 *dB*	0 *dB*	0 *dB*	0 *dB*	0 *dB*
		75% K-factor (omni)	7 *dB*	0 *dB*	0 *dB*	0 *dB*	0 *dB*
Line of Sight	Low	Power (30° ant.)	0 *dB*	-11 *dB*	-22 *dB*	-10 *dB*	-25.2 *dB*
		90% K-factor (30°)	3 *dB*	0 *dB*	0 *dB*	0 *dB*	0 *dB*
		75% K-factor (30°)	19 *dB*	0 *dB*	0 *dB*	0 *dB*	0 *dB*
		Doppler Spread	0.4 *Hz*	0.3 *Hz*	0.5 *Hz*	0.5 *Hz*	0.6 *Hz*
Antenna Correlation		$\rho_{ENV} = 0.4$					
Gain Reduction Factor		GRF = 3 *dB*					
Normalization Factor		$F_{omni} = -1.5113$ *dB*					
Omni Antenna		$\tau_{RMS} = 0.264$ μs					
Overall *K*		*K*=0.5 (90%); *K*=1.6 (75%)					
30^o Antenna		$\tau_{RMS} = 0.123$ μs					
Overall *K*		*K*=2.2 (90%); *K*=7.0 (75%)					
Max. Doppler Spread		50 *Hz*					
Coherence Time		20 *ms*					
Symbol Duration		0.1 *ms*					
Subcarrier Spacing		1000 *Hz*					
Pass-band Bandwidth		0.16 - 5.12 *GHz*					
Channel Bandwidth		0.8 – 2.56 *GHz*					
Subcarrier Bandwidth		2500 *Hz*					
Number of Subcarriers		32 – 1024					
Subcarrier Seperation		10.94 *KHz*					
Symbol Duration		102.86μs					
Number of OFDM Symbols		48 symbols per 5*ms* with CP 1/8 of the usefull symbol duration					
FFT Length		32 - 512					
User Distance		0 – 500 *m*					
Receive Antenna Beam Width		Omni directional (360^o) and 30^o with vertical polarization					
Coverage		90% cell coverage with 99.9% reliability at each location covered					
Cell Size		5 *Km*					
BS Antenna Height		20 - 30 *m*					
Receive Antenna Height		1 - 6 *m*					
BS Antenna Beam Width		120^o					
Speed		2 - 100 *Km/h*					

Table 3.2 - Channel specifications according to SUI-3 for pedestrian and vehicular enviroments.

comparisons between the examined schemes, by adopting identical channel, traffic and optimization conditions, i.e., all schedulers can handle delay constraints and are affected by

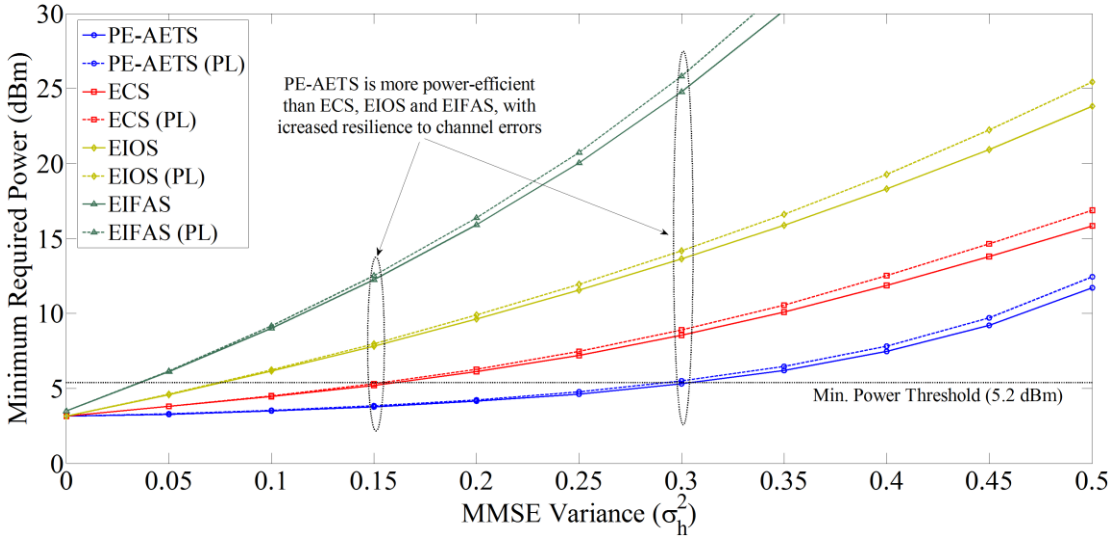

Figure 3.6 - Comparison regarding the power efficiency of PE-AETS: minimum required power versus the MMSE variance σ_h^2.

the same imperfect channel and outage conditions. Also, to clarify our simulations, in Appendix A.7 we study the impact of the channel imperfectness on the error-inconsiderate schemes EIOS [14], [20], [21], [22], [23] and EIFAS [27], [60]. However, we omit details regarding the performance gain due to multi-user diversity as they have been studied in [56]. We remark that the channel specifications have been set according to Stanford University Interim (SUI) channel model type SUI-3 [144] shown in Table 3.2. The SUI-3 channel specifications are used in IEEE 802.16 standard [5] and are considered appropriate for testing wireless systems for pedestrian and vehicular mobility in urban enviroments. Finally, all simulations have been obtained through using the programs developed by us in MatLab.

3.7.2 Simulation Results

In Figure 3.6, we consider a system with $(C_1, C_2, C_3, C_4, C_5) = (0,0,0,4,0)$, $P_{TOTAL} = 5.2\,dBm$ and homogeneous signal path-loss between users and BS with parameters $d_0 = 1m$, $d_{1,2,3,4} = 50\,m$, $\varpi = 3.5$ and $\sigma_{sd}^2 = 8\,dB$ [134]. It is obvious that EIFAS and EIOS are highly sensitive to the increase of the channel uncertainty. In fact, both schemes cannot provide the

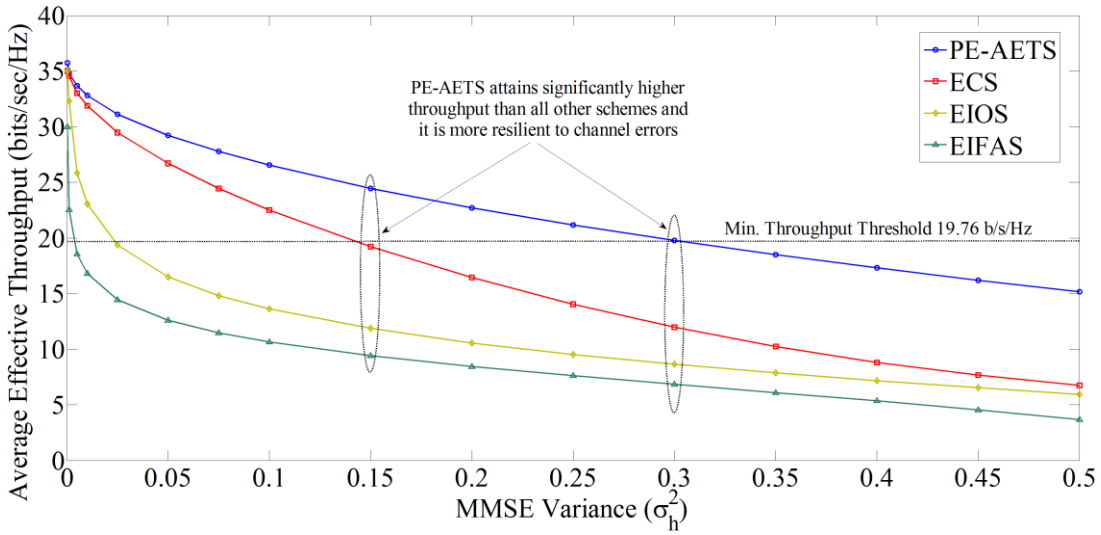

Figure 3.7 - Comparison regarding the throughput efficiency of PE-AETS: average effective throughput versus the MMSE variance σ_h^2.

minimum required throughput of 19.76*bits/sec/Hz* (see Table 3.1) even when channel uncertainty is very low, i.e., $\sigma_h^2 \geq 0.03$, as both schemes require more power than the available to the BS. On the other hand, ECS and PE-AETS perform better due to their imperfect channel considerations. Nevertheless, PE-AETS clearly outperforms ECS as it always requires less power than ECS to provide the desirable throughout. Actually, PE-AETS manages to satisfy all users under very high channel uncertainty, e.g., $\sigma_h^2 = 0.3$, where all other schemes require much higher power than $P_{TOTAL} = 5.2\ dBm$[22]. The same observations are made, when the signal path-loss between users and BS is heterogeneous, e.g., for $d_1 = 200\,m$, $d_2 = 400\,m$, $d_3 = 600\,m$ and $d_4 = 800\,m$. In this case, again PE-AETS notably outperforms ECS, EIOS and EIFAS, while all schemes require slightly more power than in the case with

[22] To clarify our model's behaviour at critical points of operation we set the value of the supplied power P_{TOTAL} congruent with the number of the heterogeneous system users and their parameters, i.e., at resource starvation we can have clear observations on the performance of the allocation descicion by setting $P_{TOTAL} = 5.2\ dBm$ and $C_4 = 4$. Similar way of simulations has been adopted in relevant studies such as [4], [15], [21], [24], [56], [114], [169]. One decibel per milli Watt (*dBm*) is computed by $dBmW = 10 \cdot \log_{10}\left(P\ /\ 1\,\text{mWatt}\right)$, where P is the terminus power [93].

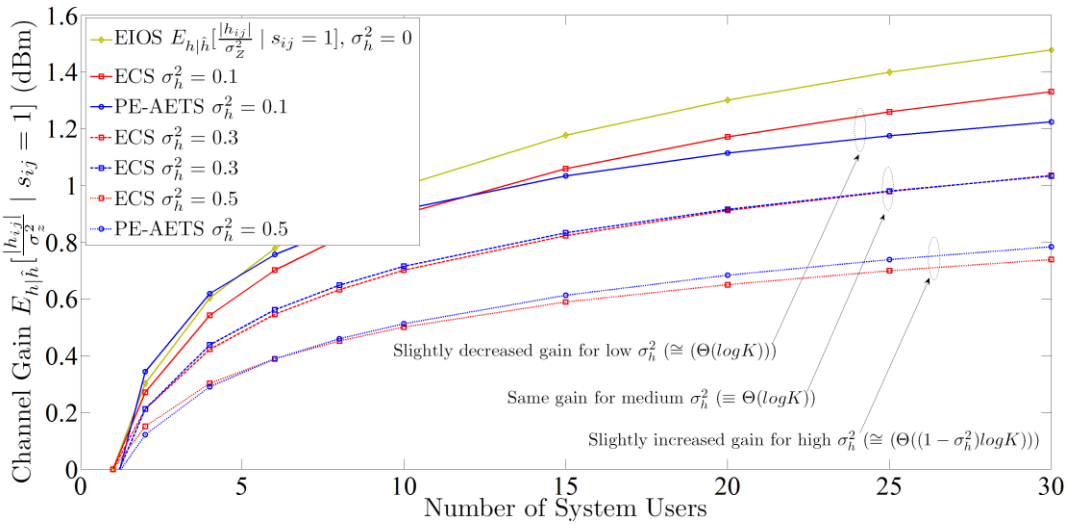

Figure 3.8 - Comparison regarding the throughput efficiency of PE-AETS: channel gain versus the number of system users.

homogeneous signal path-loss[23]. The corresponding throughput performance is shown in Figure 3.7, where PE-AETS achieves significantly higher throughput than ECS, EIOS and EIFAS under any imperfect conditions and it also provides the desirable minimum throughput at high channel uncertainty, e.g., $\sigma_h^2 > 0.3$. In addition, as depicted in Figure 3.8, thanks to opportunistic scheduling, PE-AETS appears to retain substantial throughput gain due to frequency (see Section 3.4.2) and multi-user diversity exploitation, attaining equivalent throughput gains to ECS and EIOS.

Moreover, we examine the throughput/power performance of each scheme for a larger system with $(C_1, C_2, C_3, C_4, C_5) = (1, 3, 3, 3, 0)$, where all users suffer from the same signal path-loss. From Figure 3.9a, we observe that for very low channel uncertainty from one hand all schemes satisfy the minimum required effective throughput of 128.62 *bits/sec/Hz* (see Table 3.1) but on the other hand each scheme has matching power values to result into

[23] In the following simulations, we shall omit illustrating the path-loss effect as it does not affect the behaviour of each of the examined schemes and also because large number of graphs presented in one figure may cause confusion.

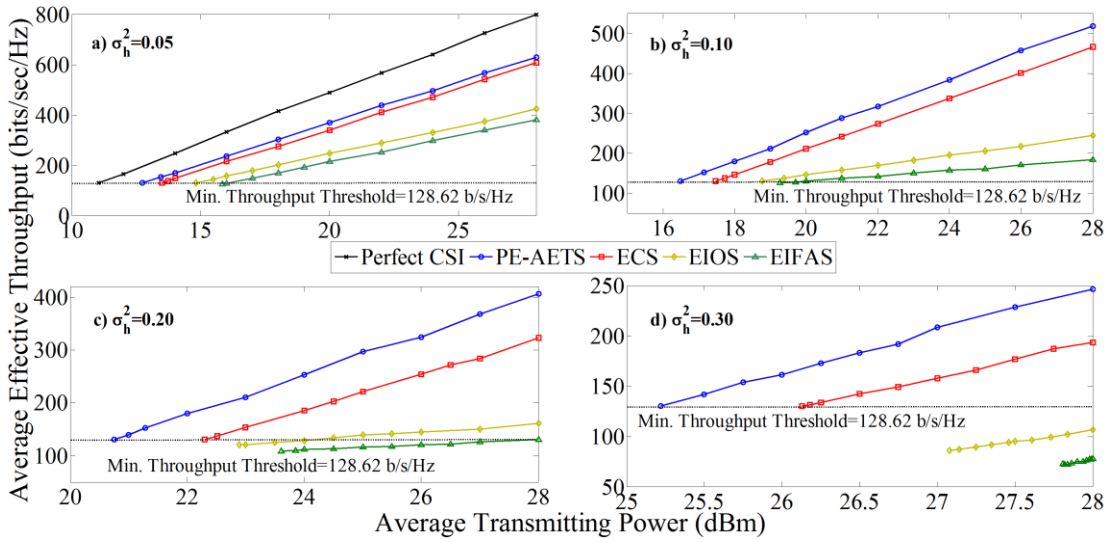

Figure 3.9 - Comparison regarding the power/throughput efficiency of PE-AETS: average effective throughput versus the average transmitting power.

different effective rates. Contrariwise, over a certain average effective throughput operation, each scheme needs extra power consumption as we swift from PE-AETS to EIFAS[24].

This difference between the power requirements of each scheme expands further when the channel uncertainty increases, as we notice from Figure 3.9b and Figure 3.9c. Figure 3.9d illustrates more obvious outlooks, where EIFAS and EIOS are unable to provide the minimum required effective throughput, while ECS maintains large deviations over PE-AETS's power/throughput curve witnessing that our scheduler bears supplementary resilience to channel error and achieves significantly power/throughput performance beyond all other schemes.

As the power/throughput efficiency and the endurance to channel errors of PE-AETS have been thoroughly demonstrated in Figure 3.6, Figure 3.7, Figure 3.8 and Figure 3.9, we

[24] Some values of the average effective throughput in Figure 3.9 may be unrealistic from a practical point of view. Nevertheless, such throughput/power performance regards the theoretical operation of the presented prototypes and implies on the comparison of each of the examined scheduler's performance at large scale practical systems, i.e., for WiMAX networks with $K > 1000$ and $N_F = 4096$. In addition, for fair comparisons and to keep consistency with relevant works, our simulation settings comply with those in [14], [17], [20], [21], [22], [23], [24], [27], [56], [60].

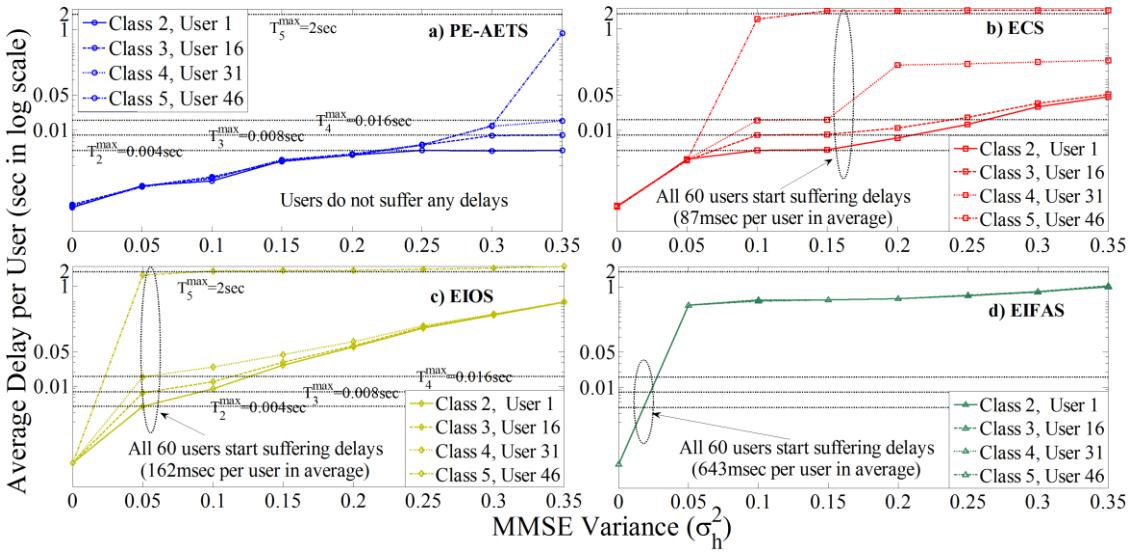

Figure 3.10 - Comparison regarding the QoS efficiency of PE-AETS: average delay per system user versus the MMSE variance σ_h^2.

shall now inspect our scheduler's QoS performance under more realistic conditions. We consider a large-scale system of 1024 subcarriers and 60 users of classes $(C_1, C_2, C_3, C_4, C_5) = (0, 15, 15, 15, 15)$. The BS is supplied with $P_{TOTAL} = 30\,dBm$ of power and the channel has total bandwidth $BW = 2.56\,MHz$. We also apply high signal path-loss by setting large distances between users and BS, e.g., $d_{1-15} = 200\,m$, $d_{16-30} = 300\,m$, $d_{31-45} = 400\,m$ and $d_{45-60} = 500\,m$. In Figure 3.10, we increase the channel uncertainty and examine the average delay of users 1, 16, 31 and 46 of Class 2, 3, 4 and 5, respectively[25]. We observe that the opportunistic schedulers PE-AETS, ECS and EIOS deliberate penalize the delay performance of the more delay tolerant user 46 to maintain the desired QoS of the less delay

[25] The average delay $E[D_j]$ per user j can be computed as follows; if $r_{required} > r_{P_{TOTAL}}$ then $E[D_j] = \left(\left(r_{required} - r_{P_{TOTAL}} \right) / K \right) \cdot t_s \cdot \left(BW / N_F \right)$ in *secs*, where $r_{P_{TOTAL}}$ is the sum of the rates of all users exploiting only the total available power at the BS P_{TOTAL} and $r_{required}$ is the sum of the rates of all users computed based on P_{TOTAL} plus any extra required power P_{extra} to support users' minimum QoS requirements e.g., $P_{extra} + P_{TOTAL}$.

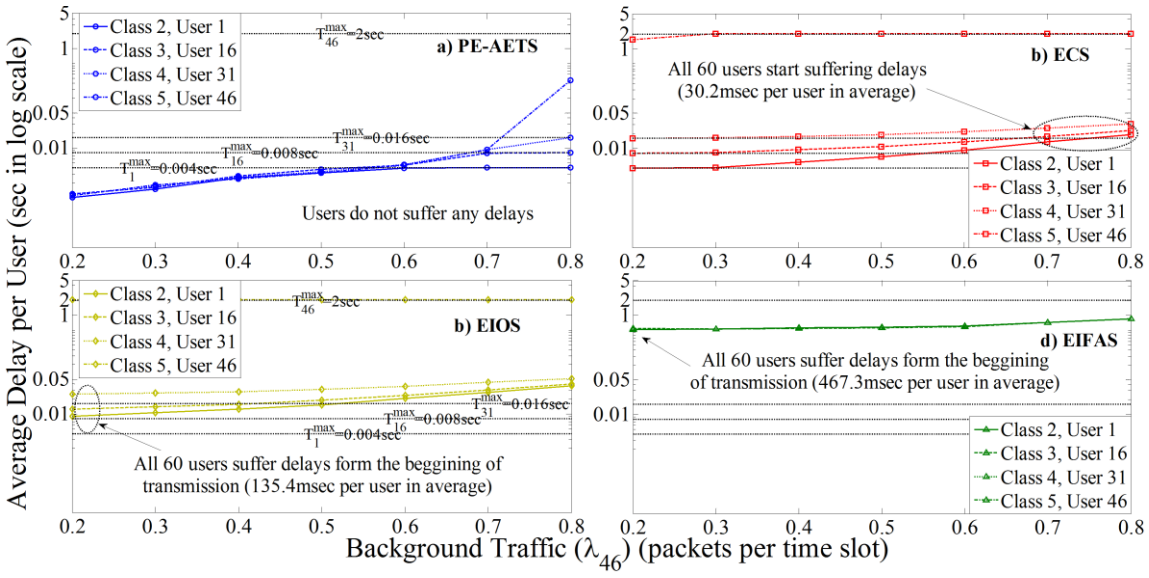

Figure 3.11 - Comparison regarding the QoS efficiency of PE-AETS: average delay per system user versus the background traffic λ_{46}.

tolerant users 1, 16 and 31, while the non-opportunistic EIFAS does not provide sufficient QoS guarantees. Nevertheless, it is straightforward that PE-AETS exhibits substantially better QoS performance over all other schedulers, as it is the only scheme where all 60 users have delays less than their the maximum delay tolerance $T_j^{\max}$. In contrary, all users suffer by 87*msec*, 162*msec* and 643*msec* average delays under ECS, EIOS and EIFAS operation.

Similar conclusions are made by inspecting in Figure 3.11, the average delay of the referenced users 1, 16, 31 and 46 versus the system's background traffic (traffic arrival rate of user 46, e.g., λ_{46}) under average channel uncertainty, e.g., $\sigma_h^2 = 0.1$. As user 46 becomes more delay-sensitive, ECS, EIOS and EIFAS require more power than the supplied to the BS to satisfy all users' minimum requirements hence, they deliver 30.2*msec*, 135.4*msec* and 467.3*msec* average delay to all 60 users, respectively. On the other hand, the supplied power to the BS, e.g., $P_{TOTAL} = 30\,dBm$, is more than enough for PE-AETS to provide ideal QoS to all users.

In sum, PE-AETS maintains better enchantments over relative schemes, in terms of power/throughput and QoS performance due to its increased resilience to channel errors.

3.8 Conclusion

In this research part, we proposed a power-efficient cross-layer scheduling scheme to provide performance enhancements in OFDMA systems with imperfect channel, packet outage and heterogeneous users considerations. Initially, we presented the imperfect channel model with its estimation procedure and we introduced a PBL process to describe the average effective data rate at the PHY layer. In continue, we performed theoretical and practical comparisons to show that our PBL process has important advantages over the existed goodput-rate oriented PBL process. Furthermore, we correlated each user's delay constraints from the upper layers with its PHY layer parameters through expressing each user's traffic at its $M/G/1/\infty/\infty$ queue, with an equivalent throughput to its PHY layer. We then formulated a cross-layer optimization problem targeting to minimize the average transmitting power subject to subcarrier, power and QoS constraints. Through applying subcarrier time-sharing relaxation, we show that our cross-layer optimization problem can be transformed into a convex optimization problem and we derived its optimal solutions via the Lagrangian optimization methodology. The proposed joint optimal adaptive power and dynamic subcarrier allocation policy has low linear complexity and performs asymptotically in terms of throughput gain due to multi-user and multi-carrier diversity exploitations. With simulation comparisons we finally demonstrated that the proposed PE-AETS has superior scheduling versatility than relevant schemes as it significantly reduces the overall transmitting power by simultaneously providing ideal QoS to heterogeneous users under very uncertain channel conditions.

Appendix A

A.1 Details on Channel Modelling

In this Appendix, we provide details for the downlink channel model in Section 3.3.1 in order to present our channel modelling in its full measure.

The elements $\mathbf{h}_j(n)=\left[h_{1j}(n),...,h_{ij}(n),...,h_{N_F j}(n)\right]^{\mathcal{T}}$ of $\mathbf{H}(n)$ are the $N_F \times 1$ channel gain vectors with entries the complex-valued channel fading random processes of user j. For example, the channel fading random process of user j on subcarrier i is given by

$$h_{ij}(n)=\sum_{\theta=0}^{\Theta} h_{j\theta}(n)e^{-\mathcal{J}2\pi i\Theta/N_F}\ , \tag{3.45}$$

where $\mathcal{J}$ indicates the imaginary part of a number. The set $\left\{h_{j\theta}(n)\right\}$ in (3.45), where $\{\cdot\}$ is the set notation, represents the Θ multiple paths for the j-th user in time domain $h_{j\theta}(n)$, which are CSCG distributed with zero mean and $\sigma_{j\theta}^2$ variance, e.g., $\mathcal{CN}\left(0,\sigma_{j\theta}^2\right)$. Moreover, each $h_{j\theta}(n)$ is modelled as a stationary and ergodic discrete-time random process meaning that $h_j(n)$ is also stationary and hence, the distribution of $\mathbf{h}_j(n)$ is independent of the OFDM block index n [59]. For this reason as well as for notational brevity we will drop the index n when it does not cause confusion.

The multiple paths are independent across the K users and correlated between subcarriers. For example, the covariance matrix of the multiple paths between the i-th and i'-th subcarrier of user j is written as

$$E\left[h_{ij}h_{i'j}^{\mathcal{H}}\right]=\frac{1}{\Theta}\cdot\left(\frac{1-e^{-\mathcal{J}2\pi\Theta(i-i')/N_F}}{1-e^{-\mathcal{J}2\pi(i-i')/N_F}}\right), \tag{3.46}$$

where $E[\cdot]$ denotes the expected value of the quantity over the ergodic realizations $h_{j\theta}$ and $[\cdot]^{\mathcal{H}}$ denotes Hermitian transpose.

Furthermore, we assume that the channel is invariant over the duration of each OFDM block hence, the channel's impulse response between the BS and the j-th user can be modelled as an Θ-th order Finite Impulse Response (FIR) filter with the coefficients the channel fading random process h_{ij} distributed as $h_{ij} \sim \left(0, \frac{1}{\Theta}\right)$ [59]. From block n to block n' the channel is slowly time varying and the channel gain vector $\mathbf{h}_j(n)$ follows the Jake's model [145], with covariance matrix $\mathbf{M}_h$ given by

$$\mathbf{M}_h = E\left[\mathbf{h}_j(n)\mathbf{h}_j^{\mathcal{H}}(n')\right] = \frac{I_0\left(2\pi f_d |n-n'| t_s\right)}{\Theta}\mathbf{I}_\Theta . \tag{3.47}$$

In (3.47) the notation $I_0(\cdot)$ denotes the zero-order Bessel function of the first kind, f_d the Doppler frequency, t_s the block duration and $\mathbf{I}_{(\cdot)}$ denotes the identity matrix.

A.2 Channel Error Covariance Matrix and MMSE Variance - Proof of *Theorem 3.1*

We recall that in our estimation process, the block of ς pilot symbols is transmitted at the beginning of every frame that contains Θ_{FR} OFDM symbols. Based on the ς pilot symbols, we can write the received pilot block vector of length $\varsigma \times 1$ as $\mathbf{y}_\varsigma(\rho) = \left[\mathbf{y}^{\mathcal{T}}(\rho \cdot \Theta_{FR}), ..., \mathbf{y}^{\mathcal{T}}\left(\left(\rho - (\varsigma - 1)\right) \cdot \Theta_{FR}\right)\right]^{\mathcal{T}}$ [26]. We can then perform ρ measurements to obtain the correlation of the scalar complex channel coefficients $\mathbf{h}$ at the frequency domain. It is noted that the complex-valued vector $\mathbf{y}(n)$ in (3.1) that describes the

[26] We omit the user index j in Appendix A.2 to avoid confusion.

channel coefficients for each user j during the n-th OFDM block, has now length $n \cdot \Theta_{FR}$, and can be written as

$$\mathbf{y}\left(n \cdot \Theta_{FR}\right) = \sqrt{N_F}\boldsymbol{\Sigma}\mathbf{W}_{\Theta}\mathbf{h}\left(n \cdot \Theta_{FR}\right) + \mathbf{z}\left(n \cdot \Theta_{FR}\right). \tag{3.48}$$

The $N_F \times N_F$ matrix $\boldsymbol{\Sigma}$ in (3.48) is given by $\boldsymbol{\Sigma} = diag\left(\varsigma_{1t},...,\varsigma_{it},...,\varsigma_{N_F t}\right)$ with entries the pilot symbols on each subcarrier at time instance t, e.g., ς_{it} is the pilot block on subcarrier i at time instance t. In addition, the $N_F \times \Theta$ matrix $\mathbf{W}_{\Theta}$ in (3.48) is the truncated unit-norm FFT matrix with entries $\left[\mathbf{W}_{\Theta}\right]_{i\theta} = \frac{1}{\sqrt{N_F}} \cdot e^{-\mathcal{J}(2\pi/N_F)i\theta}$, $i = 1,...,N_F$, $\theta = 1,...,\Theta$. For the ease of presentation, we shall compute in closed form the error covariance matrix $\mathbf{M}_{\Delta h}$ as follows.

Let us assume constant modulus pilot symbols[27] given as $\left|\varsigma_{1t}\right|^2 = ... = \left|\varsigma_{N_F t}\right|^2 = P_t$, where P_t denotes the uplink transmitting power for the CSIT estimation at time instance t. We can then define the MMSE estimator as a function $\mathbf{h}\left(\left(\rho + \delta\right)\Theta_{FR}\right)$ to estimate the channel coefficient $\mathbf{h}\left(\left(\rho + \delta\right)\Theta_{FR}\right)$ by $\hat{\mathbf{h}}$ through $\left(\rho + \delta\right)\Theta_{FR}$ measurements. By assuming that the channel gains are independent of noise, we compute the MMSE estimator as the solution of the following system of equations

$$\mathbf{M}_y \mathbf{W}_{\Theta} = \mathbf{M}_{yx}, \tag{3.49}$$

where $\mathbf{M}_y = E\left(\mathbf{y}\mathbf{y}^{\mathcal{H}}\right)$ in (3.49) is the auto-correlation matrix of the received signal and $\mathbf{M}_{yx} = E\left(\left(\sqrt{N_F}\boldsymbol{\Sigma}\mathbf{W}_{\Theta}^{\mathcal{H}}\right)\mathbf{y}^{\mathcal{H}}\right)$ the cross-correlation matrix between the received and transmitted OFDM symbols. The MMSE of $\mathbf{h}\left(\left(\rho + \delta\right)\Theta_{FR}\right)$ is given as

$$\hat{\mathbf{h}} = \mathbf{F}^{\mathcal{H}}\mathbf{y}, \tag{3.50}$$

[27] We assume a uniform power delay profile to clarify our derivations that follow. However, our results can be applied to non-uniform power delay profiles such as exponential power delay profile.

with $\mathbf{F}$ in (3.50) to denote the optimal filter. The error covariance matrix for the Minimum Square Error (MSE) estimator is as shown below

$$\begin{aligned}
\mathbf{M}_{\Delta h} &= E\left[\Delta\hat{\mathbf{h}}\Delta\hat{\mathbf{h}}^{\mathcal{H}}\right] = E\left[\left(\sqrt{N_F}\boldsymbol{\Sigma}\mathbf{W}_{\Theta}\mathbf{h} - \sqrt{N_F}\hat{\boldsymbol{\Sigma}}\hat{\mathbf{W}}_{\Theta}\right)\left(\sqrt{N_F}\boldsymbol{\Sigma}\mathbf{W}_{\Theta}\mathbf{h} - \sqrt{N_F}\hat{\boldsymbol{\Sigma}}\hat{\mathbf{W}}_{\Theta}\right)^{\mathcal{H}}\right] \\
&= E\left[\left(\sqrt{N_F}\boldsymbol{\Sigma}\mathbf{W}_{\Theta}\mathbf{h} - \sqrt{N_F}\hat{\boldsymbol{\Sigma}}\hat{\mathbf{W}}_{\Theta}\right)\left(\left(\sqrt{N_F}\boldsymbol{\Sigma}\mathbf{W}_{\Theta}\mathbf{h}\right)^{\mathcal{H}} - \mathbf{y}^{\mathcal{H}}\mathbf{F}\right)\right] \\
&\overset{(a)}{=} E\left[\left(\sqrt{N_F}\boldsymbol{\Sigma}\mathbf{W}_{\Theta}\mathbf{h} - \sqrt{N_F}\hat{\boldsymbol{\Sigma}}\hat{\mathbf{W}}_{\Theta}\right)\left(\sqrt{N_F}\boldsymbol{\Sigma}\mathbf{W}_{\Theta}\mathbf{h}\right)^{\mathcal{H}}\right] - E\left[\left(\sqrt{N_F}\boldsymbol{\Sigma}\mathbf{W}_{\Theta}\mathbf{h} - \sqrt{N_F}\hat{\boldsymbol{\Sigma}}\hat{\mathbf{W}}_{\Theta}\right)\mathbf{y}^{\mathcal{H}}\right]\mathbf{F} \\
&= E\left[\left(\sqrt{N_F}\boldsymbol{\Sigma}\mathbf{W}_{\Theta}\mathbf{h} - \mathbf{F}^{\mathcal{H}}\mathbf{y}\right)\left(\sqrt{N_F}\boldsymbol{\Sigma}\mathbf{W}_{\Theta}\mathbf{h}\right)^{\mathcal{H}}\right] \\
&= \mathbf{M}_x - \mathbf{F}^{\mathcal{H}}\mathbf{M}_{yx}
\end{aligned} \tag{3.51}$$

where $\mathbf{M}_x = E\left(\left(\sqrt{N_F}\boldsymbol{\Sigma}\mathbf{W}_{\Theta}\mathbf{h}\right)\left(\sqrt{N_F}\boldsymbol{\Sigma}\mathbf{W}_{\Theta}\mathbf{h}\right)^{\mathcal{H}}\right)$ in (3.51) is the auto-correlation matrix of the received symbol including the pilot symbols. The zero matrix on the right hand side of equation shown with (a) in (3.51) is due to the orthogonality condition of the optimal estimator.

Next, we explicitly calculate the estimator in terms of $\mathbf{h}$, $\mathbf{M}_x$ and the noise covariance matrix $\mathbf{M}_z$, which, as we have assumed constant modulus pilot symbols of transmitting power P_t and Θ paths for each of the N_F subcarriers, is written as

$$\mathbf{M}_z = E\left(\mathbf{z}\mathbf{z}^{\mathcal{H}}\right) = \frac{N_F \cdot P_{\varsigma}}{\Theta \cdot \sigma_z^2}\mathbf{I}_{\varsigma}. \tag{3.52}$$

Moreover, the following relationships can be easy verified [59].

$$\mathbf{M}_y = \mathbf{h}\mathbf{M}_x\mathbf{h}^{\mathcal{H}} + \mathbf{M}_z, \tag{3.53}$$

where $\mathbf{h}\mathbf{M}_x\mathbf{h}^{\mathcal{H}}$ is a $\varsigma \times \varsigma$ matrix, e.g., $\mathbf{M}_{\varsigma} = \mathbf{h}\mathbf{M}_x\mathbf{h}^{\mathcal{H}}$, with (i,i') entry $J_0\left(2\pi f_d \left|i-i'\right|\Theta_{FR}t_s\right)$ to denote the correlation between the received symbols based on the time-varying actual channel gain and the ς pilot symbols and

$$\mathbf{M}_{yx} = \mathbf{h}\mathbf{M}_x = \mathbf{x}_{\mathbf{M}_{\varsigma}}, \tag{3.54}$$

where $\mathbf{x}_{\mathbf{M}_{\varsigma}}$ in (3.54) is the $\varsigma \times 1$ vector that denotes the correlation between the incoming OFDM symbols on the multiple paths, which is based on the ς pilot symbols and our

$(\rho+\delta)\Theta_{FR}$ measurements, e.g., $\mathbf{x}_{\mathbf{M}_\varsigma}=\left[J_0\left(2\pi f_d\rho\Theta_{FR}t_s\right),...,J_0\left(2\pi f_d\left(\rho-(\varsigma-1)\right)\Theta_{FR}t_s\right)\right]^{\mathcal{T}}$.

Then the optimal filter $\mathbf{F}$ is given by

$$\begin{aligned}\mathbf{F}&=\left(\mathbf{h}\mathbf{M}_x\mathbf{h}^{\mathcal{H}}+\mathbf{M}_z\right)^{-1}\mathbf{h}\mathbf{M}_x\\&=\left(\mathbf{M}_\varsigma+\mathbf{M}_z\right)^{-1}\mathbf{x}_{\mathbf{M}_\varsigma}\end{aligned}. \tag{3.55}$$

Applying FFT, and accounting (3.52), (3.55) the MMSE estimator matrix is computed as

$$\begin{aligned}\hat{\mathbf{h}}&=\mathbf{F}^{\mathcal{H}}\mathbf{y}\mathbf{W}_\Theta\mathbf{W}_\Theta^{\mathcal{H}}\\&=\mathbf{M}_x\mathbf{h}^{\mathcal{H}}\left(\mathbf{h}\mathbf{M}_x\mathbf{h}^{\mathcal{H}}+\mathbf{M}_z\right)^{-1}\mathbf{y}\mathbf{W}_\Theta\mathbf{W}_\Theta^{\mathcal{H}}\\&=\mathbf{x}_{\mathbf{M}_\varsigma}^{\mathcal{H}}\left(\mathbf{M}_\varsigma+\frac{\Theta\cdot\sigma_z^2}{N_F\cdot P_\varsigma}\mathbf{I}_\varsigma\right)^{-1}\mathbf{x}_{\mathbf{M}_\varsigma}\mathbf{W}_\Theta\mathbf{W}_\Theta^{\mathcal{H}}\end{aligned} \tag{3.56}$$

and its error covariance $\mathbf{M}_{\Delta h}$ from (3.51) can be written as

$$\begin{aligned}\mathbf{M}_{\Delta h}&=E\left[\Delta\hat{\mathbf{h}}\Delta\hat{\mathbf{h}}^{\mathcal{H}}\right]\\&=\frac{N_F}{\Theta}\left(\mathbf{M}_x-\mathbf{M}_x\mathbf{h}^{\mathcal{H}}\left(\mathbf{h}\mathbf{M}_x\mathbf{h}^{\mathcal{H}}+\mathbf{M}_z\right)^{-1}\mathbf{h}\mathbf{M}_x\mathbf{W}_\Theta\mathbf{W}_\Theta^{\mathcal{H}}\right),\\&=\frac{N_F}{\Theta}\left(1-\mathbf{x}_{\mathbf{M}_\varsigma}^{\mathcal{H}}\left(\mathbf{M}_\varsigma+\frac{\Theta\cdot\sigma_z^2}{N_F\cdot P_\varsigma}\mathbf{I}_\varsigma\right)^{-1}\mathbf{x}_{\mathbf{M}_\varsigma}\mathbf{W}_\Theta\mathbf{W}_\Theta^{\mathcal{H}}\right)\end{aligned} \tag{3.57}$$

With some manipulations, the covariance in (3.57) yields (3.7) and (3.8) in *Theorem 3.1*. This completes the proof of *Theorem 3.1*. ■

Clarifications on the estimation process: If we had followed the mean feedback channel adopted in [24], [56], [18], [58], [57], the error covariance in (3.57) would have been of the form, e.g., $\mathbf{M}'_{\Delta h}=\frac{N_F}{\Theta}\left(1-\left(\frac{\Theta\cdot\sigma_z^2}{N_F\cdot P_\varsigma}\mathbf{M}_\varsigma\mathbf{I}_\varsigma\right)^{-1}\mathbf{W}_\Theta\mathbf{W}_\Theta^{\mathcal{H}}\right)$. It is easy to verify that $\mathbf{M}'_{\Delta h}$ would be a scalar multiple of the identity matrix $\mathbf{I}_\varsigma$ and hence, its diagonal entries, e.g., the channel errors Δh_{ij}, would be equal meaning i.i.d, e.g.,

$$\mathbf{M}'_{\Delta h}=\frac{N_F}{\Theta}\left(1-\left[\frac{\Theta\cdot\sigma_z^2}{N_F\cdot P_\varsigma}\times\begin{bmatrix}\alpha & 0 & \cdots & 0\\ 0 & \alpha & & 0\\ \vdots & & \ddots & \vdots\\ 0 & 0 & \cdots & \alpha\end{bmatrix}\times\begin{bmatrix}1 & 0 & \cdots & 0\\ 0 & 1 & & 0\\ \vdots & & \ddots & \vdots\\ 0 & 0 & \cdots & 1\end{bmatrix}\right]^{-1}\times\mathbf{W}_\Theta\mathbf{W}_\Theta^{\mathcal{H}}\right)=\begin{bmatrix}\hat{\alpha} & 0 & \cdots & 0\\ 0 & \hat{\alpha} & & 0\\ \vdots & & \ddots & \vdots\\ 0 & 0 & \cdots & \hat{\alpha}\end{bmatrix}.$$

Consequently, we would have had a sphericity non-adaptive estimation pattern as the error on each subcarrier would not have been estimated separately regardless each subcarrier's conditions. In contrary, from (3.57) it is straightforward that due to the vectors $\mathbf{x}_{\mathbf{M}_\varsigma}$ and $\mathbf{x}^{\mathcal{H}}_{\mathbf{M}_\varsigma}$, and the matrix $\mathbf{M}_\varsigma$, our error covariance matrix $\mathbf{M}_{\Delta h}$ is not scalar multiple of the identity matrix $\mathbf{I}_\varsigma$. This means that in our case the channel errors Δh_{ij}, would not be equal or in other words non-i.i.d. The reason is that in our case we perform estimations considering the conditions of each multi-path subcarrier meaning that our MMSE estimator valuates adaptively and thus more precisely the error correlation, e.g.,

$$\mathbf{M}_{\Delta h}=\frac{N_F}{\Theta}\left(1-\left(\begin{bmatrix}\alpha_1 & 0 & \cdots & 0\\ 0 & \alpha_2 & & 0\\ \vdots & & \ddots & \vdots\\ 0 & 0 & \cdots & \alpha_\varsigma\end{bmatrix}+\begin{bmatrix}\frac{\Theta\cdot\sigma_z^2}{N_F\cdot P_\varsigma} & 0 & \cdots & 0\\ 0 & \frac{\Theta\cdot\sigma_z^2}{N_F\cdot P_\varsigma} & & 0\\ \vdots & & \ddots & \vdots\\ 0 & 0 & \cdots & \frac{\Theta\cdot\sigma_z^2}{N_F\cdot P_\varsigma}\end{bmatrix}\right)^{-1}\times\begin{bmatrix}b_{1,\varsigma}\\ b_{2,\varsigma}\\ \vdots\\ b_{(\rho+\delta)\Theta_{FR},\varsigma}\end{bmatrix}\times\mathbf{W}_\Theta\mathbf{W}_\Theta^{\mathcal{H}}\right)$$

$$=\begin{bmatrix}\hat{\delta}_{1,\varsigma} & 0 & \cdots & 0\\ 0 & \hat{\delta}_{2,\varsigma} & & 0\\ \vdots & & \ddots & \vdots\\ 0 & 0 & \cdots & \hat{\delta}_{(\rho+\delta)\Theta_{FR},\varsigma}\end{bmatrix}$$

Therefore, we can perform non-sphericity estimations in contrast to the mean feedback channel, where the assumption of sphericity is fundamental. In practice this difference has major implication to the overall system's performance; it is obvious that, regardless the efficiency of the resource scheduler, if the MMSE variance is lumpy acquired then the scheduler would take its allocation decision on a mistaken basis.

A.3 Instantaneous Effective Data Rate – Proof of *Theorem 3.2*

From (3.10) in Section 3.4.1, it is straightforward that the actual PDF $p\left(E\left[W\left(x_{ij};y_{ij}\middle|\hat{h}_{ij}\right)\right]\right)$ of the actual instantaneous mutual information $E\left[W\left(x_{ij};y_{ij}\middle|\hat{h}_{ij}\right)\right]$ in (3.14) has mean given by $\log_2\left(1+\left(\left|\hat{h}_{ij}\right|^2 p_{ij}/\sigma_Z^2\right)\right)$ and variance $2\left|\hat{h}_{ij}\right|^2 p_{ij}^2\sigma_h^2/\left(\left|\hat{h}_{ij}\right|^2 p_{ij}+\sigma_z^2\right)^2$. Based on the actual PDF in (3.14), we can compute the condition in (3.15) by the following series expansion [146]

$$\int_0^{r_{ij}} p\left(E\left[W\left(x_{ij};y_{ij}\middle|\hat{h}_{ij}\right)\right]\right)dW=\int_0^{r_{ij}}\frac{\sigma_z^2}{p_{ij}\sigma_h^2}\exp\left(\left(W-\frac{\left|\hat{h}_{ij}\right|^2}{\sigma_h^2}-\frac{\sigma_z^2}{p_{ij}\sigma_h^2}\right)\left(\exp(W)-1\right)\right)$$
$$\times I_0\left(2\sqrt{\frac{\left|\hat{h}_{ij}\right|^2\sigma_z^2}{p_{ij}\sigma_h^4}\left(\exp(W)-1\right)}\right)dW$$

$$=\int_0^{\exp(r_{ij})-1}\frac{\sigma_z^2}{p_{ij}\sigma_h^2}\cdot\exp\left(\left(-\frac{\left|\hat{h}_{ij}\right|^2}{\sigma_h^2}-\frac{\sigma_z^2}{p_{ij}\sigma_h^2}W'\right)\sum_{\alpha=0}^{\infty}\frac{\left(\frac{\left|\hat{h}_{ij}\right|^2\sigma_z^2}{p_{ij}\sigma_h^4}W'\right)^{\alpha}}{(\alpha!)^2}dW'\right)$$

$$=\exp\left(\frac{\sigma_z^2-p_{ij}\left|\hat{h}_{ij}\right|^2-\left(\sigma_z^2\cdot\exp\left(r_{ij}\right)\right)}{p_{ij}\sigma_h^2}\right)$$
$$\times\sum_{\beta=0}^{\mathrm{B}}\sum_{\alpha=0}^{\beta-1}\left(\frac{\left(\frac{\left|\hat{h}_{ij}\right|^2}{\sigma_h^2}\right)^{\alpha}}{\alpha!}\cdot\left(\frac{\left(\frac{\sigma_z^2\left(\exp\left(r_{ij}\right)-1\right)}{p_{ij}\sigma_h^2}\right)^{\beta}}{\beta!}\right)+o\left(\frac{\left(\frac{\left|\hat{h}_{ij}\right|^2}{\sigma_h^2}\right)^{\mathrm{B}}}{\mathrm{B}!}\right)=1-P_{out} \quad , (3.58)$$

where $o(\cdot)$ is the small-*O* notation. Evaluating the series expansion in (3.58) we notice that if the MMSE variance σ_h^2 is smaller or equal than the term $p_{ij} / \left|\hat{h}_{ij}\right|^2 \sigma_z^2$, e.g., $\sigma_h^4 \le p_{ij} / \left|\hat{h}_{ij}\right|^2 \sigma_z^2$, the new condition in (3.58) can be well approximated by a Gaussian PDF with the same mean and variance, e.g.,

$$E\left[\tilde{W}\left(x_{ij}; y_{ij} \left| \hat{h}_{ij} \right.\right)\right] \sim \mathcal{N}\left(\log_2\left(1+\frac{\left|\hat{h}_{ij}\right|^2 p_{ij}}{\sigma_z^2}\right), \frac{2\left|\hat{h}_{ij}\right|^2 p_{ij}^2 \sigma_h^2}{\left(\left|\hat{h}_{ij}\right|^2 p_{ij} + \sigma_z^2\right)^2}\right). \tag{3.59}$$

The limitation $\sigma_h^4 \le p_{ij} / \left|\hat{h}_{ij}\right|^2 \sigma_z^2$ defines the validity of our approximation in (3.59) and can be written in terms of Signal-to-Noise Ratio (SNR), e.g., $\sigma_h^2 \le \sqrt{SNR_{ij} / \left|\hat{h}_{ij}\right|^2}$, with SNR_{ij} to be given by $SNR_{ij} = p_{ij}\left|\hat{h}_{ij}\right|^2 / \sigma_z^2$. Valuating the limitation $\sigma_h^2 \le \sqrt{SNR_{ij} / \left|\hat{h}_{ij}\right|^2}$ we observe that our approximation in (3.59) is not satisfied only under extremely poor channel conditions that practically never occur in reality due to, i.e., network's infrastructure. For example, for noise variance equal to one, e.g., $\sigma_z^2 = 1$, and assuming that SNR is 10*dB* then the MMSE error variance should be smaller or equal than 5.4, e.g., $\sigma_h^2 \le 5.4$, which corresponds to tremendously high channel error [28]. Hence, from the condition in (3.15) and $\tilde{W}\left(x_{ij}; y_{ij} \left| \hat{h}_{ij} \right.\right)$ in (3.59), which represents the approximated instantaneous mutual information between input x_{ij} and output y_{ij} given the estimated channel gain $\hat{h}_{ij}$ of user j on subcarrier i, we obtain the approximated instantaneous effective data rate $\tilde{r}_{ij}$ of user j on subcarrier i as presented in (3.16) in *Theorem 3.2*.

Let us now validate the accuracy of the approximated instantaneous effective data rate $\tilde{r}_{ij}$ given by (3.16) in *Theorem 3.2*, over a Rayleigh flat-fading channel. To examine the accuracy, we have to compare the performance of the approximated instantaneous effective

[28] Similar observations have been reported in [16] for single-user OFDM systems.

data rate $\tilde{r}_{ij}$ in (3.16) in *Theorem 3.2* (derived by the approximated instantaneous mutual information $E\left[\tilde{W}\left(x_{ij};y_{ij}\left|\hat{h}_{ij}\right.\right)\right]$ in (3.59)) and its exact expression r_{ij} in (3.14). The exact expression of the actual instantaneous effective data rate r_{ij} can be defined by relying on the equation (3.58) as it has been derived by the actual PDF of the instantaneous mutual information $E\left[W\left(x_{ij};y_{ij}\left|\hat{h}_{ij}\right.\right)\right]$ in (3.14). We remark that this evaluation also reveals the impact of the MMSE variance σ_h^2 on the approximated instantaneous effective data rate $\tilde{r}_{ij}$ given in (3.16) in *Theorem 3.2*. The exact expression of the actual instantaneous effective data rate r_{ij} over a Rayleigh flat-fading channel can be found as follows.

Based on the MMSE estimator presented in Section 3.3.2, we suppose that the MMSE channel estimation error $\Delta\hat{h}_{ij}$ of user j on subcarrier i is given by $\Delta\hat{h}_{ij}=h_{ij}-\hat{h}_{ij}$ and it is CSGC distributed with zero mean and σ_h^2 variance, e.g., $\Delta\hat{h}_{ij}\sim\mathcal{CN}\left(0,\sigma_h^2\right)$. We additionally assume that the MMSE channel estimation error $\Delta\hat{h}_{ij}$ is independent from the estimated channel gain $\hat{h}_{ij}$ of user j on subcarrier i. Then the channel estimator satisfies that the estimated channel gain $\hat{h}_{ij}$ is also CSGC distributed with zero mean and variance given by $1-\Delta\hat{h}_{ij}$ e.g., $\hat{h}_{ij}\sim\mathcal{CN}\left(0,1-\Delta\hat{h}_{ij}\right)$. Then, given the target data outage probability P_{out}, we use the condition in (3.58) to compute the exact expression of the average instantaneous effective data rate r_{ij} of user j on subcarrier i, averaged over the ergodic realizations of the estimated channel gains $\left\{\hat{h}_{ij}\right\}$, as follows.

$$r_{ij} = E_{\hat{h}_{ij}}\left[r_{ij}\right] \cong E_{\hat{h}_{ij}}\left[\log_2\left(1+\frac{\left|\hat{h}_{ij}\right|^2 p_{ij}}{\sigma_z^2}\right) - \frac{p_{ij}\sigma_h^2 Q^{-1}\left(1-P_{out}\right)\sqrt{\frac{2\left|\hat{h}_{ij}\right|^2}{\sigma_h^2}}}{\left|\hat{h}_{ij}\right|^2 p_{ij}+\sigma_z^2}\right]$$

$$= \int_0^{\infty}\left(\log_2\left(1+\frac{p_{ij}x}{\sigma_z^2}\right) - \frac{p_{ij}\sqrt{2\sigma_h^2 x}}{p_{ij}x+\sigma_z^2}Q^{-1}\left(1-P_{out}\right)\right)\times\frac{1}{1-\sigma_h^2}\exp\left(\frac{x}{1-\sigma_h^2}\right)dx \qquad .(3.60)$$

$$= \exp\left(\frac{\sigma_Z^2}{p_{ij}\left(1-\sigma_h^2\right)}\right)\times Ei\left(\frac{\sigma_Z^2}{p_{ij}\left(1-\sigma_h^2\right)}\right) - \left(\sqrt{\frac{2\pi\sigma_h^2}{1-\sigma_h^2}}\right.$$

$$\left. - \left(\exp\left(\frac{\sigma_Z^2}{p_{ij}\left(1-\sigma_h^2\right)}\right)\cdot\left(\frac{2\pi\sqrt{2\sigma_h^2\sigma_Z^2}}{\sqrt{p_{ij}}\left(1-\sigma_h^2\right)}\right)\cdot Q\left(\sqrt{\frac{2\sigma_Z^2}{p_{ij}\left(1-\sigma_h^2\right)}}\right)\cdot Q^{-1}\left(1-P_{out}\right)\right)\right)$$

where $Ei(\cdot)$ in (3.60) denotes the Exponential Integral Function (EIF) [59], [146]. From (3.16) and (3.60), we can compare in Figure 3.12 the exact expression of the expected value of the actual instantaneous data rate r_{ij} of user j on subcarrier i (derived by (3.58) and given by (3.60)) with the approximated instantaneous effective data rate $\tilde{r}_{ij}$ of user j on the i-th subcarrier (derived by (3.59) and given by (3.16) in *Theorem 3.2*). The comparisons regard the performance of each data rate expression versus the MMSE variance σ_h^2 under various signal-to-noise (SNR) ratios, e.g., we assume that the SNR of user j of subcarrier i is given by $SNR_{ij} = p_{ij}\left|\hat{h}_{ij}\right|^2 / \sigma_z^2$ and that it is the same for all subcarriers. From the results we observe that the graphs of both data rate expressions overlap each other with an insignificant aberrance of 0.012% in average to occur when the channel uncertainty is notably high, e.g., $\left(\left|\hat{h}_i\right|^2 / \sigma_h^2\right) \to 0$. Consequently, our approximations in (3.59) and (3.16) are accurate. This completes the proof of *Theorem 3.2*. ■

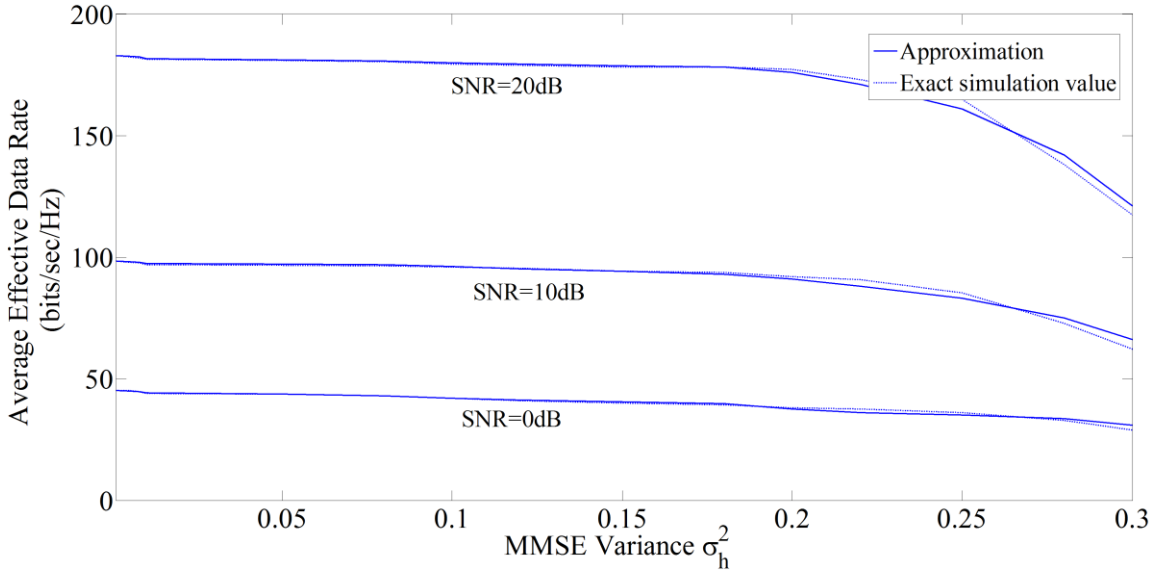

Figure 3.12 - A comparison between the approximated average effective data $\tilde{r}_{ij}$ with the actual instantaneous effective data rate r_{ij} versus the MMSE variance σ_h^2 under different SNRs.

From Figure 3.12, we can additionally detect that for large $\left(\left|\hat{h}_i\right|^2 / \sigma_h^2\right)$, our approximated instantaneous effective data rate expression in (3.16) of *Theorem 3.2*, has the property of asymptotic efficiency [147]. This means that under certain parameter regions, our estimated data rate expression $\tilde{r}_{ij}$ in (3.16) achieves higher performance than its actual expression r_{ij} in (3.60) in terms of data rate. We remark that the instantaneous power p_{ij} of user j on subcarrier i also has the property of asymptotic efficiency as it increases proportionally to $\tilde{r}_{ij}$.

A.4 Queuing Analysis - Proofs of *Lemma 3.1* and *Proposition 3.1* & *Proposition 3.2*

In our queuing analysis, we consider that the service provided by all the N_F subcarriers for each user j is considered as a server with service rate according to the system's state $\left(\hat{\mathbf{H}},\mathbf{Q}\right)$ (see Section 3.3.3) and to the user's buffer status[29]. This can be modelled as a FIFO $M/G/1/\infty/\infty$ [30] queue [59] with non-selected time slot, where each user j's average delay is described by the condition

$$E\left[D_j\right]=\frac{\lambda_j E\left[X_j{}^2\right]}{2\left(1-\lambda_j E\left[X_j\right]\right)}\le T_j^{\max}. \tag{3.61}$$

In (3.61), $E\left[X_j\right]$ represents the average service time of user *j* (in *time slots*) with second order moment given by $E\left[X_j^2\right]$. Accounting (3.61) and the QoS constraint (3.23) in the primary cross-layer optimization problem (3.18) - (3.24), we define the condition (3.25) in *Lemma 3.1*. This completes the proof of *Lemma 3.1*. ■

Furthermore, the infinite queues and the approximated instantaneous effective data rate $E\left[\tilde{r}_{ij}\right]$ in (3.16) are comparative to the Poisson arrival traffic rate λ_j value of user j. Therefore, we have to define the service time X_j to obtain the relation between the effective data rate and the delay of user j and also to establish the cross-correlation between the N_F subcarriers allocated to this user. We present our queuing analysis as follows.

[29] We remark that at some point of the allocation process the server may remain idle for a scheduling slot as subcarriers may not have been distributed to any users. Thus, modelling the distribution of the service rate of such server is highly complex and the conventional Pollaczek formula [59] is inconvenient for the calculation of each user's average service time. A traditional approach is the problem's modelling via Markov Decision Process (MDP) problem [27], [133], [181] but no closed-form analytical performance could be obtained [133] accrued by the complicated problem's solutions.

[30] This is mainly because of the fading channel, which makes the service process very hard to model. $M/G/1/\infty/\infty$ model is also very suitable for modelling various types of traffic with different QoS requirements [24], [56].

In OFDMA systems, the service time X_j represents the delay of user j and can be characterized as the number of the N_F subcarriers allocated to this user, satisfying the condition

$$X_j = \left\{ N_F \middle| q_j = F \right\}, \ \forall j . \tag{3.62}$$

In the condition (3.62), q_j represents the equivalent rate at the user j's queue, expressed as the number of bits loaded on the N_F subcarriers allocated to this user. We define the equivalent rate at the user j's queue as

$$q_j = \sum_{i=1}^{N_F} q_{ij} , \tag{3.63}$$

where q_{ij} is the number of the identically distributed bits of user j loaded to subcarrier i. Moreover, using OFDMA transmission the data streams can be grouped in a serial (in *time slots*) or parallel manner (in *number of subcarriers*). With Serial-to-Parallel (SP) and Parallel-to-Serial (PS) conventions, the perception of delay in serial grouping is translated by the equivalent delay in parallel grouping measured in the number of subcarriers, and conversely [134], [93]. Thus, we can state that the equivalent rate at the user j's queue q_j is equal to the packet size F, e.g., $q_j = F$, and that the service time X_j of user j is equal to the number of the allocated OFDM subcarriers to user j, e.g., $X_j = N_F$. Relying on our two statements and the condition in (3.62), can define the first and the second order moments of the service time X_j of user j. However, we firstly need to obtain the mean and variance of the equivalent rate at the user j's queue q_j in terms of queuing parameters.

We compute the first moment of the equivalent rate at the user j's queue q_j as follows.

$$\begin{aligned} E\left[q_j \middle| q_j\right] &= E\left[\sum_{i=1}^{N_F} q_{ij} \middle| q_j\right] \\ &= E\left[E\left[\sum_{i=1}^{N_F} q_{ij} \middle| N_F, q_j\right] \middle| q_j\right]. \\ &= E\left[N_F \cdot E\left[q_{ij} \middle| q_j\right] \middle| q_j\right] \\ &= E\left[q_{ij} \middle| q_j\right] \cdot E\left[N_F \middle| q_j\right] \end{aligned} \tag{3.64}$$

From (3.64) and our previous statements, e.g., $q_j = F$ and $X_j = N_F$, we obtain the first order moment of the service time X_j of user j as

$$E\left[X_j\right] = \frac{F}{E\left[q_{ij} \middle| q_j = F\right]}. \tag{3.65}$$

Moreover, we compute the second moment of the equivalent rate at the user j's queue q_j as follows.

$$\begin{aligned} E\left[q_j^2 \middle| q_j\right] &= E\left[\left(\sum_{i=1}^{N_F} q_{ij}\right)^2 \middle| q_j\right] \\ &= E\left[E\left[\left(\sum_{i=1}^{N_F} q_{ij}\right)^2 \middle| N_F, q_j\right] \middle| q_j\right] \\ &\overset{(1)}{=} E\left[N_F \cdot E\left[q_{ij}^2 \middle| q_j\right]\right] + \underbrace{E\left[\sum_{i \neq i'} E\left[q_{ij} q_{\tilde{i}j} \middle| q_j\right] \middle| q_j\right]} \end{aligned} \tag{3.66}$$

By using Schwartz inequality [30] and the fact that the number of the identically distributed bits of user j loaded to subcarriers i and i', $i \neq i'$ are non-negative, e.g., $q_{ij} > 0$, $q_{i'j} > 0$, we derive a lower bound for the second term of the right side of equation (1) in (3.66) as

$$E\left[q_{ij} q_{i'j}\right] \leq \sqrt{E\left[q_{ij}^2\right] E\left[q_{i'j}^2\right]} = E\left[q_{ij}^2\right]. \tag{3.67}$$

From (3.67) we conclude that the second term of the right side of equation (1) in (3.66) can be described as

$$\sum_{i \neq i'} E\left[q_{ij} q_{i'j} \middle| q_j \right] \leq N_F \left(N_F - 1 \right) E\left[q_{ij}^2 \middle| q_j \right]. \tag{3.68}$$

With substitution of (3.68) into (3.66) we continue to compute the second moment of the equivalent rate at the user j's queue q_j as below.

$$\begin{aligned} E\left[q_j^2 \middle| q_j \right] &\leq E\left[N_F \cdot E\left[q_{ij}^2 \middle| q_j \right] + N_F \left(N_F - 1 \right) E\left[q_{ij}^2 \middle| q_j \right] \right] \\ &= E\left[N_F^2 \cdot E\left[q_{ij}^2 \middle| q_j \right] \right] \\ &= E\left[q_{ij}^2 \middle| q_j \right] \cdot E\left[N_F^2 \middle| q_j \right] \end{aligned} . \tag{3.69}$$

From (3.69) and our previous statements, e.g., $q_j = F$ and $X_j = N_F$, we obtain the second order moment of the service time X_j of user j as

$$E\left[X_j^2 \right] \geq \frac{F^2}{E\left[q_{ij}^2 \middle| q_j = F \right]}. \tag{3.70}$$

In continue, we substitute the first and second order moments of the service time X_j of user j as described in (3.65) and (3.70), respectively, into the user j's average delay $E\left[D_j \right]$ as described by the condition in (3.61)[31] to derive the following relationship.

$$2T_j^{\max} - \frac{2T_j^{\max} \lambda_j F}{E\left[q_{ij} \middle| q_j = F \right]} - \frac{\lambda_j F^2}{E\left[q_{ij}^2 \middle| q_j = F \right]} \geq 0. \tag{3.71}$$

From the definition of the equivalent rate q_j at the user j's queue in (3.63) and the condition (3.71), the equivalent rate q_j at the user j's queue is defined as below.

$$\begin{aligned} &\frac{2T_j^{\max} q_j^2 - 2T_j^{\max} \lambda_j F q_j - \lambda_j F^2}{q_j^2} \geq 0 \overset{q_j^2 \geq 0}{\Leftrightarrow} \\ &2T_j^{\max} q_j^2 - 2T_j^{\max} \lambda_j F q_j - \lambda_j F^2 \geq 0 \end{aligned} . \tag{3.72}$$

[31] In our substitutions, the condition (3.70) stands for the equality e.g., we consider the minimum value of the second order moment of the service time. This corresponds to the worst case scenario as the service provided by the queuing server cannot vary at values higher than its minimum bound.

Upon solving the quadratic formula in (3.72) over q_j we define the equivalent rate q_j at the user j's queue as given in (3.27) of *Proposition 3.1*. From our queuing analysis and the equivalent rate q_j in (3.27), we conclude that the number of bits of user j loaded to the N_F allocated to this user subcarriers is low bounded according to the user j's queuing characteristics. In other words, q_j in (3.27) represents the traffic arrival rate at user j's queue by means of number of the arrival bits at user's queue over all the allocated subcarriers to this user. Hence, we can correlate the data rate of user j at the PHY layer with its equivalent rate at the MAC layer. Finally, we account the approximated instantaneous effective data rate $E\left[\tilde{r}_{ij}\right]$, the subcarrier allocation index s_{ij}, the time slot duration t_s and the bandwidth allocated to each OFDMA subcarrier $i \in N_F$, e.g., BW / N_F, to define the QoS condition in (3.26). This completes the proof of *Proposition 3.1*. ■

Furthermore, a user is delay-insensitive when it has no delay constraints or when its maximum delay tolerance $T_j^{\max}$ tends to infinite, e.g., $T_j^{\max} \to \infty$. Then from L'Hospital's rule [146] and (3.72) we get that

$$\lim_{T_j^{\max} \to \infty} \left(\frac{\partial 2T_j^{\max} q_j^2 - 2T_j^{\max} \lambda_j F q_j - \lambda_j F^2}{\partial T_j^{\max}} \right) \geq 0 \Leftrightarrow q_j - \lambda_j F \geq 0 . \qquad (3.73)$$

The condition in (3.73) is a stability condition for each user's queue as it indicates that the equivalent rate q_j must be at least equal to the bits arrival rate $F\lambda_j$ to user j's buffer, e.g., $q_j \geq F\lambda_j$. Finally, we account the approximated instantaneous effective data rate $E\left[\tilde{r}_{ij}\right]$, the subcarrier allocation index s_{ij}, the time slot duration t_s and the bandwidth allocated to each OFDMA subcarrier $i \in N_F$, e.g., BW / N_F, to define the stability condition in (3.28). This completes the proof of *Proposition 3.2*. ■

A.5 Convexity of the Power-Efficient Cross-Layer Optimization Problem - Proof of *Proposition 3.3*

In this Appendix we focus on proofing the convexity of the power-efficient cross-layer optimization problem in (3.30) - (3.35) along with the convexity and feasibility of its determined set. To avoid confusion, we separate our proofs into three different topics as below.

1) Convexity of the power-efficient cross-layer optimization problem (3.30) - (3.35) - By introducing the subcarrier time-sharing factor $\tilde{s}_{ij} \in (0,1]$ and the continue variable $\tilde{p}_{ij} = \tilde{s}_{ij} p_{ij}$, it is straightforward that the parameter $\tilde{s}_{ij}\tilde{p}_{ij}$ of the cost function in (3.30) is convex over the convex set $(\tilde{s}_{ij}, \tilde{p}_{ij})$ due to its affinity [135]. Thus, the cost function in (3.30) is also a convex function over the convex set $(\tilde{s}_{ij}, \tilde{p}_{ij})$ as any positive linear combination of convex functions is a convex function. Following the same rationality, we can show that the constraints (3.31) - (3.34) are all affine and hence, convex over the convex set $(\tilde{s}_{ij}, \tilde{p}_{ij})$.

Let us now examine the convexity of the QoS constraint (3.34). With substitution of the variables $\tilde{s}_{ij} \in (0,1]$ and $\tilde{p}_{ij} = \tilde{s}_{ij} p_{ij}$, the QoS constraint (3.34) can be represented with the function $B(\tilde{s}_{ij}, \tilde{p}_{ij})$ denoted as

$$B(\tilde{s}_{ij}, \tilde{p}_{ij}) = E\left[\sum_{i=1}^{N_F} \tilde{s}_{ij}\left(\log_2\left(1+\frac{\left|\hat{h}_{ij}\right|^2 \tilde{p}_{ij}}{\tilde{s}_{ij}\sigma_z^2}\right) - \frac{\sqrt{2}\left|\hat{h}_{ij}\right| \tilde{p}_{ij}\sigma_h Q^{-1}(1-P_{app})}{\left|\hat{h}_{ij}\right|^2 \tilde{p}_{ij} + \tilde{s}_{ij}\sigma_z^2}\right)\right] - \tilde{q}_j\left(F, T_j^{\max}, \lambda_j\right). \quad (3.74)$$

The function $B(\tilde{s}_{ij}, \tilde{p}_{ij})$ in (3.74) has the form $\log_2(1+x) - \frac{x}{x+1}$, which means that we need to prove that $B(\tilde{s}_{ij}, \tilde{p}_{ij})$ is a concave function. In other words, to show that the QoS constraint in (3.34) is convex we must prove that the Hessian matrix of the function $B(\tilde{s}_{ij}, \tilde{p}_{ij})$ in (3.74) is negative semi-definite [135]. Let us denote the Hessian matrix of the function $B(\tilde{s}_{ij}, \tilde{p}_{ij})$ in (3.74) by $\mathcal{H}_{B(\tilde{s}_{ij}, \tilde{p}_{ij})}$ and represent it as below.

$$\mathcal{H}_{B\left(\tilde{s}_{ij},\tilde{p}_{ij}\right)}=\begin{bmatrix}\dfrac{\partial^2 B\left(\tilde{s}_{ij},\tilde{p}_{ij}\right)}{\partial\tilde{p}_{ij}^2} & \dfrac{\partial^2 B\left(\tilde{s}_{ij},\tilde{p}_{ij}\right)}{\partial\tilde{s}_{ij}\partial\tilde{p}_{ij}}\\ \dfrac{\partial^2 B\left(\tilde{s}_{ij},\tilde{p}_{ij}\right)}{\partial\tilde{p}_{ij}\partial\tilde{s}_{ij}} & \dfrac{\partial^2 B\left(\tilde{s}_{ij},\tilde{p}_{ij}\right)}{\partial\tilde{s}_{ij}^2}\end{bmatrix}. \tag{3.75}$$

In order to prove that the Hessian matrix $\mathcal{H}_{B\left(\tilde{s}_{ij},\tilde{p}_{ij}\right)}$ in (3.75) is negative semi-definite, it is sufficient to show that the following conditions are satisfied.

$$\frac{\partial^2 B\left(\tilde{s}_{ij},\tilde{p}_{ij}\right)}{\partial\tilde{p}_{ij}^2}\cdot\frac{\partial^2 B\left(\tilde{s}_{ij},\tilde{p}_{ij}\right)}{\partial\tilde{s}_{ij}^2}-\frac{\partial^2 B\left(\tilde{s}_{ij},\tilde{p}_{ij}\right)}{\partial\tilde{s}_{ij}\partial\tilde{p}_{ij}}\cdot\frac{\partial^2 B\left(\tilde{s}_{ij},\tilde{p}_{ij}\right)}{\partial\tilde{p}_{ij}\partial\tilde{s}_{ij}}=0 \tag{3.76}$$

$$\frac{\partial^2 B\left(\tilde{s}_{ij},\tilde{p}_{ij}\right)}{\partial\tilde{p}_{ij}^2}\le 0, \tag{3.77}$$

$$\frac{\partial^2 B\left(\tilde{s}_{ij},\tilde{p}_{ij}\right)}{\partial\tilde{s}_{ij}^2}\le 0. \tag{3.78}$$

According to Young's Theorem [135], if the two variable function $B\left(\tilde{s}_{ij},\tilde{p}_{ij}\right)$ in (3.74) is twice continuously differentiable then the condition (3.76) is satisfied. A two variable function is twice continuously differentiable if its second derivatives do exist and are continuous. Hence, we need to perform the second order derivative test of $B\left(\tilde{s}_{ij},\tilde{p}_{ij}\right)$ in (3.74) for both its variables $\tilde{s}_{ij}$ and $\tilde{p}_{ij}$. From the second order derivative test we can also derive the concavity condition that satisfies both the conditions in (3.77) and (3.78). We perform the second order derivative test as follows.

The first derivation of $B\left(\tilde{s}_{ij},\tilde{p}_{ij}\right)$ over the variable $\tilde{p}_{ij}$ is computed as

$$\frac{\partial B\left(\tilde{s}_{ij},\tilde{p}_{ij}\right)}{\partial\tilde{p}_{ij}}=\frac{\left|\hat{h}_{ij}\right|^2}{\tilde{p}_{ij}\left|\hat{h}_{ij}\right|^2+\tilde{s}_{ij}\sigma_z^2}-\frac{\sqrt{2}\left|\hat{h}_{ij}\right|\tilde{s}_{ij}\sigma_h\sigma_z^2Q^{-1}\left(1-P_{app}\right)}{\left(\tilde{p}_{ij}\left|\hat{h}_{ij}\right|^2+\tilde{s}_{ij}\sigma_z^2\right)^2}. \tag{3.79}$$

From (3.79) we compute the second derivation of $B\left(\tilde{s}_{ij},\tilde{p}_{ij}\right)$ over the variable $\tilde{p}_{ij}$ as

$$\frac{\partial^2 B\left(\tilde{s}_{ij},\tilde{p}_{ij}\right)}{\partial \tilde{p}_{ij}^2}=\underbrace{\frac{\left|\hat{h}_{ij}\right|^4}{\left(\tilde{p}_{ij}\left|\hat{h}_{ij}\right|^2+\tilde{s}_{ij}\sigma_z^2\right)^2}}_{(1)}\cdot\underbrace{\left(\frac{2\sqrt{2}\tilde{s}_{ij}\sigma_h\sigma_z^2Q^{-1}\left(1-P_{app}\right)}{\left|\hat{h}_{ij}\right|\left(\tilde{p}_{ij}\left|\hat{h}_{ij}\right|^2+\tilde{s}_{ij}\sigma_z^2\right)}-1\right)}_{(2)}. \tag{3.80}$$

It is straightforward that the second derivative of the function $B\left(\tilde{s}_{ij},\tilde{p}_{ij}\right)$ over $\tilde{p}_{ij}$ does exist and it is also continues as $\tilde{p}_{ij}$ is continues. In addition, for the condition (3.77) of the Hessian matrix $\mathcal{H}_{B\left(\tilde{s}_{ij},\tilde{p}_{ij}\right)}$ in (3.75), it is sufficient to show that the second derivation of the function $B\left(\tilde{s}_{ij},\tilde{p}_{ij}\right)$ over $\tilde{p}_{ij}$ in (3.80) is smaller or equal to zero. We observe that the term (1) in (3.80) is positive. Hence, we need to establish a condition to ensure that the term (2) in (3.80) is smaller or equal to zero. This yields the followings.

$$\frac{2\sqrt{2}\sigma_h\sigma_z^2\tilde{s}_{ij}Q^{-1}\left(1-P_{app}\right)}{\left|\hat{h}_{ij}\right|\left(\left|\hat{h}_{ij}\right|^2\tilde{p}_{ij}+\tilde{s}_{ij}\sigma_z^2\right)}-1\le 0\Leftrightarrow 2\sqrt{2}Q^{-1}\left(1-P_{app}\right)\le\frac{\left|\hat{h}_{ij}\right|\left(\left|\hat{h}_{ij}\right|^2\tilde{p}_{ij}+\tilde{s}_{ij}\sigma_z^2\right)}{\sigma_h\tilde{s}_{ij}\sigma_z^2}\Leftrightarrow$$

$$2\sqrt{2}Q^{-1}\left(1-P_{app}\right)\le\frac{\left|\hat{h}_{ij}\right|^3\tilde{p}_{ij}+\left|\hat{h}_{ij}\right|\tilde{s}_{ij}\sigma_z^2}{\sigma_h\tilde{s}_{ij}\sigma_z^2}\Leftrightarrow 2\sqrt{2}Q^{-1}\left(1-P_{app}\right)\le\frac{\left|\hat{h}_{ij}\right|^3\tilde{p}_{ij}}{\sigma_h\tilde{s}_{ij}\sigma_z^2}+\frac{\left|\hat{h}_{ij}\right|}{\sigma_h}\Leftrightarrow$$

$$8\left(Q^{-1}\left(1-P_{app}\right)\right)^2\le\left[\frac{\left|\hat{h}_{ij}\right|^3\tilde{p}_{ij}}{\sigma_h\tilde{s}_{ij}\sigma_z^2}+\frac{\left|\hat{h}_{ij}\right|}{\sigma_h}\right]^2\Leftrightarrow 8\left(Q^{-1}\left(1-P_{app}\right)\right)^2\le\frac{\left|\hat{h}_{ij}\right|^6\tilde{p}_{ij}^2}{\sigma_h^2\tilde{s}_{ij}^2\sigma_z^4}+\frac{\left|\hat{h}_{ij}\right|^2}{\sigma_h^2}+\frac{2\left|\hat{h}_{ij}\right|^4\tilde{p}_{ij}}{\sigma_h^2\tilde{s}_{ij}\sigma_z^2}\Leftrightarrow$$

$$8\left(Q^{-1}\left(1-P_{app}\right)\right)^2\le\frac{\left|\hat{h}_{ij}\right|^2}{\sigma_h^2}\left(\frac{\left|\hat{h}_{ij}\right|^4\tilde{p}_{ij}^2}{\tilde{s}_{ij}^2\sigma_z^4}+1+\frac{2\left|\hat{h}_{ij}\right|^2\tilde{p}_{ij}}{\tilde{s}_{ij}\sigma_z^2}\right)\Leftrightarrow$$

$$8\left(Q^{-1}\left(1-P_{app}\right)\right)^2\le\frac{\left|\hat{h}_{ij}\right|^2}{\sigma_h^2}\left(1+\frac{\left|\hat{h}_{ij}\right|^2\tilde{p}_{ij}}{\tilde{s}_{ij}\sigma_z^2}\right)^2. \tag{3.81}$$

If the condition in (3.81) is satisfied, the condition (3.77) for the Hessian matrix $\mathcal{H}_{B\left(\tilde{s}_{ij},\tilde{p}_{ij}\right)}$ in (3.75) is also satisfied.

Moreover, we find the first derivation of $B\left(\tilde{s}_{ij},\tilde{p}_{ij}\right)$ over the variable $\tilde{s}_{ij}$ as follows.

$$\frac{\partial B\left(\tilde{s}_{ij},\tilde{p}_{ij}\right)}{\partial \tilde{s}_{ij}}=\log_2\left(1+\frac{\left|\hat{h}_{ij}\right|^2\tilde{p}_{ij}}{\tilde{s}_{ij}\sigma_z^2}\right)-\frac{\left|\hat{h}_{ij}\right|^2\tilde{p}_{ij}}{\left(\left|\hat{h}_{ij}\right|^2\tilde{p}_{ij}+\tilde{s}_{ij}\sigma_z^2\right)}-\frac{\sqrt{2}\left|\hat{h}_{ij}\right|^3\tilde{p}_{ij}^2\sigma_h Q^{-1}\left(1-P_{app}\right)}{\left(\left|\hat{h}_{ij}\right|^2\tilde{p}_{ij}+\tilde{s}_{ij}\sigma_z^2\right)^2}. \quad (3.82)$$

From (3.82) we compute the second derivation of $B\left(\tilde{s}_{ij},\tilde{p}_{ij}\right)$ over the variable $\tilde{s}_{ij}$ as

$$\frac{\partial^2 B\left(\tilde{s}_{ij},\tilde{p}_{ij}\right)}{\partial \tilde{s}_{ij}^2}=\frac{2\sqrt{2}\left|\hat{h}_{ij}\right|\tilde{p}_{ij}\sigma_h\sigma_z^2Q^{-1}\left(1-P_{app}\right)}{\left(\left|\hat{h}_{ij}\right|^2\tilde{p}_{ij}+\tilde{s}_{ij}\sigma_z^2\right)^2}-\frac{2\left|\hat{h}_{ij}\right|^2\tilde{p}_{ij}}{\tilde{s}_{ij}^2\sigma_z^2\left(1+\frac{\left|\hat{h}_{ij}\right|^2\tilde{p}_{ij}}{\tilde{s}_{ij}\sigma_z^2}\right)}$$

$$-\tilde{s}_{ij}\left(\frac{\left|\hat{h}_{ij}\right|^4\tilde{p}_{ij}^2}{\tilde{s}_{ij}^4\sigma_z^4\left(1+\frac{\left|\hat{h}_{ij}\right|^2\tilde{p}_{ij}}{\tilde{s}_{ij}\sigma_z^2}\right)^2}-\frac{2\left|\hat{h}_{ij}\right|^2\tilde{p}_{ij}}{\tilde{s}_{ij}^3\sigma_z^2\left(1+\frac{\left|\hat{h}_{ij}\right|^2\tilde{p}_{ij}}{\tilde{s}_{ij}\sigma_z^2}\right)}+\frac{2\sqrt{2}\left|\hat{h}_{ij}\right|\tilde{p}_{ij}\sigma_h\sigma_z^4Q^{-1}\left(1-P_{app}\right)}{\left(\left|\hat{h}_{ij}\right|^2\tilde{p}_{ij}+\tilde{s}_{ij}\sigma_z^2\right)^3}\right). \quad (3.83)$$

It is straightforward that the second derivative of the function $B\left(\tilde{s}_{ij},\tilde{p}_{ij}\right)$ over $\tilde{s}_{ij}$ does exist and it is also continues as $\tilde{s}_{ij}\in(0,1]$ is continues. Hence, the two variable function $B\left(\tilde{s}_{ij},\tilde{p}_{ij}\right)$ in (3.74) has two continues second derivatives, meaning that the function is twice differentiable and according to Young's Theorem [135], the condition (3.76) is satisfied.

In addition, for the condition (3.78) of the Hessian matrix $\mathcal{H}_{B\left(\tilde{s}_{ij},\tilde{p}_{ij}\right)}$ in (3.75), it is sufficient to show that the second derivation of the function $B\left(\tilde{s}_{ij},\tilde{p}_{ij}\right)$ over $\tilde{s}_{ij}$ in (3.83) is smaller or equal to zero. We can establish another convexity condition, which ensures that the second derivation of $B\left(\tilde{s}_{ij},\tilde{p}_{ij}\right)$ over $\tilde{s}_{ij}$ in (3.83) is smaller or equal to zero by performing the following calculations. For $\frac{\partial^2 B\left(\tilde{s}_{ij},\tilde{p}_{ij}\right)}{\partial \tilde{s}_{ij}^2}\le 0$, (3.83) becomes

$$\frac{2\sqrt{2}\left|\hat{h}_{ij}\right|\tilde{p}_{ij}\sigma_h\sigma_z^2Q^{-1}\left(1-P_{app}\right)}{\left(\left|\hat{h}_{ij}\right|^2\tilde{p}_{ij}+\tilde{s}_{ij}\sigma_z^2\right)^2}-\frac{2\left|\hat{h}_{ij}\right|^2\tilde{p}_{ij}}{\tilde{s}_{ij}\left(\left|\hat{h}_{ij}\right|^2\tilde{p}_{ij}+\tilde{s}_{ij}\sigma_z^2\right)}$$
$$-\frac{\left|\hat{h}_{ij}\right|^4\tilde{p}_{ij}^2}{\tilde{s}_{ij}\left(\left|\hat{h}_{ij}\right|^2\tilde{p}_{ij}+\tilde{s}_{ij}\sigma_z^2\right)^2}+\frac{2\left|\hat{h}_{ij}\right|^2\tilde{p}_{ij}}{\tilde{s}_{ij}\left(\left|\hat{h}_{ij}\right|^2\tilde{p}_{ij}+\tilde{s}_{ij}\sigma_z^2\right)}-\frac{2\sqrt{2}\left|\hat{h}_{ij}\right|\tilde{s}_{ij}\tilde{p}_{ij}\sigma_h\sigma_z^4Q^{-1}\left(1-P_{app}\right)}{\left(\left|\hat{h}_{ij}\right|^2\tilde{p}_{ij}+\tilde{s}_{ij}\sigma_z^2\right)^3}\le 0,$$

which with some manipulation yields that

$$\underbrace{\frac{\left|\hat{h}_{ij}\right|}{\tilde{s}_{ij}\left(\left|\hat{h}_{ij}\right|^2\tilde{p}_{ij}+\tilde{s}_{ij}\sigma_z^2\right)}}_{(1)}\left(\underbrace{\frac{2\sqrt{2}\tilde{s}_{ij}\tilde{p}_{ij}\sigma_h\sigma_z^2Q^{-1}\left(1-P_{app}\right)}{\left(\left|\hat{h}_{ij}\right|^2\tilde{p}_{ij}+\tilde{s}_{ij}\sigma_z^2\right)}-2\left|\hat{h}_{ij}\right|\tilde{p}_{ij}}_{(2)}\right.$$
$$\left.\underbrace{-\frac{\left|\hat{h}_{ij}\right|^3\tilde{p}_{ij}^2}{\left(\left|\hat{h}_{ij}\right|^2\tilde{p}_{ij}+\tilde{s}_{ij}\sigma_z^2\right)}+2\left|\hat{h}_{ij}\right|\tilde{p}_{ij}-\frac{2\sqrt{2}\tilde{s}_{ij}^2\tilde{p}_{ij}\sigma_h\sigma_z^4Q^{-1}\left(1-P_{app}\right)}{\left(\left|\hat{h}_{ij}\right|^2\tilde{p}_{ij}+\tilde{s}_{ij}\sigma_z^2\right)^2}}_{(2)}\right)\le 0 \quad . \tag{3.84}$$

As $\tilde{s}_{ij}$ and $\left|\hat{h}_{ij}\right|$ are positive variables, e.g., $\tilde{s}_{ij}\in(0,1]$ and $\left|\hat{h}_{ij}\right|\ge 0$, the term (1) in (3.84) is positive. Hence, we examine when the term (2) of (3.84) is smaller or equal to zero, e.g.,

$$\frac{2\sqrt{2}\tilde{s}_{ij}\tilde{p}_{ij}\sigma_h\sigma_z^2Q^{-1}\left(1-P_{app}\right)}{\left(\left|\hat{h}_{ij}\right|^2\tilde{p}_{ij}+\tilde{s}_{ij}\sigma_z^2\right)}-2\left|\hat{h}_{ij}\right|\tilde{p}_{ij}$$
$$-\frac{\left|\hat{h}_{ij}\right|^3\tilde{p}_{ij}^2}{\left(\left|\hat{h}_{ij}\right|^2\tilde{p}_{ij}+\tilde{s}_{ij}\sigma_z^2\right)}+2\left|\hat{h}_{ij}\right|\tilde{p}_{ij}-\frac{2\sqrt{2}\tilde{s}_{ij}^2\tilde{p}_{ij}\sigma_h\sigma_z^4Q^{-1}\left(1-P_{app}\right)}{\left(\left|\hat{h}_{ij}\right|^2\tilde{p}_{ij}+\tilde{s}_{ij}\sigma_z^2\right)^2}\le 0 \quad . \tag{3.85}$$

We continue by performing some calculations in (3.85) as below.

$$\frac{2\sqrt{2}\left|\hat{h}_{ij}\right|^2 \tilde{s}_{ij}\tilde{p}_{ij}^2\sigma_h\sigma_z^2 Q^{-1}\left(1-P_{app}\right)+2\sqrt{2}\tilde{s}_{ij}^2\tilde{p}_{ij}\sigma_h\sigma_z^4 Q^{-1}\left(1-P_{app}\right)}{\left(\left|\hat{h}_{ij}\right|^2\tilde{p}_{ij}+\tilde{s}_{ij}\sigma_z^2\right)^2}$$
$$\frac{-\left|\hat{h}_{ij}\right|^5\tilde{p}_{ij}^3-\left|\hat{h}_{ij}\right|^3\tilde{s}_{ij}\tilde{p}_{ij}^2\sigma_z^2-2\sqrt{2}\tilde{s}_{ij}^2\tilde{p}_{ij}\sigma_h\sigma_z^4 Q^{-1}\left(1-P_{app}\right)}{\left(\left|\hat{h}_{ij}\right|^2\tilde{p}_{ij}+\tilde{s}_{ij}\sigma_z^2\right)^2}\le 0 \quad . \tag{3.86}$$

The denominator of the fraction in (3.86) is positive. Hence, we examine when the nominator of the fraction in (3.86) is smaller or equal to zero as follows.

$$2\sqrt{2}\left|\hat{h}_{ij}\right|^2\tilde{s}_{ij}\tilde{p}_{ij}^2\sigma_h\sigma_z^2 Q^{-1}\left(1-P_{app}\right)-\left|\hat{h}_{ij}\right|^5\tilde{p}_{ij}^3-\left|\hat{h}_{ij}\right|^3\tilde{s}_{ij}\tilde{p}_{ij}^2\sigma_z^2\le 0 \;\Leftrightarrow$$

$$2\sqrt{2}Q^{-1}\left(1-P_{app}\right)\le\frac{\left|\hat{h}_{ij}\right|^5\tilde{p}_{ij}^3+\left|\hat{h}_{ij}\right|^3\tilde{s}_{ij}\tilde{p}_{ij}^2\sigma_z^2}{\left|\hat{h}_{ij}\right|^2\tilde{s}_{ij}\tilde{p}_{ij}^2\sigma_h\sigma_z^2}\Leftrightarrow$$

$$2\sqrt{2}Q^{-1}\left(1-P_{app}\right)\le\left|\hat{h}_{ij}\right|\left(\frac{\left|\hat{h}_{ij}\right|^2\tilde{p}_{ij}+\tilde{s}_{ij}\sigma_z^2}{\tilde{s}_{ij}\sigma_h\sigma_z^2}\right). \tag{3.87}$$

To keep consistency with the right side of the convexity condition in (3.81), we square both sides of (3.87) and get

$$8\left(Q^{-1}\left(1-P_{app}\right)\right)^2\le\frac{\left|\hat{h}_{ij}\right|^2}{\sigma_h^2}\left(1+\frac{\left|\hat{h}_{ij}\right|^2\tilde{p}_{ij}}{\tilde{s}_{ij}\sigma_z^2}\right)^2. \tag{3.88}$$

If the condition in (3.88) is satisfied, the condition (3.78) of the Hessian matrix $\mathcal{H}_{B\left(\tilde{s}_{ij},\tilde{p}_{ij}\right)}$ in (3.75) is also satisfied.

Let us now examine the concavity conditions (3.81) and (3.88). Obviously both conditions are the same. Hence, the twice continuously differentiable function $B\left(\tilde{s}_{ij},\tilde{p}_{ij}\right)$ in (3.74) is convex over the set $\left(\tilde{s}_{ij},\tilde{p}_{ij}\right)$ if the variables $\tilde{s}_{ij}$ and $\tilde{p}_{ij}$ vary in the region determined by the concavity condition (3.88). In other words, considering the concavity condition (3.88) the power-efficient cross-layer optimization problem in (3.30) - (3.35) is convex as its cost function and all constraints are convex.

2) Convexity of the determined set of the power-efficient cross-layer optimization problem in (3.30) - (3.35) - Given the subcarrier time-sharing factor $\tilde{s}_{ij} \in (0,1]$ and the variable $\tilde{p}_{ij} = \tilde{s}_{ij} p_{ij}$, the cost function (3.30) of the power-efficient cross-layer optimization problem in (3.30) - (3.35) is affine determining a convex set over $(\tilde{s}_{ij}, \tilde{p}_{ij})$ [135]. In addition, each of the constraints (3.31), (3.32), (3.33) and (3.34), determines a convex set over $(\tilde{s}_{ij}, \tilde{p}_{ij})$ due to its affinity. Also we show that the QoS constraint (3.35) is convex hence, it also determines a convex set over $(\tilde{s}_{ij}, \tilde{p}_{ij})$. Therefore, the set defined by all the five constraints (3.31) - (3.35) and by the cost function (3.30), is convex over $(\tilde{s}_{ij}, \tilde{p}_{ij})$ as it is well-known that the intersection of convex sets is also convex.

3) Feasibility of the determined set of the power-efficient cross-layer optimization problem in (3.30) - (3.35) - We shall now verify that the convex set $(\tilde{s}_{ij}, \tilde{p}_{ij})$ determined by the power-efficient cross-layer optimization problem in (3.30) - (3.35) is non-empty. Given the subcarrier time-sharing factor $\tilde{s}_{ij} \in (0,1]$ and the variable $\tilde{p}_{ij} = \tilde{s}_{ij} p_{ij}$, it is easy to obtain a $K \times N_F$ feasible set over $\tilde{s}_{ij}$ represented by, e.g., S_1, that satisfies the subcarrier constraints (3.31) and (3.32), i.e., easily we can verify that for $\tilde{s}_{ij} = 1$ the set S_1 is non-empty, e.g., $S_1 \neq \varnothing$. Similarly, there is another $K \times N_F$ feasible set over $\tilde{p}_{ij}$, e.g., S_2, that satisfies the power and QoS constraints (3.33), (3.34) and (3.35), which is also non-empty, i.e., if the convexity condition (3.88) stands then the set S_2 is non-empty, e.g., $S_2 \neq \varnothing$. Moreover, in the $(K \times N_F) + (K \times N_F)$-dimensional space $(\tilde{s}_{ij}, \tilde{p}_{ij})$, the constraints (3.31) and (3.32) of the variables $\tilde{s}_{ij}$ verify a cylinder set with base S_1, while the constraints (3.33), (3.34) and (3.35) of the variables $\tilde{s}_{ij}$ and $\tilde{p}_{ij}$ verify another cylinder set with base S_2. Consequently, the constraints in $(\tilde{s}_{ij}, \tilde{p}_{ij})$ determine the intersection of the two cylinders sets, e.g., $S_1 \cap S_2$, which it is obvious a non-empty set, e.g., $S_1 \cap S_2 = \varnothing$. Also, due to the affinity principle, the intersection $S_1 \cap S_2$ of the two cylinders sets is convex. Consequently, the power-efficient

cross-layer optimization problem in (3.30) - (3.35) is a convex optimization problem over a feasible $\left(K \times N_F\right)+\left(K \times N_F\right)$-dimensional convex set. This completes the proof of *Proposition 3.3*. ■

A.6 Optimal Allocation Policies - Proofs of *Theorem 3.3, Theorem 3.4* & *Theorem 3.5*

Given the time-sharing factor $\tilde{s}_{ij} \in (0,1]$ and the variable $\tilde{p}_{ij} = \tilde{s}_{ij} p_{ij}$, the Lagrangian function $\mathcal{L}\left(\tilde{s}_{ij}, \tilde{p}_{ij}, \xi_j, \mu, \nu_i\right)$ of the power-efficient cross-layer optimization problem in (3.30) - (3.35) is given by

$$\mathcal{L}\left(\tilde{s}_{ij}, \tilde{p}_{ij}, \xi_j, \mu, \nu_i\right) = \frac{1}{N_F}\sum_{j=1}^{K}\sum_{i=1}^{N_F}\tilde{p}_{ij} - \sum_{i=1}^{N_F}\nu_i\left(\sum_{j=1}^{K}\tilde{s}_{ij} - 1\right) - \mu\left(\frac{1}{N_F}\sum_{j=1}^{K}\sum_{i=1}^{N_F}\tilde{p}_{ij} - P_{TOTAL}\right)$$
$$+\xi_j\left(\sum_{i=1}^{N_F}\tilde{s}_{ij}\left(\log_2\left(1+\frac{\left|\hat{h}_{ij}\right|^2\tilde{p}_{ij}}{\tilde{s}_{ij}\sigma_z^2}\right) - \frac{\sqrt{2}\left|\hat{h}_{ij}\right|\tilde{p}_{ij}\sigma_h Q^{-1}\left(1-P_{app}\right)}{\left|\hat{h}_{ij}\right|^2\tilde{p}_{ij}+\tilde{s}_{ij}\sigma_z^2}\right) - \tilde{q}_j\left(F, T_j^{\max}, \lambda_j\right)\right) \quad . \quad (3.89)$$

The necessary and sufficient conditions that satisfy the global optimum solutions of the power-efficient cross-layer optimization problem in (3.30) - (3.35), are the KKT conditions defined as follows [135].

$$\left.\frac{\partial\mathcal{L}\left(\tilde{s}_{ij}, \tilde{p}_{ij}, \xi_j, \mu, \nu_i\right)}{\partial\tilde{p}_{ij}}\right|_{\left(\tilde{s}_{ij}, \tilde{p}_{ij}, \xi_j, \mu, \nu_i\right)=\left(\tilde{s}_{ij}^*, \tilde{p}_{ij}^*, \xi_j^*, \mu^*, \nu_i^*\right)} \begin{cases} < 0, \text{ if } \tilde{p}_{ij}^* = 0 \\ = 0, \text{ if } \tilde{p}_{ij}^* > 0 \end{cases}, \quad \forall i, j, \quad (3.90)$$

$$\left.\frac{\partial\mathcal{L}\left(\tilde{s}_{ij}, \tilde{p}_{ij}, \xi_j, \mu, \nu_i\right)}{\partial\tilde{s}_{ij}}\right|_{\left(\tilde{s}_{ij}, \tilde{p}_{ij}, \xi_j, \mu, \nu_i\right)=\left(\tilde{s}_{ij}^*, \tilde{p}_{ij}^*, \xi_j^*, \mu^*, \nu_i^*\right)} \begin{cases} > 0, \text{ if } \tilde{s}_{ij}^* = 1 \\ = 0, \text{ if } 0 < \tilde{s}_{ij}^* < 1 \end{cases}, \quad \forall i, j, \quad (3.91)$$

$$\tilde{p}_{ij}^* \geq 0, \quad \forall i, j, \quad (3.92)$$

$$\xi_j^* \geq 0, \quad \forall j, \quad (3.93)$$

$$\mu^* \geq 0, \quad (3.94)$$

$$\nu_i^* \geq 0, \quad \forall i, \quad (3.95)$$

$$\sum_{j=1}^{K} \tilde{s}_{ij}^{*} \le 1, \quad \forall i , \tag{3.96}$$

$$\sum_{i=1}^{N_F} \nu_i^{*} \left(\sum_{j=1}^{K} \tilde{s}_{ij}^{*} - 1 \right) \le 0 , \quad \forall j , \tag{3.97}$$

$$\frac{1}{N_F} \sum_{j=1}^{K} \sum_{i=1}^{N_F} \tilde{p}_{ij}^{*} \le P_{TOTAL} , \tag{3.98}$$

$$\mu^{*} \left(\frac{1}{N_F} \sum_{j=1}^{K} \sum_{i=1}^{N_F} \tilde{p}_{ij}^{*} - P_{TOTAL} \right) = 0 , \tag{3.99}$$

$$\sum_{i=1}^{N_F} \tilde{s}_{ij}^{*} \tilde{r}_{ij}^{*} \ge \tilde{q}_j \left(F, T_j^{\max}, \lambda_j \right), \quad \forall j , \tag{3.100}$$

$$\xi_j^{*} \left(\sum_{i=1}^{N_F} \tilde{s}_{ij}^{*} \tilde{r}_{ij}^{*} - \tilde{q}_j \left(F, T_j^{\max}, \lambda_j \right) \right) = 0 . \tag{3.101}$$

According to the KKT condition (3.90), differentiating the Lagrangian function $\mathcal{L}\left(\tilde{s}_{ij}, \tilde{p}_{ij}, \xi_j, \mu, \nu_i \right)$ in (3.89) over the optimal instantaneous transmitting power $\tilde{p}_{ij}^{*}$ of user j on subcarrier i, results to

$$\left. \frac{\partial \mathcal{L}\left(\tilde{s}_{ij}, \tilde{p}_{ij}, \xi_j, \mu, \nu_i \right)}{\partial \tilde{p}_{ij}} \right|_{\left(\tilde{s}_{ij}, \tilde{p}_{ij}, \xi_j, \mu, \nu_i \right) = \left(\tilde{s}_{ij}^{*}, \tilde{p}_{ij}^{*}, \xi_j^{*}, \mu^{*}, \nu_i^{*} \right)} = \frac{1}{N_F} - \frac{\mu^{*}}{N_F} + \tilde{s}_{ij}^{*} \xi_j^{*} \left(\frac{\left| \hat{h}_{ij} \right|^2}{\left| \hat{h}_{ij} \right|^2 \tilde{p}_{ij}^{*} + \tilde{s}_{ij}^{*} \sigma_z^2} - \frac{\sqrt{2} \left| \hat{h}_{ij} \right| \tilde{s}_{ij}^{*} \sigma_h \sigma_z^2 Q^{-1}\left(1 - P_{out} \right)}{\left(\left| \hat{h}_{ij} \right|^2 \tilde{p}_{ij}^{*} + \tilde{s}_{ij}^{*} \sigma_z^2 \right)^2} \right) = 0 \tag{3.102}$$

It is easy to verify that (3.102) results to

$$\tilde{p}_{ij}^{*} = \frac{N_F \tilde{s}_{ij}^{*} \xi_j^{*}}{2 \left| \hat{h}_{ij} \right|^2 \left(\mu^{*} - 1 \right)} \left(\underbrace{\sqrt{\left| \hat{h}_{ij} \right| \left(\left| \hat{h}_{ij} \right|^3 - 4\sqrt{2} \sigma_h \sigma_z^2 Q^{-1}\left(1 - P_{app} \right) \frac{\left(\mu^{*} - 1 \right)}{N_F \xi_j^{*}} \right)}}_{\beta_{ij}} - \left| \hat{h}_{ij} \right|^2 + \frac{2\sigma_z^2}{N_F} \frac{\left(\mu^{*} - 1 \right)}{\xi_j^{*}} \right) . \tag{3.103}$$

From equation (3.103) we derive the variable β_{ij} in (3.38) and the optimal transmitting power allocation policy as defined in (3.37) of *Theorem 3.3*.

Moreover, according to the KKT condition (3.91), differentiating the Lagrangian function $\mathcal{L}\left(\tilde{s}_{ij},\tilde{p}_{ij},\xi_j,\mu,\nu_i\right)$ in (3.89) over the optimal subcarrier allocation index $\tilde{s}_{ij}^*$ of user j on subcarrier i, results to

$$\left.\frac{\partial\mathcal{L}\left(\tilde{s}_{ij},\tilde{p}_{ij},\xi_j,\mu,\nu_i\right)}{\partial\tilde{s}_{ij}}\right|_{\left(\tilde{s}_{ij},\tilde{p}_{ij},\xi_j,\mu,\nu_i\right)=\left(\tilde{s}_{ij}^*,\tilde{p}_{ij}^*,\xi_j^*,\mu^*,\nu_i^*\right)}=\log_2\left(1+\frac{\left|\hat{h}_{ij}\right|^2\tilde{p}_{ij}^*}{\sigma_z^2\tilde{s}_{ij}^*}\right)-\frac{\left|\hat{h}_{ij}\right|^2\tilde{p}_{ij}^*}{\ln 2\cdot\tilde{s}_{ij}^*\sigma_z^2\left(1+\frac{\left|\hat{h}_{ij}\right|^2\tilde{p}_{ij}^*}{\tilde{s}_{ij}^*\sigma_z^2}\right)}$$

$$-\frac{\sqrt{2}\left|\hat{h}_{ij}\right|^3\tilde{p}_{ij}^{2*}\xi_j\sigma_h Q^{-1}\left(1-P_{app}\right)}{\left(\left|\hat{h}_{ij}\right|^2\tilde{p}_{ij}^*+\tilde{s}_{ij}^*\sigma_z^2\right)^2}-\frac{\nu_i}{\xi_j}\begin{cases}>0, \text{ if } \tilde{s}_{ij}^*=1\\ =0, \text{ if } 0<\tilde{s}_{ij}^*<1\end{cases} \tag{3.104}$$

By substituting the instantaneous optimal transmitting power $\tilde{p}_{ij}^*$ in equation (3.103) in equation (3.104), with some manipulation we get that the left side of equation (3.104) becomes

$$\log_2\left(N_F\xi_j^*\left|\hat{h}_{ij}\right|^2\cdot\frac{\beta_{ij}+\left|\hat{h}_{ij}\right|^2}{2\sigma_z^2\left(\mu^*-1\right)}\right)-\frac{\left(\frac{\beta_{ij}+\left|\hat{h}_{ij}\right|^2}{2\sigma_z^2\left(\mu^*-1\right)}-\frac{1}{N_F\xi_j^*}\right)}{\ln 2\cdot\left(\frac{\beta_{ij}+\left|\hat{h}_{ij}\right|^2}{2\sigma_z^2\left(\mu^*-1\right)}\right)}-\frac{\nu_i}{\xi_j}$$

$$-\frac{\sqrt{2}N_F\xi_j^*\left|\hat{h}_{ij}\right|\left(\frac{\beta_{ij}+\left|\hat{h}_{ij}\right|^2}{2\sigma_z^2\left(\mu^*-1\right)}-\frac{1}{N_F\xi_j^*}\right)^2\sigma_h Q^{-1}\left(1-P_{app}\right)}{\left[N_F\xi_j^*\left|\hat{h}_{ij}\right|^2\left(\left(\frac{\beta_{ij}+\left|\hat{h}_{ij}\right|^2}{2\sigma_z^2\left(\mu^*-1\right)}-\frac{1}{N_F\xi_j^*}\right)\right)^2+\frac{1}{N_F\xi_j^*\left|\hat{h}_{ij}\right|^2}+\frac{1}{2\sigma_z^4}\left(\frac{\beta_{ij}+\left|\hat{h}_{ij}\right|^2}{2\sigma_z^2\left(\mu^*-1\right)}-\frac{1}{N_F\xi_j^*}\right)\right]} \tag{3.105}$$

In continue, by introducing the variable $\beta_{ij}'=\beta_{ij}+\left|\hat{h}_{ij}\right|^2$, for notational brevity, the left side of equation (3.104) in (3.105) can be written as

$$\log_2\left(N_F\xi_j^*\left|\hat{h}_{ij}\right|^2\cdot\beta_{ij}'\right)-\frac{\left(\beta_{ij}'-\frac{1}{N_F\xi_j^*}\right)}{\ln 2\cdot\beta_{ij}'} - \frac{\sqrt{2}\left|\hat{h}_{ij}\right|N_F\xi_j^*\left(\beta_{ij}'-\frac{1}{N_F\xi_j^*}\right)^2\sigma_h Q^{-1}\left(1-P_{app}\right)}{\left[N_F\xi_j^*\left|\hat{h}_{ij}\right|^2\left(\left(\beta_{ij}'-\frac{1}{N_F\xi_j^*}\right)\right)^2+\frac{1}{N_F\xi_j^*\left|\hat{h}_{ij}\right|^2}+\frac{1}{2\sigma_z^4}\left(\beta_{ij}'-\frac{1}{N_F\xi_j^*}\right)\right]}-\frac{\nu_i}{\xi_j} \quad . \quad (3.106)$$

Moreover, we introduce the variable $\beta_{ij}''=N_F\xi_j^*\beta_{ij}'-1$ and the left side of equation (3.104) in (3.106) becomes

$$\underbrace{\xi_j^*\left(\log_2\left(\left|\hat{h}_{ij}\right|^2\cdot\left(\beta_{ij}''+1\right)\right)-\frac{\beta_{ij}''}{\ln 2\cdot\left(\beta_{ij}''+1\right)}-\frac{\sqrt{2}\left|\hat{h}_{ij}\right|\beta_{ij}''^2\sigma_h Q^{-1}\left(1-P_{app}\right)}{\left|\hat{h}_{ij}\right|^2\beta_{ij}''^2+\frac{1}{\left|\hat{h}_{ij}\right|^2}+\frac{1}{2\sigma_z^4}\beta_{ij}''}\right)}_{\hat{H}_{ij}}-\nu_i\,, \quad (3.107)$$

which yields the variable $\hat{H}_{ij}$ as defined in (3.40) of *Theorem 3.4*. Finally, from (3.107) and the KKT condition (3.91) we get that the derivation of the Lagrangian function $\mathcal{L}\left(\tilde{s}_{ij},\tilde{p}_{ij},\xi_j,\mu,\nu_i\right)$ in (3.89) over the optimal subcarrier allocation index $\tilde{s}_{ij}^*$ of user j on subcarrier i, yields that

$$\left.\frac{\partial\mathcal{L}\left(\tilde{s}_{ij},\tilde{p}_{ij},\xi_j,\mu,\nu_i\right)}{\partial\tilde{s}_{ij}}\right|_{\left(\tilde{s}_{ij},\tilde{p}_{ij},\xi_j,\mu,\nu_i\right)=\left(\tilde{s}_{ij}^*,\tilde{p}_{ij}^*,\xi_j^*,\mu^*,\nu_i^*\right)}=\xi_j^*\cdot\hat{H}_{ij}\left(\xi_j^*,\mu^*\right)-\nu_i^*\begin{cases}>0, \text{ if } \tilde{s}_{ij}^*=1\\ =0, \text{ if } 0<\tilde{s}_{ij}^*<1\end{cases} \quad . \quad (3.108)$$

From (3.108) we conclude that the optimal subcarrier allocation index $\tilde{s}_{ij}^*$ is equal to zero, e.g., $\tilde{s}_{ij}^*=0$ if the optimal LM ν_i^* is larger than $\xi_j^*\cdot\hat{H}_{ij}$, e.g., $\nu_i^*>\xi_j^*\cdot\hat{H}_{ij}$ and that the optimal subcarrier allocation index $\tilde{s}_{ij}^*$ is equal to one, e.g., $\tilde{s}_{ij}^*=1$ if the optimal LM ν_i^* is smaller than $\xi_j^*\cdot\hat{H}_{ij}$, e.g., $\nu_i^*<\xi_j^*\cdot\hat{H}_{ij}$, as expressed in (3.39) of *Theorem 3.4*.

In addition the search for the optimal user j^* as given in (3.41) of *Theorem 3.4* is always feasible for the following reason. From the subcarrier allocation constrain in (3.32)

and the time-sharing factor $\tilde{s}_{ij}^{*} \in (0,1]$, for each subcarrier i we know that if the variables $\hat{H}_{ij}$ given in (3.107) are different for all j, only the user j with the largest $\hat{H}_{ij}$ can use that subcarrier i, i.e., $\tilde{s}_{ij^*}^{*}=1$, $\tilde{s}_{ij}^{*}=0$ for all $j \neq j^*$. As the CSIT realizations, e.g., $|h_{ij}|^2$, are i.i.d then the imperfect CSIT realizations, e.g., $|\hat{h}_{ij}|^2$ are also i.i.d for different user j meaning that the chance for $\hat{H}_{ij}$ to be the same for different users happens only with probability 0. This completes the proof of *Theorem 3.4*. ■

Finally, with direct substitution of the optimal transmitting power allocation in (3.103) and the optimal subcarrier allocation index $\tilde{s}_{ij}^{*}$ in (3.108), in PE-AETS's PBL process in (3.16) we derive the optimal allocation policy $\mathbf{R}^{*}\left[\hat{h}_{ij}\right]=\left[\tilde{r}_{ij}^{*}\right]$ as given in (3.42). This completes the proof of *Theorem 3.5*. ■

A.7 Impact of Channel Imperfectness on Channel-Error-Inconsiderate Schemes (EIOS and EIFAS)

In this Appendix, we investigate the impact of channel imperfectness on the channel-error-inconsiderate schemes EIOS [14], [20], [21], [22], [23] and EIFAS [27], [60]. When EIOS and EIFAS scheduling is considered the time-shared data rate allocation policies $r_{ij,EIOS}$ and $r_{ij,EIFAS}$ of user j on subcarrier i are given by

$$r_{ij,EIOS}=r_{ij,EIFAS}=E_{\hat{h}_{ij}}\left[\tilde{s}_{ij}\log_2\left(1+\frac{\tilde{p}_{ij}\left|\hat{h}_{ij}\right|^2}{\tilde{s}_{ij}\sigma_z^2}\right)E_{h_{ij}|\hat{h}_{ij}}\left[1_{\left(|\hat{h}_{ij}|^2\le|h_{ij}|^2\right)}\right]\right].^{32} \qquad (3.109)$$

Under channel error, e.g., when $\sigma_h^2>0$, EIOS and EIFAS cannot perform appropriate scheduling. However, we can compute the minimum power requirements and average

[32] We recall that $1_{(\cdot)}$ denotes the indicator factor.

effective data rates of EIOS and EIFAS focusing on the most strict equivalent data rate requirement of each user, e.g., $\tilde{q}_j\left(F,T_j^{\max},\lambda_j\right)$, since obviously $\tilde{q}_j\left(F,T_j^{\max},\lambda_j\right)$ is enough to satisfy each user's delay constraints. In other words, the only criterion we can rely on to define the impact of channel imperfectness on channel-error-inconsiderate schemes is the minimum rate requirement derived by the upper-layer parameters, e.g., $\tilde{q}_j\left(F,T_j^{\max},\lambda_j\right)$. To avoid confusion, we separate the presentation of the specifications of EIOS and EIFAS as below.

EIOS - In EIOS's strategy, if C_j represents the class of each user j then, similarly to the definition of the optimal approximated effective data rate $\tilde{r}_{ij}^*$ in (3.42), the minimum required power $P_{\min,EIOS}$ is calculated as follows.

$$\begin{aligned}\max_{C_j}\tilde{q}_{C_j}\left(F,T_{C_j}^{\max},\lambda_{C_j}\right) &\cong E_{\hat{h}_{ij}}\left[\sum_{i=1}^{N_F}\tilde{s}_{ij}\log_2\left(\frac{P_{\min,EIOS}\eta_{ij}\left|\hat{h}_{ij}\right|^2}{\tilde{s}_{ij}\sigma_z^2}\right)E_{h_{ij}|\hat{h}_{ij}}\left[1_{\left(|\hat{h}_{ij}|^2\le|h_{ij}|^2\right)}\right]\right]\\ &= \frac{N_F}{2K}\log_2\left(P_{\min,EIOS}E_{\hat{h}_{ij}}\left[\frac{\eta_{ij}\left|\hat{h}_{ij}\right|^2}{\tilde{s}_{ij}\sigma_z^2}\middle|\tilde{s}_{ij}=1\right]\right)\end{aligned}. \quad (3.110)$$

It is shown in [21] that the term $E_{\hat{h}_{ij}}\left[\left(\eta_{ij}\left|\hat{h}_{ij}\right|^2/\sigma_z^2\right)\middle|\tilde{s}_{ij}=1\right]$ in (3.110) is computed as

$$E_{\hat{h}_{ij}}\left[\frac{\eta_{ij}\left|\hat{h}_{ij}\right|^2}{\sigma_z^2}\middle|\tilde{s}_{ij}=1\right]=\Theta\left(\left(1-\sigma_h^2\right)\log_2\left(K\right)\right).^{33} \quad (3.111)$$

In addition, apparently the term $E_{\hat{h}_{ij}}\left[E_{h_{ij}|\hat{h}_{ij}}\left[1_{\left(|\hat{h}_{ij}|^2\le|h_{ij}|^2\right)}\right]\right]$ in (3.110) equals to $1/2$. By (3.110) and (3.111), we can compute the minimum required power $P_{\min,EIOS}$ of EIOS under imperfect channel conditions as

[33] We recall that $\Theta\left(b_x\right)=a_x$ if $\limsup_{x\to\infty}|a_x|/|b_x|<\infty$ and $\limsup_{x\to\infty}|b_x|/|a_x|<\infty$.

$$P_{\min,EIOS} = \Theta\left(\frac{2^{\max\limits_{C_j}\tilde{q}_{C_j}\left(F,T_{C_j}^{\max},\lambda_{C_j}\right)\frac{2K}{N_F}}}{\left(1-\sigma_h^2\right)\log_2\left(K\right)}\right),\ \ \sigma_h^2 > 0. \tag{3.112}$$

Let us now consider that ΔP expresses the difference between the average available power to the BS P_{TOTAL} and the minimum required power $P_{\min,EIOS}$ of EIOS in (3.112), e.g., $\Delta P = P_{TOTAL} - P_{\min,EIOS}$. If $r_{P_{\min,EIOS}+\Delta P}$ is the data rate under power $P_{\min,EIOS}+\Delta P$ and $r_{P_{\min,EIOS}}$ the data rate under power $P_{\min,EIOS}$ then difference $\Delta r = r_{P_{\min,EIOS}+\Delta P} - r_{P_{\min,EIOS}}$ expresses the average system's effective throughput among all the N_F subcarriers and it is computed as

$$\Delta r = r_{P_{\min,EIOS}+\Delta P} - r_{P_{\min,EIOS}} = \frac{N_F}{2}\log_2\left(1+\frac{\Delta P}{P_{\min,EIOS}}\right).$$

Hence, under channel uncertainty, the EIOS's total average effective data rate is given by

$$\sum_{C_j=1}^{C_{\max}}\left(K_{C_j}\tilde{q}_{C_j}\left(F,T_{C_j},\lambda_{C_j}\right)\right)+\Delta r,$$

where $C_{\max}$ the total number of users' classes.

EIFAS - In EIFAS's strategy, the channel uncertainty realization $\left|\hat{h}_{ij}\right|^2$ is treated as the actual channel realization $\left|h_{ij}\right|^2$. As fixed subcarrier allocation is considered the scheme is also unaware of the subcarrier index $\tilde{s}_{ij}$ and hence, the target is to maximize the equivalent rate constraint $\tilde{q}_{C_j}\left(F,T_{C_j},\lambda_{C_j}\right)$ of the class $C_j \in C_{\max}$ users as follows.

$$\begin{aligned}\max_{C_j}\tilde{q}_C\left(F,T_{C_j}^{\max},\lambda_{C_j}\right) &\cong E_{\hat{h}_{ij}}\left[\sum_{i=1}^{N_F}\log_2\left(\frac{P_{\min,EIOS}\eta_{ij}\left|\hat{h}_{ij}\right|^2}{\sigma_z^2}\right)E_{h_{ij}|\hat{h}_{ij}}\left[1_{\left(\left|\hat{h}_{ij}\right|^2\le\left|h_{ij}\right|^2\right)}\right]\right]\\ &= \frac{N_F}{2K}E_{\hat{h}_{ij}}\left[\log_2\left(\frac{P_{\min,EIFAS}\eta_{ij}\left|\hat{h}_{ij}\right|^2}{\sigma_z^2}\right)E_{h_{ij}|\hat{h}_{ij}}\left[1_{\left(\left|\hat{h}_{ij}\right|^2\le\left|h_{ij}\right|^2\right)}\right]\right].\end{aligned} \tag{3.113}$$

From [21] we can show that the term $E_{\hat{h}_{ij}}\left[\eta_{ij}\left|\hat{h}_{ij}\right|^2/\sigma_h^2\right]$ in (3.113) is computed as

$$E_{\hat{h}_{ij}}\left[\eta_{ij}\left|\hat{h}_{ij}\right|^2/\sigma_h^2\right]=\left(1-\sigma_h^2\right). \tag{3.114}$$

In addition, apparently the term $E_{\hat{h}_{ij}}\left[E_{h_{ij}|\hat{h}_{ij}}\left[1_{\left(|\hat{h}_{ij}|^2\le|h_{ij}|^2\right)}\right]\right]$ in (3.113) equals to $1/2$.

Thus, by (3.113) and (3.114) we can compute the minimum required power $P_{\min,EIFAS}$ of EIFAS under imperfect channel conditions as

$$P_{\min,EIFAS}=\Theta\left(\frac{2^{\left(\max\limits_{C_j}\tilde{q}_{C_j}\left(F,T_{C_j}^{\max},\lambda_{C_j}\right)\right)\frac{2K}{N_F}}-1}{1-\sigma_h^2}\right),\ \sigma_h^2>0. \tag{3.115}$$

Let us now consider that $\Delta P'$ expresses the difference between the average available power to the BS P_{TOTAL} and the minimum required power $P_{\min,EIFAS}$ of EIFAS in (3.115), e.g., $\Delta P'=P_{TOTAL}-P_{\min,EIFAS}$. If $r_{P_{\min,EIFAS}+\Delta P'}$ is the data rate under power $P_{\min,EIFAS}+\Delta P'$ and $r_{P_{\min,EIFAS}}$ the data rate under power $P_{\min,EIFAS}$ then difference $\Delta r'=r_{P_{\min,EIFAS}+\Delta P'}-r_{P_{\min,EIFAS}}$ expresses the average system's effective throughput among all the N_F subcarriers and it is given by

$$\Delta r'=r_{P_{\min,EIFAS}+\Delta P'}-r_{P_{\min,EIFAS}}=\frac{N_F}{2}\log_2\left(1+\frac{\Delta P'}{P_{\min,EIFAS}}\right).$$

Hence, under channel uncertainty, the EIFAS's total average effective data rate is given by

$$\sum_{C_j=1}^{C_{\max}}\left(K_{C_j}\tilde{q}_{C_j}\left(F,T_{C_j},\lambda_{C_j}\right)\right)+\Delta r'.$$

Chapter 4

Game-Theoretic Cross-Layer Design

4.1 Introduction

In this Chapter, we focus on novel scheduling issues involved in designing, operating and managing power-efficient and fairness-aware cross-layer designs. In particular, we rely on the asymmetric Nash bargaining concept to introduce the first analytical NBS-based resource allocation policy for real-time operation in OFDMA systems. More precisely, we introduce a weighted proportional fair PBL process to allocate both power and data in fully compliance with the A-NBS Axioms. Relying on our PBL process we aim to maximize the overall effective throughput subject to channel, power and QoS distribution constraints with additional price rules regarding the heterogeneous users' asymmetric payoffs. Upon applying subcarrier time-sharing relaxation, we formulate a convex optimization problem to obtain the optimal solutions via closed-form analysis. In our analysis we exploit Lambert-*W* function properties and develop an innovative methodology to solve transcendental algebraic equations that appear during the optimization process due to the recursive origin of the A-NBS problem [44]. With our methodology, we achieve deriving the first joint power and subcarrier optimal allocation policy for the A-NBS problem by means of final formulas. In addition, we introduce a new scope for the solution concept of cross-layer designs that further enhances power efficiency and guarantees iteration-independent allocation policies. Finally, we demonstrate that the proposed A-NBS scheduling can be employed to typify ideal resource allocation for real-time operation in next-generation broadband wireless networks, where the terminus is to enhance system's performance in terms of queuing delay, fairness, QoS support and power consumption with the comparable total throughput. The key contributions and the

proposed methodology of this research part have been thoroughly discussed in Section 1.2 of Chapter 1.

4.2 Literature Review

Consecutive studies witness the importance of developing cross-layer schemes to improve resource allocation efficiency in OFDMA networks [21], [23], [56], [148]. However, by only maximizing throughput or minimizing power a frequent and detrimental phenomenon occurs when users with good channel conditions are over-allocated by resources, which are discounted from users in bad channel conditions. Hence, a new challenge emerges on the design of game-theoretic cross-layer schemes that balance resource scheduling efficiency and fairness provision. Fairness in conjunction with efficiency is concerned in non-cooperative game theoretic strategies [34], [35], [72] causing Nash equilibrium [40] issues that lower performance as compared to cooperative game theoretical approaches [41], [37]. Therefore, recent viewpoints believe that cooperative game theory is more suitable for cross-layer resource allocation [37], [38], [149], where NBS [40] is one promising candidate.

Although its major importance this research field is currently at a very early stage. The reasons are firstly that all optimal allocation strategies regard single-layer resource scheduling and secondly that no straight analytical solution to the NBS problem has been yet proposed [37], [38], [42], [43], [68], [76], [77], [150]. In their majority, relevant studies obtain sub-optimal NBS-based allocation policies via either numerical or graphical solution concepts [68], [76], [77], [150] with performances to be obviously questioned. On the other hand, we can discriminate only the four works in [37], [42], [43] and [149] where authors propose cooperative S-NBS-based game theoretical schemes on a per-layer resource scheduling basis. However, even in those cases, it is straightforward that the S-NBS property is only ostensibly adopted and also that the validity of the analytical solutions is quite biased. This can be firstly justified for the reason that the authors clearly modify the S-NBS rule, i.e., NBS properties are frequently considered as optimization constraints instead of being incorporated into the cost function and secondly because the reported optimal strategies are in partial compliment with the S-NBS allocation of power disrespecting the S-NBS allocation of subcarriers. For example, in [37] the authors develop a game theoretical model based on

modified S-NBS properties only to address the power control for the opportunistic spectrum access problem and to show that their S-NBS-based approach achieves the best trade-off between fairness and efficiency among two other bargaining solutions: the Egalitarian and Kalai-Smorodinsky [41]. Similarly, in [42] and [43] the authors adjust the S-NBS properties to propose cooperative game theoretical schemes aiming to address the power-control for reliable transmission opportunities to users in CR networks. In addition, the study in [149] attempts S-NBS-based joint power and subcarrier allocation using both sum power minimization strategy and fair throughput maximization approach by proposing the *N*-dimensional decomposition method as solution to the problem. Nevertheless, it is well known that decomposing the complex joint allocation problem into *N* single subcarrier sub-problems increases significantly the complexity of the solution meaning that the optimal allocation policy could not provide real-time service.

Through examining the A-NBS problem our first observation is that the key factor preventing the above works to derive straight analytical solutions in compliance with the NBS of both power and subcarrier allocation is the difficulty of solving transcendental algebraic equations of the form, i.e., $\log(x)^x = ax + b$, $a,b > 0$. Such equations appear during the optimization process due to the logarithmic origin of the A-NBS meaning that upon applying the KKT optimality conditions, recursions between the optimization variables unavoidably occur. The recursive origin of the A-NBS [59], [41] bears for numerical or graphical approaches and hence, new analytical solutions emerge. Therefore, we propose an intelligent methodology to solve such equations that allows us to derive the optimal policy for the actual A-NBS of both power and subcarrier allocation by means of final formulas. Our second observation is that all the afore-mentioned works consider single-layer S-NBS-based resource scheduling neglecting five important parameters for next-generation OFDMA networks. i) Heterogeneity of users' minimum requirements ii) data outage due to imperfect channel conditions, iii) complexity of the implementation algorithm, iv) various payoffs of system users and v) improvements on transmitting power-efficiency. For that reason, we address the above issues by introducing our game-theoretic resource scheduling scheme from the cross-layer perspective and also by relying on the A-NBS fairness concept. Our third observation is that the traditional scope for solving any kind of cross-layer problems can be significantly

improved in terms of power efficiency and complexity. Therefore, we rely on uniform transmitting power allocation among subcarrier time-sharing factors to introduce a different approach on the solution of cross-layer problems that favours power-efficiency and also delivers iteration-independent optimal scheduling policies.

For the ease of reference, in this Chapter we name the Error-Considerate cross-layer Scheduler adopted in [17], [24], [56] as ECS, the Error-Inconsiderate Opportunistic Scheduler adopted in [14], [20], [21], [22], [23] as EIOS, the Error-Inconsiderate Fixed power and subcarrier Assignment Scheduler utilised in [27], [60] as EIFAS, the Max-Min fairness scheduler adopted in [32], [151], [152] as MM and the Weighted Max-Min fairness scheme in [153], [154], [155] as WMM.

4.3 System Model

This Section outlines the downlink OFDMA system model, which is the basis of the proposed A-NBS cross-layer resource allocation problem formulated in Section 4.5. As illustrated in Figure 4.1, our system involves N_F subcarriers and K heterogeneous users with each user having its own minimum QoS requirements u_j^0 and q_j, and an asymmetric payoff denoted by the weight w_j. The minimum requirements u_j^0 and q_j of user j are always positive or equal to zero, e.g., $u_j^0 \geq 0$, $q_j \geq 0$, and express the user's minimum QoS demand to start cooperating with others for the NBS game to be feasible and user's minimum QoS requirement from higher layers, respectively. As we will see later, although u_j^0 and q_j are related, they are not necessarily equal as there may be instances where resources are enough for the S-NBS game to be feasible but not enough to satisfy all QoS from higher layers. Nevertheless, even in such cases we must ensure that the available resources will be fairly distributed among SUs according to the A-NBS property. On the other hand, the payoff w_j of user j takes positive values up to one, e.g., $w_j \in (0,1]$, and indicates the importance of the user in the network in terms of extra QoS provision from the BS to the user. For example, some users may belong to emergency or sensitive classes, e.g., medical, military divisions, or

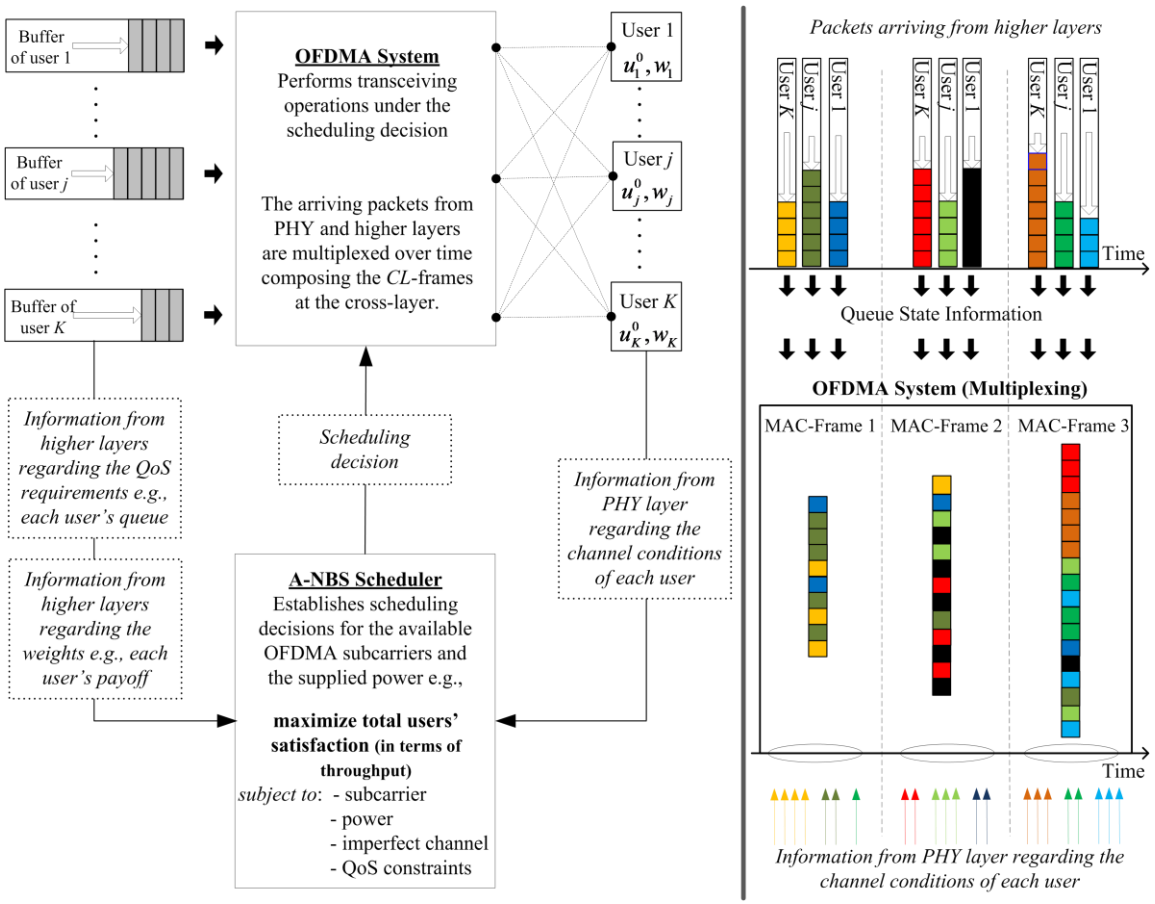

Figure 4.1 - Multi-user downlink OFDMA cross-layer scheduler under imperfect channel modelling with heterogeneous users' applications and payoffs (left). Packet multiplexing process over time for 3 *MAC*-frames (right).

may just pay higher price to the network's service provider than some other users, demanding for ideal QoS under any circumstances as, i.e., network overloading.

Prior to the scheduling decision, the proposed A-NBS scheduler collects the CSI and the QSI of all users. The CSI includes information about the channel conditions and it is obtained in the beginning of each scheduling interval through performing MMSE estimation of the imperfect channel in TDD operation[34] as presented in Sections 3.3.1 and 3.3.2 of

[34] The system can also operate under FDD, where perfect feedback of DL CSIT from mobile users is required.

Chapter 3. The QSI includes information about each user's QoS requirements q_j from higher layers and it is obtained according to an incremental update algorithm [133], [134] by observing the current backlogs in each user's independent buffer[35]. Hence, instead of updating the QoS information before each time slot as in [14], [17], [20], [21], [22], [23], [24], [27], [32], [56], [60], [151], [152], [153], [154] the A-NBS scheme uses the incremental update algorithm to reduce its pre-processing process. In addition, we use another incremental update algorithm to acquire users' payoffs and minimum QoS requirements u_j^0 to join the A-NBS game. In that case, information is acquired through UL sub-channels transmitted by each user and updates are performed according to how frequently the state of each user's mobility or significance changes. Furthermore, assuming perfect CSIR, our scheduler takes its scheduling decision once every time slot based on the estimated CSI, QSI and users' weights, and passes the resource allocation result to the OFDMA transmitter. The subcarrier and transmitting power allocation decision made by the BS transmitter is assumed to be announced to individual mobile user through a separate control DL channel.

4.3.1 Downlink Channel Modelling and CSIT Estimation from Imperfect Channel

In this Section, we adopt the channel modelling presented in Section 3.3 of Chapter 3, where the received OFDM symbol vector for the j-th user at each OFDM block is given by

$$\mathbf{y}_j = \mathbf{H} \cdot \mathbf{x}_j + \mathbf{z}_j . \tag{4.1}$$

We recall that $\mathbf{y}_j = \left[y_{ij} \right]^{\mathcal{T}}$ and $\mathbf{x}_j = \left[x_{ij} \right]^{\mathcal{T}}$ in (4.1) are the complex-valued vectors of the received and transmitted OFDM blocks y_{ij} and x_{ij} of user j on the i-th subcarrier, respectively. We also evoke that $\mathbf{H} = diag\left(\mathbf{h}_j\right)$ represents the channel gain matrix with the

[35] To avoid buffer overflow we assume that users' buffers are sufficiently large enough for storing packets arrived from higher layer. In addition, as we discuss later, we also consider that packets arriving from higher and PHY layers are multiplexed over time comprising *MAC*-frames as shown in Figure 4.1.

channel gains vectors $\mathbf{h}_j$ having entries the i.i.d actual channel gain feedback h_{ij} of user j on subcarrier i. Regarding the noise vector $\mathbf{z}_j = \left[z_{ij} \right]^{\mathcal{T}}$, we consider that its entries z_{ij} signify the channel noise of user j on subcarrier i and are CSCG i.i.d variables, e.g., $z_{ij} \sim \mathcal{CN}\left(0, \sigma_z^2\right)$, with zero mean and σ_z^2 variance given by $\sigma_z^2 = N_0 \cdot BW / N_C$, where N_0 and BW is the noise density and channel bandwidth, respectively.

The power $\mathbb{P}$ and data rate $\mathbb{R}$ allocation policies of the A-NBS scheme at the PHY layer are denoted by the matrices $\mathbb{P} = \left[p_{ij} \right]$ and $\mathbb{R} = \left[r_{ij} \right]$ with $p_{ij} = E\left[\left| x_{ij} \right|^2 \right]$ and r_{ij} to represent the instantaneous transmitting power and data rate allocated from the scheduler at the BS to user j through subcarrier i, respectively. In addition, for the efficiency of the transmission between BS and users, we consider M-QAM modulation with the Bit-Error-Rate (BER) of user j on subcarrier i to be given by

$$BER_{ij} \approx 0.2 \cdot \exp\left(\frac{-1.5 \cdot SNR_{ij}}{2^{r_{ij}} - 1} \right), \tag{4.2}$$

where SNR_{ij} in (4.2) represents the signal-to-noise (SNR) ratio of user j on subcarrier i given by $SNR_{ij} = p_{ij} \left| h_{ij} \right|^2 / \sigma_z^2$ [156]. Depending on the number of bits assigned to a subcarrier, the adaptive modulator uses a corresponding M-QAM modulation scheme, and the transmitting power level is adjusted according to the combined power, subcarrier and bit allocation decision. In other words, the adaptive modulator adjusts the number of bits loaded on the i-th subcarrier of user j by allowing the instantaneous data rate r_{ij} to take values from the set $\mathbf{D}$, e.g., $r_{ij} \in \left[0, D \right]$. The set $\mathbf{D}$ expresses the possible number of information that can be transmitted by a subcarrier and it is denoted by $\mathbf{D} = \left\{ 0,1,...,D \right\}$, where D is the maximum number of information that can be transmitted by each subcarrier.

Moreover, the subcarrier allocation policy at the PHY layer is represented by the matrix $\mathbb{S} = \left[s_{ij} \right]$, where $s_{ij} \in \left\{ 0,1 \right\}$ is the subcarrier allocation index meaning that $s_{ij} = 1$ when subcarrier i is allocated to user j otherwise $s_{ij} = 0$. Hence, to ensure that during a time slot

each subcarrier is allocated to one user only, we define a necessary subcarrier allocation condition as

$$\sum_{i=1}^{N_F} s_{ij} \leq 1. \tag{4.3}$$

In addition, we term a transmitting power allocation rule as

$$E\left[\frac{1}{N_F}\sum_{j=1}^{K}\sum_{i=1}^{N_F} s_{ij} p_{ij}\right] \leq P_{TOTAL}, \tag{4.4}$$

to guarantee that the average transmitting power over all users and subcarriers should be smaller or equal than the average total available power at the BS denoted by P_{TOTAL} [36].

In continue, we model the imperfect channel by representing the independent distributed estimated channel gain $\hat{h}_{ij}$ of user j on subcarrier i, as

$$\hat{h}_{ij} = h_{ij} + \Delta\hat{h}_{ij}, \tag{4.5}$$

where h_{ij} in (4.5) is the actual channel gain feedback and Δh_{ij} the zero mean CSCG channel error term of user j on subcarrier i with known PDF. To increase the system's resilience to CSI errors and also to enhance its throughput efficiency, we perform non-spheristic estimation of the imperfect channel utilizing our effective MMSE channel estimation process presented in Section 3.3.2 of Chapter 3. We recall that in our estimation process the channel errors $\{\Delta h_{ij}\}$ and the estimated channel gains $\{\hat{h}_{ij}\}$ are uncorrelated, while the estimation errors among each user's subcarriers are correlated with MMSE variance σ_h^2 to be depended on each subcarrier's parameters.

[36] The left side of (4.4) is divided by the number of subcarriers N_F as we refer to average quantities. This means that P_{TOTAL} is the total available power at the BS taking into consideration the effects such as PAPR , i.e., P_{TOTAL} is the total available power at the BS considering both the average transmitting power allowed by the BS and the PAPR of OFDM signals.

4.3.2 MAC and Upper Layer Modelling from Cross-Layer Perspective

Packets from upper layers arrive to each user j's buffer according to a Poisson arrival process with independent arrival rate denoted by λ_j (in *packets per time slot*). In our source modelling the K users have heterogeneous applications in nature and consequently each user has a maximum delay tolerance denoted by $T_j^{\max}$. Hence, users with heavier traffic load have higher arrival rate λ_j, while uses that are more delay-sensitive have stringent maximum delay tolerance $T_j^{\max}$. As in our previous work, we characterize the QoS parameters of each user j by the tuple $\left[F, T_j^{\max}, \lambda_j\right]$, where F denotes the size of each packet in *bits*.

The MAC layer is responsible for the A-NBS cross-layer resource scheduling at every fading block based on the current system dynamics. We recall that system dynamics change dynamically over time and express the perception of the A-NBS scheduler at the MAC layer regarding the current system state, e.g., CSI from PHY layer and QSI and users' payoffs from the upper layers. We denote A-NBS's system state as $\left(\hat{\mathbb{H}}, \mathbb{Q}, \mathbb{U}^0, \mathbb{W}\right)$, where $\hat{\mathbb{H}}$, $\mathbb{Q}$, $\mathbb{U}^0$ and $\mathbb{W}$ are the system dynamics; $\hat{\mathbb{H}}$ is the $N_F \times K$ matrix of the estimated channel gain given by $\hat{\mathbb{H}} = E\left[\left|\hat{h}_{ij}\right|^2\right]$, while $\mathbb{Q}$ is the $K \times 1$ vector of the QSI given by $\mathbb{Q} = \left[q_j\right]$ with its j-th component q_j to denote the user's QoS requirement from higher layers in terms of number of packets remaining in user j's buffer. In addition, $\mathbb{U}^0$ is the $K \times 1$ vector of users' minimum QoS demand to join the A-NBS game given by $\mathbb{U}^0 = \left[u_j^0\right]$ and $\mathbb{W}$ is the $K \times 1$ vector of users' payoffs given by $\mathbb{W} = \left[w_j\right]$.

At the beginning of every OFDM frame, the BS estimates the CSIT from dedicated uplink pilot symbols and observes the current backlogs in the buffer according to an incremental update algorithm as described in Section 3.3 of Chapter 3. Based on the obtained CSIT, QSI and payoffs, A-NBS at the cross-layer determines the subcarrier allocation from the policy $\mathbb{S}\left[\hat{\mathbb{H}}, \mathbb{Q}, \mathbb{U}^0, \mathbb{W}\right]$, the transmitting power allocation from the policy

$\mathbb{P}\left[\hat{\mathbb{H}},\mathbb{Q},\mathbb{U}^0,\mathbb{W}\right]$ and the throughput allocation from the policy $\mathbb{R}\left[\hat{\mathbb{H}},\mathbb{Q},\mathbb{U}^0,\mathbb{W}\right]$. The scheduling results are then broadcasted on downlink common channels to all users before subsequent downlink packets transmissions at scheduled rates.

4.4 Effective Data Rate under Imperfect CSIT, Channel Outage and Asymmetric Weights of System Users - Fairness Aware PBL Process for OFDMA Systems

In this Section, we design a novel fairness-aware PBL process that fully complies with the A-NBS allocation of power and subcarrier considering channel imperfectness, channel outage and asymmetric weights of system users. To explore different potentials we approach the fairness aware PBL process with a different scope than our power-efficient PBL process defined in Chapter 3. For the ease of presentation, we separate the formulation of the A-NBS-based PBL process into two parts: the first part regards the imperfect channel and outage considerations, while the second part concerns the asymmetric fairness awareness.

4.4.1 Imperfect Channel and Outage Considerations - Part A

As we thoroughly explained in Section 3.4 of Chapter 3, imperfect channel may result in scheduled rates greater than the maximum channel's capacity [136]. Hence, we shall firstly address the systematic effect of packet error due to channel noise and outage to define the effective instantaneous data rate r_{ij} of the A-NBS scheme.

Looking through the definition of the BER in (4.2), the instantaneous data rate r_{ij} allocated to user j through subcarrier i, has been defined as a function of the actual channel realization h_{ij} hence, it is in fact the maximum achievable capacity c_{ij} of subcarrier i allocated to user j during a fading slot. From the Shannon's capacity theorem [136] and by defining the variable $\eta_{ij} = -1.5/\left(\sigma_z^2 \cdot \ln\left(5 \cdot BER_{ij}\right)\right)$ for brevity, we can define the maximum achievable capacity c_{ij} of subcarrier i allocated to user j as

$$c_{ij} = \log_2\left(1+\eta_{ij} p_{ij} \left|h_{ij}\right|^2\right). \tag{4.6}$$

Our target is to define a PBL process to describe the maximum possible data rate transmission under channel outage. In our PBL process, the instantaneous effective data rate r_{ij} should firstly be smaller or equal than the maximum achievable capacity c_{ij} in (4.6), e.g., $r_{ij} \le c_{ij}$, and secondly it should be defined as the maximum instantaneous data successfully delivered to user j through subcarrier i, e.g.,

$$r_{ij} = 1_{\left(r_{ij} \le c_{ij}\right)} \cdot c_{ij}\,. \tag{4.7}$$

The notation $1_{(\cdot)}$ denotes the indicator function, which in (4.7) is given by $1_{\left(r_{ij} \le c_{ij}\right)} = \begin{cases} 1, & r_{ij} \le c_{ij} \\ 0, & r_{ij} > c_{ij} \end{cases}$, $\forall i, j$. Hence, accounting the imperfect channel realization $\hat{h}_{ij}$ in (4.6), we can compute the instantaneous effective data rate r_{ij} in (4.7) as

$$\begin{aligned} r_{ij} &= E_{\hat{h}_{ij}}\left[E_{h_{ij}|\hat{h}_{ij}}\left[1_{\left(r_{ij} \le c_{ij}\right)} \cdot c_{ij}\right]\right] \\ &= E_{\hat{h}_{ij}}\left[1_{\left(r_{ij} \le c_{ij}\right)} \cdot c_{ij}\right] \\ &= E_{\hat{h}_{ij}}\left[\left(\Pr\left(r_{ij} \le c_{ij} \middle| \hat{h}_{ij}\right)\right) \cdot c_{ij}\right] \\ &= E_{\hat{h}_{ij}}\left[\left(1-\mathbb{P}_{out,ij}\right) \cdot c_{ij}\right] \end{aligned}, \tag{4.8}$$

where $\mathbb{P}_{out,ij}$ represents the target channel outage probability of each subcarrier i allocated to user j and it is given by $\mathbb{P}_{out,ij} = 1 - \Pr\left[E_{\hat{h}_{ij}}\left[c_{ij}\right] \le c_{ij} \middle| \hat{h}_{ij}\right]$. In other words, $\mathbb{P}_{out,ij}$ in (4.8) indicates the target channel outage probability determined by the probability where the maximum achievable capacity c_{ij} is smaller than the capacity $E_{\hat{h}_{ij}}\left[c_{ij}\right]$ as perceived by the system due to the imperfect channel. For simplicity, we assume that the target channel outage probability $\mathbb{P}_{out,ij}$ is the same for each user and subcarrier, e.g., $\mathbb{P}_{out,ij} = \mathbb{P}_{out}$. Furthermore, from the definitions of the instantaneous effective data rate r_{ij} in (4.8) and of the maximum

achievable capacity c_{ij} in (4.6) we can define the PBL process of the effective data rate r_j allocated to user j as

$$\begin{aligned} r_j &= E_{\hat{h}_{ij}}\left[\sum_{i=1}^{N_F}\left(1-\mathbb{P}_{out}\right)\cdot s_{ij}\cdot c_{ij}\right] \\ &= E_{\hat{h}_{ij}}\left[\sum_{i=1}^{N_F}\left(1-\mathbb{P}_{out}\right)\cdot s_{ij}\cdot \log_2\left(1+\eta_{ij}\,p_{ij}\left|h_{ij}\right|^2\right)\right], \end{aligned} \tag{4.9}$$

where $1-\mathbb{P}_{out}=\Pr\left[E_{\hat{h}_{ij}}\left[c_{ij}\right]\le c_{ij}\left|\hat{h}_{ij}\right.\right]$ is the probability of successfully transmitting information and the subcarrier allocation index s_{ij} is used to indicate which subcarriers are assigned to user j. The definition of our PBL process in (4.9), on one hand considers channel imperfectness and channel outage but on the other hand it does not have not yet include the asymmetric weights of the system users.

4.4.2 A-NBS Fairness Considerations - Part B

To include the asymmetric weights of the system users in our PBL process we follow the A-NBS Axioms as presented in Section 2.4 of Chapter 2. Examining *Lemma 2.2*, we observe that we cannot apply the A-NBS property in our PBL function in (4.9) as it is not convex yet. The reason is that the definition of the effective data rate r_j of user j in (4.9) includes the discrete variable of the subcarrier index s_{ij}, e.g., $s_{ij}\in\{0,1\}$, and the continues variable of the instantaneous transmitting power p_{ij}. To achieve convexity we transform the discrete variable of the subcarrier index s_{ij} through utilizing subcarrier time-sharing relaxation [140] that allows us to define the continue variable $\tilde{s}_{ij}\in(0,1]$ (see Section 3.6.1 of Chapter 3 for more details). The subcarrier time-sharing $\tilde{s}_{ij}$ of each subcarrier i bears the definition of the variables $\tilde{r}_{ij}=\tilde{s}_{ij}r_{ij}$ and $\tilde{p}_{ij}=\tilde{s}_{ij}p_{ij}$, which express the instantaneous effective data rate and the instantaneous transmitting power of user j on subcarrier i scaled by the same factor $\tilde{s}_{ij}$. In other words, we can write our PBL process in (4.9) as

$$\tilde{r}_j = E_{\hat{h}_{ij}}\left[\sum_{i=1}^{N_F}\left(1-\mathbb{P}_{out}\right)\cdot\tilde{s}_{ij}\cdot\log_2\left(1+\frac{\eta_{ij}\tilde{p}_{ij}\left|h_{ij}\right|^2}{\tilde{s}_{ij}}\right)\right], \tag{4.10}$$

with the M-QAM modulator allowing the instantaneous effective data rate $\tilde{r}_{ij}$ of user j on subcarrier i to take values from the set $\tilde{\mathbf{D}}=\left\{0,1,...,\tilde{s}_{ij}\cdot D\right\}$ e.g., $\tilde{r}_{ij}\in\left[0,\tilde{s}_{ij}\cdot D\right]$.

Theorem 4.1 - Given the subcarrier time-sharing factor $\tilde{s}_{ij}\in(0,1]$ and the new power transmission variable $\tilde{p}_{ij}=\tilde{s}_{ij}p_{ij}$, the PBL function in (4.10) that expresses the effective data rate $\tilde{r}_j$ allocated to user j is a concave function over the non-empty and convex set $\left(\tilde{s}_{ij},\tilde{p}_{ij}\right)$.

Proof - The proof of *Theorem 4.1* is presented in Appendix B.1 . ■

Since in *Theorem 4.1* we prove that our PBL function in (4.10) is concave over the non-empty and convex set $\left(\tilde{s}_{ij},\tilde{p}_{ij}\right)$, we can now apply the A-NBS property on the instantaneous effective data rate $\tilde{r}_j$ of user j. More precisely, we consider each user j's weight $w_j\in(0,1]$ and its minimum requirement $u_j^0\geq 0$ to define the following Theorem according to the A-NBS property as given in *Lemma 2.2* of Section 2.4.

Theorem 4.2 - For each weight $w_j\in(0,1]$ of user j, an asymmetric Nash bargaining point $\left(\tilde{s}_{ij},\tilde{p}_{ij}\right)$ is determined by the instantaneous subcarrier allocation index $\tilde{s}_{ij}$ and the instantaneous transmitting power $\tilde{p}_{ij}$, which is a concave function of the effective data rate $\tilde{r}_j$ of user $j\in K$ defined as $\tilde{r}_j\geq u_j^0$, $\forall\tilde{s}_{ij}\in(0,1],\tilde{p}_{ij}\geq 0$, and gives the unique solution to the maximization problem

$$\max_{\tilde{s}_{ij},\tilde{p}_{ij}}\prod_{j\in K}\left(\tilde{r}_j-u_j^0\right)^{w_j}. \tag{4.11}$$

Proof - The proof of *Theorem 4.2* is similar to the proof of the A-NBS property presented in [40] and in *Lemma 2.2*, and has been omitted from this Thesis due to space limitations. ■

In *Theorem 4.2*, we describe an un-constrained throughput maximization problem with its cost function to express each user j's throughput satisfaction in the A-NBS game strategy. In other words, the physical meaning of the cost function in (4.11) is the amount of extra resources allocated to user j, i.e., excess throughput obtained by user j. To present the A-NBS throughput maximization problem in its full measure, we substitute in the problem (4.11) the effective data rate $\tilde{r}_j$ of user j given in (4.10) and by taking advantage of the strictly increasing property of the logarithm function we define a new A-NBS throughput maximization problem as below

$$\max_{\tilde{s}_{ij},\tilde{p}_{ij}} \prod_{j\in K} \left(\tilde{r}_j - u_j^0\right)^{w_j} \Leftrightarrow$$

$$\max_{\tilde{s}_{ij},\tilde{p}_{ij}} \sum_{j=1}^{K} w_j \ln\left(\tilde{r}_j - u_j^0\right) \Leftrightarrow \quad . \tag{4.12}$$

$$\max_{\tilde{s}_{ij},\tilde{p}_{ij}} \sum_{j=1}^{K} w_j \ln\left(E_{\hat{h}_{ij}}\left[\sum_{i=1}^{N_F} \left(1-\mathbb{P}_{out}\right)\cdot \tilde{s}_{ij} \cdot \log_2\left(1+\frac{\eta_{ij}\tilde{p}_{ij}\left|h_{ij}\right|^2}{\tilde{s}_{ij}}\right)\right] - u_j^0\right)$$

Nevertheless, although we have taken into consideration the strictly increasing property of the logarithm function, it is not ensured that the new problem in (4.12) is equivalent to the A-NBS-based maximization problem in (4.11). The reason is that the cost function of the new problem in (4.12) is uncertain to result a unique solution over $\left(\tilde{s}_{ij}, \tilde{p}_{ij}\right)$, which ensures that the effective data rate r_j allocated to user j is larger than the user j's minimum requirement, e.g., $\tilde{r}_j > u_j^0$. Hence, to prove the equivalency between the two problems in (4.11) and (4.12), it is sufficient to show that the cost function of the new problem in (4.12) strictly increases for all $\left(\tilde{s}_{ij}, \tilde{p}_{ij}\right)$ such that $\tilde{r}_j > u_j^0$. Showing that the new cost function strictly increases it is then straightforward that the solution $\left(\tilde{s}_{ij}, \tilde{p}_{ij}\right)$ is unique and that it fully complies with the A-NBS property as given in *Lemma 2.2* in Section 2.4. Let us denote the cost function of the new problem in (4.12) as U. Then from (4.12) it stands that $U = \sum_{j=1}^{K} U_j$, where the utility function U_j of user j is given by

$$U_j = w_j \ln\left(E_{\hat{h}_{ij}}\left[\sum_{i=1}^{N_F} (1 - \mathbb{P}_{out}) \cdot \tilde{s}_{ij} \cdot \log_2\left(1 + \frac{\eta_{ij} \tilde{p}_{ij} \left| h_{ij} \right|^2}{\tilde{s}_{ij}} \right) \right] - u_j^0 \right), \tag{4.13}$$

Relying on (4.13) we can then define the following Theorem.

Theorem 4.3 - The problem in (4.12) is equivalent to the A-NBS throughput maximization problem in (4.11) and its cost function $U = \sum_{j=1}^{K} U_j$ is designed based on the A-NBS Theorem matching the metric of weighted proportional fairness for resource sharing [157].

Proof - The proof of *Theorem 4.3* is presented in Appendix B.2. ■

From *Theorem 4.3* we prove that our PBL process in (4.13) expresses the user j's satisfaction in fully compliance with the A-NBS of power and subcarrier allocation including the effects of channel imperfectness and channel outage along with each user j's asymmetric weight.

The key differences between our PBL process in (4.13) and the utilities defined by the relevant studies [37], [13], [42] and [43] are now easy to be verified. Firstly, our PBL process includes imperfect channel and outage considerations, while others do not. Secondly, our utility function U_j in (4.13) includes both the subcarrier $\tilde{s}_{ij}$ and power $\tilde{p}_{ij}$ allocation variables inside the logarithm, imposed by the A-NBS principle, while others consider only the transmitting power allocation variable meaning that in those cases the subcarrier allocation policy does not comply either with the S-NBS or A-NBS rules. In follow, we rely on the A-NBS problem in (4.12) to formulate the cross-layer A-NBS optimization problem constrained on several system parameters.

4.5 A-NBS-based Cross-Layer Problem Formulation

In this Section, we formulate the A-NBS cross-layer design for heterogeneous users with imperfect channel and outage considerations as a constrained optimization problem based on the OFDMA system modelling described in Section 4.3.

4.5.1 Formulation of the A-NBS Cross-Layer Optimization Problem

We represent the optimal subcarrier allocation policy with the $N_F \times K$ matrix $\mathbb{S}^* = \left[\tilde{s}_{ij}^*\right]$ whose (i, j)-th element is the optimal time-sharing subcarrier allocation factor $\tilde{s}_{ij}^*$ of user j on subcarrier i. In addition, we denote the optimal transmitting power allocation policy with the $N_F \times K$ matrix $\mathbb{P}^* = \left[\tilde{p}_{ij}^*\right]$ whose (i, j)-th element is the optimal instantaneous transmitting power allocation $\tilde{p}_{ij}^*$ of user j on subcarrier i. In continue, we can formulate the A-NBS cross-layer optimization problem as follows.

Find optimal subcarrier and transmitting power resource allocation policies $\mathbb{S}^*\left[\hat{\mathbb{H}}, \mathbb{Q}, \mathbb{U}^0, \mathbb{W}\right]$ and $\mathbb{P}^*\left[\hat{\mathbb{H}}, \mathbb{Q}, \mathbb{U}^0, \mathbb{W}\right]$, respectively

such that:
$$\max_{\tilde{s}_{ij}, \tilde{p}_{ij}} E\left[\sum_{j=1}^{K} w_j \ln\left(E_{\hat{h}_{ij}}\left[\sum_{i=1}^{N_F}\left(1-\mathbb{P}_{out}\right)\cdot\tilde{s}_{ij}\cdot\log_2\left(1+\frac{\eta_{ij}\tilde{p}_{ij}\left|h_{ij}\right|^2}{\tilde{s}_{ij}}\right)\right]-u_j^0\right)\right] \tag{4.14}$$

subject to:
$$\tilde{s}_{ij} \in (0,1], \quad \forall i, j, \tag{4.15}$$
$$\sum_{j=1}^{K} \tilde{s}_{ij} \le 1, \quad \forall i, \tag{4.16}$$
$$\tilde{p}_{ij} \ge 0, \quad \forall i, j, \tag{4.17}$$
$$E\left[\frac{1}{N_F}\sum_{j=1}^{K}\sum_{i=1}^{N_F}\tilde{p}_{ij}\right] \le P_{TOTAL}, \tag{4.18}$$
$$E\left[D_j\right] \le T_j^{\max}, \quad \forall j, \tag{4.19}$$
$$\mathbb{P}_{out,ij} = \mathbb{P}_{out} = \mathbb{P}_{app}, \quad \forall i, j, \tag{4.20}$$
$$\sum_{j=1}^{K} w_j = 1 \ . \tag{4.21}$$

The A-NBS cross-layer optimization problem (4.14) - (4.21) is a utility maximization problem over the instantaneous transmitting power $\tilde{p}_{ij}$ and the time-sharing subcarrier allocation factor $\tilde{s}_{ij}$. The problem is constrained over QoS, channel and packet outage, subcarrier and power allocation constraints. More precisely, the cost function in (4.14) expresses the total level of satisfaction of all the system users in terms of throughput allocated from the BS to the K heterogeneous users over all the N_F subcarriers in terms of weighted fair resource allocation according to the A-NBS principle. The subcarrier allocation constraints (4.15) and (4.16) are used to certify that only one user j can occupy a time-share of a subcarrier i at a specific time slot. Moreover, the power allocation constraints (4.17) and (4.18) ensure that the power cannot take negative values and that the total transmitting power from the BS to the K users cannot exceed the average total available power at the BS P_{TOTAL}. Constraint (4.19) is the QoS constraint in terms of average delay of each heterogeneous user j, denoted by $E\left[D_j\right]$[37], and of the maximum delay tolerance $T_j^{\max}$ specified by user j's queuing characteristics[38]. Furthermore, the outage constraint (4.20) limits the impact of the imperfect CSIT by guaranteeing that the target channel outage probability $\mathbb{P}_{out,ij} = \mathbb{P}_{out}$ at the PHY layer, satisfies a target packet outage probability $\mathbb{P}_{app}$. The target packet outage probability $\mathbb{P}_{app}$, given by $\mathbb{P}_{app} = 1 - \Pr\left(E\left[D_j\right] \le T_j^{\max}\right)$, represents the packet transmission failure and it is usually specified by the application requirements of each user. Finally, the weight constraint (4.21) guarantees that the summation of the users' payoffs should be lied in the feasible system's payoff region, e.g., it should be equal to one.

It is straightforward that the QoS constraint (4.19) and the outage constraint (4.20) have been defined in terms of higher layer parameters meaning that both constraints do not comply with the cross-layer structure. Hence, the A-NBS cross-layer optimization problem in

[37] The average delay is adopted in the literature i.e., [18], [24], [56], [27] as a performance measure of the delay performance. In short, it is recognized that average delay is a good characterization of overall delay performance.

[38] In our model, we assume that users have enough traffic waited in the queue, which is ready to be transmitted. Therefore, if a network resource is allocated to a user, that network resource is used up by that user.

(4.14) - (4.21) cannot be directly solved unless we express the two constraints (4.19) and (4.20) by means of PHY layer parameters.

4.5.2 Correlation between Outage and QoS Constraints of the A-NBS Cross-Layer Optimization Problem

In this Section, we express the outage constraint (4.20) and the QoS constraint (4.19) of the A-NBS cross-layer optimization problem in (4.14) - (4.21) in terms of PHY layer optimization variables.

In particular, we observe that given the imperfect channel realization $\hat{h}_{ij}$, the actual channel realization h_{ij} in the cost function of the optimization problem in (4.14) - (4.21) is CSGC distributed with mean the estimated channel gain $\hat{h}_{ij}$, e.g., $E_{h_{ij}|\hat{h}_{ij}}\left[h_{ij} \middle| \hat{h}_{ij} \right] = \hat{h}_{ij}$, and variance the MMSE variance σ_h^2, e.g., $E_{h_{ij}|\hat{h}_{ij}}\left[\left(h_{ij} - \hat{h}_{ij} \right)\left(h_{ij} - \hat{h}_{ij} \right) \middle| \hat{h}_{ij} \right] = \sigma_h^2$. As the actual channel realization h_{ij} is CSGC distributed, e.g., $h_{ij} \sim \mathcal{CN}\left(\hat{h}_{ij}, \sigma_h^2 \right)$, the term $\left| h_{ij} \right|^2 / \sigma_h^2$ is a non-central random chi-squared variable with two degrees of freedom[39] and non-centrality parameter the term $\left| \hat{h}_{ij} \right|^2 / \sigma_h^2$ [146], [59], [156]. Relying on these statistics we present the following Theorem to define the A-NBS cross-layer optimization problem in (4.14) - (4.21) in terms of the outage constraint (4.20).

[39] The degrees of freedom express the number of independent pieces of information available to estimate another piece of information and define the sensitivity of an estimation pattern. To specify the orientation of the term $\left| h_{ij} \right|^2 / \sigma_h^2$ we involve two of its independent displacements: the imperfect channel realization $\hat{h}_{ij}$ and the channel error $\Delta\hat{h}_{ij}$ meaning that the term $\left| h_{ij} \right|^2 / \sigma_h^2$ has two degrees of freedom.

Theorem 4.4 - The cost function of the A-NBS cross-layer optimization problem (4.14) - (4.21) satisfies the outage constraint (4.20), e.g., $\mathbb{P}_{out} = \mathbb{P}_{app}$ when the utility function U_j of user j in (4.13) is given by the following equation[40]

$$U_j = w_j \ln\left(\sum_{i=1}^{N_F}\left(1-\mathbb{P}_{app}\right)\cdot\tilde{s}_{ij}\cdot\log_2\left(1+\frac{\eta_{ij}\tilde{p}_{ij}\sigma_h^2}{\tilde{s}_{ij}}\cdot\mathbb{F}^{-1}_{\left(\frac{\left|\hat{h}_{ij}\right|^2}{\sigma_h^2}\right)_2}\left(\mathbb{P}_{app}\right)\right)-u_j^0\right), \qquad (4.22)$$

where $F^{-1}_{\left(\left|\hat{h}_{ij}\right|^2/\sigma_h^2\right)_2}\left(\mathbb{P}_{app}\right)$ is the inverse non-central chi-squared CDF of $\mathbb{P}_{app}$ with non-centrality parameter the term $\left|\hat{h}_{ij}\right|^2/\sigma_h^2$ and two degrees of freedom.

Proof - The proof of *Theorem 4.4* is presented in Appendix B.3. ■

From the definition of the utility function U_j of user j in (4.22) of *Theorem 4.4* and Appendix B.3, we can now define the instantaneous effective data rate $\tilde{r}_{ij}$ of user j on subcarrier i in terms of time-sharing as

$$\tilde{r}_{ij} = \left(1-\mathbb{P}_{app}\right)\cdot\log_2\left(1+\frac{\eta_{ij}\tilde{p}_{ij}\sigma_h^2}{\tilde{s}_{ij}}\cdot\mathbb{F}^{-1}_{\left(\frac{\left|\hat{h}_{ij}\right|^2}{\sigma_h^2}\right)_2}\left(\mathbb{P}_{app}\right)\right) \qquad (4.23)$$

and the time-shared instantaneous effective data rate $\tilde{r}_j$ of user j in (4.10) as

$$\tilde{r}_j = \sum_{i=1}^{N_F}\left(1-\mathbb{P}_{app}\right)\cdot\tilde{s}_{ij}\cdot\log_2\left(1+\frac{\eta_{ij}\tilde{p}_{ij}\sigma_h^2}{\tilde{s}_{ij}}\cdot\mathbb{F}^{-1}_{\left(\frac{\left|\hat{h}_{ij}\right|^2}{\sigma_h^2}\right)_2}\left(\mathbb{P}_{app}\right)\right). \qquad (4.24)$$

[40] From this point in this Section, the expectation operator $E[\cdot]$ refers to the average of the quantity over the ergodic realizations of the actual and the estimated channel gains e.g., $\{h_{ij}\}$ and $\{\hat{h}_{ij}\}$, respectively. For notational brevity, we omit its characterization i.e., "expected" or "averaged".

Furthermore, we aim to transform the QoS constraint (4.19) of the A-NBS cross-layer optimization problem in (4.14) - (4.21) in terms of PHY layer optimization variables. Based on our queuing analysis presented in Section 3.5.2 of Chapter 3, we can easily establish a relationship between the instantaneous effective data rate $\tilde{r}_j$ of user j in (4.24) and its traffic characteristic tuple $\left[F, T_j^{\max}, \lambda_j\right]$ as described in Section 3.3.3. More precisely, we adopt the traffic arrival rate $\tilde{q}_j\left(F, T_j^{\max}, \lambda_j\right)$ at the user j's queue (see Appendix A.4 of Chapter 3) given by

$$\tilde{q}_j\left(F, T_j^{\max}, \lambda_j\right) = \left(\frac{1}{t_s} / \frac{BW}{N_F}\right) \cdot \left(\frac{F}{2T_j^{\max}} \cdot \left(\sqrt{T_j^{\max}\lambda_j\left(T_j^{\max}\lambda_j + 2\right)} + \lambda_j T_j^{\max}\right)\right), \tag{4.25}$$

to define that instantaneous effective data rate $\tilde{r}_j$ of user j in (4.24) must be at least equal to the traffic arrival rate $\tilde{q}_j\left(F, T_j^{\max}, \lambda_j\right)$, e.g.,

$$\tilde{r}_j \geq \tilde{q}_j\left(F, T_j^{\max}, \lambda_j\right).^{41} \tag{4.26}$$

Although we can include the QoS condition (4.26) into the A-NBS cross-layer optimization problem (4.14) - (4.21), for consistency reasons we shall reform it in terms of the utility function U_j of user j. In addition, by reformatting the QoS condition (4.26) we can correlate the minimum requirement u_j^0 of user j and its traffic arrival rate $\tilde{q}_j\left(F, T_j^{\max}, \lambda_j\right)$. More precisely, by firstly subtracting the minimum requirement u_j^0 from both sides of the inequality (4.26), we can then consider the logarithm of both sides and multiply it by the weight w_j of user j to get the following relationship.

[41] We remark that when the maximum delay tolerance $T_j^{\max}$ of a user j is sufficiently large e.g., $T_j^{\max} \to \infty$, then the QoS condition (4.26) becomes $\tilde{r}_j \geq \left(\left(1/t_s\right)/\left(N_F / BW\right)\right) \cdot F\lambda_j$ (for more details see Section 3.5.2and Appendix A.4 of Chapter 3).

$$\begin{aligned} \tilde{r}_j &\geq \tilde{q}_j\left(F, T_j^{\max}, \lambda_j\right) \Leftrightarrow \\ \tilde{r}_j - u_j^0 &\geq \tilde{q}_j\left(F, T_j^{\max}, \lambda_j\right) - u_j^0 \Leftrightarrow \\ \ln\left(\tilde{r}_j - u_j^0\right) &\geq \ln\left(\tilde{q}_j\left(F, T_j^{\max}, \lambda_j\right) - u_j^0\right) \Leftrightarrow \\ w_j \ln\left(\tilde{r}_j - u_j^0\right) &\geq w_j \ln\left(\tilde{q}_j\left(F, T_j^{\max}, \lambda_j\right) - u_j^0\right) \Leftrightarrow \end{aligned} . \quad (4.27)$$

From the reformulation of the QoS condition in (4.27) we can make two conclusions. The first conclusion is that we can establish a QoS condition, which specifies that the utility function U_j of user j should be at least equal to the term $w_j \ln\left(\tilde{q}_j\left(F, T_j^{\max}, \lambda_j\right) - u_j^0\right)$. In other words, we can describe the equivalent to U_j level of satisfaction of user j based on the traffic arrival rate $\tilde{q}_j\left(F, T_j^{\max}, \lambda_j\right)$ at the user j's queue as

$$U_j \geq w_j \ln\left(\tilde{q}_j\left(F, T_j^{\max}, \lambda_j\right) - u_j^0\right). \quad (4.28)$$

The second conclusion is that we can define a correlation condition between the minimum requirement u_j^0 of user j and its traffic arrival rate $\tilde{q}_j\left(F, T_j^{\max}, \lambda_j\right)$. More precisely, the logarithm at the right side of (4.27) is valid if it's inside part is at least equal to one, e.g., $\tilde{q}_j\left(F, T_j^{\max}, \lambda_j\right) - u_j^0 \geq 1$. Hence, we can easily determine that the minimum requirement u_j^0 of user j must be at least equal to its traffic arrival rate $\tilde{q}_j\left(F, T_j^{\max}, \lambda_j\right)$ minus one *bit/sec/Hz*, e.g.,

$$\tilde{q}_j\left(F, T_j^{\max}, \lambda_j\right) - 1 \geq u_j^0 \geq 0 .^{42} \quad (4.29)$$

The correlation in (4.29) has practical significance as it ensures that the A-NBS game is feasible even if the allocated data rate is less than the incoming traffic arrival rate to each user's queue. In other words, a user may not be totally satisfied but it still cooperates to ensure fair allocation of the available resources. Hence, in the frequent case where the

[42] We remark that when the maximum delay tolerance $T_j^{\max}$ of a user j is sufficiently large e.g., $T_j^{\max} \to \infty$, then the correlation condition (4.29) becomes $u_j^0 \leq \left(\left(1/t_s\right)/\left(N_F / BW\right)\right) \cdot F\lambda_j - 1$ (for more details see Section 3.5.2 and Appendix A.4 of Chapter 3).

available power at the BS is not enough to support all users' QoS requirements, the scheduling decision is taken on the A-NBS principle ensuring weighted proportional fairness.

4.5.3 Reformulation of the A-NBS-based Cross-Layer Optimization Problem

Considering the new definition of the utility function U_j of user j in (4.22) of *Theorem 4.4* as well as the QoS condition in (4.28) along with the correlation condition in (4.29), we can reformulate the A-NBS cross-layer optimization problem in (4.14) - (4.21) as follows.

Find optimal subcarrier and transmitting power resource allocation policies $\mathbb{S}^*\left[\hat{\mathbb{H}},\mathbb{Q},\mathbb{U}^0,\mathbb{W}\right]$ and $\mathbb{P}^*\left[\hat{\mathbb{H}},\mathbb{Q},\mathbb{U}^0,\mathbb{W}\right]$, respectively

such that:

$$\max_{\tilde{s}_{ij},\tilde{p}_{ij}} E\left[\sum_{j=1}^{K} w_j \ln\left(\sum_{i=1}^{N_F}\left(1-\mathbb{P}_{app}\right)\cdot\tilde{s}_{ij}\cdot\log_2\left(1+\frac{\eta_{ij}\tilde{p}_{ij}\sigma_h^2}{\tilde{s}_{ij}}\cdot\mathbb{F}^{-1}_{\left(\frac{|\hat{h}_{ij}|^2}{\sigma_h^2}\right)_2}\left(\mathbb{P}_{app}\right)\right)-\left(\tilde{q}_j\left(F,T_j^{\max},\lambda_j\right)-1\right)\right)\right] \tag{4.30}$$

subject to:

$$\tilde{s}_{ij}\in(0,1], \quad \forall i,j, \tag{4.31}$$

$$\sum_{j=1}^{K}\tilde{s}_{ij}\le 1, \quad \forall i, \tag{4.32}$$

$$\tilde{p}_{ij}\ge 0, \quad \forall i,j, \tag{4.33}$$

$$E\left[\frac{1}{N_F}\sum_{j=1}^{K}\sum_{i=1}^{N_F}\tilde{p}_{ij}\right]\le P_{TOTAL}, \tag{4.34}$$

$$E\left[w_j\ln\left(\sum_{i=1}^{N_F}\left(1-\mathbb{P}_{app}\right)\cdot\tilde{s}_{ij}\cdot\log_2\left(1+\frac{\eta_{ij}\tilde{p}_{ij}\sigma_h^2}{\tilde{s}_{ij}}\cdot\mathbb{F}^{-1}_{\left(\frac{|\hat{h}_{ij}|^2}{\sigma_h^2}\right)_2}\left(\mathbb{P}_{app}\right)\right)-\left(\tilde{q}_j\left(F,T_j^{\max},\lambda_j\right)-1\right)\right)\right]\ge w_j\ln\left(\tilde{q}_j\left(F,T_j^{\max},\lambda_j\right)-u_j^0\right), \quad \forall j, \tag{4.35}$$

$$\sum_{j=1}^{K} w_j = 1 \ . \qquad (4.36)$$

In the A-NBS cross-layer optimization problem (4.30) - (4.36), the cost function in (4.30) has been reformulated according to the outage condition (4.20) of the primary A-NBS optimization problem (4.14) - (4.21) considering the worst case scenario of the correlation condition in (4.29), e.g., accounting the maximum minimum utility u_j^0 of user j given by $u_j^0 = \tilde{q}_j\left(F, T_j^{\max}, \lambda_j\right) - 1$. Moreover, the subcarrier, power and weight constraints (4.31) - (4.34) and (4.36) are the same with constraints (4.15) - (4.18) and (4.21) of the primary A-NBS problem, respectively. The new QoS constraint (4.35) is the transformed QoS constraint (4.19) including the outage constraint (4.20) of the A-NBS cross-layer optimization problem in (4.14) - (4.21) and signifies that each user j's satisfaction at the PHY layer must be at least equal to the equivalent level of satisfaction depended on user j's queue.

Let us now examine the convexity of the A-NBS cross-layer optimization problem (4.30) - (4.36).

Proposition 4.1 - Given the subcarrier time-sharing factor $\tilde{s}_{ij} \in (0,1]$ and the new power transmission variable $\tilde{p}_{ij} = \tilde{s}_{ij} p_{ij}$, the A-NBS cross-layer optimization problem (4.30) - (4.36) is a convex optimization problem over the non-empty and convex set $\left(\tilde{s}_{ij}, \tilde{p}_{ij}\right)$.

Proof - The proof of *Proposition 4.1* is presented in Appendix B.4. ■

In *Proposition 4.1* we show that the A-NBS cross-layer optimization problem (4.30) - (4.36) has a unique global optimal solution, which can be obtained in polynomial time. In the following Section, we present the optimal resource allocation strategies approaching their solution concept with a new scope to outcome iteration-independent and power-efficient policies.

4.6 Convex Optimization-based Game Theoretic Optimal Allocation Strategies in Compliance with the A-NBS Principle

In this Section, we initialize convex optimization to derive the optimal solutions of the A-NBS cross-layer problem (4.30) - (4.36).

As we consider subcarrier time-sharing relaxation, the optimal time-sharing subcarrier allocation factor $\tilde{s}_{ij}^*$ is a real number indicating the faction of time that subcarrier i requires to transmit an amount of information for user j [140]. Hence, we can directly define the optimal time-sharing subcarrier allocation factor $\tilde{s}_{ij}^*$ of user j subcarrier i based on the following Theorem.

Theorem 4.5 - Given the imperfect channel realization $\hat{h}_{ij}$, the optimal subcarrier allocation policy $\mathbb{S}^*\left[\hat{h}_{ij}\right]=\left[\tilde{s}_{ij}^*\right]$ has individual matrix elements the A-NBS-based optimal time-sharing subcarrier allocation factor $\tilde{s}_{ij}^*$ of user j on subcarrier i given by

$$\tilde{s}_{ij}^* = \Phi_{ij}^{-1}\left(\nu_i^*\right). \tag{4.37}$$

The function $\Phi_{ij}^{-1}(\cdot)$ is the inverse function of $\Phi_{ij}(\cdot)$, which represents the first derivative of the utility function U_j of user j over $\tilde{s}_{ij}^*$, ν_i^* is the optimal LM related with the subcarrier allocation constraint (4.32) given by $\nu_i^* = \Xi^{-1}(1)$ and the function $\Xi^{-1}(\cdot)$ is the inverse function of the function $\Xi(\cdot)$ given by $\Xi(\cdot) \equiv \sum_{j=1}^{K} \Phi_{ij}^{-1}(\cdot)$.

Proof - The proof of *Theorem 4.5* is presented in Appendix B.5. ■

To define the optimal subcarrier index $\tilde{s}_{ij}^*$ in (4.37), we must firstly determine the function $\Phi_{ij}^{-1}\left(\nu_i^*\right)$. However, the function $\Phi_{ij}^{-1}\left(\nu_i^*\right)$ cannot be yet defined as the optimal transmitting power $\tilde{p}_{ij}^*$ is still unknown. To define the function $\Phi_{ij}^{-1}\left(\nu_i^*\right)$, we can assume that an amount of power, e.g., $\tilde{p}_{ij}^* = P_{TOTAL} / \left(BW \cdot N_F\right)$, is uniformly allocated among the N_F

subcarriers. Upon applying uniform transmitting power allocation, we can establish from *Theorem 4.5* the optimal subcarrier allocation matrix $\mathbb{S}^*\left[\hat{h}_{ij}\right]$ with elements the optimal subcarrier allocation indexes $\tilde{s}_{ij}^*$ to indicate, which subcarriers are in good conditions and which are not. For example, by allocating the same amount of power among all subcarriers and if subcarrier i is in better conditions than subcarrier i' then subcarrier i should require less time to transfer the same amount of information than subcarrier i'. Hence, their optimal subcarrier allocation indexes would differ, e.g., subcarrier i should have larger optimal subcarrier allocation index $\tilde{s}_{ij}^*$ than subcarrier i', e.g., $\tilde{s}_{ij}^* < \tilde{s}_{i'j}^*$, with the chance of each optimal subcarrier allocation index $\tilde{s}_{ij}^*$ to be the same with another to be equal to zero (see Appendix B.5).

Accounting the optimal subcarrier allocation matrix $\mathbb{S}^*\left[\hat{h}_{ij}\right]$ given by *Theorem 4.5* we can determine the optimal transmitting power allocation policy as below.

Theorem 4.6 - Given the imperfect channel realization $\hat{h}_{ij}$ and the optimal subcarrier allocation matrix $\mathbb{S}^*\left[\hat{h}_{ij}\right]$, the optimal transmitting power allocation policy $\mathbb{P}^*\left[\hat{h}_{ij}\right]=\left[\tilde{p}_{ij}^*\right]$ has individual matrix elements the optimal instantaneous transmitting power $\tilde{p}_{ij}^*$ of user j on subcarrier i, which is always positive and it is given by

$$\tilde{p}_{ij}^* = \frac{\tilde{s}_{ij}^*}{\eta_{ij}\sigma_h^2 \cdot \mathbb{F}^{-1}_{\left(\frac{\left|\hat{h}_{ij}\right|^2}{\sigma_h^2}\right)_2}\left(\mathbb{P}_{app}\right)} \left(2^{\frac{\left(\tilde{q}_j\left(F,T_j^{\max},\lambda_j\right)-1\right)}{\tilde{s}_{ij}^*\left(1-\mathbb{P}_{app}\right)}} \cdot \exp\left(W\left(\ln\left(2^{\left(\frac{N_F\left(1+\xi_j^*\right)w_j\eta_{ij}\sigma_h^2 \cdot \mathbb{F}^{-1}_{\left(\frac{\left|\hat{h}_{ij}\right|^2}{\sigma_h^2}\right)_2}\left(\mathbb{P}_{app}\right)}{\tilde{s}_{ij}^* \cdot \ln 2 \cdot \mu^* \cdot 2^{\left(\frac{\left(\tilde{q}_j\left(F,T_j^{\max},\lambda_j\right)-1\right)}{\tilde{s}_{ij}^*\left(1-\mathbb{P}_{app}\right)}\right)}} \right)} \right) \right) \right) - 1 \right), \quad (4.38)$$

where ξ_j^* and μ^* are the optimal LM related to the QoS constraint (4.35) and the transmitting power allocation constraint (4.34), respectively, while the notation $W(\cdot)$ denotes the

Lambert-*W* function [158]. In addition, the optimal transmitting power allocation policy $\mathbb{P}^*\left[\hat{h}_{ij}\right]$ is decoupled among the N_F OFDM subcarriers to obtain the optimal user denoted by j^* with the following searching process, which is always feasible.

$$\text{For } i=1 \text{ to } N_F \text{ find } j^* = \arg\min \tilde{p}_{ij}^* \text{ and set } \tilde{p}_{ij}^* = \begin{cases} \tilde{p}_{ij}^*, \text{ if } j = j^* \\ 0, \text{ otherwise} \end{cases}, \ \tilde{s}_{ij}^* = \begin{cases} \tilde{s}_{ij}^*, \text{ if } \tilde{p}_{ij}^* > 0 \\ 0, \text{ otherwise} \end{cases} \quad (4.39)$$

Proof - The proof of *Theorem 4.6* presented in Appendix B.6. ■

From *Theorem 4.6*, we establish the optimal transmitting power matrix $\mathbb{P}^*\left[\hat{h}_{ij}\right]$, which can be perceived as an $N_F \times K$ map of various elements each one indicating the required by each user power to transmit a fixed amount of information on each subcarrier. With the linear search in (4.39), we can easily choose the optimal users that require less transmitting power to be satisfied than others. We can also reformulate the optimal subcarrier allocation matrix $\mathbb{S}^*\left[\hat{h}_{ij}\right]$ by setting equal to zero the optimal time-sharing subcarrier allocation factor $\tilde{s}_{ij}^*$ in (4.37) for the non-optimal users. Later we will see that our linear search in (4.39) enhances system's power efficiency.

Moreover, having defined the optimal subcarrier allocation matrix $\mathbb{S}^*\left[\hat{h}_{ij}\right]$ and the optimal transmitting power allocation policy $\mathbb{P}^*\left[\hat{h}_{ij}\right]$ in *Theorem 4.6*, we can define the optimal effective data rate allocation policy $\mathbb{R}^*\left[\hat{h}_{ij}\right]$ as below.

Theorem 4.7 - Given the optimal transmitting power matrix $\mathbb{P}^*\left[\hat{h}_{ij}\right]$ and the optimal subcarrier allocation policy $\mathbb{S}^*\left[\hat{h}_{ij}\right]$ the optimal effective data rate allocation policy $\mathbb{R}^*\left[\hat{h}_{ij}\right]=\left[\tilde{r}_{ij}^*\right]$ has individual matrix elements the optimal effective data rate $\tilde{r}_{ij}^*$ of user j on subcarrier i given by

$$\tilde{r}_{ij}^{*}=\left(1-\mathbb{P}_{app}\right)\cdot\tilde{s}_{ij}^{*}\cdot\log_2\left(2^{\frac{\left(\tilde{q}_j\left(F,T_j^{\max},\lambda_j\right)-1\right)}{\tilde{s}_{ij}^{*}\left(1-\mathbb{P}_{app}\right)}}\cdot\exp\left(W\left(\ln\left(2^{\left(\frac{N_F\left(1+\xi_j^{*}\right)w_j\eta_{ij}\sigma_h^2\cdot F^{-1}\left(\mathbb{P}_{app}\right)}{\left(\frac{\left|\hat{h}_{ij}\right|^2}{\sigma_h^2}\right)_2}\right)\frac{\left(\tilde{q}_j\left(F,T_j^{\max},\lambda_j\right)-1\right)}{\tilde{s}_{ij}^{*}\left(1-\mathbb{P}_{app}\right)}}\right)\right)\right)\right). \quad (4.40)$$

Proof - The optimal effective data rate $\tilde{r}_{ij}^{*}$ of user j on subcarrier i in (4.40) is derived with direct substitution of the optimal time-sharing subcarrier allocation factor $\tilde{s}_{ij}^{*}$ in (4.37) and the optimal instantaneous transmitting power $\tilde{p}_{ij}^{*}$ in (4.38) into the effective data rate $\tilde{r}_{ij}$ of user j on subcarrier i in (4.23). This completes the proof of *Theorem 4.7*. ■

In the next Sections, we discuss the implementation process of the optimal allocation policies presented in *Theorem 4.6* and *Theorem 4.7* as well as some specifications of the A-NBS scheme.

4.6.1 Implementation Process of the Optimal Allocation Policies

The block diagram of our cross-layer iteration-independent optimal scheduling is shown in Figure 4.2. The optimal transmitting power allocation policy in *Theorem 4.6* has the form of multi-user water-filling strategy with power water-level of each user j to be given by $\left(\xi_j^{*}+1\right)/\mu^{*}$. This means that the optimal power is allocated according to the CSIT across subcarriers, the weight w_j and the QSI of each user j. The optimal LMs μ^{*} and ξ_j^{*} can be perceived as the resource scheduling calibrators of the system, e.g., the users that participate in the A-NBS game with urgent packets to transmit and high weights are allocated with a high power water-level $\left(\xi_j^{*}+1\right)/\mu^{*}$, while the users with non-urgent packets and low weights are assigned with lower water-levels $\left(\xi_j^{*}+1\right)/\mu^{*}$. Moreover, the optimal subcarrier allocation in

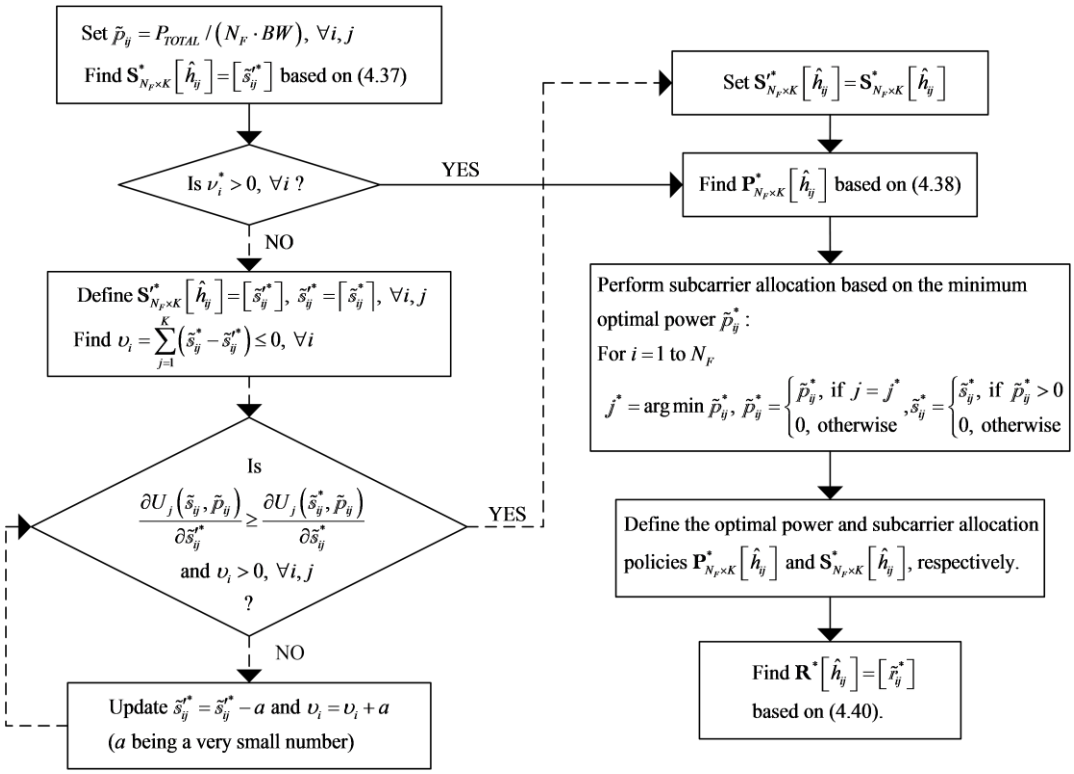

Figure 4.2 - Block diagram of the A-NBS optimal cross-layer resource scheduling based on the proposed iteration-independent methodology.

can be interpreted as a policy, where a user with high urgency and significance (defined by its weight w_j and the LM ξ_j^*, which is depended on the urgency of the delay requirements) has higher chance of being allocated with subcarriers, while users with the same urgency level and significance (the weights w_j and the LMs ξ_j^* are the same) have the same chance and subcarriers are fairly allocated to all users in the group according to the NBS principle. Later, in our simulations we will demonstrate that resource allocation fairness among users of same class and significance is almost perfect, in contrary to many other proposals [17], [20], [21], [22], [23], [24], [27], [34], [35], [37], [41], [56], [60], [72] including our previously presented PE-AETS, where fairness is randomly distributed. Finally, as shown in Figure 4.2, we develop a sub-mechanism to ensure that the optimal LMs ν_i^* s are always positive. However,

we report that such process is extremely rare to be utilized as they are only needed in cases, where allocation is infeasible due to insufficient resources.

Let us now show that he proposed A-NBS scheme is iteration-independent and inspect its total computational complexity. From the KKT conditions (4.69) - (4.87), the differentiations of the Lagrangian function $\mathcal{L}\left(\tilde{s}_{ij},\tilde{p}_{ij},\xi_j,\mu,\nu_i,\varepsilon\right)$ in (4.68) over the LMs $\left\{\xi_j\right\}$ and μ yield the optimal LMs $\left\{\xi_j^*\right\}$ and μ^*, respectively to be global maxima. For example, from the KKT condition (4.72), the differentiation of $\mathcal{L}\left(\tilde{s}_{ij},\tilde{p}_{ij},\xi_j,\mu,\nu_i,\varepsilon\right)$ over μ yields that $\frac{1}{N_F}\sum_{j=1}^{K}\sum_{i=1}^{N_F}\tilde{p}_{ij}^{*}=P_{TOTAL}$. With substitution of the optimal instantaneous transmitting power $\tilde{p}_{ij}^{*}$ in (4.38) we get that

$$\underbrace{\sum_{j=1}^{K}\sum_{i=1}^{N_F}\frac{\tilde{s}_{ij}^{*}}{\eta_{ij}\sigma_h^2\cdot\mathbb{F}^{-1}_{\left(\frac{\left|\hat{h}_{ij}\right|^2}{\sigma_h^2}\right)_2}\left(\mathbb{P}_{app}\right)}}_{A_{ij}}\left(2^{\underbrace{\frac{\left(\tilde{q}_j\left(F,T_j^{\max},\lambda_j\right)-1\right)}{\tilde{s}_{ij}^{*}\left(1-\mathbb{P}_{app}\right)}}_{B_{ij}}}\cdot\exp\left(W\left(\ln\left(2^{\underbrace{\frac{N_F\left(1+\xi_j^*\right)w_j\eta_{ij}\sigma_h^2\cdot\mathbb{F}^{-1}_{\left(\frac{\left|\hat{h}_{ij}\right|^2}{\sigma_h^2}\right)_2}\left(\mathbb{P}_{app}\right)}{\tilde{s}_{ij}^{*}\cdot\ln 2\cdot\mu^{*}\cdot 2^{\frac{\left(\tilde{q}_j\left(F,T_j^{\max},\lambda_j\right)-1\right)}{\tilde{s}_{ij}^{*}\left(1-\mathbb{P}_{app}\right)}}}}_{C_{ij}}}\right)\right)\right)-1\right)=N_F P_{TOTAL}. \tag{4.41}$$

If we set $A_{ij}=\tilde{s}_{ij}^{*}/\left(\eta_{ij}\sigma_h^2\cdot\mathbb{F}^{-1}_{\left(\left|\hat{h}_{ij}\right|^2/\sigma_h^2\right)_2}\left(\mathbb{P}_{app}\right)\right)$, $B_{ij}=\left(\tilde{q}_j\left(F,T_j^{\max},\lambda_j\right)-1\right)/\left(\tilde{s}_{ij}^{*}\left(1-\mathbb{P}_{app}\right)\right)$, $C_{ij}=N_F\left(1+\xi_j^*\right)w_j\eta_{ij}\sigma_h^2\cdot\mathbb{F}^{-1}_{\left(\left|\hat{h}_{ij}\right|^2/\sigma_h^2\right)_2}\left(\mathbb{P}_{app}\right)/\left(\tilde{s}_{ij}^{*}\cdot\ln 2\cdot\mu^{*}\cdot 2^{\left(\left(\tilde{q}_j\left(F,T_j^{\max},\lambda_j\right)-1\right)/\left(\tilde{s}_{ij}^{*}\left(1-\mathbb{P}_{app}\right)\right)\right)}\right)$ and $D_{ij}=2^{B_{ij}}\cdot\exp\left(W\left(\ln\left(C_{ij}\right)\right)\right)$ then (4.41) becomes $\sum_{j=1}^{K}\sum_{i=1}^{N_C}\left(A_{ij}\cdot\left(D_{ij}-1\right)\right)-P_{TOTAL}=0$, which with some manipulation becomes

$$\sum_{j=1}^{K}\sum_{i=1}^{N_C} A_{ij}D_{ij} = \sum_{j=1}^{K}\sum_{i=1}^{N_C}\left(\frac{P_{TOTAL}}{K\cdot N_F} + A_{ij}\right). \tag{4.42}$$

We observe that the right side of (4.42) is known and it can be resolved into a single constant, e.g., $Y = \sum_{j=1}^{K}\sum_{i=1}^{N_C}\left(\left(P_{TOTAL}/\left(KN_F\right)\right) + A_{ij}\right)$. Hence, we can write (4.42) as

$$\sum_{j=1}^{K}\sum_{i=1}^{N_C} A_{ij}D_{ij} = Y. \tag{4.43}$$

Since A_{ij}, B_{ij}, C_{ij} and D_{ij} are all non-negative integers, the function in (4.43) is monotonic, meaning that it has at most one solution on μ^*. However, except the unknown variable μ^*, the equation (4.43) involves another K unknown variables ξ_j^*s on its left side[43].

From the KKT condition in (4.71) we can likewise show that each unknown variable ξ_j^* has its own monotonic function, which also involves K unknown variables, e.g., the rest of the $K-1$ unknown variables ξ_j^*s and the unknown LM μ^*. Consequently, we build a system with $K+1$ monotonic equations, e.g., K for the ξ_j^*s plus one for μ^*, which are all correlated by each other. In other words, we can obtain the LMs ξ_j^*s and μ^* through solving $K+1$ equations at once without performing iteration-dependent searches. Hence, the introduced scheme is iteration-independent and its total actual complexity is dependent on the $N_F \times K$ linear search of the optimal user j^* in (4.39) and the system of $K+1$ equations. In other words, our proposal has total complexity of $\mathcal{O}\left(\left(N_F \times K\right)+K+1\right)$. We recall from Section 3.6.3 of Chapter 3 that iteration-dependent schemes [37], [13], [42], [43] (including our PE-AETS presented in Chapter 3) have complexity of $\mathcal{O}\left(N_F \times K\right)$ plus an extra complexity of $\mathcal{O}\left(l\left[N_F \times K \times \Delta_{\{\xi_j^*\}} + \left(K \times \Delta_{\mu^*} - 1\right)\right]\right)$ due to their root-finding mechanism.

[43] We recall that the optimal subcarrier allocation indexes $\tilde{s}_{ij}^*$s have been already defined in *Theorem 4.6*.

Hence, iteration-dependent schemes have $\mathcal{O}\left(N_F \times K^2 \times l\left[N_F \times \Delta_{\{\xi_j^*\}} + \left(\Delta_{\mu^*} - 1\right)\right]\right)$ complexity in total, where l is the number of loops, $\Delta_{\{\xi_j^*\}}$ is the number of iterations required in one loop to find ξ_j^* and $\Delta_{\mu'^*}$ is the number of iterations required to find μ'^*. Apparently, such complexity is huge compared to our proposal.

In addition, as we do not utilize iteration-dependent mechanisms, it is obvious that the convergence of our scheme to optimal solutions is guaranteed. In conclusion, our cross-layer design methodology allows us to design iteration-independent schemes that converge to A-NBS-based optimal solutions much more rapid than the traditional iteration-dependent approach ensuring that way better real-time system operation.

4.6.2 Specifications on A-NBS-based Scheduling

To gain insight of the behaviour of the A-NBS-based optimal scheduling, in this Section we discuss the feasibility of our A-NBS scheduling proposal, its power-efficiency, the asymptotic performance gain due to multi-user diversity, the impact of the imperfect channel on the service time of each packet, the packet multiplexing process and the accuracy of our optimal policy. To avoid confusion, we separate our discussions into four different topics as below.

1) Feasibility Criterion - The existence of the optimal time-sharing subcarrier allocation factor $\tilde{s}_{ij}^*$ and the optimal instantaneous transmitting power $\tilde{p}_{ij}^*$ of user j on subcarrier i given by *Theorem 4.5* and *Theorem 4.6*, respectively, does not imply the feasibility of the A-NBS cross-layer optimization problem (4.30) - (4.36). The reason is that the minimum requirement u_j^0 of user j (considered equal to $\tilde{q}_j\left(F, T_j^{\max}, \lambda_j\right) - 1$) sometimes may be larger than the instantaneous effective data rate $\tilde{r}_j$ of user j in (4.24). Hence, we establish the feasibility of the A-NBS cross-layer optimization problem (4.30) - (4.36) by setting the following feasibility criterion.

Proposition 4.2 - The A-NBS cross-layer optimization problem (4.30) - (4.36) is feasible if and only if the following condition stands

$$\frac{\sum_{i=1}^{N_F}\left(1-\mathbb{P}_{app}\right)\cdot\tilde{s}_{ij}^{*}\cdot\log_2\left(1+\frac{\eta_{ij}\tilde{p}_{ij}^{*}\sigma_h^2}{\tilde{s}_{ij}^{*}}\cdot\mathbb{F}^{-1}_{\left(\frac{|\hat{h}_{ij}|^2}{\sigma_h^2}\right)_2}\left(\mathbb{P}_{app}\right)\right)-\left(\tilde{q}_j\left(F,T_j^{\max},\lambda_j\right)-1\right)}{\left(\tilde{q}_j\left(F,T_j^{\max},\lambda_j\right)-u_j^0\right)}\geq e^1. \quad (4.44)$$

Proof - Given the optimal time-sharing subcarrier allocation factor $\tilde{s}_{ij}^{*}$ and the optimal instantaneous transmitting power $\tilde{p}_{ij}^{*}$ in *Theorem 4.6*, the rest of constraints (4.35) and (4.36) result in the criterion in (4.44). This completes the proof of *Proposition 4.2*. ■

From the feasibility criterion (4.44) in *Proposition 4.2* the scheduler can be ensured in prior to its allocation decision about if the A-NBS game can be established by means of total fair resource allocation among users. In the case where the minimum requirement u_j^0 of all users is high enough bearing the A-NBS game not to be feasible then the fairness performance decreases. Nevertheless, we avoid in feasible allocation in such cases by designing the proposed A-NBS scheduler to operate under the consideration that the minimum users' requirements $\left\{u_j^0\right\}$ to participate to the A-NBS game should be less than their minimum QoS requirements minus 1 bit, e.g., $\left\{\tilde{q}_j\left(F,T_j^{\max},\lambda_j\right)-1\right\}$, which always satisfies the feasibility criterion. In the case where we had not considered correlation between the minimum A-NBS requirement u_j^0 and the minimum QoS demand $\tilde{q}_j\left(F,T_j^{\max},\lambda_j\right)$, e.g., $u_j^0\leq\tilde{q}_j\left(F,T_j^{\max},\lambda_j\right)-1$, but we had assumed that u_j^0 and $\tilde{q}_j\left(F,T_j^{\max},\lambda_j\right)$ are uncorrelated then the feasibility criterion would not been satisfied in the case where the total available power to the BS P_{TOTAL} was not enough.

2) Power-Efficiency - The A-NBS-based joint power and subcarrier allocation policy presented in *Theorem 4.5* and *Theorem 4.6* enhances system's power efficiency for two reasons. The first reason is that it bears imperfect channel and packet outage considerations.

Hence, accounting realistic network conditions, our proposed scheme is more power-efficient than schemes unaware to channel imperfections [20], [21], [22], [23], [24], [27]. The second reason is that the optimal subcarrier allocation in *Theorem 4.5* is performed based on the choice of the user that requires less power to transmit than others and not on the time-share of subcarriers. For example, the resource allocation could have been performed by a linear search among the N_F subcarriers based on the optimal subcarrier allocation policy as defined in *Theorem 4.5*, i.e., for $i=1$ to N_F find the optimal user j^* from $j^* = \arg\min \tilde{s}_{ij}^*$ and then allocate to each of the optimal users the corresponding power as given in (4.38). Although the aforementioned subcarrier allocation process would provide NBS fairness, it would not always guarantee maximum power efficiency as it considers only the subcarrier allocation constraints (4.31) and (4.32), and not the power and QoS constraints (4.34) and (4.35), respectively (see Appendices B.3and B.4). Hence, when the QoS or weight heterogeneity between users is high, then supposing that subcarrier i is in better channel conditions from subcarrier i' for a specific user, e.g., $\tilde{s}_{ij}^* < \tilde{s}_{i'j}^*$, it does not necessarily mean that the transmitting power on subcarrier i would also be less that the transmitting power on subcarrier i', e.g., $\tilde{p}_{ij}^* < \tilde{p}_{i'j}^*$, and vice versa. In conclusion, in contrary to all relevant imperfect-channel-aware studies (including our previous presented PE-AETS) where subcarrier allocation is performed on the subcarrier indexes we can further increase our scheme's power efficiency as our new methodology allows us to perform subcarrier allocation on the transmitting power basis.

3) Asymptotic Multi-User Diversity Gain - The optimal effective data rate allocation policy in *Theorem 4.7* enhances system's throughput by exploiting multi-carrier and multi-user diversity. The throughput gain due to multi-carrier diversity exploitation for such schemes is thoroughly presented in [21] and [93]. Regarding the throughput gain due to multi-user diversity exploitation we can discuss the followings. From the subcarrier i's perspective the optimal user j^* of class, e.g., C_1 can be perceived as [21]

$$j^*\left(C_1,i\right)=\arg\max_{j\in C_1}\left(\frac{\left(\xi_j^*+1\right)\left(1-\mathbb{P}_{app}\right)}{\mu^*}\cdot\frac{\eta_{ij}\sigma_h^2}{\tilde{s}_{ij}}\cdot\mathbb{F}^{-1}_{\left(\frac{\left|\hat{h}_{ij}\right|^2}{\sigma_h^2}\right)_2}\left(\mathbb{P}_{app}\right)\right)^{\frac{\left(\xi_j^*+1\right)\left(1-\mathbb{P}_{app}\right)}{\mu^*}}. \quad (4.45)$$

Hence, we are able to compute the throughput gain due to multi-user diversity as shown in the below *Lemma*.

Lemma 4.1 - The conditional cross-layer throughput gains for same class users $j\in C_1$, with $C_1\in K$, is given by

$$E\left[\tilde{s}_{ij}^*\eta_{ij}\sigma_h^2\cdot\mathbb{F}^{-1}_{\left(\frac{\left|\hat{h}_{ij}\right|^2}{\sigma_h^2}\right)_2}\left(\mathbb{P}_{app}\right)\middle|\tilde{s}_{ij}^*=1,\, j\in C_1\right]=\Theta\left(\left(1-\sigma_h^2\right)\log_2\left(K\right)\right).$$

Proof - The proof of *Lemma 4.1* is similar to the proofs presented in [21] and [56] regarding the multi-user diversity gains, and it has been omitted from this Thesis due to space limitations. ■

4) Impact of Channel Imperfectness on Service Time, Packet Multiplexing and Accuracy of the Optimal Policy - The proposed A-NBS scheme has same specifications on these topics with our previously presented scheduler PE-AETS. For brevity purposes, we refer the reader to Section 3.6.4 of Chapter 3, where we have thoroughly presented these subject matters.

4.7 Simulations

In this Section, we present simulations to examine the performance of the proposed A-NBS scheduler in comparison with the relative schemes PE-AETS [148], ECS [17], [24], [56],

	Class 1	Class 2	Class 3	Class 4	Class 5
Poission arrival rate λ_j (*packets/time slot*)	0.8	0.5	0.4	0.15	0.15
Min. delay requirement $T_j^{\max}$ (*time slot*)	2	2	4	8	1000
Min. delay requirement $T_j^{\max}$ (*sec*)	0.004	0.004	0.008	0.016	2
Min.eEquivalent rate $\tilde{q}_j\left(F, T_j^{\max}, \lambda_j\right)$ (*bits/sec/Hz*)	25.00	17.08	12.50	4.94	3.75
Max. min. utility of each user to join the A-NBS game u_j^0 (*bits/sec/Hz*)	24.00	16.08	11.50	3.94	2.75
Weight w_j of each user (dependent on classes)	0.30	0.25	0.20	0.15	0.10

Table 4.1- Minimum requirements of each heterogeneous class of users, depended on each user's QoS demands and weight.

EIOS [14], [20], [21], [22], [23], EIFAS [27], [60], MM [32], [151], [152] and WMM [153], [154], [155][44].

4.7.1 Simulation Modelling

We consider a prototype single-cell OFDMA system with channel bandwidth of $BW = 80\,KHz$ equally distributed among $N_F = 32$ subcarriers, each one having five independent paths, e.g., $\Theta = 5$. In addition, we specify five different classes of users denoted by $\left(C_1, C_2, C_3, C_4, C_5\right)$, with the QoS requirements of each class to be characterized by the tuple $\left(\boldsymbol{\lambda}, \mathbf{T}, \mathbf{F}\right) = \left(\left(0.8, 2, 125\right), \left(0.5, 3, 125\right), \left(0.4, 4, 125\right), \left(0.15, 8, 125\right), \left(0.15, 1000, 125\right)\right)$ and each class's weights to be given by $\mathbf{w} = \left(w_{C_1}, w_{C_2}, w_{C_3}, w_{C_4}, w_{C_5}\right)$. From the tuple and payoff

[44] We remark that the impact of channel imperfectness on the channel-error-inconsiderate EIOS and EIFAS has been studied in Appendix A.7 of Chapter 3. Note that although in this research part we consider adaptive modulation schemes, represented by the variable η_{ij}, we have set $\eta_{ij} = 1$ to keep consistency between simulation comparisons of the examined schemes.

structure we clarify in Table 4.1 each user's minimum requirements in terms of average approximated effective data rate. Furthermore, we set the scheduling slot duration to $t_s = 2$ *msec* and we assume that each packet has size of $F = 125\,bits$. To be compliant with the BER approximation in (4.2) we assume that the adaptive modulator operates with BER_{ij} smaller or equal to 0.001, e.g., $BER_{ij} = 4.4626 \times 10^{-5}$, and the noise variance equals to one, e.g., $\sigma_z^2 = 1$, (meaning that $\eta_{ij} = 1$). To make our simulation model more realistic, we consider that all the heterogeneous users suffer signal path-loss from the BS. The signal path-loss PL_j of user j is computed by [134]

$$PL_j = PL(d_0) + 10\varpi \log_{10}(d_j / d_0) + sd_{\sigma_{sd}^2} \text{ (in } dBm)^{45}, \tag{4.46}$$

where $PL(d_0)$ is the reference path loss at a reference distance d_0, d_j is the distance of user j from the BS, ϖ is the path loss component and $sd_{\sigma_{sd}^2}$ is the Gaussian random variable for shadowing with standard deviation σ_{sd}^2. We remark that we keep consistency among comparisons between the examined schemes, by adopting identical channel, traffic and optimization conditions, i.e., all schedulers can handle delay constraints and are affected by the same imperfect channel and outage conditions. Also, to clarify our simulations, we present details in Appendix B.7 regarding the impact of the channel imperfectness on the channel-error-inconsiderate schemes MM [32], [151], [152] and WMM [153], [154], [155]. We finally remanrk that the channel specifications have been set according to the type SUI-3 [144] channel model shown in Table 3.2 of Section 3.7.1 at Chapter 3. The SUI-3 model is considered that reflects realistic channel conditions for pedestrian and vehicular mobility in urban enviroments. All simulations have been obtained through using computer software developed by us in MatLab.

[45] One *dBm* is computed by the formula $dBmW = 10 \cdot \log_{10}(P\ /1\,\text{mWatt})$, where P is the terminus power [93].

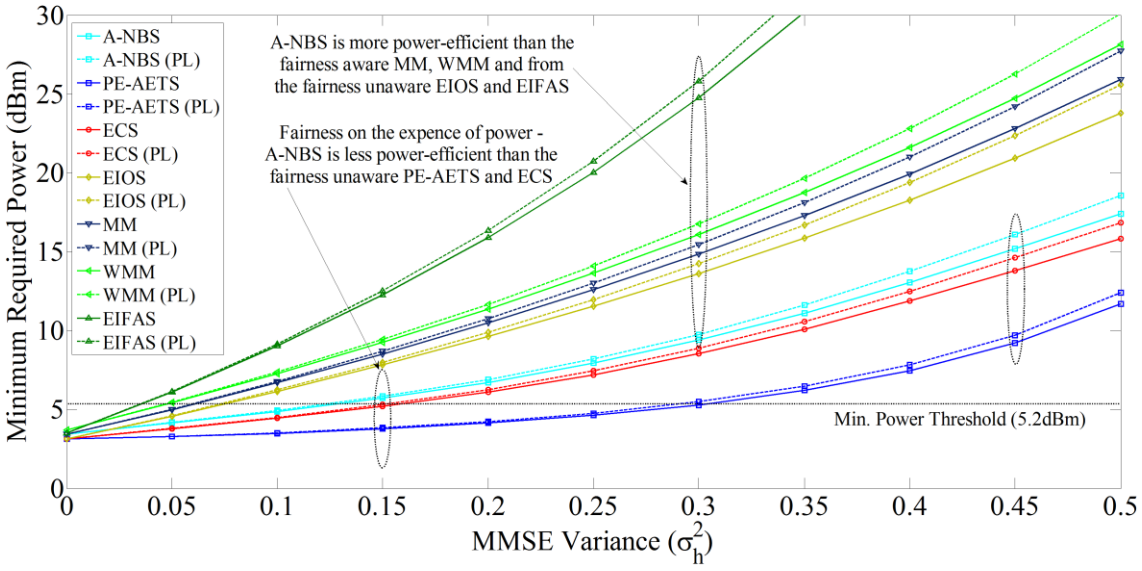

Figure 4.3 - Comparison regarding the power efficiency of the A-NBS scheme: minimum required power versus MMSE variance σ_h^2.

4.7.2 Simulation Results

In Figure 4.3, we consider a system with $(C_1, C_2, C_3, C_4, C_5) = (0,0,0,4,0)$, $P_{TOTAL} = 5.2\,dBm$ and homogeneous signal path-loss between users and BS with parameters $d_0 = 1m$, $d_{1,2,3,4} = 50\,m$, $\varpi = 3.5$ and $\sigma_{sd}^2 = 8\,dB$. Apparently, MM, WMM, EIFAS and EIOS are highly sensitive to the increase of the channel uncertainty. In fact, the schemes cannot provide the minimum required throughput of 19.76*bits/sec/Hz* (see Table 4.1) even when channel uncertainty is very low, i.e., $\sigma_h^2 \geq 0.03$, as all four schemes require more power than the available to the BS. On the other hand, A-NBS, ECS and PE-AETS perform better due to their imperfect channel considerations. We observe that the weighted fairness considerations of A-NBS increase the scheme's power demands compared to ECS and PE-AETS. Nevertheless, the A-NBS scheme seems to provide better trade-off between fairness and efficiency than ECS, as it requires slightly more power (0.5*dBm* in average) to support the same QoS requirements with ECS but with the additional advantage of NBS fair distribution of the wireless resources. The same observations are made, when the signal path-loss between

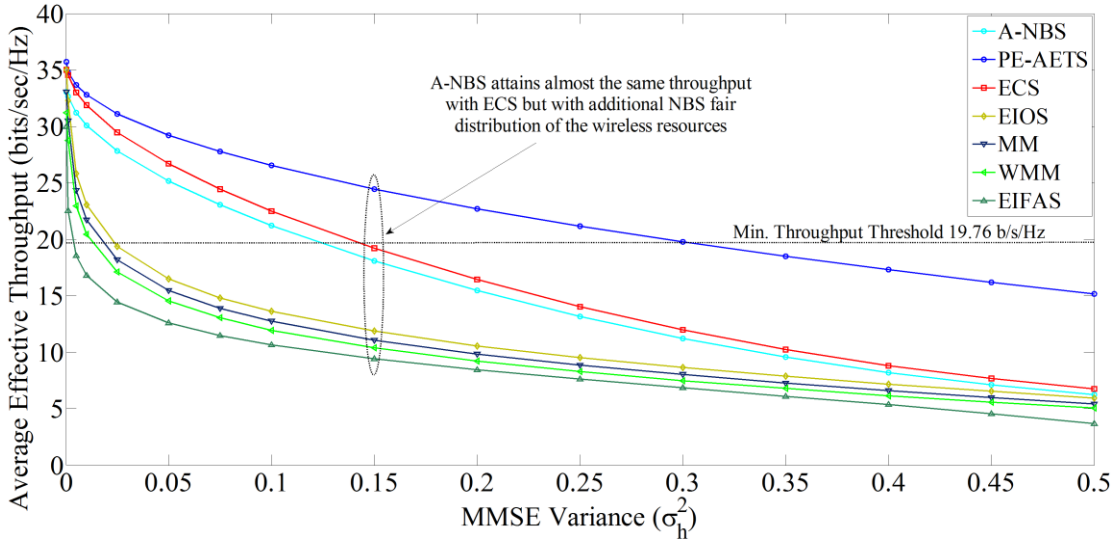

Figure 4.4 - Comparison regarding the throughput efficiency of the A-NBS scheme: average effective throughput versus MMSE variance σ_h^2.

users and BS is heterogeneous, e.g., for $d_1 = 200\,m$, $d_2 = 400\,m$, $d_3 = 600\,m$ and $d_4 = 800\,m$. In this case, all schemes behave the same as in homogeneous signal path-loss but with slightly higher power demands[46]. The corresponding throughput performance is shown in Figure 4.4, where the A-NBS scheduler achieves marginally lower average effective throughput than ECS but significantly higher than EIOS, MM, WMM and EIFAS under any channel imperfectness. In general, it is indeed expected the fairness-considerate schemes A-NBS, MM and WMM to spend more resources than the corresponding fairness-inconsiderate schedulers ECS and EIOS. In addition, weighted fair scheduling has higher resource cost than the non-weighted. This can be seen by observing that the WMM scheme, which, due to users' payoffs, has slightly decreased power and throughput performance than MM.

Let us now examine the power/throughput performance of each scheme considering a larger system with $(C_1, C_2, C_3, C_4, C_5) = (1,3,3,3,0)$, where all users suffer from the same

[46] In the following simulations, we shall omit illustrating the path-loss effect as it does not affect the behaviour of each of the examined schemes and also because large number of graphs presented in one figure may cause confusion.

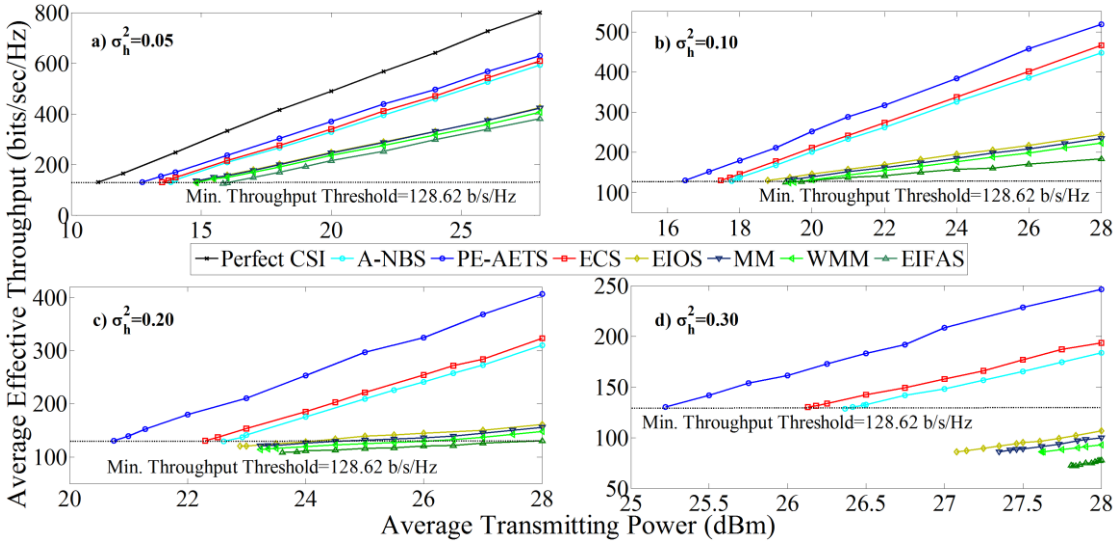

Figure 4.5 - Comparison regarding the power/throughput efficiency of the A-NBS scheme: average effective throughput versus average transmitting power.

signal path-loss. From Figure 4.5a, we observe that for very low channel uncertainty on one hand all schemes satisfy the minimum required effective throughput of 128.62 *bits/sec/Hz* (see Table 4.1) but on the other hand each scheme has matching power values to result into different effective throughputs. Contrariwise, over a certain average effective throughput operation, each scheme needs extra power consumption as we swift from PE-AETS to EIFAS. This difference between the power requirements of each scheme expands further when the channel uncertainty increases, as we notice from Figure 4.5b and Figure 4.5c. Figure 4.5d illustrates more obvious outlooks, where EIFAS, MM, WMM and EIOS are unable to provide the minimum required effective throughput. However, the proposed A-NBS has notable behaviour under any channel uncertainty, maintaining slightly less performance than ECS, even though the involved system users specify heterogeneous payoffs.

In continue, we consider a large-scale system to examine the fairness and the QoS performance of the proposed A-NBS scheme. In particular, we examine a wireless system of 1024 subcarriers and 60 users of classes $(C_1, C_2, C_3, C_4, C_5) = (0, 15, 15, 15, 15)$. The BS is supplied with $P_{TOTAL} = 30\, dBm$ of power and the channel has total bandwidth $BW = 2.56\, MHz$. In Figure 4.6, we can see the superiority of the proposed A-NBS scheme over the examined schedulers in terms of fairness s performance. More precisely, considering average channel

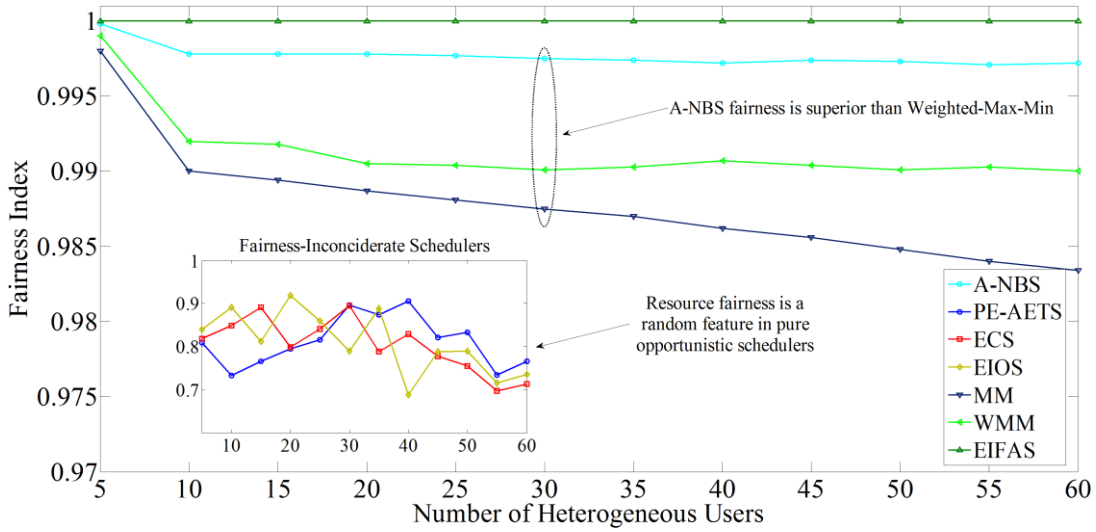

Figure 4.6 - Comparison regarding the fairness efficiency of the A-NBS scheme: fairness index versus number of heterogeneous users.

uncertainty, e.g., $\sigma_h^2 = 0.1$ and upon adding at each measurement five heterogeneous users from class C_2 to class C_5, we observe that A-NBS's fairness performance is clearly the best; our scheme's Fairness Index (FI)[47] tends to obtain the ideal level, e.g., $\mathrm{FI} = 1$, which of course is EIFAS's privilege due to its fixed resource allocation strategy. Evidently, Max-Min fairness is not as effective as NBS since both the MM and WMM schemes result in lower FIs than the A-NBS's scheduler, e.g., 0.986 and 0.991 in average, respectively. However, WMM performs better than MM as the scheme in the former case has a more precise perception about users' priorities/weights. Moreover, despite their high throughput/power performance, the opportunistic schemes PE-AETS, ECS and EIOS do not manage to allocate the wireless resources fairly among users, with their FIs to fluctuate at low levels, e.g., 0.8123, 0.8046, 0.8097 in average, respectively.

[47] For each of the examined schemes the FI is calculated by $\mathrm{FI} = \left(\sum_{j=1}^{K} R_j / R_j^{\min} \right)^2 / \left(K \cdot \sum_{j=1}^{K} \left(R_j / R_j^{\min} \right)^2 \right)$, where R_j represents the allocated rate to user j and $R_j^{\min}$ the user's minimum required data rate [55].

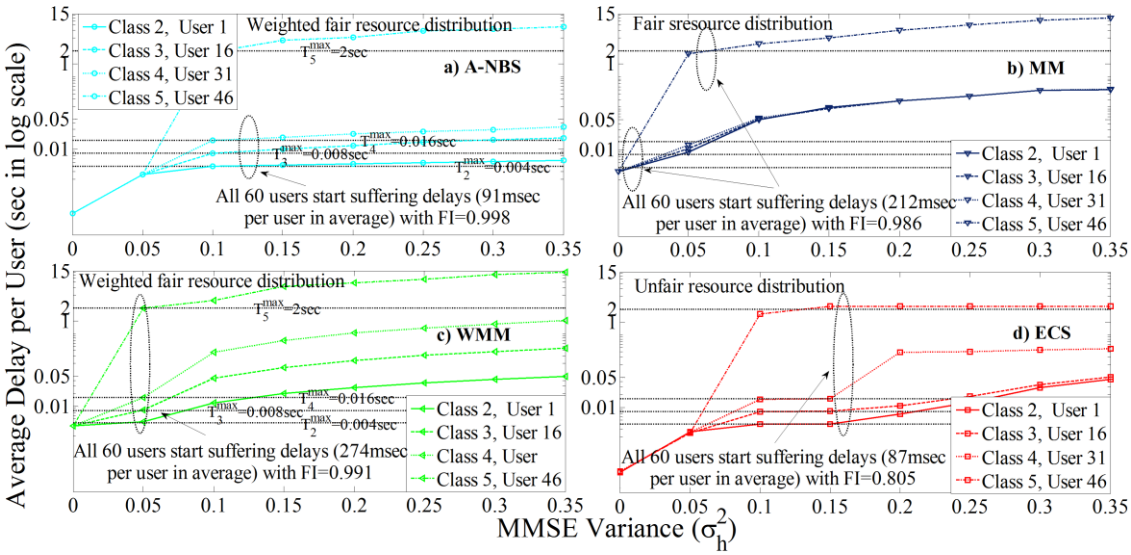

Figure 4.7 - Comparison regarding the QoS efficiency of the A-NBS scheme: average delay per system user versus MMSE variance σ_h^2.

To inspect the QoS efficiency of the proposed A-NBS scheme we consider a large-scale system of 60 users of classes $(C_1, C_2, C_3, C_4, C_5) = (0,15,15,15,15)$ and 1024 subcarriers of total bandwidth $BW = 2.56\,MHz$. We keep consistency with our simulations in Section 3.7.2 by supplying the BS with $P_{TOTAL} = 30\,dBm$ and considering the same signal path-loss between users and BS, e.g., $d_{1-15} = 200\,m$, $d_{16-30} = 300\,m$, $d_{31-45} = 400\,m$ and $d_{45-60} = 500\,m$. In Figure 4.7, we increase the channel uncertainty and observe the differences regarding the resource distribution of A-NBS, MM, WMM and ECS. More precisely, the weighted-fairness considerate schemes A-NBS and WMM have better perception about users' priorities than MM and ECS. For example, although the total supplied power to the BS is on purpose not enough for all schemes to support the minimum users' QoS requirements, A-NBS and WMM scheduling make the most delay sensitive user 1 with the higher payoff to suffer by less delay comparably, e.g., to user 16 or user 31. In contrary, the weighted-fairness inconsiderate MM distributes evenly the resources among users without considering payoffs causing all users to

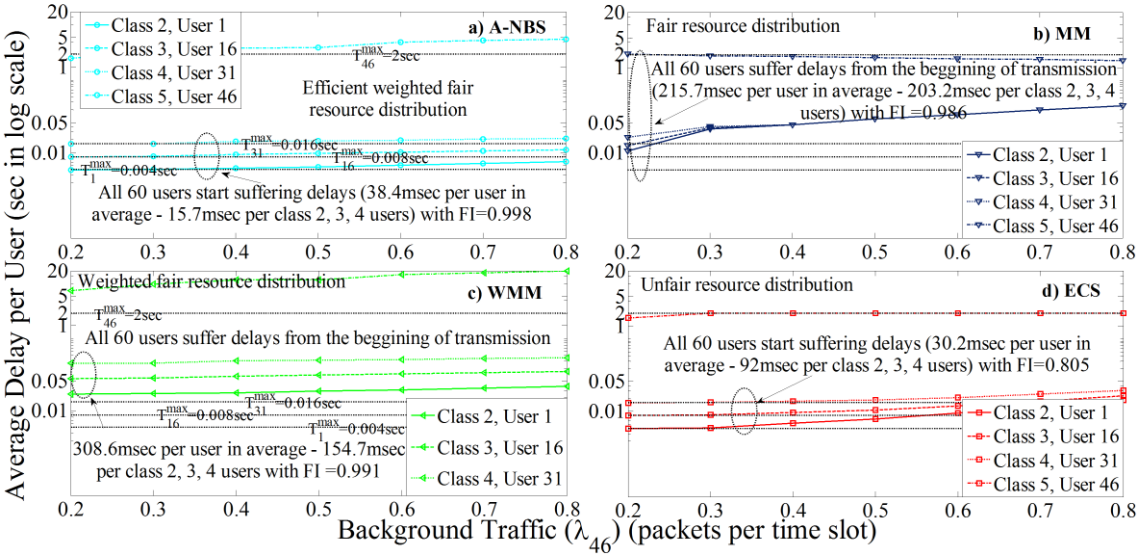

Figure 4.8 - Comparison regarding the QoS efficiency of the A-NBS scheme: average delay per system user versus background traffic λ_{46}.

suffer by 212*msec* delay in average, while ECS's[48] behaviour is purely opportunistic. Nevertheless, A-NBS performs better than WMM as users in the first case suffer by 91*msec* delays, while in the second case by 274*msec* delays in average. The impact of users' payoffs on A-NBS and WMM scheduling decision is visible from the fact that user 1's delay has lower increase pace than user 16's, which in turn has lower increase pace than user 31's etc. This observation is clearer at the A-NBS case, where due to its weight user 1 has slightly more delay than its maximum limit, while user 16 has marginally more delay increase etc. It is notable that among the examined schemes A-NBS provides the best QoS support at the more delay sensitive and higher priority users; our scheme prefers to astrict resources from the delay-insensitive and lowest priority user 46 and distribute those resources to the rest of the users according to their delay tolerances and priorities.

Similar conclusions are made by inspecting Figure 4.8, the average delay of users 1, 16, 31 and 46 versus the system's background traffic (traffic arrival rate λ_{46} of user 46) under

[48] For comparison purposes in this simulation, we refer to the ECS as its performance is closer to A-NBS, MM and WMM than PE-AETS, EIOS or EIFAS.

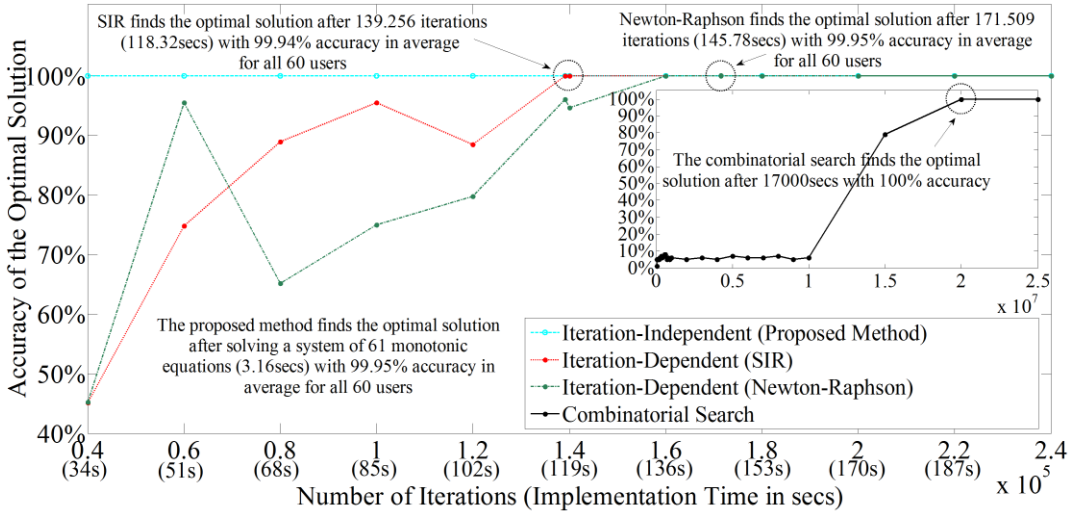

Figure 4.9 - Comparison regarding the implementation efficiency of the A-NBS scheme: accuracy of the optimal solution versus number of iterations and implementation time.

average channel uncertainty, e.g., $\sigma_h^2 = 0.1$. As user 46 becomes more delay-sensitive, all schemes require more power than the supplied to the BS to satisfy all users' minimum requirements causing delays to users. However, we observe that A-NBS provides the best QoS support at the delay sensitive and higher priority users imperviousing to support the delay-insensitive and lower priority user 46 under power starvation, e.g., $\lambda_{45} > 0.35$. For example, under the proposed A-NBS scheme class 2, 3 and 4 users suffer by low delays of 15.7*msec* in average per user, while when MM, WMM and ECS scheduling is applied, users suffer by higher delays of 203,2*msec*, 154.7*msec* and 92*msec*, respectively.

Finally, we demonstrate in Figure 4.9 that the proposed A-NBS scheme achieves 99.95% accurate solutions in average with incomparable lower implementation time than others. More precisely, we simulate a system with 60 users and 1024 subcarriers in MatLab and observe that the proposed iteration-independent method obtains the optimal solutions only in 3.16*sec*, while the iteration-dependent schemes, e.g., PE-AETS, ECS, EIOS, MM, WMM and EIFAS, require either 118.32*sec* or 145.78*sec* under using SIR or Newton-

Raphson root-finding mechanisms, respectively[49]. In addition, although the combinatorial search is 100% accurate, its implementation time is extremely high, while we have experienced several convergence issues during our simulations.

In sum, it is evident from our simulations that the proposed A-NBS scheme delivers the best trade-off between throughput efficiency and fair resource distribution over relative schemes with incomparable lower implementation complexity in networks with heterogeneous QoS support.

4.8 Conclusion

In this research part, we proposed an iteration-independent game-theoretic cross-layer scheduling scheme to provide performance enhancements in OFDMA systems with imperfect channel, packet outage, heterogeneous QoS and asymmetric users' payoffs. Relying on the imperfect channel modelling and estimation procedure presented in the first research part of this Thesis, we initially introduced a PBL process to describe each weighted user's level of satisfaction in terms of effective throughput under channel and packet outage. We show that our PBL process fully complies with the A-NBS of power and subcarrier allocation in contrary to existing approaches that consider only the NBS of power. Furthermore, by adopting the throughput correlation between each user's delay constraints from the upper layers with its PHY layer parameters presented in the first research part of this Thesis, we established a relationship between each user's minimum requirement to join the A-NBS game and its traffic arrival rate ensuring that way the feasibility of the A-NBS game. We then formulated a game-theoretic cross-layer optimization problem that targets to maximize the average users' satisfaction in terms of throughput, subject to subcarrier, power, QoS and weight constraints. Through applying subcarrier time-sharing relaxation, we show that our game-theoretic cross-layer optimization problem can be transformed into a convex

[49] We remark that our reported measurements have been obtained through using a personal computer with 3.2GHz Central Processing Unit (CPU) power. Obviously the implementation time of iteration-dependent and iteration-independent schemes can be significantly reduced through using dedicated hardware as e.g., System-on-Chip (SoC).

optimization problem. We utilized Lagrangian optimization and approached the solution of our cross-layer problem with a different than existed scope that results iteration-independent optimal policies and enhances system's power efficiency. In addition, within our scope we introduced an innovative methodology to provide solutions by means of final formulas to the transcendental algebraic equations that appear during the optimization process due to the recursive origin of the A-NBS problem. We show that the proposed joint optimal game-theoretic adaptive-power and dynamic-subcarrier-allocation policy has actual linear complexity in the number of users and subcarriers and it also performs asymptotically in terms of throughput gain due to multi-user and multi-carrier diversity exploitations. With simulations we demonstrated that the proposed A-NBS scheme provides close to ideal weighted fair scheduling by maintaining the system's effective throughput at remarkably high levels under various uncertain channel conditions. Finally, simulation comparisons with relevant approaches witnessed that the proposed game-theoretic scheme achieves the best trade-off between fairness and throughput/power efficiency by simultaneously providing superior QoS support according to heterogeneous users requirements and asymmetric weights.

Appendix B

B.1 Convexity of the A-NBS-based PBL Function - Proof of *Theorem 4.1*

From the logarithmic origin of the PBL function in (4.10) it is straightforward that the function should be concave. However, to show that the PBL function in (4.10) is concave over $\tilde{s}_{ij}$, $\tilde{p}_{ij}$, we must prove that its Hessian matrix is negative semi-definite [135]. Let us denote the Hessian matrix of the function $\tilde{r}_j$ in (4.10) by $\mathcal{H}_{\tilde{r}_j}$ and represent it as below.

$$\mathcal{H}_{\tilde{r}_j} = \begin{bmatrix} \dfrac{\partial \tilde{r}_j}{\partial \tilde{p}_{ij}^2} & \dfrac{\partial \tilde{r}_j}{\partial \tilde{s}_{ij}\tilde{p}_{ij}} \\ \dfrac{\partial \tilde{r}_j}{\partial \tilde{p}_{ij}\tilde{s}_{ij}} & \dfrac{\partial \tilde{r}_j}{\partial \tilde{s}_{ij}^2} \end{bmatrix}. \tag{4.47}$$

To prove that the Hessian matrix $\mathcal{H}_{\tilde{r}_j}$ in (4.47) is negative semi-definite, it is sufficient to show that the following conditions are satisfied.

$$\frac{\partial \tilde{r}_j}{\partial \tilde{p}_{ij}^2} \cdot \frac{\partial \tilde{r}_j}{\partial \tilde{s}_{ij}^2} - \frac{\partial \tilde{r}_j}{\partial \tilde{s}_{ij}\tilde{p}_{ij}} \cdot \frac{\partial \tilde{r}_j}{\partial \tilde{p}_{ij}\tilde{s}_{ij}} = 0 \tag{4.48}$$

$$\frac{\partial \tilde{r}_j}{\partial \tilde{p}_{ij}^2} < 0\,, \tag{4.49}$$

$$\frac{\partial \tilde{r}_j}{\partial \tilde{s}_{ij}^2} < 0\,. \tag{4.50}$$

According to Young's Theorem [135], if the two variable function $\tilde{r}_j$ in (4.10) is twice continuously differentiable then the condition (4.48) is satisfied. A two variable function is twice continuously differentiable if its second derivatives do exist and are continuous. Hence, we need to perform the second order derivative test of $\tilde{r}_j$ in (4.10) for both its variables $\tilde{s}_{ij}$ and $\tilde{p}_{ij}$. From the second order derivative test we can also derive the

concavity condition that satisfies both the conditions (4.49) and (4.50). We perform the second order derivative test as follows.

The first derivation of $\tilde{r}_j$ over the variable $\tilde{p}_{ij}$ is computed as

$$\frac{\partial \tilde{r}_j}{\partial \tilde{p}_{ij}} = \left(1 - \mathbb{P}_{out}\right) \cdot \frac{\tilde{s}_{ij} \eta_{ij} \left|h_{ij}\right|^2}{\ln 2 \cdot \left(\tilde{s}_{ij} + \eta_{ij} \tilde{p}_{ij} \left|h_{ij}\right|^2\right)}. \tag{4.51}$$

From (4.51) we compute the second derivation of $\tilde{r}_j$ over $\tilde{p}_{ij}$ as

$$\frac{\partial \tilde{r}_j}{\partial \tilde{p}_{ij}^2} = -\left(1 - \mathbb{P}_{out}\right) \cdot \frac{\tilde{s}_{ij} \eta_{ij}^2 \left|h_{ij}\right|^4}{\ln 2 \cdot \left(\tilde{s}_{ij} + \eta_{ij} \tilde{p}_{ij} \left|h_{ij}\right|^2\right)^2} < 0. \tag{4.52}$$

From (4.52) it is straightforward that the second derivative of $\tilde{r}_j$ over $\tilde{p}_{ij}$ does exist, is continues, as $\tilde{p}_{ij}$ is continues, and it is negative. Hence, the condition (4.49) of the Hessian $\mathcal{H}_{\tilde{r}_j}$ in (4.47) is always satisfied.

Moreover, for the condition (4.50) of the Hessian matrix $\mathcal{H}_{\tilde{r}_j}$ in (4.47), it is sufficient to show that the second derivation of the function $\tilde{r}_j$ over $\tilde{s}_{ij}$ in (4.10) is negative. The first derivation of $\tilde{r}_j$ over the variable $\tilde{s}_{ij}$ is computed as

$$\frac{\partial \tilde{r}_j}{\partial \tilde{s}_{ij}} = \left(1 - \mathbb{P}_{out}\right) \left(\log_2 \left(1 + \frac{\eta_{ij} \tilde{p}_{ij} \left|h_{ij}\right|^2}{\tilde{s}_{ij}} \right) - \frac{\eta_{ij} \tilde{p}_{ij} \left|h_{ij}\right|^2}{\ln 2 \left(\tilde{s}_{ij} + \eta_{ij} \tilde{p}_{ij} \left|h_{ij}\right|^2\right)} \right). \tag{4.53}$$

From (4.53) we compute the second derivation of $\tilde{r}_j$ over the variable $\tilde{s}_{ij}$ as

$$\frac{\partial \tilde{r}_j}{\partial \tilde{s}_{ij}^2} = \left(1 - \mathbb{P}_{out}\right) \left(\frac{\eta_{ij} \tilde{p}_{ij} \left|h_{ij}\right|^2}{\ln 2 \left(\tilde{s}_{ij} + \eta_{ij} \tilde{p}_{ij} \left|h_{ij}\right|^2\right)^2} - \frac{\eta_{ij} \tilde{p}_{ij} \left|h_{ij}\right|^2}{\tilde{s}_{ij} \ln 2 \left(\tilde{s}_{ij} + \eta_{ij} \tilde{p}_{ij} \left|h_{ij}\right|^2\right)} \right). \tag{4.54}$$

Evaluating the negativity of (4.54), e.g., $\partial \tilde{r}_j / \partial \tilde{s}_{ij}^2 < 0$, the second derivation of $\tilde{r}_j$ over $\tilde{s}_{ij}$ in (4.54) yields that $-\eta_{ij} \tilde{p}_{ij} \left| h_{ij} \right|^2 < 0$, which always stands[50]. Hence, the second derivative of $\tilde{r}_j$ over $\tilde{s}_{ij}$ does exist, is continues, as $\tilde{s}_{ij} \in (0,1]$ is continues, and it is negative meaning that the condition (4.50) of the Hessian $\mathcal{H}_{\tilde{r}_j}$ in (4.47) is always satisfied. Recalling that the function $\tilde{r}_j$ in (4.10) is twice continuously differentiable and thus, the condition (4.48) is also satisfied. In conclusion, the Hessian matrix $\mathcal{H}_{\tilde{r}_j}$ in (4.47) is negative semi-definite yielding that the PBL function in (4.10) is concave over the $K \times N_F$ convex set $(\tilde{s}_{ij}, \tilde{p}_{ij})$. Finally, the set $(\tilde{s}_{ij}, \tilde{p}_{ij})$ is non-empty as for example for $\tilde{s}_{ij} = 1$ and $\tilde{p}_{ij} = 0$ the function $\tilde{r}_j$ is equal to zero, e.g., $\tilde{r}_j = 0$ meaning that the set $(\tilde{s}_{ij}, \tilde{p}_{ij})$ indeed exists. This completes the proof of *Theorem 4.1*. ■

B.2 Equivalency between the Problem in (4.12) and the A-NBS Throughput Maximization Problem in (4.11) - Proof of *Theorem 4.3*

To prove that the problem in (4.12) is equivalent to the A-NBS throughput maximization problem in (4.11), it is sufficient to show that the utility function U_j in (4.13) strictly increases for all $(\tilde{s}_{ij}, \tilde{p}_{ij})$, which satisfy that the effective data rate r_j allocated to user j is larger than the user j's minimum requirement, e.g., $\tilde{r}_j > u_j^0$. To prove that the utility function U_j in (4.13) strictly increases, we examine its first derivative over $\tilde{p}_{ij}$, given by

[50] We remark that although we have set $\eta_{ij} = -1.5 / \left(\sigma_z^2 \cdot \ln\left(5 \cdot BER_{ij}\right) \right)$, the variable η_{ij} is always positive e.g., $\eta_{ij} > 0$, as the term BER_{ij} takes only negative values [93].

$$\frac{\partial U_j}{\partial \tilde{p}_{ij}} = \frac{\left(1-\mathbb{P}_{out}\right)\cdot \tilde{s}_{ij}\eta_{ij}\left|h_{ij}\right|^2}{\ln 2\left(\tilde{s}_{ij}+\eta_{ij}\tilde{p}_{ij}\left|h_{ij}\right|^2\right)\left(\underbrace{\left(1-\mathbb{P}_{out}\right)\cdot \tilde{s}_{ij}\cdot \log_2\left(1+\frac{\eta_{ij}\tilde{p}_{ij}\left|h_{ij}\right|^2}{\tilde{s}_{ij}}\right)}_{\tilde{r}_j}-u_j^0\right)}. \tag{4.55}$$

From (4.55), it is straightforward that the first derivative of the utility function U_j in (4.13) over $\tilde{p}_{ij}$ is positive, e.g., $\partial U_j / \partial \tilde{p}_{ij} > 0$. Hence, U_j in (4.13) strictly increases for all $\tilde{p}_{ij} > 0$, which satisfy that $\tilde{r}_j > u_j^0$. Let us now denote the function $\Phi_{ij}\left(\tilde{s}_{ij}\right)$ to represent the first-order derivative of U_j in (4.13) over $\tilde{s}_{ij}$, e.g., $\partial U_j / \partial \tilde{s}_{ij}$, given by

$$\Phi_{ij}\left(\tilde{s}_{ij}\right) \equiv \frac{\partial U_j}{\partial \tilde{s}_{ij}} = \left(1-\mathbb{P}_{out}\right)\cdot w_j \cdot \left(\frac{\log_2\left(1+\frac{\eta_{ij}\tilde{p}_{ij}\left|h_{ij}\right|^2}{\tilde{s}_{ij}}\right)-\frac{\eta_{ij}\tilde{p}_{ij}\left|h_{ij}\right|^2}{\ln 2\left(\tilde{s}_{ij}+\eta_{ij}\tilde{p}_{ij}\left|h_{ij}\right|^2\right)}}{\underbrace{\left(1-\mathbb{P}_{out}\right)\cdot \tilde{s}_{ij}\cdot \log_2\left(1+\frac{\eta_{ij}\tilde{p}_{ij}\left|h_{ij}\right|^2}{\tilde{s}_{ij}}\right)}_{\tilde{r}_j}-u_j^0}\right). \tag{4.56}$$

Recalling that $\tilde{p}_{ij} > 0$, the denominator of the function $\Phi_{ij}\left(\tilde{s}_{ij}\right)$ in (4.56) is positive for all $\tilde{s}_{ij}$ satisfying $\tilde{r}_j > u_j^0$. Thus, to prove the strictly increasing property of U_j in (4.13) it is sufficient to show that the numerator of the function $\Phi_{ij}\left(\tilde{s}_{ij}\right)$ in (4.56) is also positive for $\tilde{s}_{ij} > \tilde{s}_{ij}^{\min}$, where $\tilde{s}_{ij}^{\min} > 0$ is the unique solution of $\tilde{r}_j = u_j^0$. The numerator of the function $\Phi_{ij}\left(\tilde{s}_{ij}\right)$ in (4.56) can be represented by the function $\mathrm{T}(\tau)$ denoted by

$$\mathrm{T}(\tau) = \frac{\log_2(1+\tau)-\tau}{\ln 2\cdot(1+\tau)}, \tag{4.57}$$

where the variable τ is given by $\tau = \eta_{ij}\tilde{p}_{ij}\left|h_{ij}\right|^2 / \tilde{s}_{ij}$ and it is positive, e.g., $\tau > 0$. It is easy to verify that the first-order derivative of the function $\mathrm{T}(\tau)$ over τ is positive when $\tau > 0$, i.e.,

$$\frac{\partial \mathrm{T}(\tau)}{\partial \tau} = \frac{\tau}{\ln 2 \cdot (1+\tau)^2} > 0,\ \tau > 0.$$

Therefore, not only the function $\mathrm{T}(\tau)$ strictly increases but also we can reduce the numerator of the function $\Phi_{ij}(\tilde{s}_{ij})$ in (4.56) into $\left((1-\mathbb{P}_{out})\cdot w_j / \ln 2\right)\cdot \mathrm{T}\left(\eta_{ij}\tilde{p}_{ij}\left|h_{ij}\right|^2 / \tilde{s}_{ij}\right)$ as from (4.57) it stands that $\mathrm{T}(\tau) > \mathrm{T}(0) = 0$. Thus, the function $\Phi_{ij}(\tilde{s}_{ij})$ in (4.56) is positive, e.g., $\Phi_{ij}(\tilde{s}_{ij}) > 0$, as both its nominator and denominator are positive. Consequently the first derivations of the utility function U_j in (4.13) over $\tilde{p}_{ij}$ and $\tilde{s}_{ij}$ are positive. In conclusion, the utility function U_j in (4.13) strictly increases for all $(\tilde{s}_{ij}, \tilde{p}_{ij})$, which satisfy $\tilde{r}_j > u_j^0$, meaning that the two problems in (4.11) and (4.12) are equivalent.

In continue, we prove that the utility function U_j in (4.13) is designed based on the A-NBS theorem matching the metric of weighted proportional fairness of resource sharing [157]. We consider the $K \times 1$ vector $\tilde{\mathbb{r}}$ given by

$$\tilde{\mathbb{r}} = \left[\left(\tilde{r}_1 - u_1^0\right)^{w_1}, ..., \left(\tilde{r}_K - u_K^0\right)^{w_K}\right]^T, \tag{4.58}$$

which expresses the users' satisfaction. In addition, we define the $K \times 1$ vector of users' weights $\mathbb{W}$ denoted by $\mathbb{W} = [w_1, ..., w_K]$. Then we can define the $K \times 1$ utility vector $\mathbf{U}(\tilde{\mathbb{r}}, \mathbb{W})$ with entries the utility function of each user j, e.g.,

$$\mathbf{U}(\tilde{\mathbb{r}}, \mathbb{W}) = \prod_{j \in K} \left(\tilde{r}_j - u_j^0\right)^{w_j}. \tag{4.59}$$

For the purpose of equilibrium analysis, we set the disagreement points of the utility function U_j in (4.13) to be equal to zero, e.g., $u_j^0 = 0$, reducing the utility vector $\mathbf{U}(\tilde{\mathbb{r}}, \mathbb{W})$ in (4.59) to

$$\mathbf{U}(\tilde{\mathbb{r}}, \mathbb{W}) = \prod_{j \in K} \left(\tilde{r}_j\right)^{w_j}. \tag{4.60}$$

As we have proven that the two problems in (4.11) and (4.12) are equivalent, the utility vector $\mathbf{U}(\tilde{\mathbb{r}}, \mathbb{W})$ in (4.60) can be written as

$$\begin{aligned}\mathbf{U}\left(\tilde{\mathbb{r}},\mathbb{W}\right) &= \sum_{j=1}^{K} w_j \ln\left(\tilde{r}_j\right) \\ &= \mathbb{W}\cdot\ln\tilde{\mathbb{r}}\end{aligned}. \tag{4.61}$$

Moreover, assuming that the optimal allocation index and power are given by $\tilde{s}_{ij}^{*}$ and $\tilde{p}_{ij}^{*}$, respectively then we can define the $K\times 1$ vector $\tilde{\mathbb{r}}^{*}$ with entries the optimal effective data rate of each of the K users, e.g., $\tilde{\mathbb{r}}^{*}=\left[\tilde{\mathbb{r}}_1^{*},...,\tilde{\mathbb{r}}_K^{*}\right]^{\mathcal{T}}$. From utility theory [33], a vector of rates, e.g., $\tilde{\mathbb{r}}^{*}$, is said to be weighted proportionally fair with weights, e.g., $\mathbb{W}$, if and only if it is feasible and for any other feasible rate vector $\tilde{\mathbb{r}}$ it satisfies that $\mathbb{W}\cdot\left(\tilde{\mathbb{r}}-\tilde{\mathbb{r}}^{*}\right)/\tilde{\mathbb{r}}^{*}\le 0$ [157]. Hence, we examine the first derivative of the utility vector $\mathbf{U}\left(\tilde{\mathbb{r}},\mathbb{W}\right)$ in (4.61) at the point $\tilde{\mathbb{r}}=\tilde{\mathbb{r}}^{*}$, e.g.,

$$\left(\tilde{\mathbb{r}}-\tilde{\mathbb{r}}^{*}\right)\cdot\left.\frac{\partial\mathbf{U}\left(\tilde{\mathbb{r}},\mathbb{W}\right)}{\partial\tilde{\mathbb{r}}}\right|_{\left(\tilde{\mathbb{r}},\mathbb{W}\right)=\left(\tilde{\mathbb{r}}^{*},\mathbb{W}\right)} = \mathbb{W}\cdot\left(\frac{\tilde{\mathbb{r}}-\tilde{\mathbb{r}}^{*}}{\tilde{\mathbb{r}}^{*}}\right)\le 0\,. \tag{4.62}$$

We observe that the first derivative of the utility vector $\mathbf{U}\left(\tilde{\mathbb{r}},\mathbb{W}\right)$ at the point $\tilde{\mathbb{r}}=\tilde{\mathbb{r}}^{*}$ in (4.62) is indeed smaller or equal to zero. Consequently, the utility vector $\mathbf{U}\left(\tilde{\mathbb{r}},\mathbb{W}\right)$ in (4.61) guarantees the weighted proportional fairness condition of spectrum sharing because any movement along any direction $\tilde{\mathbb{r}}-\tilde{\mathbb{r}}^{*}$ at the optimum rate vector $\tilde{\mathbb{r}}^{*}$ cannot improve the utility vector $\mathbf{U}\left(\tilde{\mathbb{r}},\mathbb{W}\right)$. Hence, the optimal allocation index $\tilde{s}_{ij}^{*}$ and transmitting power $\tilde{p}_{ij}^{*}$ provide weighted proportionally fair resource allocation when considered in the utility function U_j in (4.13). This completes the proof of *Theorem 4.3*. ■

B.3 Definition of the Cost Function of the A-NBS Optimization Problem under Imperfect CSIT and Channel Outage - Proof of *Theorem 4.4*

In this Appendix, we aim to express the cost function of the A-NBS cross-layer optimization problem (4.14) - (4.21) in terms of the outage constraint (4.20), e.g., $\mathbb{P}_{out}=\mathbb{P}_{app}$.

Let us firstly consider the case where the channel is perfect. From the maximum achievable capacity c_{ij} in (4.6) and the time-sharing variables $\tilde{s}_{ij}$ and $\tilde{p}_{ij}$ we can define the time-shared maximum achievable capacity $\tilde{c}_{ij}$ of user j on subcarrier i under perfect channel conditions as

$$\tilde{c}_{ij} = \log_2\left(1 + \frac{\eta_{ij}\tilde{p}_{ij}\left|h_{ij}\right|^2}{\tilde{s}_{ij}}\right). \tag{4.63}$$

Considering (4.63) and the outage constraint (4.20), e.g., $\mathbb{P}_{out} = \mathbb{P}_{app}$, the instantaneous effective data rate r_{ij} of user j on subcarrier i in (4.8) can be written in terms of time-sharing as $\tilde{r}_{ij} = E_{\hat{h}_{ij}}\left[\left(1-\mathbb{P}_{app}\right)\cdot\tilde{c}_{ij}\right]$ and the instantaneous effective data rate $\tilde{r}_j$ of user j in (4.10) becomes $\tilde{r}_j = \sum_{i=1}^{N_F}\tilde{s}_{ij}\cdot\tilde{r}_{ij} = E_{\hat{h}_{ij}}\left[\sum_{i=1}^{N_F}\left(1-\mathbb{P}_{app}\right)\cdot\tilde{s}_{ij}\cdot\tilde{c}_{ij}\right]$. Hence, as we define that $U = \sum_{j=1}^{K}U_j$, from (4.11) the utility function U_j in (4.13) can be rewritten in terms of time-shared maximum achievable capacity $\tilde{c}_{ij}$ as

$$\begin{aligned} U_j &= E\left[w_j \ln\left(\tilde{r}_j - u_j^0\right)\right] \\ &= E\left[w_j \ln\left(\left(\sum_{i=1}^{N_F}\cdot\tilde{s}_{ij}\cdot\tilde{r}_{ij}\right) - u_j^0\right)\right] \\ &= E\left[w_j \ln\left(E_{\hat{h}_{ij}}\left[\sum_{i=1}^{N_F}\left(1-\mathbb{P}_{app}\right)\cdot\tilde{s}_{ij}\cdot\tilde{c}_{ij}\right] - u_j^0\right)\right] \end{aligned} . \tag{4.64}$$

Examining (4.64) and our new definition of the utility function U_j of user j in (4.22) it is straightforward that in order to prove *Theorem 4.4* it is sufficient to show that under imperfect channel conditions the capacity $E_{\hat{h}_{ij}}\left[\tilde{c}_{ij}\right]$ as perceived by the system satisfies the outage constraint (4.20), e.g., $\mathbb{P}_{out} = \mathbb{P}_{app}$, if

$$E_{\hat{h}_{ij}}\left[\tilde{c}_{ij}\right]=\log_2\left(1+\frac{\eta_{ij}\tilde{p}_{ij}\sigma_h^2}{\tilde{s}_{ij}}\cdot\mathcal{F}^{-1}_{\left(\frac{|\hat{h}_{ij}|^2}{\sigma_h^2}\right)_2}\left(\mathcal{P}_{app}\right)\right). \tag{4.65}$$

From the definition of the target outage probability $\mathcal{P}_{out}$ in Section 4.4.1 and our assumption in (4.65) we can express $\mathcal{P}_{out}$ as follows.

$$\begin{aligned}
\mathcal{P}_{out} &= 1-\Pr\left[E_{\hat{h}_{ij}}\left[\tilde{c}_{ij}\right]\le\tilde{c}_{ij}\,\middle|\,\hat{h}_{ij}\right]\\
&=\Pr\left[\tilde{c}_{ij}\le E_{\hat{h}_{ij}}\left[\tilde{c}_{ij}\right]\middle|\,\hat{h}_{ij}\right]\\
&=\Pr\left[\log_2\left(1+\frac{\eta_{ij}\tilde{p}_{ij}\left|h_{ij}\right|^2}{\tilde{s}_{ij}}\right)<\log_2\left(1+\frac{\eta_{ij}\tilde{p}_{ij}\sigma_h^2}{\tilde{s}_{ij}}\cdot\mathcal{F}^{-1}_{\left(\frac{|\hat{h}_{ij}|^2}{\sigma_h^2}\right)_2}\left(\mathcal{P}_{app}\right)\right)\middle|\,\hat{h}_{ij}\right]\\
&=\Pr\left[\left|h_{ij}\right|^2<\sigma_h^2\cdot\mathcal{F}^{-1}_{\left(\frac{|\hat{h}_{ij}|^2}{\sigma_h^2}\right)_2}\left(\mathcal{P}_{app}\right)\middle|\,\hat{h}_{ij}\right]\\
&=\Pr\left[\frac{\left|h_{ij}\right|^2}{\sigma_h^2}<\mathcal{F}^{-1}_{\left(\frac{|\hat{h}_{ij}|^2}{\sigma_h^2}\right)_2}\left(\mathcal{P}_{app}\right)\middle|\,\hat{h}_{ij}\right].
\end{aligned} \tag{4.66}$$

We recall that the actual channel realization h_{ij} in (4.66) is CSGC distributed, e.g., $h_{ij}\sim\mathcal{CN}\left(\hat{h}_{ij},\sigma_h^2\right)$, the term $\left|h_{ij}\right|^2/\sigma_h^2$ is a non-central random chi-squared variable with two degrees of freedom and non-centrality parameter the term $\left|\hat{h}_{ij}\right|^2/\sigma_h^2$. Hence, we can define the non-central chi-squared CDF $\mathcal{F}_{(\cdot)}\left(x\right)$ of the random variable x with non-centrality

parameter $\left|\hat{h}_{ij}\right|^2 / \sigma_h^2$ and two degrees of freedom, e.g., $\mathbb{F}_{\left(\left|\hat{h}_{ij}\right|^2/\sigma_h^2\right)_2}\left(x\right)$ [51] to rewrite the condition in (4.66) as

$$\begin{aligned}\mathbb{P}_{out} &= \Pr\left[\left.\frac{\left|h_{ij}\right|^2}{\sigma_h^2} < \mathbb{F}^{-1}_{\left(\frac{\left|\hat{h}_{ij}\right|^2}{\sigma_h^2}\right)_2}\left(\mathbb{P}_{app}\right)\right|\hat{h}_{ij}\right] \\ &= \mathbb{F}_{\left(\frac{\left|\hat{h}_{ij}\right|^2}{\sigma_h^2}\right)_2}\left[\mathbb{F}^{-1}_{\left(\frac{\left|\hat{h}_{ij}\right|^2}{\sigma_h^2}\right)_2}\left(\mathbb{P}_{app}\right)\right] \quad .^{[52]} \\ &= \mathbb{P}_{app}\end{aligned} \tag{4.67}$$

From (4.67) we verify that our definition of the capacity $E_{\hat{h}_{ij}}\left(\tilde{c}_{ij}\right)$ as perceived by the system in (4.65) verifies the outage condition (4.20), e.g., $\mathbb{P}_{out} = \mathbb{P}_{app}$. Consequently, the utility function U_j of user j in (4.64) can be written as

$$U_j = E\left[w_j \ln\left(E_{\hat{h}_{ij}}\left[\sum_{i=1}^{N_F}\left(1-\mathbb{P}_{app}\right)\cdot\tilde{s}_{ij}\cdot\tilde{c}_{ij}\right]-u_j^0\right)\right] \Leftrightarrow$$

$$U_j = w_j \ln\left(\sum_{i=1}^{N_F}\left(1-\mathbb{P}_{app}\right)\cdot\tilde{s}_{ij}\cdot\log_2\left(1+\frac{\eta_{ij}\tilde{p}_{ij}\sigma_h^2}{\tilde{s}_{ij}}\cdot\mathbb{F}^{-1}_{\left(\frac{\left|\hat{h}_{ij}\right|^2}{\sigma_h^2}\right)_2}\left(\mathbb{P}_{app}\right)\right)-u_j^0\right),$$

[51] The non-central CDF of x with two degrees of freedom and non-centrality parameter a is given by $\mathbb{F}_{\left(a^a\right)_2}\left(x\right) = 1-\mathbb{Q}_1\left(\sqrt{x}\cdot\sqrt{a^2}\right)$, where $\mathbb{Q}_1\left(\cdot\right)$ denotes the Marcum Q-function of the first order [59].

[52] Through defining the inverse non-central chi-squared CDF $\mathbb{F}^{-1}_{(\cdot)}\left(\cdot\right)$ of the random variable y, with non-centrality parameter $\left|\hat{h}_{ij}\right|^2 / \sigma_h^2$ and two degrees of freedom e.g., $\mathbb{F}^{-1}_{\left(\left|\hat{h}_{ij}\right|^2/\sigma_h^2\right)_2}\left(y\right)$, we can utilize the property of the CDF [156], which specifies that $\mathbb{F}_{\left(\left|\hat{h}_{ij}\right|^2/\sigma_h^2\right)_2}\left(x\right) = y \Leftrightarrow \mathbb{F}^{-1}_{\left(\left|\hat{h}_{ij}\right|^2/\sigma_h^2\right)_2}\left(y\right) = x$, to compute the equation in (4.67)

which resolves (4.22). This completes the proof of *Theorem 4.4*. ■

B.4 Convexity of the A-NBS Optimization Problem - Proof of *Proposition 4.1*

In this Appendix we focus on proofing the convexity of the A-NBS cross-layer optimization problem (4.30) - (4.36) along with the convexity and feasibility of its determined set. To avoid confusion, we separate our proofs into three different topics as below.

1) Convexity of the A-NBS cross-layer optimization problem (4.30) - (4.36). By introducing the subcarrier time-sharing factor $\tilde{s}_{ij} \in (0,1]$ and the continues variable $\tilde{p}_{ij} = \tilde{s}_{ij} p_{ij}$, the cost function in (4.30) as well as of the QoS constraint (4.35) have the form $w_j \ln\left(\tilde{r}_{ij} - \left(\tilde{q}_j\left(F, T_j^{\max}, \lambda_j\right) - 1\right)\right)$, which is a concave function over the non-empty and convex set $\left(\tilde{s}_{ij}, \tilde{p}_{ij}\right)$ due to its logarithmic origin [135] (see *Theorem 4.1* for more details). Thus, the cost function in (4.30) and the QoS constraint (4.35) are also concave functions over the convex set $\left(\tilde{s}_{ij}, \tilde{p}_{ij}\right)$ as any positive linear combination of concave functions is a concave function. In addition, it is straightforward that the subcarrier, power and weight constraints (4.31) - (4.34) and (4.36) are all affine over $\tilde{s}_{ij}$ or $\tilde{p}_{ij}$ and hence, they are convex functions over the convex set $\left(\tilde{s}_{ij}, \tilde{p}_{ij}\right)$.

2) Convexity of the determined set of the A-NBS cross-layer optimization problem (4.30) - (4.36). Given the subcarrier time-sharing factor $\tilde{s}_{ij} \in (0,1]$ and the variable $\tilde{p}_{ij} = \tilde{s}_{ij} p_{ij}$, the cost function (4.30) of the A-NBS cross-layer optimization problem (4.30) - (4.36) is concave determining a convex set over $\left(\tilde{s}_{ij}, \tilde{p}_{ij}\right)$ [135]. In addition, each of the constraints (4.31) - (4.34) and (4.36), determines a convex set over $\left(\tilde{s}_{ij}, \tilde{p}_{ij}\right)$ due to its affinity. Also the QoS constraint (4.35) is concave hence, it also determines a convex set over $\left(\tilde{s}_{ij}, \tilde{p}_{ij}\right)$. Therefore,

the set defined by all the five constraints (4.31) - (4.36) and by the cost function (4.30), is convex over $\left(\tilde{s}_{ij}, \tilde{p}_{ij}\right)$ as it is well-known that the intersection of convex sets is also convex.

3) Feasibility of the determined set of the A-NBS cross-layer optimization problem (4.30) - (4.36). We shall now verify that the convex set $\left(\tilde{s}_{ij}, \tilde{p}_{ij}\right)$ determined by the A-NBS cross-layer optimization problem (4.30) - (4.36) is non-empty. Given the subcarrier time-sharing factor $\tilde{s}_{ij} \in (0,1]$ and the variable $\tilde{p}_{ij} = \tilde{s}_{ij} p_{ij}$, it is easy to obtain a $K \times N_F$ feasible set over $\tilde{s}_{ij}$ represented by, e.g., $\mathcal{S}_1$, that satisfies the subcarrier constraints (4.31) and (4.32), i.e., easily we can verify that for $\tilde{s}_{ij} = 1$ the set $\mathcal{S}_1$ is non-empty, e.g., $\mathcal{S}_1 \neq \varnothing$. Similarly, there is another $K \times N_F$ feasible set over $\tilde{p}_{ij}$, e.g., $\mathcal{S}_2$, that satisfies the power and QoS constraints (4.33) - (4.36) and the cost function (4.30) which is also non-empty, i.e., if $\tilde{s}_{ij} = 1$ then for $\tilde{p}_{ij} > \tilde{s}_{ij}\left(\left(2^{\tilde{q}_j\left(F, T_j^{\max}, \lambda_j\right)/\left((1-P_{app})\tilde{s}_{ij}\right)} - 1\right) / \left(\eta_{ij}\sigma_h^2 \mathbb{F}^{-1}_{\left(\left|\hat{h}_{ij}\right|^2/\sigma_h^2\right)_2}\left(P_{app}\right)\right)\right)$[53] the set S_2 is non-empty, e.g., $S_2 \neq \varnothing$. Moreover, in the $\left(K \times N_F\right) + \left(K \times N_F\right)$-dimensional space $\left(\tilde{s}_{ij}, \tilde{p}_{ij}\right)$, the constraints (4.31) and (4.32) of the variables $\tilde{s}_{ij}$ verify a cylinder set with base $\mathcal{S}_1$, while the constraints (4.33) - (4.36) and the cost function (4.30) of the variables $\tilde{p}_{ij}$ verify another cylinder set with base $\mathcal{S}_2$. Consequently, the constraints in $\left(\tilde{s}_{ij}, \tilde{p}_{ij}\right)$ determine the intersection of the two cylinders sets, e.g., $\mathcal{S}_1 \cap \mathcal{S}_2$, which it is obvious a non-empty set, e.g., $\mathcal{S}_1 \cap \mathcal{S}_2 = \varnothing$. Also, due to the affinity principle, the intersection $\mathcal{S}_1 \cap \mathcal{S}_2$ of the two cylinders sets is convex. Consequently, the A-NBS cross-layer optimization problem (4.30) - (4.36) is a convex

[53] The condition can be easily derived upon assuming that the cost function is positive, e.g., $w_j \ln\left(\left(1-P_{app}\right)\cdot\tilde{s}_{ij}\cdot\log_2\left(1+\eta_{ij}\tilde{p}_{ij}\sigma_h^2\mathbb{F}^{-1}_{\left(\left|\hat{h}_{ij}\right|^2/\sigma_h^2\right)_2}\left(P_{app}\right)/\tilde{s}_{ij}\right) - \left(\tilde{q}_j\left(F, T_j^{\max}, \lambda_j\right) - 1\right)\right) > 0$.

optimization problem over a feasible $\left(K\times N_F\right)+\left(K\times N_F\right)$-dimensional convex set. This completes the proof of *Proposition 4.1*. ■

B.5 Optimal Subcarrier Allocation Index in Compliance with the A-NBS Principle - *Theorem 4.5*

In this Appendix we determine the optimal subcarrier allocation index $\tilde{s}_{ij}^{*}$ for user j on subcarrier i. Let us firstly define the Lagrangian function $\mathcal{L}\left(\tilde{s}_{ij},\tilde{p}_{ij},\xi_j,\mu,\nu_i,\varepsilon\right)$ of the A-NBS cross-layer optimization problem (4.30) - (4.36) as

$$\mathcal{L}\left(\tilde{s}_{ij},\tilde{p}_{ij},\xi_j,\mu,\nu_i,\varepsilon\right)=\mu\left(P_{TOTAL}-\frac{1}{N_F}\left(\sum_{j=1}^{K}\sum_{i=1}^{N_F}\tilde{p}_{ij}\right)\right)-\nu_i\left(\sum_{j=1}^{K}\tilde{s}_{ij}-1\right)+\varepsilon\left(\sum_{j=1}^{K}w_j-1\right)$$

$$+\sum_{j=1}^{K}w_j\ln\left(\sum_{i=1}^{N_F}\left(1-\mathbb{P}_{app}\right)\cdot\tilde{s}_{ij}\cdot\log_2\left(1+\frac{\eta_{ij}\tilde{p}_{ij}\sigma_h^2}{\tilde{s}_{ij}}\cdot\mathbb{F}^{-1}_{\left(\frac{\left|\hat{h}_{ij}\right|^2}{\sigma_h^2}\right)_2}\left(\mathbb{P}_{app}\right)\right)-\left(\tilde{q}_j\left(F,T_j^{\max},\lambda_j\right)-1\right)\right) \quad , (4.68)$$

$$+\xi_j\left(w_j\ln\left(\sum_{i=1}^{N_F}\left(1-\mathbb{P}_{app}\right)\cdot\tilde{s}_{ij}\cdot\log_2\left(1+\frac{\eta_{ij}\tilde{p}_{ij}\sigma_h^2}{\tilde{s}_{ij}}\cdot\mathbb{F}^{-1}_{\left(\frac{\left|\hat{h}_{ij}\right|^2}{\sigma_h^2}\right)_2}\left(\mathbb{P}_{app}\right)\right)-\left(\tilde{q}_j\left(F,T_j^{\max},\lambda_j\right)-1\right)\right)\right)$$

where ξ_j, μ, ν_i and ε are the LMs related with the QoS constraint (4.35), the power constraint (4.34), the subcarrier constraint (4.32) and the weight constraint (4.36), respectively. The necessary and sufficient conditions that satisfy the global optimum solutions of the A-NBS cross-layer optimization problem (4.30) - (4.36), are the KKT conditions defined as follows [135].

$$\left.\frac{\partial\mathcal{L}\left(\tilde{s}_{ij},\tilde{p}_{ij},\xi_j,\mu,\nu_i,\varepsilon\right)}{\partial\tilde{p}_{ij}}\right|_{\left(\tilde{s}_{ij},\tilde{p}_{ij},\xi_j,\mu,\nu_i,\varepsilon\right)=\left(\tilde{s}_{ij}^{*},\tilde{p}_{ij}^{*},\xi_j^{*},\mu^{*},\nu_i^{*},\varepsilon^{*}\right)}\begin{cases}<0, \text{ if } \tilde{p}_{ij}^{*}=0\\ =0, \text{ if } \tilde{p}_{ij}^{*}>0\end{cases},\quad \forall i,j, \qquad (4.69)$$

$$\left.\frac{\partial \mathcal{L}\left(\tilde{s}_{ij},\tilde{p}_{ij},\xi_j,\mu,\nu_i,\varepsilon\right)}{\partial \tilde{s}_{ij}}\right|_{\left(\tilde{s}_{ij},\tilde{p}_{ij},\xi_j,\mu,\nu_i,\varepsilon\right)=\left(\tilde{s}_{ij}^*,\tilde{p}_{ij}^*,\xi_j^*,\mu^*,\nu_i^*,\varepsilon^*\right)} \begin{cases} >0, \text{ if } \tilde{s}_{ij}^*=1 \\ =0, \text{ if } 0<\tilde{s}_{ij}^*<1 \end{cases}, \quad \forall i,j, \tag{4.70}$$

$$\left.\frac{\partial \mathcal{L}\left(\tilde{s}_{ij},\tilde{p}_{ij},\xi_j,\mu,\nu_i,\varepsilon\right)}{\partial \xi_j}\right|_{\left(\tilde{s}_{ij},\tilde{p}_{ij},\xi_j,\mu,\nu_i,\varepsilon\right)=\left(\tilde{s}_{ij}^*,\tilde{p}_{ij}^*,\xi_j^*,\mu^*,\nu_i^*,\varepsilon^*\right)} \begin{cases} >0, \text{ if } \xi_j^*<0 \\ =0, \text{ if } \xi_j^*\geq 0 \end{cases}, \quad \forall j, \tag{4.71}$$

$$\left.\frac{\partial \mathcal{L}\left(\tilde{s}_{ij},\tilde{p}_{ij},\xi_j,\mu,\nu_i,\varepsilon\right)}{\partial \mu}\right|_{\left(\tilde{s}_{ij},\tilde{p}_{ij},\xi_j,\mu,\nu_i,\varepsilon\right)=\left(\tilde{s}_{ij}^*,\tilde{p}_{ij}^*,\xi_j^*,\mu^*,\nu_i^*,\varepsilon^*\right)} \begin{cases} >0, \text{ if } \mu^*<0 \\ =0, \text{ if } \mu^*\geq 0 \end{cases}, \tag{4.72}$$

$$\left.\frac{\partial \mathcal{L}\left(\tilde{s}_{ij},\tilde{p}_{ij},\xi_j,\mu,\nu_i,\varepsilon\right)}{\partial \nu_i}\right|_{\left(\tilde{s}_{ij},\tilde{p}_{ij},\xi_j,\mu,\nu_i,\varepsilon\right)=\left(\tilde{s}_{ij}^*,\tilde{p}_{ij}^*,\xi_j^*,\mu^*,\nu_i^*,\varepsilon^*\right)} \begin{cases} >0, \text{ if } \nu_i^*<0 \\ =0, \text{ if } \nu_i^*\geq 0 \end{cases}, \quad \forall i, \tag{4.73}$$

$$\left.\frac{\partial \mathcal{L}\left(\tilde{s}_{ij},\tilde{p}_{ij},\xi_j,\mu,\nu_i,\varepsilon\right)}{\partial \varepsilon}\right|_{\left(\tilde{s}_{ij},\tilde{p}_{ij},\xi_j,\mu,\nu_i,\varepsilon\right)=\left(\tilde{s}_{ij}^*,\tilde{p}_{ij}^*,\xi_j^*,\mu^*,\nu_i^*,\varepsilon^*\right)} \begin{cases} >0, \text{ if } \varepsilon^*<0 \\ =0, \text{ if } \varepsilon^*\geq 0 \end{cases}, \tag{4.74}$$

$$\tilde{p}_{ij}^* \geq 0, \quad \forall i,j, \tag{4.75}$$

$$\xi_j^* \geq 0, \quad \forall j, \tag{4.76}$$

$$\mu^* \geq 0, \tag{4.77}$$

$$\nu_i^* \geq 0, \quad \forall i, \tag{4.78}$$

$$\varepsilon^* \geq 0, \tag{4.79}$$

$$\sum_{j=1}^{K} \tilde{s}_{ij}^* \leq 1, \quad \forall i, \tag{4.80}$$

$$\sum_{i=1}^{N_F} \nu_i^* \left(1-\sum_{j=1}^{K} \tilde{s}_{ij}^*\right) \geq 0, \quad \forall j, \tag{4.81}$$

$$P_{TOTAL} - \frac{1}{N_F}\sum_{j=1}^{K}\sum_{i=1}^{N_F} \tilde{p}_{ij}^* \geq 0, \tag{4.82}$$

$$\mu^* \left(P_{TOTAL} - \frac{1}{N_F}\sum_{j=1}^{K}\sum_{i=1}^{N_F} \tilde{p}_{ij}^*\right) = 0, \tag{4.83}$$

$$w_j \ln\left(\sum_{i=1}^{N_F} \tilde{r}_{ij} - \left(\tilde{q}_j\left(F, T_j^{\max}, \lambda_j\right) - 1\right)\right) \geq 0\,, \quad \forall j\,, \tag{4.84}$$

$$\xi_j^*\left(\sum_{j=1}^{K} w_j \ln\left(\tilde{r}_{ij} - \left(\tilde{q}_j\left(F, T_j^{\max}, \lambda_j\right) - 1\right)\right)\right) = 0\,, \quad \forall j\,, \tag{4.85}$$

$$1 - \sum_{j=1}^{K} w_j \geq 0\,, \tag{4.86}$$

$$\varepsilon^*\left(\sum_{j=1}^{K} w_j - 1\right) = 0\,. \tag{4.87}$$

where ξ_j^*, μ^*, ν_i^* and ε^* are the optimal LMs of ξ_j, μ, ν_i and ε, respectively. Considering the correlation condition (4.29) and the definition of the function $\Phi_{ij}\left(\tilde{s}_{ij}\right)$ in (4.56), the differentiation of the Lagrangian function $\mathcal{L}\left(\tilde{s}_{ij}, \tilde{p}_{ij}, \xi_j, \mu, \nu_i, \varepsilon\right)$ in (4.68) over $\tilde{s}_{ij}$, represented by the KKT condition (4.70), yields that

$$\left.\frac{\partial \mathcal{L}\left(\tilde{s}_{ij}, \tilde{p}_{ij}, \xi_j, \mu, \nu_i, \varepsilon\right)}{\partial \tilde{s}_{ij}}\right|_{\left(\tilde{s}_{ij}, \tilde{p}_{ij}, \xi_j, \mu, \nu_i, \varepsilon\right) = \left(\tilde{s}_{ij}^*, \tilde{p}_{ij}^*, \xi_j^*, \mu^*, \nu_i^*, \varepsilon^*\right)} =$$

$$\underbrace{\left(1 - \mathbb{P}_{app}\right) w_j \left(\frac{\log_2\left(1 + \dfrac{\eta_{ij}\tilde{p}_{ij}^*\left|h_{ij}\right|^2}{\tilde{s}_{ij}^*}\right) - \dfrac{\eta_{ij}\tilde{p}_{ij}^*\left|h_{ij}\right|^2}{\ln 2\left(\tilde{s}_{ij}^* + \eta_{ij}\tilde{p}_{ij}^*\left|h_{ij}\right|^2\right)}}{\left(1 - \mathbb{P}_{app}\right)\tilde{s}_{ij}^* \log_2\left(1 + \dfrac{\eta_{ij}\tilde{p}_{ij}^*\left|h_{ij}\right|^2}{\tilde{s}_{ij}^*}\right) - \left(\tilde{q}_j\left(F, T_j^{\max}, \lambda_j\right) - 1\right)}\right)}_{\Phi\left(\tilde{s}_{ij}^*\right)} - \nu_i^* = \Phi_{ij}\left(\tilde{s}_{ij}^*\right) - \nu_i^* = 0\,. \tag{4.88}$$

From (4.88) we conclude the following relationship between the function $\Phi_{ij}\left(\tilde{s}_{ij}^*\right)$ and the optimal LM ν_i^*

$$\Phi_{ij}\left(\tilde{s}_{ij}^*\right) = \nu_i^*\,. \tag{4.89}$$

Differentiating the function $\Phi_{ij}\left(\tilde{s}_{ij}^{*}\right)$ with respect to $\tilde{s}_{ij}^{*}$, it is easy to verify that the derivation is negative, e.g., $\partial\Phi_{ij}\left(\tilde{s}_{ij}^{*}\right)/\partial\tilde{s}_{ij}^{*}<0$ for all $\tilde{s}_{ij}^{*}>\tilde{s}_{ij}^{\min}$ [54]. Hence, the function $\Phi_{ij}\left(\tilde{s}_{ij}^{*}\right)$ strictly decreases and its inverse function $\Phi_{ij}^{-1}\left(\tilde{s}_{ij}^{*}\right)$ exists for $\tilde{s}_{ij}^{*}>0$, e.g.,

$$\tilde{s}_{ij}^{*}=\Phi_{ij}^{-1}\left(\nu_{i}^{*}\right). \tag{4.90}$$

Moreover, differentiating the Lagrangian function $\mathcal{L}\left(\tilde{s}_{ij},\tilde{p}_{ij},\xi_{j},\mu,\nu_{i},\varepsilon\right)$ in (4.68) over ν_{i}^{*}, which corresponds to the KKT condition (4.73), we get that

$$\left.\frac{\partial\mathcal{L}\left(\tilde{s}_{ij},\tilde{p}_{ij},\xi_{j},\mu,\nu_{i},\varepsilon\right)}{\partial\nu_{i}}\right|_{\left(\tilde{s}_{ij},\tilde{p}_{ij},\xi_{j},\mu,\nu_{i},\varepsilon\right)=\left(\tilde{s}_{ij}^{*},\tilde{p}_{ij}^{*},\xi_{j}^{*},\mu^{*},\nu_{i}^{*},\varepsilon^{*}\right)}=\left(\sum_{j=1}^{K}\tilde{s}_{ij}^{*}\right)-1=0. \tag{4.91}$$

Hence, accounting (4.90) and (4.91) we conclude the following relationship

$$\sum_{j=1}^{K}\Phi_{ij}^{-1}\left(\nu_{i}^{*}\right)=1. \tag{4.92}$$

Proposition 4.3 - If the function Ξ is defined as $\Xi\equiv\sum_{j=1}^{K}\Phi_{ij}^{-1}\left(\nu_{i}^{*}\right)$ then its inverse function Ξ^{-1} exists for $\Xi\left(\nu_{i}^{*}\right)$.

Proof - From the fact that that the derivation of $\Phi_{ij}\left(\tilde{s}_{ij}^{*}\right)$ over $\tilde{s}_{ij}^{*}$ is negative, e.g., $\partial\Phi_{ij}\left(\tilde{s}_{ij}^{*}\right)/\partial\tilde{s}_{ij}^{*}<0$ we can compute that the derivation of $\Xi\left(\nu_{i}^{*}\right)$ over ν_{i}^{*} is also negative, e.g.,

$$\frac{\partial\Xi\left(\nu_{i}^{*}\right)}{\partial\nu_{i}^{*}}=\frac{\partial\sum_{j=1}^{K}\Phi_{ij}^{-1}\left(\nu_{i}^{*}\right)}{\partial\nu_{i}^{*}}=\sum_{j=1}^{K}\left\{\frac{1}{\frac{\partial\Phi_{ij}\left(\tilde{s}_{ij}^{*}\right)}{\partial\tilde{s}_{ij}^{*}}}\right\}<0,\ \forall i. \tag{4.93}$$

[54] We recall that $\tilde{s}_{ij}^{\min}>0$ is the unique solution of $\tilde{r}_{j}=\left(\tilde{q}_{j}\left(F,T_{j}^{\max},\lambda_{j}\right)-1\right)$.

Thus, $\Xi\left(\nu_i^*\right)$ strictly decreases and its inverse function $\Xi^{-1}(\cdot)$ does exist. This completes the proof of *Proposition 4.3*. ■

From (4.92) and *Proposition 4.3* we can define the optimal LM ν_i^* as

$$\nu_i^* = \Xi^{-1}(1),\ \forall i\,. \tag{4.94}$$

From (4.94) and (4.90) we finally derive the optimal subcarrier allocation index $\tilde{s}_{ij}^*$ as

$$\tilde{s}_{ij}^* = \Phi_{ij}^{-1}\left(\nu_i^*\right),\ \forall i, j\,,$$

which resolves equation (4.37) in *Theorem 4.5*. This completes the proof of *Theorem 4.5*. ■

We remark that in equation (4.37) of *Theorem 4.5* the chance for the optimal subcarrier allocation index $\tilde{s}_{ij}^*$ to be the same for different users happens only with probability 0. This is because the imperfect channel realizations $\left|\hat{h}_{ij}\right|^2$ are i.i.d. for different users, e.g., for users j and j' it stands that $\left|\hat{h}_{ij}\right|^2 \neq \left|\hat{h}_{ij'}\right|^2$, hence it is ensured that the function $\Phi_{ij}^{-1}\left(\nu_i^*\right)$ is also different for different users, e.g., $\Phi_{ij}^{-1}\left(\nu_i^*\right) \neq \Phi_{ij'}^{-1}\left(\nu_i^*\right), \forall i, j \neq j'$.

B.6 Optimal Transmitting Power in Compliance with the A-NBS Principle - Proofs of *Theorem 4.6*

In this Appendix we determine the optimal transmitting power allocation $\tilde{p}_{ij}^*$ for user j on subcarrier i. From the KKT condition (4.69), the differentiation of the Lagrangian function $\mathcal{L}\left(\tilde{s}_{ij}, \tilde{p}_{ij}, \xi_j, \mu, \nu_i, \varepsilon\right)$ in (4.68) over $\tilde{p}_{ij}$ yields the optimal channel allocation index $\tilde{p}_{ij}^* > 0$ of user j on subcarrier i to be global maxima, e.g.,

$$\left.\frac{\partial \mathcal{L}\left(\tilde{s}_{ij}, \tilde{p}_{ij}, \xi_j, \mu, \nu_i, \varepsilon\right)}{\partial \tilde{p}_{ij}}\right|_{\left(\tilde{s}_{ij}, \tilde{p}_{ij}, \xi_j, \mu, \nu_i\right) = \left(\tilde{s}_{ij}^*, \tilde{p}_{ij}^*, \xi_j^*, \mu^*, \nu_i^*\right)} = 0 \qquad \Leftrightarrow$$

$$\left(1+\xi_j^*\right)w_j \frac{\dfrac{\eta_{ij}\sigma_h^2 \cdot \mathbb{F}^{-1}_{\left(\left|\hat{h}_{ij}\right|^2/\sigma_h^2\right)_2}\left(\mathbb{P}_{app}\right)}{\ln 2 \cdot \left(1+\dfrac{\eta_{ij}\tilde{p}_{ij}^*\sigma_h^2}{\tilde{s}_{ij}^*} \cdot \mathbb{F}^{-1}_{\left(\left|\hat{h}_{ij}\right|^2/\sigma_h^2\right)_2}\left(\mathbb{P}_{app}\right)\right)}}{\tilde{s}_{ij}^* \cdot \log_2\left(1+\dfrac{\eta_{ij}\tilde{p}_{ij}^*\sigma_h^2}{\tilde{s}_{ij}^*} \cdot \mathbb{F}^{-1}_{\left(\left|\hat{h}_{ij}\right|^2/\sigma_h^2\right)_2}\left(\mathbb{P}_{app}\right)\right)-\dfrac{\left(\tilde{q}_j\left(F,T_j^{\max},\lambda_j\right)-1\right)}{\left(1-\mathbb{P}_{app}\right)}} - \frac{1}{N_F}\mu^* = 0 \Leftrightarrow$$

$$\left(\tilde{s}_{ij}^* \cdot \log_2\left(1+\frac{\eta_{ij}\tilde{p}_{ij}^*\sigma_h^2}{\tilde{s}_{ij}^*} \cdot \mathbb{F}^{-1}_{\left(\left|\hat{h}_{ij}\right|^2/\sigma_h^2\right)_2}\left(\mathbb{P}_{app}\right)\right)-\frac{\left(\tilde{q}_j\left(F,T_j^{\max},\lambda_j\right)-1\right)}{\left(1-\mathbb{P}_{app}\right)}\right)$$

$$\times\left(1+\frac{\eta_{ij}\tilde{p}_{ij}^*\sigma_h^2}{\tilde{s}_{ij}^*} \cdot \mathbb{F}^{-1}_{\left(\left|\hat{h}_{ij}\right|^2/\sigma_h^2\right)_2}\left(\mathbb{P}_{app}\right)\right) = \frac{N_F\left(1+\xi_j^*\right)w_j\eta_{ij}\sigma_h^2 \cdot \mathbb{F}^{-1}_{\left(\left|\hat{h}_{ij}\right|^2/\sigma_h^2\right)_2}\left(\mathbb{P}_{app}\right)}{\ln 2 \cdot \mu^*}. \quad (4.95)$$

For notational brevity, let us define the variables χ_{ij}^* and ζ_{ij}^* denoted by

$$\chi_{ij}^* = 1+\frac{\eta_{ij}\tilde{p}_{ij}^*\sigma_h^2}{\tilde{s}_{ij}^*} \cdot \mathbb{F}^{-1}_{\left(\left|\hat{h}_{ij}\right|^2/\sigma_h^2\right)_2}\left(\mathbb{P}_{app}\right) \quad (4.96)$$

and

$$\zeta_{ij}^* = \frac{N_F\left(1+\xi_j^*\right)w_j\eta_{ij}\sigma_h^2 \cdot \mathbb{F}^{-1}_{\left(\left|\hat{h}_{ij}\right|^2/\sigma_h^2\right)_2}\left(\mathbb{P}_{app}\right)}{\ln 2 \cdot \mu^*}, \quad (4.97)$$

respectively. Then from (4.96) and (4.97) the equation in (4.95) becomes

$$\chi_{ij}^*\left(\tilde{s}_{ij}^* \cdot \log_2\left(\chi_{ij}^*\right)-\frac{\left(\tilde{q}_j\left(F,T_j^{\max},\lambda_j\right)-1\right)}{\left(1-\mathbb{P}_{app}\right)}\right) = \zeta_{ij}^* \Leftrightarrow$$

$$\tilde{s}_{ij}^* \cdot \log_2\left(\chi_{ij}^*\right)^{\chi_{ij}^*} = \chi_{ij}^*\frac{\left(\tilde{q}_j\left(F,T_j^{\max},\lambda_j\right)-1\right)}{\left(1-\mathbb{P}_{app}\right)} + \zeta_{ij}^*. \quad (4.98)$$

It is easy to discriminate that the equation in (4.98) is a transcendental algebraic equation over the variable χ_{ij}^*, e.g., it has the form $\log(x)^x = ax+b$, $a,b>0$. Although other studies provide numerical or graphical solutions to equations similar to (4.95), we propose the

following solution methodology to define the optimal transmitting power $\tilde{p}_{ij}^{*}$ of the A-NBS problem by means of final formulas.

Let us suppose that the term $\left(\tilde{q}_j\left(F,T_j^{\max},\lambda_j\right)-1\right)/\left(1-\mathbb{P}_{app}\right)$ at the right side of the equation in (4.98) is equal to $\tilde{s}_{ij}^{*}\log_2\left(\upsilon_{ij}^{*}\right)$, e.g.,

$$\frac{\left(\tilde{q}_j\left(F,T_j^{\max},\lambda_j\right)-1\right)}{\left(1-\mathbb{P}_{app}\right)}=\tilde{s}_{ij}^{*}\log_2\left(\upsilon_{ij}^{*}\right), \tag{4.99}$$

with the variable υ_{ij}^{*} to be defined as

$$\upsilon_{ij}^{*}=2^{\frac{\left(\tilde{q}_j\left(F,T_j^{\max},\lambda_j\right)-1\right)}{\tilde{s}_{ij}^{*}\left(1-\mathbb{P}_{app}\right)}}>1. \tag{4.100}$$

Then from (4.99) and (4.100) the equation in (4.98) becomes

$$\tilde{s}_{ij}^{*}\cdot\log_2\left(\chi_{ij}^{*}\right)^{\chi_{ij}^{*}}=\tilde{s}_{ij}^{*}\log_2\left(\upsilon_{ij}^{*}\right)^{\chi_{ij}^{*}}+\zeta_{ij}^{*}\Leftrightarrow$$

$$\tilde{s}_{ij}^{*}\cdot\log_2\left(\chi_{ij}^{*}\right)^{\chi_{ij}^{*}}-\tilde{s}_{ij}^{*}\log_2\left(\upsilon_{ij}^{*}\right)^{\chi_{ij}^{*}}=\zeta_{ij}^{*}\Leftrightarrow$$

$$\tilde{s}_{ij}^{*}\cdot\log_2\left(\frac{\chi_{ij}^{*}}{\upsilon_{ij}^{*}}\right)^{\chi_{ij}^{*}}=\zeta_{ij}^{*}\quad . \tag{4.101}$$

Multiplying both sides of (4.101) with $1/\upsilon_{ij}^{*}$ it becomes

$$\frac{1}{\upsilon_{ij}^{*}}\tilde{s}_{ij}^{*}\cdot\log_2\left(\frac{\chi_{ij}^{*}}{\upsilon_{ij}^{*}}\right)^{\chi_{ij}^{*}}=\frac{1}{\upsilon_{ij}^{*}}\zeta_{ij}^{*}\Leftrightarrow$$

$$\tilde{s}_{ij}^{*}\cdot\log_2\left(\frac{\chi_{ij}^{*}}{\upsilon_{ij}^{*}}\right)^{\frac{\chi_{ij}^{*}}{\upsilon_{ij}^{*}}}=\frac{\zeta_{ij}^{*}}{\upsilon_{ij}^{*}}. \tag{4.102}$$

Defining the variable φ_{ij}^{*} as

$$\varphi_{ij}^{*}=\frac{\chi_{ij}^{*}}{\upsilon_{ij}^{*}}, \tag{4.103}$$

then equation (4.102) becomes

$$\tilde{s}_{ij}^{*}\cdot\log_2\left(\varphi_{ij}^{*}\right)^{\varphi_{ij}^{*}}=\frac{\zeta_{ij}^{*}}{\upsilon_{ij}^{*}}\Leftrightarrow$$

$$\varphi_{ij}^{*\varphi_{ij}^{*}}=2^{\frac{\zeta_{ij}^{*}}{\upsilon_{ij}^{*}\tilde{s}_{ij}^{*}}}. \tag{4.104}$$

To solve the equation (4.104) over φ_{ij}^{*} we use the Lambert-*W* function's property [158] according to which if $x^x=z$ then $z=\exp\left(W\left(\ln\left(z\right)\right)\right)$ or $z=\ln\left(z\right)/W\left(\ln\left(z\right)\right)$, where $W\left(\cdot\right)$ denotes the Lambert-*W* function. Hence, (4.104) yields that

$$\varphi_{ij}^{*}=\exp\left(W\left(\ln\left(2^{\frac{\zeta_{ij}^{*}}{\upsilon_{ij}^{*}\tilde{s}_{ij}^{*}}}\right)\right)\right),^{55} \tag{4.105}$$

In continue, with in sequence substitutions of the variables φ_{ij}^{*}, υ_{ij}^{*}, ζ_{ij}^{*} and χ_{ij}^{*} given by (4.103), (4.100), (4.97) and (4.96), respectively, into equation (4.105), we easily derive the optimal transmitting power $\tilde{p}_{ij}^{*}$, e.g.,

$$\tilde{p}_{ij}^{*}=\frac{\tilde{s}_{ij}^{*}}{\eta_{ij}\sigma_h^2\cdot\mathbb{F}^{-1}_{\left(\frac{\left|\hat{h}_{ij}\right|^2}{\sigma_h^2}\right)_2}\left(\mathbb{P}_{app}\right)}\cdot\left(2^{\frac{\left(\tilde{q}_j\left(F,T_j^{\max},\lambda_j\right)-1\right)}{\tilde{s}_{ij}^{*}\left(1-\mathbb{P}_{app}\right)}}\cdot\exp\left(W\left(\ln\left(2^{\frac{N_F\left(1+\xi_j^{*}\right)w_j\eta_{ij}\sigma_h^2\cdot\mathbb{F}^{-1}_{\left(\frac{\left|\hat{h}_{ij}\right|^2}{\sigma_h^2}\right)_2}\left(\mathbb{P}_{app}\right)}{\tilde{s}_{ij}^{*}\cdot\ln 2\cdot\mu^{*}\cdot 2^{\left(\frac{\left(\tilde{q}_j\left(F,T_j^{\max},\lambda_j\right)-1\right)}{\tilde{s}_{ij}^{*}\left(1-\mathbb{P}_{app}\right)}\right)}}}\right)\right)\right)-1\right) \tag{4.106}$$

which yields the formula of the optimal transmitting power in (4.38) of *Theorem 4.6*. Finally, it is apparent that the optimal instantaneous transmitting power $\tilde{p}_{ij}^{*}$ in (4.106) is always larger or equal to zero, e.g., $\tilde{p}_{ij}^{*}\geq 0$.

[55] We remark that according to Lambert-*W* function's property, equation (4.105) can be also written as $\varphi_{ij}^{*}=\ln\left(2^{\zeta_{ij}^{*}/\left(\upsilon_{ij}^{*}\tilde{s}_{ij}^{*}\right)}\right)/W\left(\ln\left(2^{\zeta_{ij}^{*}/\left(\upsilon_{ij}^{*}\tilde{s}_{ij}^{*}\right)}\right)\right)$.

In conclusion, $\tilde{p}_{ij}^{*}$ in (4.106) indicates the amount of the instantaneous optimal transmitting power on subcarrier i of each user j. To increase power efficiency, we need to discriminate which users require less power than others and consider them as optimal users. This can be achieved by a simple linear search among the N_F subcarriers for the optimum user j^*, given by $j^* = \arg\min \tilde{p}_{ij}^{*}$. Our search would be always feasible for the reason that the chance for the optimal instantaneous transmitting power $\tilde{p}_{ij}^{*}$ to be the same for different users happens only with probability 0, as the imperfect channel realizations $\left|\hat{h}_{ij}\right|^2$ are i.i.d. This completes the proof of *Theorem 4.6*. ■

B.7 Impact of Channel Imperfectness on Channel-Error-Inconsiderate Game Theoretic Schemes (MM and WMM)

In this Appendix, we investigate the impact of channel imperfectness on the channel-error-inconsiderate schemes MM [151], [152], [32] and WMM [153], [154], [155]. When MM and WMM scheduling is considered the time-shared data rate allocation policies $r_{ij,MM}$ and $r_{ij,WMM}$ of user j on subcarrier i are given by

$$r_{ij,MM} = E_{\hat{h}_{ij}}\left[\tilde{s}_{ij}\log_2\left(1+\frac{\tilde{p}_{ij}\left|\hat{h}_{ij}\right|^2}{\tilde{s}_{ij}\sigma_z^2}\right)E_{h_{ij}|\hat{h}_{ij}}\left[1_{\left(\left|\hat{h}_{ij}\right|^2\le\left|h_{ij}\right|^2\right)}\right]\right] \quad \text{and} \tag{4.107}$$

$$r_{ij,WMM} = w_j E_{\hat{h}_{ij}}\left[\tilde{s}_{ij}\log_2\left(1+\frac{\tilde{p}_{ij}\left|\hat{h}_{ij}\right|^2}{\tilde{s}_{ij}\sigma_z^2}\right)E_{h_{ij}|\hat{h}_{ij}}\left[1_{\left(\left|\hat{h}_{ij}\right|^2\le\left|h_{ij}\right|^2\right)}\right]\right],^{56} \tag{4.108}$$

respectively. Under channel error, e.g., when $\sigma_h^2 > 0$, MM and WMM cannot perform appropriate scheduling. However, we can compute the minimum power requirements and average effective data rates of MM and WMM focusing on the most strict equivalent data rate

[56] We recall that $1_{(\cdot)}$ denotes the indicator factor.

requirement of each user, e.g., $\tilde{q}_j\left(F,T_j^{\max},\lambda_j\right)$, since obviously $\tilde{q}_j\left(F,T_j^{\max},\lambda_j\right)$ is enough to satisfy each user's delay constraints. In other words, the only criterion we can rely on to define the impact of channel imperfectness on channel-error-inconsiderate schemes is the minimum rate requirement derived by the upper-layer parameters, e.g., $\tilde{q}_j\left(F,T_j^{\max},\lambda_j\right)$. To avoid confusion, we separate the presentation of the specifications of MM and WMM as below.

MM - In MM's strategy, if C_j represents the class of each user j then the target is to maximize the equivalent rate of the most delay-insensitive class, e.g., $\max_{C_j}\min\tilde{q}_C\left(F,T_{C_j}^{\max},\lambda_{C_j}\right)$. Similarly to the definition of the optimal effective data rate $\tilde{r}_{ij}^*$ in (4.40), the minimum required power $P_{\min,MM}$ is calculated as follows.

$$\begin{aligned}\max_{C_j}\min\tilde{q}_{C_j}\left(F,T_{C_j}^{\max},\lambda_{C_j}\right) &\cong E_{\hat{h}_{ij}}\left[\sum_{i=1}^{N_F}\tilde{s}_{ij}\log_2\left(\frac{P_{\min,MM}\eta_{ij}\left|\hat{h}_{ij}\right|^2}{\tilde{s}_{ij}\sigma_z^2}\right)E_{h_{ij}|\hat{h}_{ij}}\left[1_{\left(\left|\hat{h}_{ij}\right|^2\le\left|h_{ij}\right|^2\right)}\right]\right] \\ &= \frac{N_F}{2K}\log_2\left(P_{\min,MM}E_{\hat{h}_{ij}}\left[\frac{\eta_{ij}\left|\hat{h}_{ij}\right|^2}{\tilde{s}_{ij}\sigma_z^2}\middle|\tilde{s}_{ij}=1\right]\right)\end{aligned}. \quad (4.109)$$

As shown in [21] the term $E_{\hat{h}_{ij}}\left[\left(\eta_{ij}\left|\hat{h}_{ij}\right|^2/\left(\tilde{s}_{ij}\sigma_z^2\right)\right)\middle|\tilde{s}_{ij}=1\right]$ in (4.109) is computed as

$$E_{\hat{h}_{ij}}\left[\frac{\eta_{ij}\left|\hat{h}_{ij}\right|^2}{\tilde{s}_{ij}\sigma_z^2}\middle|\tilde{s}_{ij}=1\right]=\Theta\left(\left(1-\sigma_h^2\right)\log_2\left(K\right)\right).^{57} \quad (4.110)$$

[57] We recall that $\Theta\left(b_x\right)=a_x$ if $\limsup_{x\to\infty}\left|a_x\right|/\left|b_x\right|<\infty$ and $\limsup_{x\to\infty}\left|b_x\right|/\left|a_x\right|<\infty$.

In addition, it is obvious that the term $E_{\hat{h}_{ij}}\left[E_{h_{ij}|\hat{h}_{ij}}\left[1_{\left(|\hat{h}_{ij}|^2 \le |h_{ij}|^2\right)}\right]\right]$ in (4.109) equals to $1/2$. By (4.109) and (4.110), we can compute the minimum required power $P_{\min,MM}$ of MM under imperfect channel conditions as

$$P_{\min,MM} = \Theta\left(\frac{2^{\max\limits_{C_j} \min \tilde{q}_{C_j}\left(F, T_{C_j}^{\max}, \lambda_{C_j}\right)\frac{2K}{N_F}}}{\left(1-\sigma_h^2\right)\log_2\left(K\right)}\right). \tag{4.111}$$

Let us now consider that $\Delta\mathbb{P}$ expresses the difference between the average available power to the BS P_{TOTAL} and the minimum required power $P_{\min,MM}$ of MM in (4.111), e.g., $\Delta\mathbb{P} = P_{TOTAL} - P_{\min,MM}$. If $r_{P_{\min,MM}+\Delta\mathbb{P}}$ is the data rate under power $P_{\min,MM} + \Delta\mathbb{P}$ and $r_{P_{\min,MM}}$ the data rate under power $P_{\min,MM}$ then difference $\Delta\mathbb{r} = r_{P_{\min,MM}+\Delta\mathbb{P}} - r_{P_{\min,MM}}$ expresses the average system's effective throughput among all the N_F subcarriers and it is computed as

$$\Delta\mathbb{r} = r_{P_{\min,MM}+\Delta\mathbb{P}} - r_{P_{\min,MM}} = \frac{N_F}{2}\log_2\left(1+\frac{\Delta\mathbb{P}}{P_{\min,MM}}\right).$$

Hence, under channel uncertainty, the MM's total average effective data rate is given by

$$\sum_{C_j=1}^{C_{\max}}\left(K_{C_j}\tilde{q}_{C_j}\left(F, T_{C_j}, \lambda_{C_j}\right)\right) + \Delta\mathbb{r}.$$

WMM - From the time-shared data rate allocation policy $r_{ij,WMM}$ in (4.108) , the minimum required power $P_{\min,WMM}$ in WMM scheduling is calculated as follows.

$$\begin{aligned}\max_{C_j} \tilde{q}_{C_j}\left(F, T_{C_j}^{\max}, \lambda_{C_j}\right) &\cong w_j E_{\hat{h}_{ij}}\left[\sum_{i=1}^{N_F}\tilde{s}_{ij}\log_2\left(\frac{P_{\min,WMM}\eta_{ij}\left|\hat{h}_{ij}\right|^2}{\tilde{s}_{ij}\sigma_z^2}\right)E_{h_{ij}|\hat{h}_{ij}}\left[1_{\left(|\hat{h}_{ij}|^2 \le |h_{ij}|^2\right)}\right]\right] \\ &= \frac{N_F}{2K}w_j\log_2\left(P_{\min,WMM}E_{\hat{h}_{ij}}\left[\frac{\eta_{ij}\left|\hat{h}_{ij}\right|^2}{\tilde{s}_{ij}\sigma_z^2}\middle|\tilde{s}_{ij}=1\right]\right)\end{aligned}. \tag{4.112}$$

As shown in [21], the term $E_{\hat{h}_{ij}}\left[\left(\eta_{ij}\left|\hat{h}_{ij}\right|^2/\left(\tilde{s}_{ij}\sigma_z^2\right)\right)\middle|\tilde{s}_{ij}=1\right]$ in (4.112) is computed as

$$E_{\hat{h}_{ij}}\left[\frac{\eta_{ij}\left|\hat{h}_{ij}\right|^2}{\tilde{s}_{ij}\sigma_z^2}\middle|\tilde{s}_{ij}=1\right]=\Theta\left(\left(1-\sigma_h^2\right)\log_2\left(K\right)\right). \tag{4.113}$$

In addition, it is obvious that the term $E_{\hat{h}_{ij}}\left[E_{h_{ij}|\hat{h}_{ij}}\left[1_{\left(|\hat{h}_{ij}|^2\le|h_{ij}|^2\right)}\right]\right]$ in (4.112) equals to $1/2$. By (4.112) and (4.113), we can compute the minimum required power $P_{\min,WMM}$ of WMM under imperfect channel conditions as

$$P_{\min,WMM}=\Theta\left(\frac{2^{\max\limits_{C_j}\tilde{q}_{C_j}\left(F,T_{C_j}^{\max},\lambda_{C_j}\right)\frac{2K}{w_jN_F}}}{\left(1-\sigma_h^2\right)\log_2\left(K\right)}\right). \tag{4.114}$$

Let us now consider that $\Delta\mathbb{P}'$ expresses the difference between the average available power to the BS P_{TOTAL} and the minimum required power $P_{\min,WMM}$ of WMM in (4.114), e.g., $\Delta\mathbb{P}'=P_{TOTAL}-P_{\min,WMM}$. If $r_{P_{\min,WMM}+\Delta\mathbb{P}'}$ is the data rate under power $P_{\min,WMM}+\Delta\mathbb{P}'$ and $r_{P_{\min,WMM}}$ the data rate under power $P_{\min,WMM}$ then difference $\Delta\mathbb{r}'=r_{P_{\min,WMM}+\Delta\mathbb{P}'}-r_{P_{\min,WMM}}$ expresses the average system's effective throughput among all the N_F subcarriers and it is computed as

$$\Delta\mathbb{r}'=r_{P_{\min,WMM}+\Delta\mathbb{P}'}-r_{P_{\min,WMM}}=\frac{N_F}{2}\log_2\left(1+\frac{\Delta\mathbb{P}'}{P_{\min,WMM}}\right).$$

Hence, under channel uncertainty, the WMM's total average effective data rate is given by

$$\sum_{C_j=1}^{C_{\max}}\left(K_{C_j}\tilde{q}_{C_j}\left(F,T_{C_j},\lambda_{C_j}\right)\right)+\Delta\mathbb{r}'.$$

Chapter 5

Game Theoretic Cross-Layer Design for Cognitive Radios

5.1 Introduction

In this Chapter, we propose a new NBS-based cooperative game-theoretic scheduling framework for joint channel and power allocation in OFDMA cognitive radio (CR) systems with channel uncertainty. In particular, our objectives are to maximize the overall throughput of the CR network and simultaneously to achieve the proportional fair resource distribution with the protection of each licenced user (or Primary User (PU)) transmission, while guaranteeing each CR user (or Secondary User (SU)) minimum rate requirement and the proportional fairness and efficient power distribution among SUs. We rely on the symmetric Nash bargaining concept to introduce an analytical NBS-based cross-layer resource allocation policy for real-time operation in OFDMA CR systems. More precisely, we introduce a proportional fair PBL process with channel outage considerations to allocate both power and subcarriers in fully compliance with the S-NBS Axioms. Relying on our PBL process we aim to maximize the overall effective throughput of heterogeneous CR users subject to subcarrier, power and QoS constraints. Using channel time-sharing relaxation, we formulate a convex optimization problem and establish a feasibility condition for the determined convex set to satisfy all constraints. Moreover, we obtain the optimal solutions via closed-form analysis by introducing a contemporary solution methodology that involves Lambert-*W* function properties. With our methodology, we successfully solve transcendental algebraic equations that appear during the NBS oriented optimization process and achieve deriving the first joint power and channel optimal allocation policy for the S-NBS problem in CR systems by means of final formulas. In addition, due to our new solution concept of cross-layer designs we enhance the CR system's power efficiency and establish low complexity implementation

mechanisms, which do not require iterative processes as usual to search the optimal solution numerically. Finally, through simulation comparisons we demonstrate that the proposed cross-layer scheme for CR networks outperforms the existing maximal rate, fixed assignment and max-min fairness, and converges in real-time to accurate Pareto optimal solutions. The key contributions of this research part have been numbered and discussed in Section 1.2 of Chapter 1.

5.2 Literature review

It is certain that the rapid growth of wireless services has led to growing demand for radio spectrum. Nevertheless, although radio spectrum is limited, valuable, and increasingly congested, recent spectrum-measurement campaigns indicate that most of the licensed spectrum is underutilized [12]. To deal with the dilemma between spectrum congestion and spectrum underutilization, CR technology has been proposed and advocated as an enabling technique that promises to overcome the problem of spectrum scarcity caused by the current way of fixed spectrum allocation [48], [49]. Dynamic spectrum access or spectrum-sharing is considered as one critical merit provided by CR technology [159]. In such a case, a CR user is able to intelligently detect radio spectrums that are temporarily unused by licensed PUs and to dynamically utilize those spectrums available, so-called white spaces. The coexistence of PU and SU networks is described by three basic spectrum-sharing scenarios; spectrum overlay, where the SU network utilizes a license band when the PU network is using the band [55]**,** spectrum underlay, where simultaneous transmissions of PU and SU networks are allowed under the condition that the SU network interferes lower than a certain threshold with the PU network [34]**,** [160]**,** [161] and inter-weaved spectrum, which combines the above two spectrum-sharing methods [162]. In particular, under inter-weaved spectrum-sharing the SU system can utilize the unused license band, i.e., a white space, when the spectrum is typically under-utilized. The secondary transmitter in this mode needs to operate in real-time to monitor spectrum and detect the white space that changes with time and geographic location.

There is an abundance of studies for CR network resource allocation in the relevant literature [53], [163], [164], [165], [166], [167], [168], [169], [170], [171], [172]. Resource allocation for OFDM-based CR networks is examined in [163] and [164], where optimal

schemes derived via Lagrangian formulation are proposed to maximize the DL capacities of a single and multiple SUs, respectively while guaranteeing the interference to the PUs being below a specified threshold. The study in [165] proposes a partitioned iterative water-filling algorithm that enhances the capacity of an OFDM CR system, while the issue of DL channel assignment and power control for FDMA-based CR is addressed in [166], where the locations of the wireless users are considered fixed. Moreover, the authors in [167] and [168] utilize dual frameworks to provide centralized and distributed algorithms that improve the total achievable sum rate of SU OFDMA networks subject to interference constraints specified at the PUs' receivers. In addition, the works in [169] and [170] examine the aspect of dynamic PU activity in OFDM CR systems investigating the case where channels are not always available to SUs. The authors in [53] and [171] study the information theoretical capacity of point-to-point CR channels under various scenarios. However, although the above mentioned studies are very fundamental on the analysis of CR systems, they all assume that SUs have perfect knowledge of the CSI and also have been designed on a single-layer basis. To the best of our knowledge, only [53] and [172] address the resource allocation problem in OFDM-based CR systems with partial CSI but without cross-layer considerations.

On the other hand, the previously reported studies do not deliberate game-theoretic scheduling, which are widely recognized as powerful tools for distributed resource allocation and decision making in interactive multiuser CR systems. Mainly implemented through heuristic techniques, Nash Equilibrium Solutions (NES) are proposed in [34], [38], [39], [50], [51], [52], [53], [54], [55], [160], [161], [162], [173], where the topic of resource allocation is addressed through non-cooperative game scenarios. Additionally, pricing NES-based schemes that improve network utility are introduced in [52], [53], [174]. However, as NES have been proven to be inefficient [41], the achievable network sum utility can be low compared with centralized optimization in cooperative game scenarios. This is because in CR networks, SUs are motivated to cooperate with each other to enhance their own transmission opportunities and achieve high spectrum efficiency. Hence, cooperative game theory favours distributed resource allocation in CR networks, where efficiency and fairness are two of the most concerned metrics. Arising from the Nash Axioms, the Pareto optimality in the cooperative game theoretic schemes in [37], [42], [43], [149], [175] guarantee efficiency and proportional fairness. For example, [175] investigates resource allocation using the Nash bargaining game

and the coalition game in OFDMA networks, whereas [149] focuses on the issues of efficiency, fairness, and QoS guarantee using the framework of the NBS. Among all the afore-mentioned studies only the approaches in [37], [42], [43], [149] introduce analytical solutions using S-NBS resource allocation in CR networks by solely addressing the NBS allocation of power. However, examining the analysis presented in those studies we are quite biased for the validity of the optimal solutions as the authors do not prove the existence of the convex set, which satisfies all the power constraints of the CR optimization problems.

Although recent efforts our first observation is that either in general or especially for CR networks no study has yet proposed the actual S-NBS of both subcarrier and power allocation. Through our experience, we evaluate that this major insufficiency in the field of wireless networking comes from the difficulty of solving transcendental algebraic equations of the form, i.e., $\log(x)^x = ax + b$, $a,b > 0$ that appear during the S-NBS-based convex optimization process [59], [41][58]. We also estimate that this is the reason that most of the afore-mentioned CR approaches propose numerical or even graphical solutions. Therefore, we introduce an intelligent methodology to solve such equations that allows us to derive the optimal policy for the actual S-NBS of both power and channel allocation by means of final formulas. Our second observation is that five important parameters for next-generation CR networks have not been yet combined in any of the previously stated approaches. i) Heterogeneity of SUs ii) data outage due to imperfect channel conditions, iii) complexity of the implementation algorithm, iv) improvements on transmitting power-efficiency and v) cross-layer structure. Hence, we address the above issues by introducing an aggregate game-theoretic resource scheduling scheme from the cross-layer perspective considering inter-weaved spectrum-sharing. Our third observation is that although it is essential for the CR transmitter to operate in real-time, no study reports efforts on iterative-independent and non-heuristic implementation algorithms. For this reason, we rely on uniform transmitting power allocation among channel time-sharing factors to introduce a different approach on the solution of S-NBS-based optimization problems that favours power-efficiency and also

[58] We remark that in this research part we focus on S-NBS-based fairness instead of A-NBS for the reason that various weights are not necessary to be considered in CR systems as SUs exploit the available resources from the primary network opportunistically.

delivers iterative-independent optimal CR scheduling policies. Our fourth observation is that although the plurality of relevant researches the convexity of the NBS-based optimization problem in many studies is not sufficiently proven. In particular, it is well-known that a CR optimization problem involves interference cancelation constraints between PUs and SUs in terms of power thresholds. These interference cancelation constraints on one hand are related but on the other hand they frequently contradict each other due to different requirements of PUs and SUs, channel conditions and spectrum availability. Hence, as we further explain in Section 5.5.3, the convexity of such problems is not always guaranteed as some constraints may not be satisfied and thus, the optimal results often are infeasible. For this reason we establish a condition for our optimization problem to be convex over a convex and non-empty set that satisfies all constraints.

For the ease of reference, in this Chapter we name the proposed S-NBS-based Scheduler for CR networks as S-NBS-CR, the Error-Inconsiderate Scheduler for CR networks developed in our previous work [176] as EIS-NBS-CR, the Error-Considerate opportunistic Scheduler for CR networks adopted in [17], [24], [56] as ECS-CR, the Error-Inconsiderate Power-NBS-based Scheduler for CR networks adopted in [37], [42], [43], [149], [175] as EIP-NBS-CR, the Error-Inconsiderate Fixed power and channel Assignment Scheduling scenario for CR networks utilised in [27], [37], [60] as EIFAS-CR and the Max-Min fairness scheduler for CRs adopted in [32], [151], [152] as MM-CR.

5.3 System Model

This Section outlines the DL OFDMA system model, which is the basis of the proposed S-NBS-CR cross-layer resource allocation problem formulated in Section 5.3. As illustrated in Figure 5.1 , in our CR modelling two wireless multi-user systems coexist; the primary and the secondary network. The primary network includes K' PUs that refers to the users, which own the permanent or legacy rights on the usage of the wireless spectrum. On the other hand the secondary network encompasses K heterogeneous SUs, N_C orthogonal subcarriers and the BS that operates under S-NBS-CR scheduling. Each SU $j \in K$ can exploit the spectrum holes and simultaneously transmit with PUs in a way where interference to PUs is avoided. In

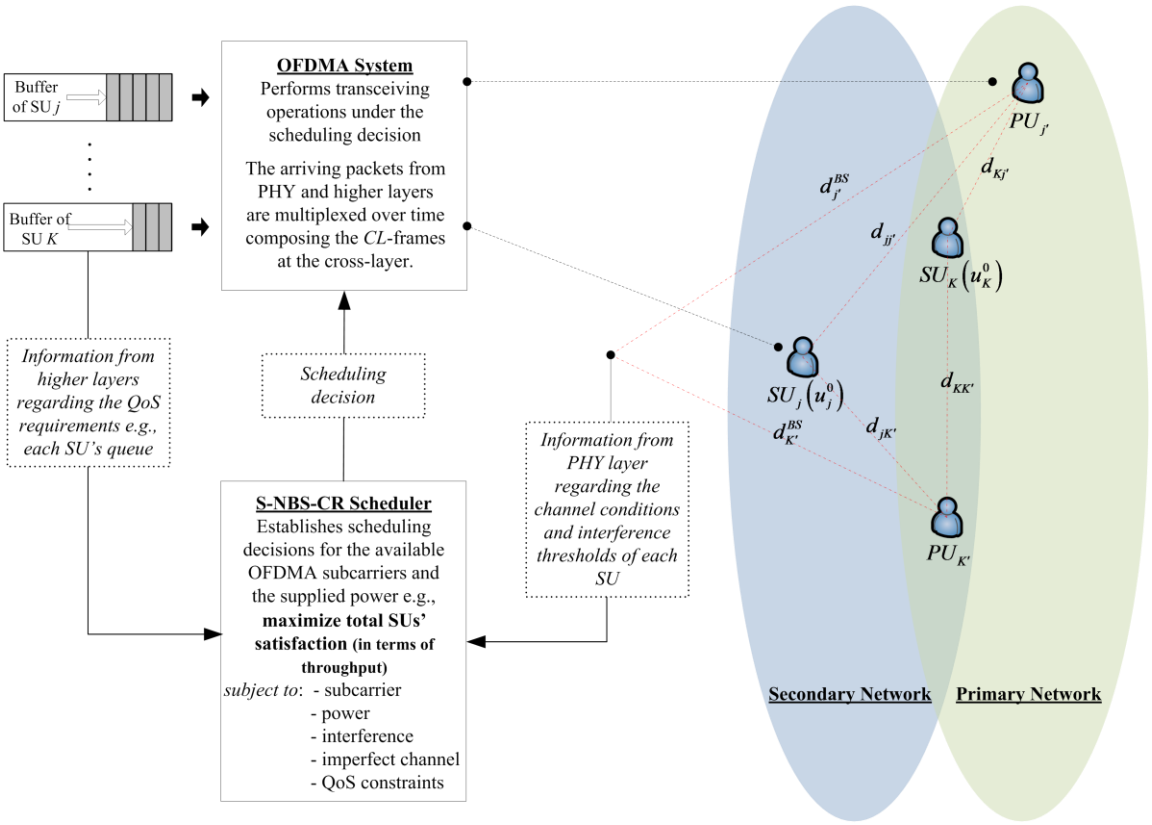

Figure 5.1 - System model for a CR system involving two multi-user networks. Downlink OFDMA resource scheduling based on the S-NBS principle with imperfect channel and heterogeneous QoS requirements of the SUs.

other words, the S-NBS-CR scheduling decision firstly needs to comply with cognitive capabilities, such as sensing the spectrum reliably to check whether it is being used by a PU $j' \in K'$ and secondly to change the radio parameters to exploit the unused part of the spectrum without interfering any transmission of PUs. To avoid transmission interference each SU is constrained by power threshold rules, which as we will see later in Section 5.3.3 can be defined based on the affined distances d between PUs and SUs, e.g., $d_{jj'}$, $d_{jK'}$, $d_{Kj'}$, $d_{KK'}$, and PUs and BS, e.g., $d_{j'}^{BS}$, $d_{K'}^{BS}$. In addition, in our modelling we consider that each SU j has its own minimum QoS requirement u_j^0 in order to start cooperating with others for the NBS game to be feasible. The minimum QoS requirement u_j^0 is always positive or equal

to zero, e.g., $u_j^0 \geq 0$ and it is directly related with user's QoS requirements from higher layers. However, the minimum requirement u_j^0 is not necessarily equal to each SU's j minimum QoS from higher layers; in fact it should be smaller. The reason is that there may be instances, i.e., channel is highly imperfect, where on one hand the S-NBS game may be feasible, e.g., wireless resources may be enough to satisfy all u_j^0 s, but on the other hand the minimum QoS requirements of SUs from higher layers may not be completely satisfied. Nevertheless, even in such cases we must ensure that the available resources will be fairly distributed among SUs according to the S-NBS property.

The main operation of the S-NBS-CR is related to our previously proposed PE-AETS and A-NBS schemes with main differences due to networks' coexistence. In particular, prior to the scheduling decision, S-NBS-CR collects the CSI and the QoS requirements of the SUs as well as the positioning of each PU and SU. More precisely, the CSI is obtained at the beginning of each scheduling interval through performing MMSE estimation of the imperfect channel in TDD operation[59] as described in Sections 3.3.2 and 3.3.2 of Chapter 3. Furthermore, the QSI is attained according to an incremental update algorithm [133], [134], which observes the current backlogs in each SU's independent buffer[60]. In addition, the QSI is updated according to how frequently the state of the SU's mobility and positioning changes in relation with those of PUs. In other words, instead of updating the QoS information before each time slot as in [14], [17], [20], [21], [22], [23], [24], [27], [32], [56], [60], [151], [152], [153], [154] S-NBS-CR uses the incremental update algorithm to reduce its pre-processing process. Moreover, the positioning of each PU and SU is specified by information acquired by space-based systems such as GPS [177] via UL feedback channels transmitted by each PU and SU. Assuming perfect CSIR, the S-NBS-CR scheduling descision is taken once every time slot based on the estimated CSI, QSI and users' positioning information, and passes the resource allocation result to the OFDMA transmitter. Finally, we assume that the subcarrier

[59] The system can also operate under FDD, where perfect feedback of DL CSIT from mobile users is required.

[60] To avoid buffer overflow we assume that users' buffers are sufficiently large enough for storing packets arrived from higher layer.

and transmitting power allocation decision made by the BS transmitter at the secondary network is announced to individual SU through a separate control channel.

5.3.1 Downlink Channel Modelling and CSIT Estimation from Imperfect Channel

In this Section, we adopt the channel modelling presented in Section 3.3 of Chapter 3, where the received OFDM symbol vector for the j-th SU at each OFDM block is given by

$$\mathbf{y}_j = \mathbf{H} \cdot \mathbf{x}_j + \mathbf{z}_j . \tag{5.1}$$

We recall that $\mathbf{y}_j = \left[y_{ij} \right]^{\mathcal{T}}$ and $\mathbf{x}_j = \left[x_{ij} \right]^{\mathcal{T}}$ in (5.1) are the complex-valued vectors of the received and transmitted OFDM blocks y_{ij} and x_{ij} of SU j on the i-th subcarrier, respectively. We also evoke that $\mathbf{H} = diag\left(\mathbf{h}_j\right)$ represents the channel gain matrix with the channel gains vectors $\mathbf{h}_j$ having entries the i.i.d actual channel gain feedback h_{ij} of SU j on subcarrier i. Regarding the noise vector $\mathbf{z}_j = \left[z_{ij} \right]^{\mathcal{T}}$, we consider that its entries z_{ij} signify the channel noise of SU j on subcarrier i and are CSCG i.i.d variables, e.g., $z_{ij} \sim \mathcal{CN}\left(0, \sigma_z^2\right)$, with zero mean and σ_z^2 variance given by $\sigma_z^2 = N_0 \cdot BW / N_C$, where N_0 and BW is the noise density and channel bandwidth, respectively.

The power $\mathcal{P}$ and data rate $\mathcal{R}$ allocation policies of the S-NBS-CR scheme at the PHY layer are denoted by the matrices $\mathcal{P} = \left[p_{ij} \right]$ and $\mathcal{R} = \left[r_{ij} \right]$ with $p_{ij} = E\left[\left| x_{ij} \right|^2 \right]$ and r_{ij} to represent the instantaneous transmitting power and data rate allocated from the scheduler at the BS to SU j through subcarrier i, respectively. In addition, for the efficiency of the transmission between BS and users, we consider M-QAM modulation with the Bit-Error-Rate (BER) of SU j on subcarrier i to be given by [67], [92], [106]

$$\mathcal{BER}_{ij} \approx 0.2 \cdot \exp\left(\frac{-1.5 \cdot \mathcal{SNR}_{ij}}{2^{r_{ij}} - 1} \right), \tag{5.2}$$

The term $\mathcal{SNR}_{ij}$ in (5.2) represents the signal-to-noise (SNR) ratio of SU j on subcarrier i given by $\mathcal{SNR}_{ij} = \mathcal{p}_{ij}\left|h_{ij}\right|^2 / \sigma_z^2$ [156]. Depending on the number of bits assigned to a subcarrier, the adaptive modulator uses a corresponding M-QAM modulation scheme, and the transmitting power level is adjusted according to the combined power, subcarrier and bit allocation decision. Hence, the adaptive modulator adjusts the number of bits loaded on the i-th subcarrier of SU j by allowing the instantaneous data rate r_{ij} to take values from the set $\mathcal{D}$, e.g., $r_{ij} \in [0, \mathcal{D}]$. The set $\mathcal{D}$ expresses the possible number of information that can be transmitted by a subcarrier and it is denoted by $\mathcal{D} = \{0,1,...,\mathcal{D}\}$, where $\mathcal{D}$ is the maximum number of information that can be transmitted by each subcarrier.

Moreover, the subcarrier allocation policy at the PHY layer is represented by the matrix $\mathcal{S} = [s_{ij}]$, where $s_{ij} \in \{0,1\}$ is the subcarrier allocation index meaning that $s_{ij} = 1$ when subcarrier i is allocated to SU j otherwise $s_{ij} = 0$. Hence, to ensure that during a time slot each subcarrier is allocated to one SU only, we define a necessary subcarrier allocation condition as

$$\sum_{i=1}^{N_C} s_{ij} \le 1, \ \forall i . \tag{5.3}$$

In addition, we term a transmitting power allocation rule as

$$E\left[\frac{1}{N_C}\sum_{j=1}^{K}\sum_{i=1}^{N_C} s_{ij}\mathcal{p}_{ij}\right] \le P_{TOTAL}, \tag{5.4}$$

[61]

guaranteeing that the average transmitting power over all users and subcarriers should be smaller or equal than the average total available power at the BS denoted by P_{TOTAL}.

In continue, we model the imperfect channel by representing the independent distributed estimated channel gain $\hat{h}_{ij}$ of SU j on subcarrier i, as

[61] The left side of (5.4) is divided by the number of subcarriers N_C as we refer to average quantities. This means that P_{TOTAL} is the total available power at the BS taking into consideration the effects such as PAPR maximizing that way the utilization of all subcarriers.

$$\hat{h}_{ij} = h_{ij} + \Delta\hat{h}_{ij}, \tag{5.5}$$

where h_{ij} in (5.5) is the actual channel gain feedback and Δh_{ij} the zero mean CSCG channel error term of user j on subcarrier i with known PDF. To increase the system's resilience to CSI errors and also to enhance its throughput efficiency, we perform non-spheristic estimation of the imperfect channel utilizing our effective MMSE channel estimation process presented in Section 3.3.2 of Chapter 3. We recall that in our estimation process the channel errors $\{\Delta h_{ij}\}$ and the estimated channel gains $\{\hat{h}_{ij}\}$ are uncorrelated, while the estimation errors among each user's subcarriers are correlated with MMSE variance σ_h^2 to be depended on each subcarrier's parameters.

5.3.2 MAC and Upper Layer Modelling from Cross-Layer Perspective

Packets from upper layers arrive to each SU j's buffer according to a Poisson arrival process with independent arrival rate denoted by λ_j (in *packets per time slot*). In our source modelling the K SUs have heterogeneous applications in nature and consequently each SU has a maximum delay tolerance denoted by $T_j^{\max}$. Hence, upon spectrum availability SUs with heavier traffic load have higher arrival rate λ_j, while SUs who are more delay-sensitive have stringent maximum delay tolerance $T_j^{\max}$. As in our previous works, we characterize the QoS parameters of each SU j by the tuple $\left[F, T_j^{\max}, \lambda_j\right]$, where F denotes the size of each packet in *bits*.

The MAC layer is responsible for the S-NBS-CR scheduling at every fading block based on the current system dynamics. We recall that system dynamics change dynamically over time and express the perception of the S-NBS-CR scheduler at the MAC layer regarding the current system state, e.g., CSI from PHY layer and QSI and PUs', SUs' positioning. We denote S-NBS-CR's system state as $\left(\hat{\mathcal{H}}, \mathcal{Q}, \mathcal{M}\right)$, where $\hat{\mathcal{H}}$, $\mathcal{Q}$ and $\mathcal{M}$ are the system

dynamics; $\hat{\mathcal{H}}$ is the $N_C \times K$ matrix of the estimated channel gain given by $\hat{\mathcal{H}} = E\left[\left|\hat{h}_{ij}\right|^2\right]$, $\mathcal{Q}$ is the $K \times 1$ vector of the QSI given by $\mathcal{Q} = \left[q_j\right]$ with its j-th component q_j to denote the number of packets remains in SU j's buffer and $\mathcal{M}$ is the $K \times 1$ vector of SUs' positions given by $\mathcal{M} = \left[m_j\right]$.

At the beginning of every OFDM frame, the BS of the secondary network estimates the CSIT from dedicated UL pilot symbols and observes the current backlogs in the buffer according to an incremental update algorithm as described in Section 3.3 of Chapter 3. Based on the obtained CSIT and QSI, S-NBS-CR at the cross-layer determines the subcarrier allocation from the policy $\mathcal{S}\left[\hat{\mathcal{H}}, \mathcal{Q}, \mathcal{M}\right]$, the transmitting power allocation from the policy $\mathcal{P}\left[\hat{\mathcal{H}}, \mathcal{Q}, \mathcal{M}\right]$ and the throughput allocation from the policy $\mathcal{R}\left[\hat{\mathcal{H}}, \mathcal{Q}, \mathcal{M}\right]$. The scheduling results are then broadcasted on downlink channels to all users before subsequent downlink packet transmissions at scheduled rates.

5.3.3 Power-Driven Interference Cancelation Conditions and QoS Considerations

Let us now establish the CR system's regulations for transmission interference cancelation that ensure successful and simultaneous transmissions of PUs and SUs. As discussed previously one of the most important features of a CR system is to allow multiple SUs to dynamically access white spaces in order to improve efficiency of the overall network spectrum utilization. In the coexistence scenario shown in Figure 5.1, SUs' opportunistic transmissions give rise to interference with PUs. To quantify and manage the interference, proper interference power constraints must be imposed to protect active PUs from harmful interference caused by SUs. Hence, to protect potential transmission of PUs and at the same time guarantee their QoS, the received Signal to Interference-plus-Noise Ratio (SINR) at the j'-th PU must be above a certain level, e.g., a predefined threshold to protect the PU's

communication given by $\gamma_{PU}^{\min}$. If the distance between the BS and the j'-th PU is denoted by $d_{j'}^{BS}$, then we can obtain an interference cancelation rule as [178] [62]

$$\frac{P_{j'}^{PU}\left(d_{j'}^{BS}\right)^{-\rho}}{\left(\sum_{i=1}^{N_C}\left(s_{ij}\wp_{ij}\right)\right)\cdot\left(d_{jj'}\right)^{-\rho}+BW\cdot N_0^{j'}}\geq\gamma_{PU}^{\min}, \tag{5.6}$$

where $P_{j'}^{PU}$ in (5.6) denotes the transmitting power of the j'-th PU, $d_{jj'}$ the distance between the j-th CR user and the j'-th PU, ρ the exponent of propagation loss and $N_0^{j'}$ the noise power of the j'-th PU. In our system the affined distances $d_{jj'}$ and $d_{j'}^{BS}$ are specified by space-based systems such as the Global Positioning System (GPS) [177], while the BS acquires information for each PUs' transmitting power $P_{j'}^{PU}$ via feedback channels. Furthermore, accounting the definition of the instantaneous transmitting power $\wp_{ij}$ and the subcarrier allocation index s_{ij} in Section 5.3.1, the interference cancelation regulation in (5.6) can be expressed in terms of interference power constraint as

$$E\left[\sum_{i=1}^{N_C}\left(s_{ij}\wp_{ij}\right)\right]\leq P_j^{\max}, \tag{5.7}$$

where the variable $P_j^{\max}$ in (5.7) denotes the maximum interference power tolerated by the j'-th PU and is calculated by

$$P_j^{\max}=\left(\frac{P_{j'}^{PU}}{\gamma_{PU}^{\min}}\right)\cdot\left(\frac{d_{j'}^{BS}}{d_{jj'}}\right)^{-\rho}-\frac{BW\cdot N_0^{j'}}{\left(d_{jj'}\right)^{-\rho}}. \tag{5.8}$$

In other words, the power-driven interference cancelation condition in (5.7) indicates that PUs' QoS is satisfied and their communication is protected when the total transmit power of each SU j on all its allocated subcarriers is constrained by the maximum interference power tolerated $P_j^{\max}$, which is depended on several dynamic parameters of the involved system users.

[62] In this work, only propagation losses are considered when the scheduler calculates the channel gains of a PU. Similar analysis can be done when the channel fading gains are also considered for PUs.

Nevertheless, by only considering the condition in (5.7) elimination of transmission interference among PUs and SUs is not ensured. The reason is that we have not yet considered the QoS regulation that describes SUs' demand to satisfy their minimum requirements without interfering with the PUs. To clarify further we need to establish an additional condition, which should also be expressed in terms of transmitting power for consistency reasons, to maintain minimum communication quality for the SUs and at the same time not to invalidate the interference cancelation condition of the PUs in (5.7). Let us assume that each SU j requires its SINR not to be smaller than a predefined cut-off power threshold denoted by $\gamma_j^{\min}$. Recalling from (5.3) that our system does not allow more than one SUs to occupy a subcarrier we can define the power-driven QoS condition for SUs as[63]

$$E\left[\sum_{i=1}^{N_C} s_{ij}\, p_{ij} \left|\hat{h}_{ij}\right|^2\right] / \sigma_z^2 \geq \gamma_j^{\min}, \tag{5.9}$$

which can be further simplified to

$$E\left[\sum_{i=1}^{N_C}\left(s_{ij}\, p_{ij} \left|\hat{h}_{ij}\right|^2\right)\right] \geq P_j^{\min}, \tag{5.10}$$

The variable $P_j^{\min}$ in (5.10) expresses the minimum power required by the j-th SU to satisfy its minimum QoS requirements without interfering with PUs and it is calculated by

$$P_j^{\min} = \gamma_j^{\min} \cdot \sigma_z^2 = \frac{\gamma_j^{\min} \cdot BW \cdot N_0}{N_C}. \tag{5.11}$$

Evidently, the interference cancelation power constraints in (5.7) and (5.10) indicate the admissible worst radio-frequency environment for the PUs and SUs, respectively. Later in Section 5.5, we will formulate the cross-layer resource allocation problem for the CR system as a traditional optimization problem under power-driven interference cancelation conditions imposed for PU protection, in addition to the requirements on the minimum SINR for the SUs. We remark that the cut-off power threshold $\gamma_j^{\min}$ of each SU is directly related with its

[63] We remark that the interference among system's subcarriers is out of the scope of this work as from the condition in (5.3) it is straightforward that subcarrier allocations are assumed to be perfectly orthogonal among SUs.

minimum requirement u_j^0 to join the S-NBS game as well as with its minimum QoS demand from higher layers. In contrary to many relevant studies, in Section 5.5.2 we shall correlate each SU's cut-off power threshold $\gamma_j^{\min}$ in (5.11) with its equivalent data rate at higher layers and its minimum requirement u_j^0 to join the S-NBS game. In addition, we will establish a feasibility condition that correlates the power-driven CR constraints, e.g., $P_j^{\min}$ in (5.11), $P_j^{\max}$ in (5.8) and the total available power at the BS P_{TOTAL} in (5.4). Such feasibility condition is vital for the validity of the scheduling decision as it is frequent the interference cancelation conditions to contradict each other.

5.4 Effective Data Rate under Imperfect CSIT and Channel Outage - Fairness Aware PBL Process for OFDMA-based CR Systems

In this Section, we design a novel fairness aware PBL process that fully complies with the S-NBS of power and subcarrier allocation considering imperfect channel and outage conditions. Our approach is similar to the PBL process developed in Section 4.4 of Chapter 4 with key differences to occur due to symmetric fairness considerations. Hence, to clarify every fold of our new research topic, we present the S-NBS-based PBL process in its full measure. For the ease of presentation, we separate the formulation of the S-NBS-based PBL process into two parts: the first part regards the imperfect channel and outage considerations, while the second part concerns the symmetric fairness awareness.

5.4.1 Imperfect Channel and Outage Considerations - Part A

As we thoroughly explained in Section 3.4 of Chapter 3, imperfect channel may result in scheduled rates greater than the maximum channel's capacity [136]. Hence, we shall firstly address the systematic effect of packet error due to channel noise and outage to define the effective instantaneous data rate r_{ij} of the S-NBS-CR.

By the definition of the BER in (5.2), the instantaneous data rate r_{ij} allocated to SU j through subcarrier i, has been defined as a function of the actual channel realization h_{ij} hence, it is in fact the maximum achievable capacity c_{ij} of subcarrier i allocated to SU j during a fading slot. From the Shannon's capacity theorem [136] and by defining the variable $\hbar_{ij} = -1.5/\left(\sigma_z^2 \cdot \ln\left(5 \cdot \mathcal{BER}_{ij}\right)\right)$ for brevity, we can define the maximum achievable capacity c_{ij} of subcarrier i allocated to SU j as

$$c_{ij} = \log_2\left(1 + \hbar_{ij} p_{ij} \left|h_{ij}\right|^2\right). \tag{5.12}$$

Our target is to define a PBL process to describe the maximum possible data rate transmission under channel outage. In our PBL process, the instantaneous effective data rate r_{ij} should firstly be smaller or equal than the maximum achievable capacity c_{ij} in (5.12), e.g., $r_{ij} \le c_{ij}$, and secondly it should be defined as the maximum instantaneous data successfully delivered to SU j through subcarrier i, e.g.,

$$r_{ij} = 1_{\left(r_{ij} \le c_{ij}\right)} \cdot c_{ij}, \tag{5.13}$$

where the indicator function $1_{\left(r_{ij} \le c_{ij}\right)}$ in (5.13) is given by $1_{\left(r_{ij} \le c_{ij}\right)} = \begin{cases} 1, & r_{ij} \le c_{ij} \\ 0, & r_{ij} > c_{ij} \end{cases}$, $\forall i, j$. Hence, accounting the imperfect channel realization $\hat{h}_{ij}$ in (5.12), the instantaneous effective data rate r_{ij} in (5.13) is computed as

$$\begin{aligned} r_{ij} &= E_{\hat{h}_{ij}}\left[E_{h_{ij}|\hat{h}_{ij}}\left[1_{\left(r_{ij} \le c_{ij}\right)} \cdot c_{ij}\right]\right] \\ &= E_{\hat{h}_{ij}}\left[1_{\left(r_{ij} \le c_{ij}\right)} \cdot c_{ij}\right] \\ &= E_{\hat{h}_{ij}}\left[\left(\Pr\left(r_{ij} \le c_{ij} \middle| \hat{h}_{ij}\right)\right) \cdot c_{ij}\right] \\ &= E_{\hat{h}_{ij}}\left[\left(1 - \mathcal{P}_{out,ij}\right) \cdot c_{ij}\right] \end{aligned}, \tag{5.14}$$

where $\mathcal{P}_{out,ij}$ represents the target channel outage probability of each subcarrier i allocated to SU j and it is given by $\mathcal{P}_{out,ij} = 1 - \Pr\left[E_{\hat{h}_{ij}}\left[c_{ij}\right] \le c_{ij} \middle| \hat{h}_{ij}\right]$. In other words, $\mathcal{P}_{out,ij}$ in (5.14)

indicates the target channel outage probability determined by the probability where the maximum achievable capacity c_{ij} is smaller than the capacity $E_{\hat{h}_{ij}}\left[c_{ij}\right]$ as perceived by the system due to the imperfect channel realizations $\hat{h}_{ij}$. For simplicity, we assume that the target channel outage probability $\mathcal{P}_{out,ij}$ is the same for each user and subcarrier, e.g., $\mathcal{P}_{out,ij}=\mathcal{P}_{out}$. Furthermore, from the definitions of the instantaneous effective data rate r_{ij} in (5.14) and of the maximum achievable capacity c_{ij} in (5.12) we can define the PBL process of the effective data rate r_j allocated to SU j as

$$\begin{aligned} r_j &= E_{\hat{h}_{ij}}\left[\sum_{i=1}^{N_C}\left(1-\mathcal{P}_{out}\right)\cdot s_{ij}\cdot c_{ij}\right] \\ &= E_{\hat{h}_{ij}}\left[\sum_{i=1}^{N_C}\left(1-\mathcal{P}_{out}\right)\cdot s_{ij}\cdot \log_2\left(1+\frac{p_{ij}\left|h_{ij}\right|^2}{\Gamma}\right)\right], \end{aligned} \tag{5.15}$$

where $1-\mathcal{P}_{out}=\Pr\left[E_{\hat{h}_{ij}}\left[c_{ij}\right]\le c_{ij}\left|\hat{h}_{ij}\right.\right]$ is the probability of successfully transmitting information. The definition of our PBL process in (5.15), on one hand considers channel imperfectness and channel outage but on the other hand it does not have not yet include symmetric fairness considerations.

5.4.2 S-NBS Fairness Considerations - Part B

We shall now apply the S-NBS property in the PBL process in (5.15). Examining equation (5.15), we observe that we cannot directly apply the S-NBS property as we have not yet shown that our function is convex. In fact, our PBL function is not convex as it includes the discrete variable of the subcarrier index s_{ij}, e.g., $s_{ij}\in\{0,1\}$, and the continues variable of the instantaneous transmitting power p_{ij}. To achieve convexity we transform the discrete variable of the subcarrier index s_{ij} through utilizing subcarrier time-sharing relaxation [140] that allows us to define the continue variable $\tilde{s}_{ij}\in(0,1]$ (see Section 3.6.1 of Chapter 3 for more details). The subcarrier time-sharing $\tilde{s}_{ij}$ of each subcarrier i bears the definition of the

variables $\tilde{r}_{ij} = \tilde{s}_{ij} r_{ij}$ and $\tilde{p}_{ij} = \tilde{s}_{ij} p_{ij}$, which express the instantaneous effective data rate and the instantaneous transmitting power of SU j on subcarrier i scaled by the same factor $\tilde{s}_{ij}$. In other words, we can write our PBL process in (5.15) in terms of subcarrier time-sharing as

$$\tilde{r}_j = E_{\hat{h}_{ij}}\left[\sum_{i=1}^{N_C}\left(1-\mathcal{P}_{out}\right)\cdot \tilde{s}_{ij}\cdot \log_2\left(1+\frac{\hat{\kappa}_{ij}\,\tilde{p}_{ij}\left|h_{ij}\right|^2}{\tilde{s}_{ij}}\right)\right], \tag{5.16}$$

with the M-QAM modulator allowing the instantaneous effective data rate $\tilde{r}_{ij}$ of SU j on subcarrier i to take values from the set $\tilde{\mathcal{D}} = \left\{0,1,...,\tilde{s}_{ij}\cdot\mathcal{D}\right\}$ e.g., $\tilde{r}_{ij} \in \left[0, \tilde{s}_{ij}\cdot\mathcal{D}\right]$.

Theorem 5.1 - Given the subcarrier time-sharing factor $\tilde{s}_{ij} \in (0,1]$ and the new power transmission variable $\tilde{p}_{ij} = \tilde{s}_{ij} p_{ij}$, the PBL function in (5.16) that expresses the effective data rate $\tilde{r}_j$ allocated to SU j, is a concave function over the non-empty and convex set $\left(\tilde{s}_{ij}, \tilde{p}_{ij}\right)$.

Proof - The proof of *Theorem 5.1* is similar to the proof of *Theorem 4.1* in Chapter 4 and has been omitted from this Thesis due to space limitations. ■

Since in *Theorem 5.1* we prove that our PBL function (5.16) is concave over the non-empty and convex set $\left(\tilde{s}_{ij}, \tilde{p}_{ij}\right)$, we can now apply the S-NBS property on the instantaneous effective data rate $\tilde{r}_j$ of SU j. More precisely, we consider each SU j's minimum QoS requirement $u_j^0 \geq 0$ to join the S-NBS game along with the S-NBS property and its Axioms as described in Lemma 2.1 and Section 2.4, respectively to define the following Theorem.

Theorem 5.2 – As the function $\tilde{r}_j$ in (5.16) is convex upper-bounded defined on the non-empty and convex set $\left(\tilde{s}_{ij}, \tilde{p}_{ij}\right)$, there exists a symmetric Nash bargaining point that verifies $\tilde{r}_j \geq u_j^0$, $\forall \tilde{s}_{ij} \in (0,1]$, $\tilde{p}_{ij} \geq 0$ and comprises the unique solution of the maximization problem

$$\max_{\tilde{s}_{ij}, \tilde{p}_{ij}} \prod_{j\in K}\left(\tilde{r}_j - u_j^0\right). \tag{5.17}$$

Proof - The proof of *Theorem 5.2* is similar to the proof of Lemma 2.1 and to the S-NBS property presented in [40] and has been omitted from this Thesis due to space limitations. ■

In *Theorem 5.2*, we describe an un-constrained throughput maximization problem with its cost function to express each SU j's throughput satisfaction in the S-NBS game strategy. The physical meaning of the cost function of the problem (5.17) is the amount of extra resources allocated to SU j, i.e., excess throughput obtained by SU j. Moreover, to present the S-NBS throughput maximization problem in its full measure, we substitute in the problem (5.17) the effective data rate $\tilde{r}_j$ of SU j given by (5.16) and by taking advantage of the strictly increasing property of the logarithm function we define a new S-NBS throughput maximization problem as below

$$\max_{\tilde{s}_{ij},\tilde{p}_{ij}} \prod_{j\in K}\left(\tilde{r}_j - u_j^0\right) \Leftrightarrow$$
$$\max_{\tilde{s}_{ij},\tilde{p}_{ij}} \sum_{j=1}^{K} \ln\left(E_{\hat{h}_{ij}}\left[\sum_{i=1}^{N_C}\left(1-\mathcal{P}_{out}\right)\cdot \tilde{s}_{ij}\cdot \log_2\left(1+\frac{\hbar_{ij}\,\tilde{p}_{ij}\left|h_{ij}\right|^2}{\tilde{s}_{ij}}\right)\right] - u_j^0\right). \tag{5.18}$$

Nevertheless, although we have taken into consideration the strictly increasing property of the logarithm function, it is not ensured that the new problem (5.18) is equivalent to the S-NBS-based maximization problem (5.17). The reason is that it is still uncertain that the cost function of the new problem (5.18) can provide a unique solution over $\left(\tilde{s}_{ij}, \tilde{p}_{ij}\right)$, which ensures that the effective data rate $\tilde{r}_j$ allocated to SU j is larger than the user j's minimum requirement, e.g., $\tilde{r}_j > u_j^0$. To prove the equivalency between the two problems it is sufficient to show that the cost function of the new problem (5.18) strictly increases for all $\left(\tilde{s}_{ij}, \tilde{p}_{ij}\right)$ such that $\tilde{r}_j > u_j^0$. Showing that the new cost function strictly increases it is then straightforward that the solution $\left(\tilde{s}_{ij}, \tilde{p}_{ij}\right)$ is unique and that it fully complies with the S-NBS property as explained in Section 4.4 of Chapter 4. Let us denote the cost function of the new problem (5.18) by the utility function $\mathcal{U} = \sum_{j=1}^{K} \mathcal{U}_j$, with $\mathcal{U}_j$ to represent the utility function of SU j given by

$$\mathcal{U}_j = \ln\left(E_{\hat{h}_{ij}}\left[\sum_{i=1}^{N_C} (1-\mathcal{P}_{out}) \cdot \tilde{s}_{ij} \cdot \log_2\left(1+\frac{\hbar_{ij}\,\tilde{p}_{ij}\left|h_{ij}\right|^2}{\tilde{s}_{ij}} \right) \right] - u_j^0 \right). \tag{5.19}$$

The following Theorem follows readily from (5.19).

Theorem 5.3 - The problem (5.18) is equivalent to the S-NBS throughput maximization problem (5.17) and its cost function $\mathcal{U} = \sum_{j=1}^{K} \mathcal{U}_j$ is designed based on the S-NBS Theorem matching the metric of proportional fairness for resource sharing [157].

Proof - The proof of *Theorem 5.3* is presented in Appendix C.1. ■

From *Theorem 5.3* we prove that our PBL process (5.19) expresses the user j's satisfaction in full compliance with the S-NBS of power and subcarrier allocation including the effects of channel imperfectness and channel outage along with each user j's asymmetric weight.

The key differences between our PBL process (5.19) and the utilities defined by the relevant studies [37], [13], [42] and [43] are now easy to be verified. Firstly, our PBL process includes imperfect channel and outage considerations, while others do not. Secondly, our utility function $\mathcal{U}_j$ in (5.19) includes both the subcarrier $\tilde{s}_{ij}$ and power $\tilde{p}_{ij}$ allocation variables inside the logarithm, imposed by the S-NBS principle, while others consider only the transmitting power allocation variable only. This means that in those cases the subcarrier allocation policy does not comply either with the S-NBS or A-NBS rules. In the following, we will formulate the S-NBS-based cross-layer optimization problem for CR networks relying on (5.18).

5.5 S-NBS-based Cross-Layer Problem Formulation

In this Section, we formulate the S-NBS cross-layer design for heterogeneous users with imperfect channel and outage considerations as a constrained optimization problem based on the OFDMA system modelling described in Section 5.3.

5.5.1 Formulation of the S-NBS Cross-Layer Optimization Problem

We represent the optimal subcarrier allocation policy with the $N_C \times K$ matrix $\boldsymbol{\mathcal{S}}^* = \left[\tilde{s}_{ij}^*\right]$ whose (i,j)-th element is the optimal time-sharing subcarrier allocation factor $\tilde{s}_{ij}^*$ of SU j on subcarrier i. In addition, we denote the optimal transmitting power allocation policy with the $N_C \times K$ matrix $\boldsymbol{\mathcal{P}}^* = \left[\tilde{p}_{ij}^*\right]$ whose (i,j)-th element is the optimal instantaneous transmitting power allocation $\tilde{p}_{ij}^*$ of SU j on subcarrier i. In continue, we can formulate the S-NBS cross-layer optimization problem as follows.

Find optimal subcarrier and transmitting power resource allocation policies $\boldsymbol{\mathcal{S}}\left[\hat{\boldsymbol{\mathcal{H}}}, \boldsymbol{\mathcal{Q}}, \boldsymbol{\mathcal{M}}\right]$ and $\boldsymbol{\mathcal{P}}\left[\hat{\boldsymbol{\mathcal{H}}}, \boldsymbol{\mathcal{Q}}, \boldsymbol{\mathcal{M}}\right]$, respectively

$$\textit{such that: } \max_{\tilde{s}_{ij}, \tilde{p}_{ij}} E\left[\sum_{j=1}^{K} \ln\left(E_{\hat{h}_{ij}}\left[\sum_{i=1}^{N_C}\left(1-\mathcal{P}_{out}\right)\cdot \tilde{s}_{ij}\cdot \log_2\left(1+\frac{\mathcal{H}_{ij}\tilde{p}_{ij}\left|h_{ij}\right|^2}{\tilde{s}_{ij}}\right)\right]-u_j^0\right)\right] \quad (5.20)$$

$$\textit{subject to: } \tilde{s}_{ij} \in (0,1], \quad \forall i,j, \quad (5.21)$$

$$\sum_{j=1}^{K} \tilde{s}_{ij} \le 1, \quad \forall i, \quad (5.22)$$

$$\tilde{p}_{ij} \ge 0, \quad \forall i,j, \quad (5.23)$$

$$E\left[\sum_{i=1}^{N_C} \tilde{p}_{ij}\right] \le P_j^{\max}, \quad \forall j, \quad (5.24)$$

$$E\left[\sum_{i=1}^{N_C}\left(\tilde{p}_{ij}\left|\hat{h}_{ij}\right|^2\right)\right] \ge P_j^{\min}, \quad \forall j, \quad (5.25)$$

$$E\left[\frac{1}{N_C}\sum_{j=1}^{K}\sum_{i=1}^{N_C}\tilde{p}_{ij}\right] \le P_{TOTAL}, \quad (5.26)$$

$$E\left[D_j\right] \le T_j^{\max}, \quad \forall j, \quad (5.27)$$

$$\mathcal{P}_{out,ij} = \mathcal{P}_{out} = \mathcal{P}_{app}, \quad \forall i, j. \qquad (5.28)$$

The S-NBS cross-layer optimization problem (5.20) - (5.28) is a utility maximization problem over the instantaneous transmitting power $\tilde{p}_{ij}$ and the time-sharing subcarrier allocation factor $\tilde{s}_{ij}$. The problem includes power-driven constraints for transmission interference cancelation between PUs and SUs, channel and packet outage limitations due to imperfect channel, subcarrier and power allocation rules. More precisely, the cost function in (5.20) expresses the total level of satisfaction of all the SUs in the CR network. The level of satisfaction is expressed according to the S-NBS principle in terms of throughput allocated from the BS to the K heterogeneous SUs over all the N_C subcarriers. The subcarrier allocation constraints (5.21) and (5.22) are used to certify that only one SU j can occupy a time-share of a subcarrier i at a specific time slot. Moreover, the power allocation constraint (5.23) ensures that the instantaneous transmitting power $\tilde{p}_{ij}$ is always larger or equal to zero, while constraint (5.24) is the PUs' interference cancelation regulation (5.7) expressed in terms of the time-sharing factor $\tilde{p}_{ij}$. In addition, constraint (5.25) corresponds to (5.10), which guarantees that the SUs will get their minimum QoS requirement in terms of power and simultaneously that they will not interfere with PUs transmission. Furthermore, we express the system rule (5.4) in terms of $\tilde{p}_{ij}$ to write the cross-layer constraint (5.26), which warrants that the total transmitting power from the BS to the K SUs cannot exceed the average total available power at the BS P_{TOTAL}. We remark that (5.24) and (5.26) are independent constraints; $P_j^{\max}$ is determined by the SNIR requiremtn of the PUs, while P_{TOTAL} is the total power available for cognitive radio users. Furthermore, constraint (5.27) is the QoS constraint in terms of average delay of each heterogeneous SU j, denoted by $E\left[D_j\right]$[64], and of the

[64] The average delay is adopted in the literature i.e., [24], [56], [27] as a performance measure of the delay performance. In short, it is recognized that average delay is a good characterization of overall delay performance.

maximum delay tolerance $T_j^{\max}$ specified by SU j's queuing characteristics[65]. Furthermore, the outage constraint (5.28) limits the impact of the imperfect CSIT by guaranteeing that the target channel outage probability $\mathcal{P}_{out,ij} = \mathcal{P}_{out}$ at the PHY layer, satisfies a target packet outage probability $\mathcal{P}_{app}$. The target packet outage probability $\mathcal{P}_{app}$, given by $\mathcal{P}_{app} = 1 - \Pr\left(E\left[D_j\right] \le T_j^{\max}\right)$, represents the packet transmission failure and it is usually specified by the application requirements of each user.

It is straightforward that the QoS constraint (5.27) and the outage constraint (5.28) have been defined in terms of higher layer parameters meaning that both constraints do not comply with the cross-layer structure. In addition, the power constraint (5.25) is related with the QoS constraint (5.27) as both constraints try to ensure the SUs' minimum requirements. In fact, considering one of those two constraints would result the other constraint to be redundant in our problem. Hence, the S-NBS cross-layer optimization problem (5.20) - (5.28) cannot be directly solved unless we express constraints (5.27) and (5.28) by means of PHY layer parameters and correlate (5.27) with (5.25).

5.5.2 Correlation between Transmission Interference Cancelation, Outage and QoS Constraints of the S-NBS Cross-Layer Optimization Problem

In this Section, we correlate the power-driven transmission interference cancelation constraint (5.25) with the QoS constraint (5.27) and express the derived regulation along with the outage constraint (5.28) of the S-NBS cross-layer optimization problem (5.20) - (5.28) in terms of PHY layer optimization variables.

Correlation between Outage and QoS Constraints. Regarding the outage constraint (5.28), we observe that given the imperfect channel realization $\hat{h}_{ij}$, the actual channel realization h_{ij} in the cost function of the optimization problem (5.20) - (5.28) is CSGC distributed with

[65] In our model, we assume that users have enough traffic waited in the queue, which is ready to be transmitted. Therefore, if a network resource is allocated to a user, that network resource is used up by that user.

mean the estimated channel gain $\hat{h}_{ij}$, e.g., $E_{h_{ij}|\hat{h}_{ij}}\left[h_{ij}\left|\hat{h}_{ij}\right.\right]=\hat{h}_{ij}$, and variance the MMSE variance σ_h^2, e.g., $E_{h_{ij}|\hat{h}_{ij}}\left[\left(h_{ij}-\hat{h}_{ij}\right)\left(h_{ij}-\hat{h}_{ij}\right)\left|\hat{h}_{ij}\right.\right]=\sigma_h^2$. As the actual channel realization h_{ij} is CSGC distributed, e.g., $h_{ij}\sim\mathcal{CN}\left(\hat{h}_{ij},\sigma_h^2\right)$, the term $\left|h_{ij}\right|^2/\sigma_h^2$ is a non-central random chi-squared variable with two degrees of freedom[66] and non-centrality parameter the term $\left|\hat{h}_{ij}\right|^2/\sigma_h^2$ [146], [59], [156]. Relying on these statistics we present the following Theorem to define the S-NBS cross-layer optimization problem (5.20) - (5.28) in terms of the outage constraint (5.28).

Theorem 5.4 - The cost function of the S-NBS cross-layer optimization problem (5.20) - (5.28) satisfies the outage constraint (5.28), e.g., $\mathcal{P}_{out}=\mathcal{P}_{app}$ when the utility function $\mathcal{U}_j$ of SU j in (5.19) is given by the following equation[67]

$$\mathcal{U}_j=\ln\left(\sum_{i=1}^{N_C}\left(1-\mathcal{P}_{app}\right)\cdot\tilde{s}_{ij}\cdot\log_2\left(1+\frac{\mathcal{h}_{ij}\tilde{p}_{ij}\sigma_h^2}{\tilde{s}_{ij}}\cdot\mathcal{F}^{-1}_{\left(\frac{\left|\hat{h}_{ij}\right|^2}{\sigma_h^2}\right)_2}\left(\mathcal{P}_{app}\right)\right)-u_j^0\right), \tag{5.29}$$

where $F^{-1}_{\left(\left|\hat{h}_{ij}\right|^2/\sigma_h^2\right)_2}\left(\mathcal{P}_{app}\right)$ is the inverse non-central chi-squared CDF of $\mathcal{P}_{app}$ with non-centrality parameter the term $\left|\hat{h}_{ij}\right|^2/\sigma_h^2$ and two degrees of freedom.

Proof - The proof of *Theorem 5.4* is presented in Appendix C.2. ■

[66] The degrees of freedom express the number of independent pieces of information available to estimate another piece of information and define the sensitivity of an estimation pattern. To specify the orientation of the term $\left|h_{ij}\right|^2/\sigma_h^2$ we involve two of its independent displacements: the imperfect channel realization $\hat{h}_{ij}$ and the channel error $\Delta\hat{h}_{ij}$ meaning that the term $\left|h_{ij}\right|^2/\sigma_h^2$ has two degrees of freedom.

[67] From this point in this Section, the expectation operator $E\left[\cdot\right]$ refers to the average of the quantity over the ergodic realizations of the actual and the estimated channel gains e.g., $\left\{h_{ij}\right\}$ and $\left\{\hat{h}_{ij}\right\}$, respectively. For notational brevity, we omit its characterization i.e., "expected" or "averaged".

From the definition of the utility function $\mathcal{U}_j$ of SU j in (5.29) and AppendixC.2, we can now define the instantaneous effective data rate $\tilde{r}_{ij}$ of user j on subcarrier i in terms of time-sharing as

$$\tilde{r}_{ij} = \left(1-\mathcal{P}_{app}\right)\cdot \log_2\left(1+\frac{\hbar_{ij}\tilde{p}_{ij}\sigma_h^2}{\tilde{s}_{ij}}\cdot \mathbb{F}^{-1}_{\left(\frac{|\hat{h}_{ij}|^2}{\sigma_h^2}\right)_2}\left(\mathcal{P}_{app}\right)\right). \tag{5.30}$$

Similarly, we can denote the time-shared instantaneous effective data rate $\tilde{r}_j$ of SU j in (5.16) as

$$\tilde{r}_j = \sum_{i=1}^{N_C}\left(1-\mathcal{P}_{app}\right)\cdot \tilde{s}_{ij}\cdot \log_2\left(1+\frac{\hbar_{ij}\tilde{p}_{ij}\sigma_h^2}{\tilde{s}_{ij}}\cdot \mathbb{F}^{-1}_{\left(\frac{|\hat{h}_{ij}|^2}{\sigma_h^2}\right)_2}\left(\mathcal{P}_{app}\right)\right). \tag{5.31}$$

Furthermore, we aim to transform the QoS constraint (5.27) in terms of PHY layer optimization variables and also correlate it with the power-driven transmission interference cancelation constraint (5.25). Based on our queuing analysis presented in Section 3.5.2 of Chapter 3, we can easily establish a relationship between the instantaneous effective data rate $\tilde{r}_j$ of SU j in (5.31) and its traffic characteristic tuple $\left[F, T_j^{\max}, \lambda_j\right]$ (see Section 5.3.2). More precisely, we adopt the traffic arrival rate $\tilde{q}_j\left(F, T_j^{\max}, \lambda_j\right)$ at the user j's queue (see Appendix A.4 of Chapter 3) given by

$$\tilde{q}_j\left(F, T_j^{\max}, \lambda_j\right) = \left(\frac{1}{t_s}/\frac{BW}{N_F}\right)\cdot\left(\frac{F}{2T_j^{\max}}\cdot\left(\sqrt{T_j^{\max}\lambda_j\left(T_j^{\max}\lambda_j+2\right)}+\lambda_j T_j^{\max}\right)\right), \tag{5.32}$$

to define that instantaneous effective data rate $\tilde{r}_j$ of SU j in (5.31) must be at least equal to the traffic arrival rate $\tilde{q}_j\left(F, T_j^{\max}, \lambda_j\right)$, e.g.,

$$\tilde{r}_j \geq \tilde{q}_j\left(F, T_j^{\max}, \lambda_j\right).^{68} \tag{5.33}$$

Although we can include the QoS condition (5.27) into the S-NBS cross-layer optimization problem (5.20) - (5.28), we can further reform it in terms of the utility function $\mathcal{U}_j$ of SU j. In addition, by reformatting the QoS condition (5.27) we can correlate the minimum requirement u_j^0 of SU j and its traffic arrival rate $\tilde{q}_j\left(F, T_j^{\max}, \lambda_j\right)$. More precisely, by initially subtracting the minimum requirement u_j^0 from both sides of the inequality (5.33), we can then consider the logarithm of both sides and derive the following relationship.

$$\begin{aligned} \tilde{r}_j &\geq \tilde{q}_j\left(F, T_j^{\max}, \lambda_j\right) \Leftrightarrow \\ \tilde{r}_j - u_j^0 &\geq \tilde{q}_j\left(F, T_j^{\max}, \lambda_j\right) - u_j^0 \Leftrightarrow . \\ \ln\left(\tilde{r}_j - u_j^0\right) &\geq \ln\left(\tilde{q}_j\left(F, T_j^{\max}, \lambda_j\right) - u_j^0\right) \Leftrightarrow \end{aligned} \tag{5.34}$$

From the reformulation of the QoS condition in (5.34) we conclude two things. Firstly, that we can establish a QoS condition, which specifies that the utility function $\mathcal{U}_j$ of SU j should be at least equal to the term $\ln\left(\tilde{q}_j\left(F, T_j^{\max}, \lambda_j\right) - u_j^0\right)$. In other words, we can describe the equivalent to $\mathcal{U}_j$ level of satisfaction of user j based on the traffic arrival rate $\tilde{q}_j\left(F, T_j^{\max}, \lambda_j\right)$ at the user j's queue as

$$\mathcal{U}_j \geq \ln\left(\tilde{q}_j\left(F, T_j^{\max}, \lambda_j\right) - u_j^0\right). \tag{5.35}$$

Secondly, we can define a correlation condition between the minimum requirement u_j^0 of SU j and its traffic arrival rate $\tilde{q}_j\left(F, T_j^{\max}, \lambda_j\right)$. More precisely, the logarithm at the right side of (5.34) is valid if it's inside part is at least equal to one, e.g., $\tilde{q}_j\left(F, T_j^{\max}, \lambda_j\right) - u_j^0 \geq 1$. Hence, we can easily determine that the minimum requirement u_j^0 of

[68] We remark that when the maximum delay tolerance $T_j^{\max}$ of a SU j is sufficiently large e.g., $T_j^{\max} \to \infty$, then the QoS condition (5.35) becomes $\tilde{r}_j \geq \left(\left(1/t_s\right)/\left(N_F / BW\right)\right) \cdot F\lambda_j$ (for more details see Section 3.5.2 and Appendix A.4 of Chapter 3).

SU j must be at least equal to its traffic arrival rate $\tilde{q}_j\left(F,T_j^{\max},\lambda_j\right)$ minus one *bit/sec/Hz*, e.g.,

$$0 \le u_j^0 \le \tilde{q}_j\left(F,T_j^{\max},\lambda_j\right)-1.^{69} \tag{5.36}$$

The correlation in (5.36) has practical significance as it ensures that the S-NBS game is feasible even if the allocated data rate is less than the incoming traffic arrival rate to each SU's queue. In other words, a user may not be totally satisfied but it still cooperates to ensure fair allocation of the available resources. Hence, in the frequent case where the available power at the BS is not enough to support all SUs' QoS requirements, the scheduling decision is taken on the S-NBS principle ensuring proportional fair resource allocation.

Correlation between Power-Driven Transmission Interference Cancelation and QoS Constraints. Examining the S-NBS cross-layer optimization problem (5.20) - (5.28), it is straightforward that the cross-layer constraint (5.35) is related to the transmission interference cancelation constraint (5.25). For example, in the former case we express the minimum QoS requirements of each SU in terms of throughput, while in the latter case in terms of power. Hence, as throughput depends on power and vice versa, it is unnecessary to consider in our problem both constraints (5.25) and (5.35). However, their properties are necessary to be deliberated as, e.g., (5.25) not only ensures the minimum QoS satisfaction of each SU but it also guarantees that this SU will not interfere with the PUs.

For this reason, we correlate the traffic arrival rate $\tilde{q}_j\left(F,T_j^{\max},\lambda_j\right)$ of each SU j with its minimum required power $P_j^{\min}$ in (5.10). More precisely, as the BS can perfectly acquire the QSI from the upper layers, the equivalent data rate $\tilde{q}_j\left(F,T_j^{\max},\lambda_j\right)$ is known to our scheduler. So, the information exchange between the cross and higher layers is performed with the same way like between the cross and PHY layers under a Gaussian channel, e.g., with perfect CSI. In a Gaussian channel if we assume that the channel's capacity is known or

[69] We remark that when the maximum delay tolerance $T_j^{\max}$ of a user j is sufficiently large e.g., $T_j^{\max}\to\infty$, then the correlation condition (5.36) becomes $u_j^0 \le \left(\left(1/t_s\right)/\left(N_F/BW\right)\right)\cdot F\lambda_j - 1$ (for more details see Section 3.5.2 and Appendix A.4 of Chapter 3).

fixed we can directly compute the SNR by $SNR = 2^{capacity} - 1$ [136]. Back to our case, for known data rate $\tilde{q}_j\left(F, T_j^{\max}, \lambda_j\right)$, we can compute the corresponding minimum power $P_j^{\min}$ of each SU by [179]

$$P_j^{\min} \cong 2^{\frac{N_C}{BW} \cdot \tilde{q}_j\left(F, T_j^{\max}, \lambda_j\right)} - 1. \tag{5.37}$$

Equation (5.37) is not a cross-layer constraint but expresses our scheduler's perception about how much minimum power each SU requires based only on the QSI. To define a cross-layer constraint with properties of both (5.27) and (5.25) we can consider the QoS-driven power constraint (5.25), with $P_j^{\min}$ to be computed by (5.37).

We remark that relevant studies [34], [37], [38], [39], [42], [43], [50], [51], [52], [53], [54], [55], [149], [160], [161], [162], [173], [175] do not present analysis for the computation of the minimum required power $P_j^{\min}$. In fact, it is frequently assumed that $P_j^{\min}$ is announced to the BS through uplink channels. However, as next generation CR networking requires integrated proposals that meet reality, in contemporary designs $P_j^{\min}$ should be defined by mans of final formulas. In contrary to existing work, we achieve to correlate the QoS and transmission interference constraints and thanks to our queue modelling to derive a specific formula that computes the minimum required power $P_j^{\min}$ of each SU j.

5.5.3 Reformulation of the S-NBS-based Cross-Layer Optimization Problem

Considering the new definition of the utility function $\mathcal{U}_j$ of SU j in (5.29) of *Theorem 5.4* along with the correlation condition (5.36), we can reformulate the S-NBS cross-layer optimization problem (5.20) - (5.28) as follows.

Find optimal subcarrier and transmitting power resource allocation policies $\mathcal{S}\left[\hat{\mathcal{H}},\mathcal{Q},\mathcal{M}\right]$ and $\mathcal{P}\left[\hat{\mathcal{H}},\mathcal{Q},\mathcal{M}\right]$, respectively

such that:

$$\max_{\tilde{s}_{ij},\tilde{p}_{ij}} E\left[\sum_{j=1}^{K}\ln\left(\sum_{i=1}^{N_C}\left(1-\mathcal{P}_{app}\right)\cdot\tilde{s}_{ij}\cdot\log_2\left(1+\frac{\tilde{h}_{ij}\tilde{p}_{ij}\sigma_h^2}{\tilde{s}_{ij}}\cdot\mathcal{F}^{-1}_{\left(\frac{|\hat{h}_{ij}|^2}{\sigma_h^2}\right)_2}\left(\mathcal{P}_{app}\right)\right)-\left(\tilde{q}_j\left(F,T_j^{\max},\lambda_j\right)-1\right)\right)\right] \tag{5.38}$$

subject to:

$$\tilde{s}_{ij}\in(0,1], \quad \forall i,j, \tag{5.39}$$

$$\sum_{j=1}^{K}\tilde{s}_{ij}\le 1, \quad \forall i, \tag{5.40}$$

$$\tilde{p}_{ij}\ge 0, \quad \forall i,j, \tag{5.41}$$

$$E\left[\sum_{i=1}^{N_C}\tilde{p}_{ij}\right]\le P_j^{\max}, \quad \forall j, \tag{5.42}$$

$$E\left[\sum_{i=1}^{N_C}\left(\tilde{p}_{ij}\left|\hat{h}_{ij}\right|^2\right)\right]\ge P_j^{\min}, \quad \forall j, \tag{5.43}$$

$$E\left[\frac{1}{N_C}\sum_{j=1}^{K}\sum_{i=1}^{N_C}\tilde{p}_{ij}\right]\le P_{TOTAL} \tag{5.44}$$

In the S-NBS cross-layer optimization problem (5.38) - (5.44), the cost function in (5.38) has been reformulated according to the outage condition (5.28) of the S-NBS cross-layer optimization problem (5.20) - (5.28) considering the worst case scenario of the correlation condition in (5.36), e.g., accounting the maximum minimum utility u_j^0 of user j given by $u_j^0=\tilde{q}_j\left(F,T_j^{\max},\lambda_j\right)-1$. Moreover, the subcarrier and power constraints (5.39) - (5.44) are the same with constraints (5.21) - (5.26) of the S-NBS cross-layer optimization problem (5.20) - (5.28), respectively, with the difference that the minimum power $P_j^{\min}$ in the new constraint (5.42) is computed by (5.37).

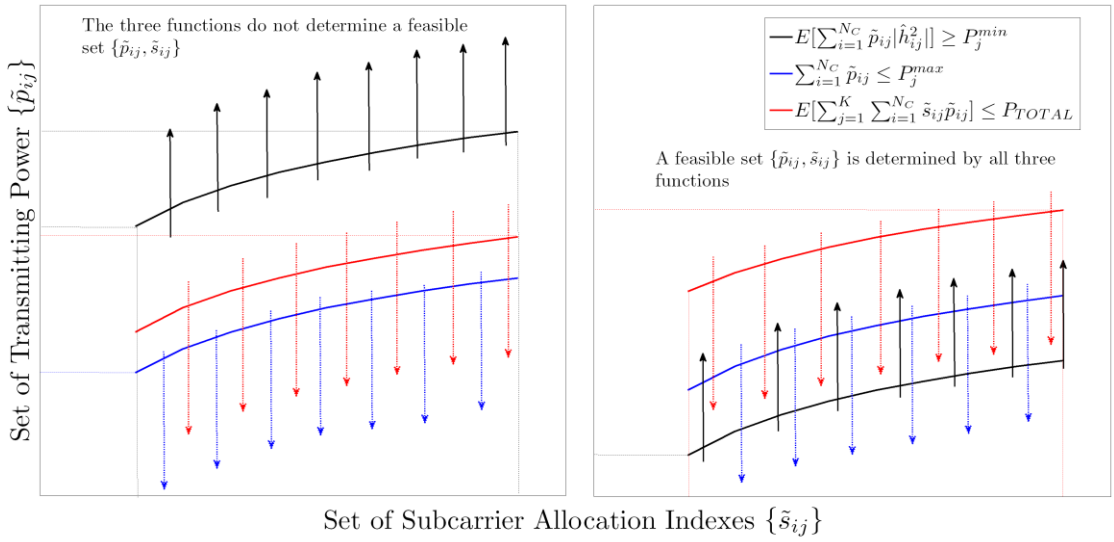

Figure 5.2 – Example regarding the validity of convex sets determined by multiple functions. In the left figure the feasible set $\left(\tilde{s}_{ij}, \tilde{p}_{ij}\right)$ that satisfies all functions is an empty set. In the right figure the set $\left(\tilde{s}_{ij}, \tilde{p}_{ij}\right)$ is non-empty as the variables $\tilde{s}_{ij}$ and $\tilde{p}_{ij}$ are determined in the feasible space that the three functions define.

Let us now examine the convexity of the S-NBS cross-layer optimization problem (5.38) - (5.44). With a quick look, the problem (5.38) - (5.44) seems to be convex. However, the set $\left(\tilde{s}_{ij}, \tilde{p}_{ij}\right)$ determined by all constraints may not be feasible. The reason is the power constraint (5.43), where its inequality sign is opposite from constraints (5.42) and (5.44). Hence, it is not ensured that we can always determine a feasible set $\left(\tilde{s}_{ij}, \tilde{p}_{ij}\right)$ that satisfies all three constraints since there may be instances, where $P_j^{\min}$ is larger than P_{TOTAL} and $P_j^{\max}$. To be more precise, we illustrate a simple example in Figure 5.2[70]. For this reason we need to obtain a feasibility condition for the S-NBS cross-layer optimization problem (5.38) - (5.44).

[70] The graphs illustrated in Figure 5.2 do not represent the real behaviour of the functions (5.42), (5.43) and (5.44) but are used only to explain the issue on the feasibility of the determined set $\left(\tilde{s}_{ij}, \tilde{p}_{ij}\right)$.

Proposition 5.1 - Given the subcarrier time-sharing factor $\tilde{s}_{ij} \in (0,1]$ and the new power transmission variable $\tilde{p}_{ij} = \tilde{s}_{ij} p_{ij}$, the S-NBS cross-layer optimization problem (5.38) - (5.44) is a convex optimization problem over convex set $\left(\tilde{s}_{ij}, \tilde{p}_{ij}\right)$ and the convex set $\left(\tilde{s}_{ij}, \tilde{p}_{ij}\right)$ is non-empty if and only if

$$\min\left\{\max\left\{E\left[\left|\hat{h}_{ij}\right|^2\right]\right\}\right\} \geq \frac{\sum_{j=1}^{K} P_j^{\min}}{\min\left(P_{TOTAL}, \sum_{j=1}^{K} P_j^{\max}\right)}. \tag{5.45}$$

Proof - The proof of *Proposition 5.1* is presented in Appendix C.3. ■

The feasibility condition (5.45) ensures that all constraints of the S-NBS cross-layer optimization problem (5.38) - (5.44) can determine a convex set $\left(\tilde{s}_{ij}, \tilde{p}_{ij}\right)$, which is non-empty. However, examining (5.45) an argument could be raised as it is not clear yet if (5.45) makes the constraint on the total transmitting power (5.44) irrelevant to the S-NBS cross-layer optimization problem (5.38) - (5.44). To clarify this issue we provide the following Proposition.

Proposition 5.2 - Given the feasibility condition (5.45), the constraint on the total transmitting power (5.44) is not redundant to the S-NBS cross-layer optimization problem (5.38) - (5.44).

Proof - The proof of *Proposition 5.2* is presented in Appendix C.3. ■

To the best of our knowledge, studies in the relevant literature do not derive such feasibility conditions [34], [38], [39], [37], [42], [43], [50], [51], [52], [53], [54], [55], [149], [160], [161], [162], [173], [175]. In those cases, authors generally assume that the minimum power $P_j^{\min}$ required to satisfy the QoS requirements of a SU is always smaller than, e.g., the minimum power $P_j^{\max}$ a SU requires to avoid interference. However, such assumptions are not pragmatic since in reality a SU may require more power than $P_j^{\max}$ to satisfy its minimum requirements and consequently in those cases the optimization problems are not feasible. In any case, a clear view on system's parameters is always convenient.

In *Proposition 5.1* we show that the S-NBS cross-layer optimization problem (5.38) - (5.44) has a unique global optimal solution, which can be obtained in polynomial time. In the following Section, we present the optimal resource allocation strategies approaching their solution concept with a new scope to outcome iteration-independent and power-efficient policies.

5.6 Convex Optimization-based Game Theoretic Optimal Allocation Strategies for CR Systems in Compliance with the S-NBS Principle

In this Section, we initialize convex optimization to derive the optimal solutions of the S-NBS cross-layer problem (5.38) - (5.44).

As we consider subcarrier time-sharing relaxation, the optimal time-sharing subcarrier allocation factor $\tilde{s}_{ij}^{*}$ is a real number indicating the faction of time that subcarrier i requires to transmit an amount of information for SU j [140]. Hence, we can directly define the optimal time-sharing subcarrier allocation factor $\tilde{s}_{ij}^{*}$ of SU j subcarrier i based on the following Theorem.

Theorem 5.5 - Given the imperfect channel realization $\hat{h}_{ij}$, the optimal subcarrier allocation policy $\boldsymbol{S}^{*}\left[\hat{h}_{ij}\right]=\left[\tilde{s}_{ij}^{*}\right]$ has individual matrix elements the S-NBS-based optimal time-sharing subcarrier allocation factor $\tilde{s}_{ij}^{*}$ of SU j on subcarrier i given by

$$\tilde{s}_{ij}^{*}=\mathcal{F}_{ij}^{-1}\left(\kappa_{i}^{*}\right). \tag{5.46}$$

The function $\mathcal{F}_{ij}^{-1}(\cdot)$ is the inverse function of $\mathcal{F}_{ij}(\cdot)$ in (5.54), which represents the first derivative of the utility function $\mathcal{U}_{j}$ of SU j over the variable κ_{i}^{*}, κ_{i}^{*} is the optimal LM related with the subcarrier allocation constraint (5.40) given by $\kappa_{i}^{*}=\mathcal{X}^{-1}(1)$ and the function $\mathcal{X}^{-1}(\cdot)$ is the inverse function of the function $\mathcal{X}(\cdot)$ given by $\mathcal{X}(\cdot)\equiv\sum_{j=1}^{K}\mathcal{F}_{ij}^{-1}(\cdot)$.

Proof - The proof of *Theorem 5.5* is presented in Appendix C.4. ■

To define the optimal subcarrier index $\tilde{s}_{ij}^{*}$ in (5.46), we must firstly determine the function $\mathcal{F}_{ij}^{-1}\left(\kappa_i^{*}\right)$. However, the function $\mathcal{F}_{ij}^{-1}\left(\kappa_i^{*}\right)$ cannot be yet defined as the optimal transmitting power $\tilde{p}_{ij}^{*}$ is still unknown. To define the function $\mathcal{F}_{ij}^{-1}\left(\kappa_i^{*}\right)$, we can assume that an amount of power, e.g., $\tilde{p}_{ij}^{*} = P_{TOTAL} / \left(BW \cdot N_C\right)$, is uniformly allocated among the N_C subcarriers. Upon applying uniform transmitting power allocation, we can establish from (5.46) the optimal subcarrier allocation matrix $\boldsymbol{S}^{*}\left[\hat{h}_{ij}\right]$ with elements the optimal subcarrier allocation indexes $\tilde{s}_{ij}^{*}$ to indicate, which subcarriers are in good conditions and which are not. For example, by allocating the same amount of power among all subcarriers and if subcarrier i is in better conditions than subcarrier i' then subcarrier i should require less time to transfer the same amount of information than subcarrier i'. Hence, their optimal subcarrier allocation indexes would differ, e.g., subcarrier i should have larger optimal subcarrier allocation index $\tilde{s}_{ij}^{*}$ than subcarrier i', e.g., $\tilde{s}_{ij}^{*} < \tilde{s}_{i'j}^{*}$. We remark that the chance of each optimal subcarrier allocation index $\tilde{s}_{ij}^{*}$ to be the same with another to be equal to zero (see Appendix C.4).

Accounting the optimal subcarrier allocation matrix $\boldsymbol{S}^{*}\left[\hat{h}_{ij}\right]$ given in *Theorem 5.5* we can determine the optimal transmitting power allocation policy as below.

Theorem 5.6 - Given the imperfect channel realization $\hat{h}_{ij}$ and the optimal subcarrier allocation matrix $\boldsymbol{S}^{*}\left[\hat{h}_{ij}\right]$, the optimal transmitting power allocation policy $\mathcal{P}^{*}\left[\hat{h}_{ij}\right] = \left[\tilde{p}_{ij}^{*}\right]$ has individual matrix elements the optimal instantaneous transmitting power $\tilde{p}_{ij}^{*}$ of SU j on subcarrier i, which are always positive and are given by

$$\tilde{p}_{ij}^{*}=\frac{\tilde{s}_{ij}^{*}}{\hbar_{ij}\sigma_h^2\cdot\mathcal{F}^{-1}_{\left(\left|\hat{h}_{ij}\right|^2/\sigma_h^2\right)_2}\left(\mathcal{P}_{app}\right)}\left(2^{\frac{\left(\tilde{q}_j\left(F,T_j^{\max},\lambda_j\right)-1\right)}{\tilde{s}_{ij}^{*}\left(1-\mathcal{P}_{app}\right)}}\cdot\exp\left(W\left(\ln\left(2^{\frac{\hbar_{ij}\sigma_h^2\cdot\mathcal{F}^{-1}_{\left(\frac{\left|\hat{h}_{ij}\right|^2}{\sigma_h^2}\right)_2}\left(\mathcal{P}_{app}\right)}{\ln 2\cdot\tilde{s}_{ij}^{*}\cdot\left(\frac{1}{N_F}\vartheta^{*}+\xi_j^{*}-\iota_j^{*}\left|\hat{h}_{ij}\right|^2\right)\cdot 2^{\frac{\left(\tilde{q}_j\left(F,T_j^{\max},\lambda_j\right)-1\right)}{\tilde{s}_{ij}^{*}\left(1-\mathcal{P}_{app}\right)}}}}\right)\right)\right)-1\right) \tag{5.47}$$

where ξ_j^{*}, ϑ^{*} and ι_j^{*} are the optimal LMs with the power-driven interference cancelation constraint (5.42), the power constraint (5.44) and the power-driven QoS constraint (5.43) for SUs, respectively, while the notation $W(\cdot)$ denotes the Lambert-*W* function [158]. In addition, the optimal transmitting power allocation policy $\mathcal{P}^{*}\left[\hat{h}_{ij}\right]$ is decoupled among the N_C OFDM subcarriers to obtain the optimal SU denoted by $\jmath^{*}$ with the following searching process, which is always feasible.

$$\text{For } i=1 \text{ to } N_C \text{ find } \jmath^{*}=\arg\min \tilde{p}_{ij}^{*} \text{ and set } \tilde{p}_{ij}^{*}=\begin{cases}\tilde{p}_{ij}^{*}, \text{ if } j=\jmath^{*}\\ 0, \text{ otherwise}\end{cases}, \ \tilde{s}_{ij}^{*}=\begin{cases}\tilde{s}_{ij}^{*}, \text{ if } \tilde{p}_{ij}^{*}>0\\ 0, \text{ otherwise}\end{cases} \tag{5.48}$$

Proof - The proof of *Theorem 5.6* presented in Appendix C.5. ■

From *Theorem 5.6*, we establish the optimal transmitting power matrix $\boldsymbol{\mathcal{P}}^{*}\left[\hat{h}_{ij}\right]$, which can be perceived as an $N_C\times K$ map of various elements each one indicating the required by each SU power to transmit a fixed amount of information on each subcarrier. With the linear search in (5.48), we can easily choose the optimal SUs that require less transmitting power to be satisfied than others. We can also reformulate the optimal subcarrier allocation matrix $\boldsymbol{\mathcal{S}}^{*}\left[\hat{h}_{ij}\right]$ by setting the optimal time-sharing subcarrier allocation factor $\tilde{s}_{ij}^{*}$ in (5.46) equal to zero for the non-optimal SUs. Later we will see that our linear search in (5.48) enhances system's power efficiency.

Moreover, having defined the optimal subcarrier allocation matrix $\boldsymbol{\mathcal{S}}^*\left[\hat{h}_{ij}\right]$ and the optimal transmitting power allocation policy $\boldsymbol{\mathcal{P}}^*\left[\hat{h}_{ij}\right]$ in *Theorem 5.6*, we can define the optimal effective data rate allocation policy $\boldsymbol{\mathcal{R}}^*\left[\hat{h}_{ij}\right]$ as below.

Theorem 5.7 - Given the optimal transmitting power matrix $\boldsymbol{\mathcal{P}}^*\left[\hat{h}_{ij}\right]$ and the optimal subcarrier allocation policy $\boldsymbol{\mathcal{S}}^*\left[\hat{h}_{ij}\right]$ the optimal effective data rate allocation policy $\boldsymbol{\mathcal{R}}^*\left[\hat{h}_{ij}\right]$ has individual matrix elements the optimal effective data rate $\tilde{r}_{ij}^*$ of SU j on subcarrier i given by

$$\tilde{r}_{ij}^* = \left(1-\mathcal{P}_{app}\right)\cdot\tilde{s}_{ij}\cdot\log_2\left(2^{\frac{\left(\tilde{q}_j\left(F,T_j^{\max},\lambda_j\right)-1\right)}{\tilde{s}_{ij}^*\left(1-\mathcal{P}_{app}\right)}}\cdot\exp\left(W\left(\ln\left(2^{\frac{\hbar_{ij}\sigma_{\hat{h}}^2\cdot F^{-1}\left(\frac{|\hat{h}_{ij}|^2}{\sigma_{\hat{h}}^2}\right)_2\left(\mathcal{P}_{app}\right)}{\ln 2\cdot\tilde{s}_{ij}^*\cdot\left(\frac{1}{N_F}\vartheta^*+\xi_j^*-\iota_j^*\left|\hat{h}_{ij}\right|^2\right)\cdot 2^{\frac{\left(\tilde{q}_j\left(F,T_j^{\max},\lambda_j\right)-1\right)}{\tilde{s}_{ij}^*\left(1-\mathcal{P}_{app}\right)}}}}\right)\right)\right)\right). \quad (5.49)$$

Proof - The optimal effective data rate $\tilde{r}_{ij}^*$ of SU j on subcarrier i in (5.49) is derived with direct substitution of the optimal time-sharing subcarrier allocation factor $\tilde{s}_{ij}^*$ in (5.46) and the optimal instantaneous transmitting power $\tilde{p}_{ij}^*$ in (5.48) into the effective data rate $\tilde{r}_{ij}$ of SU j on subcarrier i in (5.30). This completes the proof of *Theorem 5.7*. ■

In the next Sections, we discuss the implementation process of the optimal allocation policies presented in *Theorem 5.6* and *Theorem 5.7* as well as some specifications of the S-NBS-CR.

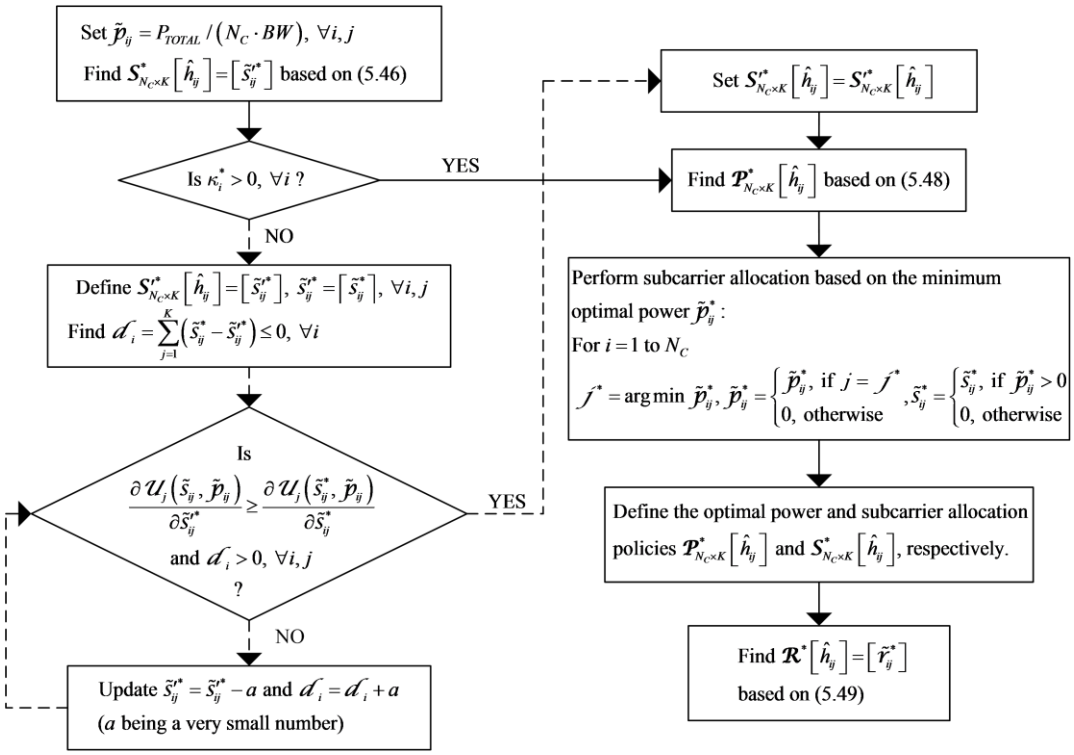

Figure 5.3 - Block diagram of the S-NBS optimal cross-layer resource scheduling for CR systems based on the proposed iterative-independent methodology.

5.6.1 Implementation Process of the S-NBS-CR Optimal Allocation Policies

The block diagram of our cross-layer iterative-independent optimal scheduling is shown in Figure 5.3. The optimal transmitting power allocation policy in *Theorem 5.6* has the form of multi-user water-filling strategy with power water-level of each SU j to be given by $1/\left(\frac{1}{N_F}\vartheta^* + \xi^*_j - \iota^*_j \left|\hat{h}_{ij}\right|^2\right)$. The optimal LMs ϑ^*, ξ^*_j and ι^*_j can be perceived as the resource scheduling calibrators of the system, e.g., the SUs that participate in the S-NBS game with urgent packets to transmit have higher LM ι^*_j than SUs with non-urgent packets. However, those SUs that may interfere with PUs have lower LM ξ^*_j than SUs with better interference

cancelation conditions. Hence, the power water-level $1/\left(\frac{1}{N_F}\vartheta^* + \xi_j^* - \iota_j^*\left|\hat{h}_{ij}\right|^2\right)$ of each SU is depended on the urgency and chance of interference with PUs, e.g., SUs with high urgency and better interference cancelation condition have higher water-level than SUs with non-urgent packets and bad interference conditions. Moreover, the optimal subcarrier allocation in can be interpreted as a policy, where a SU with high urgency and good interference cancelation conditions (defined by the LMs ι_j^* and ξ_j^*, respectively) has higher chance of being allocated with subcarriers, while SUs with the same urgency level and position (the LMs ι_j^* and ξ_j^* are same for all SUs) have the same chance and subcarriers are fairly allocated to all users in the group according to the NBS principle. Later, from our simulations we will demonstrate that resource allocation fairness among SUs of same class and interference conditions is almost perfect, in contrary to many other proposals, where resource fairness is sufficiently lower [37], [42], [43], [53] [149], [163], [164], [165], [166], [167], [168], [169], [170], [171], [172], [175]. Finally, as shown in Figure 5.3, we develop a sub-mechanism to ensure that the optimal LMs ν_i^* s are always positive. However, we report that such process is extremely rare to be utilized as they are only needed in cases, where allocation is infeasible due to insufficient resources.

Let us now show that he proposed S-NBS-CR is iteration-independent and inspect its total computational complexity. From the KKT conditions (5.86) - (5.104), the differentiations of the Lagrangian function $\mathcal{L}\left(\tilde{s}_{ij}, \tilde{p}_{ij}, \xi_j, \vartheta, \kappa_i, \iota_j\right)$ in (5.85) over the LMs $\{\xi_j\}$, ϑ and $\{\iota_j\}$ yield the optimal LMs $\{\xi_j^*\}$, ϑ^* and $\{\iota_j^*\}$, respectively to be global maxima. For example, from the KKT condition (5.88), the differentiation of $\mathcal{L}\left(\tilde{s}_{ij}, \tilde{p}_{ij}, \xi_j, \vartheta, \kappa_i, \iota_j\right)$ over ξ_j yields that $\sum_{i=1}^{N_C} \tilde{p}_{ij} = P_j^{\max}$. With substitution of the optimal instantaneous transmitting power $\tilde{p}_{ij}^*$ in (5.48) we get that

$$\sum_{i=1}^{N_C} \underbrace{\frac{\tilde{s}_{ij}^*}{\hbar_{ij}\sigma_h^2 \cdot \mathbb{F}^{-1}_{\left(\left|\hat{h}_{ij}\right|^2/\sigma_h^2\right)_2}\left(\mathcal{P}_{app}\right)}}_{\mathcal{A}_{ij}} \left(\underbrace{2^{\frac{\left(\tilde{q}_j\left(F,T_j^{\max},\lambda_j\right)-1\right)}{\tilde{s}_{ij}^*\left(1-\mathcal{P}_{app}\right)}}}_{\mathcal{B}_{ij}} \cdot \exp\left(W\left(\ln\left(\underbrace{2^{\frac{\hbar_{ij}\sigma_h^2 \cdot \mathbb{F}^{-1}_{\left(\left|\hat{h}_{ij}\right|^2/\sigma_h^2\right)_2}\left(\mathcal{P}_{app}\right)}{\ln 2 \cdot \tilde{s}_{ij}^* \cdot \left(\frac{1}{N_F}\vartheta^* + \xi_j^* - \iota_j^*\left|\hat{h}_{ij}\right|^2\right) \cdot 2^{\frac{\left(\tilde{q}_j\left(F,T_j^{\max},\lambda_j\right)-1\right)}{\tilde{s}_{ij}^*\left(1-\mathcal{P}_{app}\right)}}}}}_{\mathcal{C}_{ij}} \right) \right) \right) - 1 \right) = P_j^{\max} \tag{5.50}$$

If we set $\mathcal{A}_{ij} = \tilde{s}_{ij}^* / \hbar_{ij}\sigma_h^2 \cdot \mathbb{F}^{-1}_{\left(\left|\hat{h}_{ij}\right|^2/\sigma_h^2\right)_2}\left(\mathcal{P}_{app}\right)$, $\mathcal{B}_{ij} = \left(\tilde{q}_j\left(F,T_j^{\max},\lambda_j\right)-1\right) / \tilde{s}_{ij}^*\left(1-\mathcal{P}_{app}\right)$,

$\mathcal{C}_{ij} = \hbar_{ij}\sigma_h^2 \cdot \mathbb{F}^{-1}_{\left(\left|\hat{h}_{ij}\right|^2/\sigma_h^2\right)_2}\left(\mathcal{P}_{app}\right) / \ln 2 \cdot \tilde{s}_{ij}^* \cdot \left(\frac{1}{N_F}\vartheta^* + \xi_j^* - \iota_j^*\left|\hat{h}_{ij}\right|^2\right) \cdot 2^{\mathcal{B}_{ij}}$ and

$\mathcal{D}_{ij} = 2^{\mathcal{B}_{ij}} \cdot \exp\left(W\left(\ln\left(\mathcal{C}_{ij}\right)\right)\right)$ then (5.50) becomes $\sum_{i=1}^{N_C}\left(\mathcal{A}_{ij} \cdot \left(\mathcal{D}_{ij} - 1\right)\right) - P_j^{\max} = 0$, which can be written as

$$\sum_{i=1}^{N_C}\left(\mathcal{A}_{ij} \cdot \mathcal{D}_{ij}\right) = \sum_{i=1}^{N_C}\left(\frac{P_j^{\max}}{N_C} + \mathcal{A}_{ij}\right). \tag{5.51}$$

We observe that the right side of (5.51) is known and it can be resolved into a single constant, e.g., $\mathcal{Y} = \sum_{i=1}^{N_C}\left(\left(P_j^{\max} / N_C\right) + A_{ij}\right)$. Hence, we can write (5.51) as

$$\sum_{i=1}^{N_C} \mathcal{A}_{ij} \cdot \mathcal{D}_{ij} = \mathcal{Y}. \tag{5.52}$$

Since $\mathcal{A}_{ij}$, $\mathcal{B}_{ij}$, $\mathcal{C}_{ij}$ and $\mathcal{D}_{ij}$ are all non-negative integers, the function (5.52) is monotonic, meaning that it has at most K solutions on the optimal LMs ξ_j^*s, $j \in K$. Hence,

to find each ξ_j^* we need to solve a monotonic equation, which involves $2K$ unknown variables, e.g., the rest of the $K-1$ unknown ξ_j^*s, K unknown ι_j^*s, plus one unknown ϑ^*[71].

From the KKT condition (5.91) we can likewise show that each optimal LM ι_j^* has its own monotonic function, which also involves $2K$ unknown variables, e.g., the rest of $K-1$ unknown ι_j^*s, K unknown ξ_j^*s, plus the optimal LM ϑ^*. In addition, the optimal LM ϑ^* can be found through solving a monotonic function of $2K$ unknown variables, e.g., K unknown ξ_j^*s and K unknown ι_j^*s. Consequently, we build a system with $2K+1$ correlated monotonic equations, K for ξ_j^*s, K for ι_j^*s and one more equation for ϑ^*. In other words, we can obtain the LMs ξ_j^*s, ι_j^*s and ϑ^* through solving $2K+1$ equations at once without performing iteration-dependent searches. Hence, the introduced scheme is iteration-independent and its total actual complexity is $\mathcal{O}\left(\left(N_F \times K\right)+2K+1\right)$, e.g., $\mathcal{O}\left(N_F \times K\right)$ linear search of the optimal user j^* in (5.48) plus $\mathcal{O}\left(2K+1\right)$ from the system of equations. We recall from Section 3.6.3 of Chapter 3 that iteration-dependent schemes [37], [13], [42], [43] (including our PE-AETS presented in Chapter 3) have complexity of $\mathcal{O}\left(N_F \times K\right)$ plus an extra complexity of $\mathcal{O}\left(l\left[N_F \times K \times \Delta_{\{\xi_j^*\}}+\left(K \times \Delta_{\mu^*}-1\right)\right]\right)$ due to their root-finding mechanism. Hence, iteration-dependent schemes have $\mathcal{O}\left(N_F \times K^2 \times l\left[N_F \times \Delta_{\{\xi_j^*\}}+\left(\Delta_{\mu^*}-1\right)\right]\right)$ complexity in total, where l is the number of loops, $\Delta_{\{\xi_j^*\}}$ is the number of iterations required in one loop to find ξ_j^* and $\Delta_{\mu'^*}$ is the number of iterations required to find μ'^*. Apparently, such complexity is huge compared to our proposal.

[71] We recall that the optimal subcarrier allocation indexes $\tilde{s}_{ij}^*$s have been already defined in *Theorem 5.5*.

In addition, as we do not utilize iteration-dependent mechanisms, it is obvious that the convergence of our scheme to optimal solutions is guaranteed. In conclusion, our cross-layer design methodology allows us to design iteration-independent schemes that converge to S-NBS-based optimal solutions much more rapid than the traditional iteration-dependent approach ensuring that way better real-time system operation.

5.6.2 Specifications on S-NBS-CR Scheduling

The proposed S-NBS-CR scheme has similar specifications with our previously presented schedulers PE-AETS and A-NBS scheme on the below six topics.

- Feasibility of its optimal policy (Section 4.6.2, Chapter 4),
- power-efficiency (Section 4.6.2, Chapter 4),
- asymptotic performance gain due to multi-user diversity (Section 4.6.2, Chapter 4),
- impact of imperfect channel on the service time of each packet (Section 3.6.4, Chapter 3),
- packet multiplexing process (Section 3.6.4, Chapter 3) and
- accuracy of its optimal policy (Section 3.6.4, Chapter 3).

Due to space limitations, we omit details, referring the reader to study the corresponding Sections to each topic, where we have thoroughly presented these subject matters.

5.7 Simulations

In this Section, we present simulations to examine the performance of the proposed S-NBS-CR scheduler in comparison with the Error-Inconsiderate S-NBS-CR (EIS-NBS-CR) developed in our previous work [176], the Error-Considerate opportunistic Scheduler (ECS-CR) [17], [24], [56], the Error-Inconsiderate Power-NBS-based Scheduler for CR networks (EIP-NBS-CR) adopted in [37], [42], [43], [149], [175], the Error-Inconsiderate Fixed power and channel Assignment Scheduling scenario (EIFAS-CR) utilised for CR networks in [27],

	PUs	SU_1	SU_2	SU_3
Poission arrival rate λ_j (*packets/time slot*)	1.22	0.4	0.15	0.225
Min. delay requirement $T_j^{\max}$ (*time slot*)	2	4	8	2
Min. delay requirement $T_j^{\max}$ (*sec*)	0.004	0.008	0.016	0.004
Min. equivalent rate $\tilde{q}_j\left(F, T_j^{\max}, \lambda_j\right)$ (*bits/sec/Hz*)	35.80	12.50	4.94	3.75
Min. power $P_j^{\min}$ (*mWatt*)	-	3.5	1.4	1
Min. power $P_j^{\min}$ (*dB*)		5.4	1.46	0
Max. min. utility of each SU to join the S-NBS game u_j^0 (*bits/sec/Hz*)	-	11.50	3.94	2.75

Table 5.1 - Minimum requirements of each heterogeneous user, which participates in the CR system.

[37], [60] and the Max-Min fairness scheduler for CR networks (MM-CR) adopted in [32], [151], [152].

5.7.1 Simulation Modelling

We consider a prototype single-cell CR system consisted by two networks: the primary and the secondary. The total channel bandwidth of the secondary network is $BW = 2.56\,MHz$ and it is distributed equally among $N_F = 1024$ subcarriers, each one having five independent paths, e.g., $\Theta = 5$ [72]. We specify three different classes of SUs denoted by $\left(SU_1, SU_2, SU_3\right)$, with the QoS requirements of each class to be characterized by the tuple structure

[72] The total channel bandwidth of $BW = 2.56\,MHz$ has been set based on the number of the considered subcarriers, i.e., by myltiplying the 1024 subcarriers with the $2500Hz$ bandwidth of each subcarrier, e.g., $2500Hz \times 1024 = 2.56MHz$. The total channel bandwidth may not be practicable but it facilitates our simulation comparisons as it is consistent with simulation models used in relevant works, e.g., [17], [24], [27], [32], [37], [42], [43], [56], [60], [149], [151], [152], [175]. In addition, such total channel bandwidth has been derived based on the realistic assumption that the individual channel bandwidth is $2500Hz$, which corresponds to IEEE 802.12 and IEEE 802.11 standard channel settings [2], [5], [144].

$(\boldsymbol{\lambda}, \mathbf{T}, \mathbf{F}) = ((0.4, 4, 125), (0.15, 8, 125), (0.225, 2, 125))$. In the primary network, there exist five PUs that belong to one class, e.g., PU_1, characterized by the tuple $(\lambda_j, T_j^{\max}, F) = (1.22, 2, 125)$. From the tuple of each user that participates in the CR system we clarify in Table 5.1 each user's minimum requirements, in terms of average approximated effective data rate. Furthermore, we set the scheduling slot duration to $t_s = 2\,msec$ and we assume that each packet has size of $F = 125\,bits$. We assume the adaptive modulator operates under $\mathcal{BER}_{ij} = 4.4626 \times 10^{-5}$ and the noise variance equals to one, e.g., $\sigma_z^2 = 1$, (meaning that $\hbar_{ij} = 1$). In addition, all users suffer from 2*dB* path-loss, e.g., $PL_j = 2\,dB,\ \forall j$ [73]. To make our simulation model more realistic, we consider that all the heterogeneous users suffer signal path-loss from the BS. We remark that we keep consistency among comparisons between the examined schemes, by adopting identical channel, traffic and optimization conditions, i.e., all schedulers can handle delay constraints and are affected by the same imperfect channel and outage conditions. Also, we omit presenting the impact of the channel imperfectness on the channel-error-inconsiderate schemes EIS-NBS-CR, EIP-NBS-CR, EIOS-CR, EIFAS-CR and MM-CR as it is similar to our previously examined relative schemes studied in Appendix A.7 of Chapter 3 and Appendix B.7 of Chapter 4. The channel specifications have been set according to the type SUI-3 [144] channel model for pedestrian and vehicular mobility in urban enviroments as shown in Table 3.2 of Section 3.7.1 at Chapter 3. All simulations have been obtained through using computer software developed by us in MatLab.

[73] The signal path-loss PL_j of each SU j is computed by $PL_j = PL(d_0) + 10\varpi \log_{10}(d_j / d_0) + sd_{\sigma_{sd}^2}$ (in *dBm*), where $PL(d_0)$ is the reference path loss at a reference distance d_0, d_j is the distance of user j from the BS, ϖ is the path loss component and $sd_{\sigma_{sd}^2}$ is the Gaussian random variable for shadowing with standard deviation σ_{sd}^2 [134].

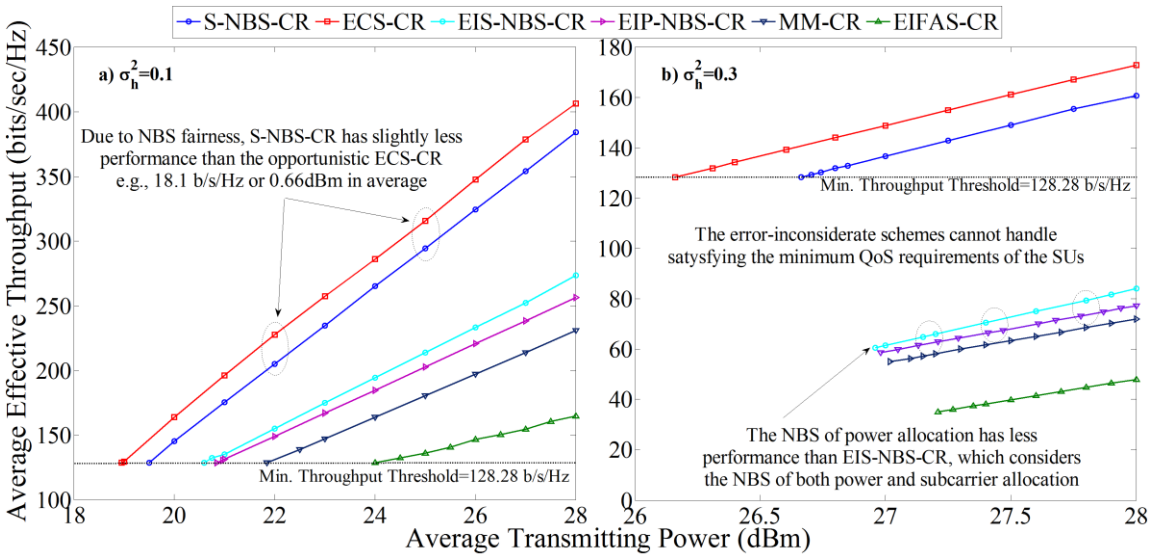

Figure 5.4 - Comparison regarding the power/throughput efficiency of S-NBS-CR: average effective throughput versus average transmitting power.

5.7.2 Simulation Results

We consider a CR system with $K=20$ heterogeneous SUs of classes $(SU_1, SU_2, SU_3)=(5,8,7)$ and $K'=5$ homogeneous PUs with parameters $P_{j'}^{PU}=10$ *mWatt* (10*dBm*), $N_0^{j'}=0.003\,mWatt$ (-25.2*dB*), $d_{j'}^{BS}=12\,m$, $d_{jj'}^{BS}=8\,m$, $\gamma_{PU}^{\min}=2\,mWatt$ (3.01*dBm*) and $\rho=2.5$ [74]. From equation (5.8) we can easily compute that the minimum power of each

[74] In our simulations we need to create critical system states, i.e., resource starvation, where the performance bounds of the proposed schemes can be easily examined. For example, in this Section we assume that $K=20$ SUs of classes $(SU_1, SU_2, SU_3)=(5,8,7)$ participate in the network. The reason is that according to the considered interference parameters, signal path loss settings, supplied power and minimum QoS requirements (128.27*bits/sec/Hz*), all schemes will burst to resource starvation states for large and realistic regions of channel uncertainties, distances between PUs and BS, and noise powers. This facilitates our examinations on the behaviour and interpretation of the results of each scheme and helps to obtain a clear view of their performance bounds under pragmatic considerations. In addition, the assumption $K=20$ SUs participate in the system is reasonable and complies with simulation setting used in [17], [24], [32], [43], [56], [60], [149], [152].

SU to avoid interference with PUs is $P_j^{\max} = 1.25\, mWatt$ $(0.96 dBm)$[75]. In Figure 5.4, we initially observe that the proposed S-NBS-CR has significantly higher power/throughput performance than other fairness-aware schemes. However, it is slightly outperformed by the opportunistic scheme ECS-CR, i.e., S-NBS-CR has 18.12*bits/sec/Hz* less throughput in average. This is something expected as NBS fairness decreases system's power/throughput efficiency by definition. Secondly, recalling the simulations in Section 4.7.2 of Chapter 4, we observe that the performance difference between ECS-CR and S-NBS-CR is larger than the performance difference between ECS-CR and S-NBS-CR. For example, in this simulation we have 18.12*bits/sec/Hz* less throughput performance than ECS-CR's, while the corresponding simulation in Figure 4.5 of Section 4.7.2 shows that the difference is only 5.76*bits/sec/Hz* in average. In other words, the performance difference between opportunistic and non-opportunistic scheduling is larger in CR systems than in non-CR systems. The physical meaning of this phenomenon is that CR systems operate opportunistically by their nature hence, pure-opportunistic schemes like ECS are favoured in such environments. Thirdly, we observe that EIS-NBS-CR performs better than EIP-NBS-CR. This means that the scheduling versatility of schemes, which consider the NBS of both power and subcarrier allocation is sufficiently higher than schemes, which deliberate the NBS of power only, i.e., [37], [42], [43], [149], [175]. Fourthly, it is obvious that Max-Min fairness is not as effective as NBS in CR systems since the MM-CR performs worse than EIS-NBS-CR and EIP-NBS-CR. Finally, it is evident that the error-inconsiderate schemes EIS-NBS-CR, EIP-NBS-CR, MM-CR and EIFAS-CR cannot satisfy the minimum QoS requirements of the SUs especially when the channel uncertainty is high, e.g., $\sigma_h^2 = 0.3$ in Figure 5.4b.

[75] One *dBm* is computed by the formula $dBmW = 10 \cdot \log_{10}\left(P\ /1\ \text{mWatt}\right)$, where P is the terminus power [93].

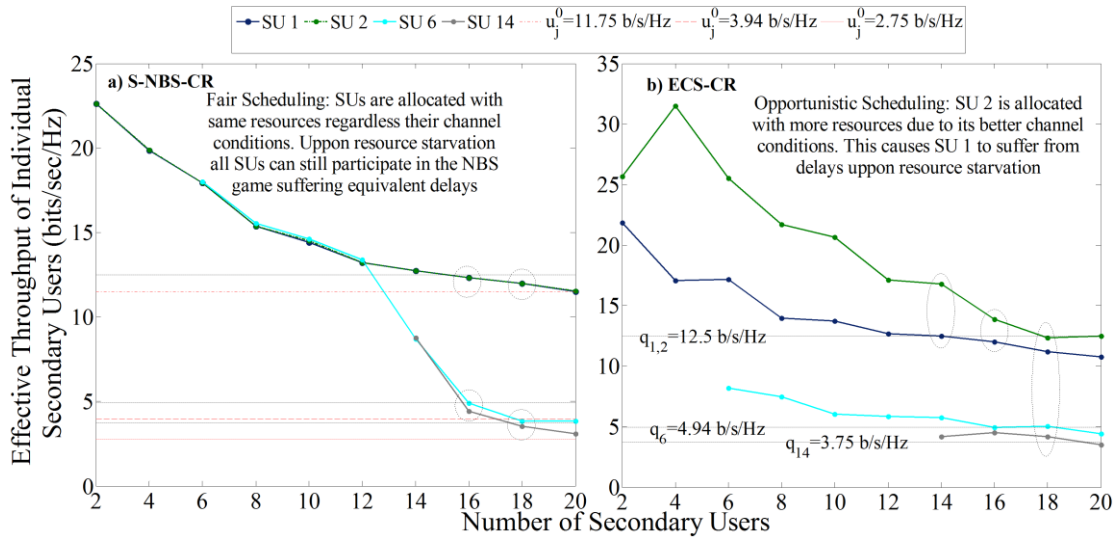

Figure 5.5 - Comparison regarding the QoS performance of S-NBS-CR: effective throughput of individual secondary users versus the number of secondary users.

Let us now gain a more microscopic view on the QoS performance of the error-considerate S-NBS-CR and ECS-CR. We illustrate in Figure 5.5 the effective throughput achieved by SUs 1, 2, 6 and 14 versus the number of SUs that join the CR system. For the purpose of investigation, the SU 2 is configured to always have a better channel condition than that of SUs 1, 6 and 14. In general, when the supplied power to the BS P_{TOTAL} is high enough it is expected that all four SUs to achieve more than their minimum required data rate. The more SUs entering the system, the higher power is required to meet their minimum QoS demands. Therefore, observing the performance at and beyond the boundary point after which the supplied power is not enough to accommodate all the SUs will clearly show how fairly each scheme treats the SUs Hence, supplying the BS with $P_{TOTAL} = 20\,dBm$ and considering average channel imperfectness, e.g., $\sigma_h^2 = 0.1$, we observe in Figure 5.5a that when the supplied power is enough, S-NBS-CR allocates almost perfectly fair resources among the SUs, i.e., when $2 \le K \le 16$ SUs 1, 2, 6 and 14 have almost the same throughput. When resource starvation occurs, i.e., $K \ge 17$, S-NBS-CR allocates more resources to the most demanded SUs, e.g., SUs 1 and 2, while it still keeps allocating fairly the resources among the less demanded SUs 6 and 14. When all SUs are considered, e.g., $K = 20$, although SUs 1, 2,

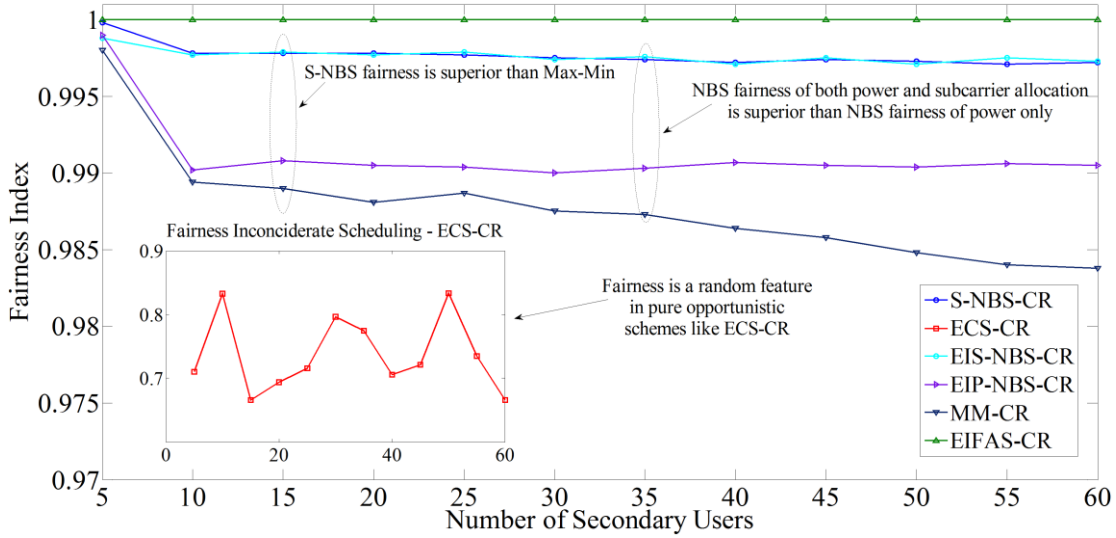

Figure 5.6 - Comparison regarding the fairness efficiency of S-NBS-CR: fairness index versus the number of secondary users.

6 and 14 are allocated with data rate slightly less than their minimum required $\tilde{q}_j$, they participate in the NBS game as they all have higher throughput than their minimum thresholds u_j^0s. On the other hand, Figure 5.5b shows that ECS-CR is rather unfair since it tends to assign most of the remaining resources to the SU with the best channel condition. When $2 \le K \le 18$, SU 2 always obtains higher data rate than SUs 1, 6 and 14 given it is in better channel condition than others. When resource starvation occurs, i.e., $K \ge 19$, SUs 1 and 14 are allocated lower data rate than their minimum requirement due to their worse channel conditions than CR users 2 and 6. Therefore, S-NBS-CR is shown to perform best in terms of fairness and QoS provision to the CR users.

The superiority of the S-NBS-CR in terms of fairness performance can be studied in Figure 5.6. More precisely, Figure 5.6 shows that both our schemes S-NBS-CR and EIS-NBS-CR attain higher fairness index (FI) than others. In fact, we show that our proposed methodology, which considers the NBS of both power and subcarrier allocation, delivers schemes that distribute resources more fairly than schedulers, which deliberate the NBS of power only, i.e., [37], [42], [43], [149], [175]. Moreover, we can again verify that considering NBS fairness is better than Max-Min, while the fixed subcarrier and power allocation in

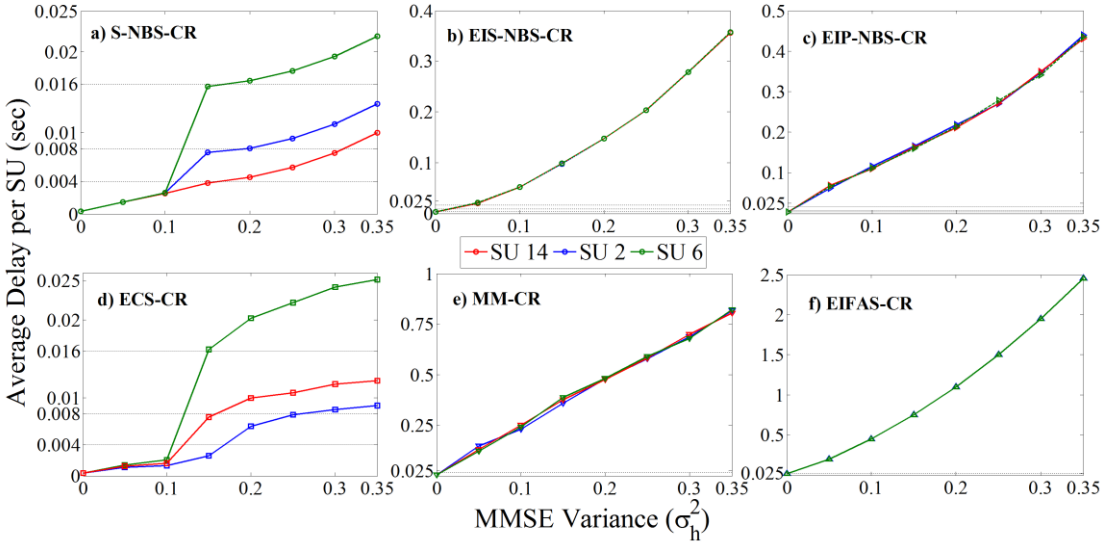

Figure 5.7 - Comparison regarding the QoS efficiency of S-NBS-CR: average delay per secondary user versus the MMSE variance σ_h^2.

EIFS-CR on one hand leads to perfect fairness but on the other hand, as shown in Figure 5.4, it significantly decreases the power/throughput performance. In addition, although ECS-CR's slightly higher performance than S-NBS-CR, it is evident that fairness in ECS-CR is a random feature.

Let us now examine the impact of fair resource distribution on the QoS provision of each scheme. We supply the BS with $P_{TOTAL} = 20\,dBm$ and we observe from Figure 5.7 that only S-NBS-CR and ECS-CR provide the required QoS to SUs 2, 6 and 14 up to certain channel imperfectness, i.e., $\sigma_h^2 = 0.15$. However, upon resource starvation, e.g., $\sigma_h^2 > 0.15$, S-NBS-CR distributes resources fairly meaning that all SUs suffer by the same delay of 3.35*msec* in average. In contrary, the opportunistic ESC-CR provides more resources to SU 2, who has been configured to have the best channel conditions among all SUs. Hence, ECS-CR scheduling provides several different delays to the SUs meaning that there are SUs who are served almost perfectly (e.g., SU 2 suffers by small delay of 0.47*msec* in average) but some others suffer by high delays (e.g., SUs 14 and 6 suffer by high delays of 4.03*msec* and 5.24*msec* in average, respectively). Consequently, although ECS-CR has better power/throughput performance than S-NBS-CR, in the latter case the QoS provision is more

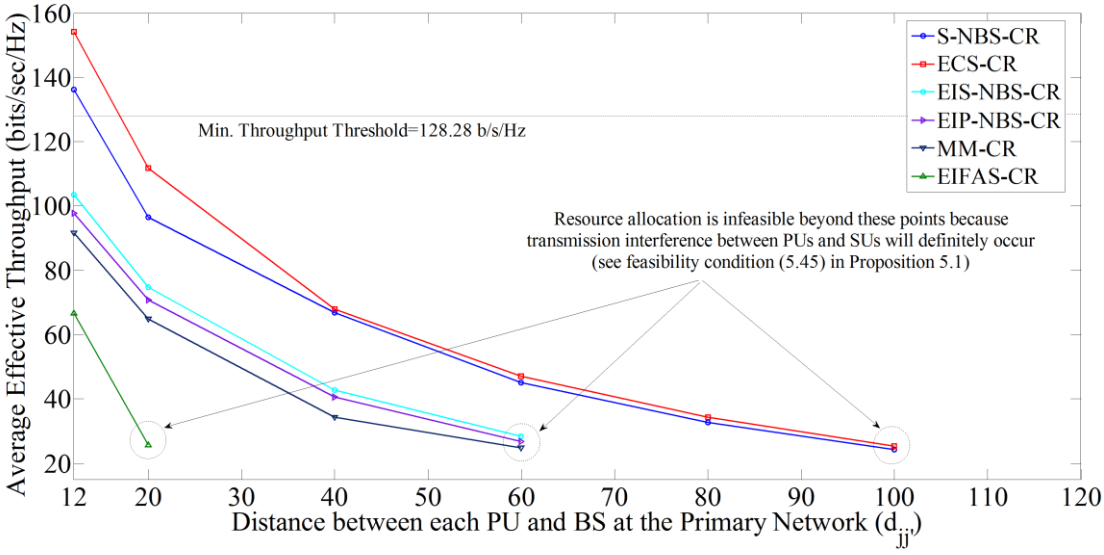

Figure 5.8 - Comparison regarding the impact of the primary users' conditions on the secondary network: average effective throughput versus the distance $d_{jj'}$ between primary users and the base station at the primary network.

guaranteed than in the former case. Moreover, the error-inconsiderate schemes cannot guarantee satisfying QoS as they provide extremely high delays from low to high channel uncertainty. Nevertheless, we can still observe that EIS-NBS-CR out performs EIP-NBS-CR, MM-CR and EIFAS-CR due to its increased NBS-based scheduling versatility. In conclusion, in Figure 5.7 we show that the overall QoS performance increases as wireless resources are being distributed more fairly to the system users.

We have not so far considered the impact of the PUs requirements and channel conditions on the secondary network. In Figure 5.8 we increase the distance between each PU from the BS decreasing that way the maximum interference power $P_j^{\max}$ tolerated by each PU. In other words, as the distance between PUs and BS at the primary network increases, the transmission interference between PUs and SUs is more imminent and thus, the scheduler at the secondary network requires more resources to satisfy the SUs. We supply the BS at the secondary network with $P_{TOTAL} = 20\,dBm$ and consider average channel imperfectness, e.g., $\sigma_h^2 = 0.1$. We observe that PUs' conditions remarkably affect the overall throughput of the secondary network. For example, none of the examined schedulers can satisfy the QoS

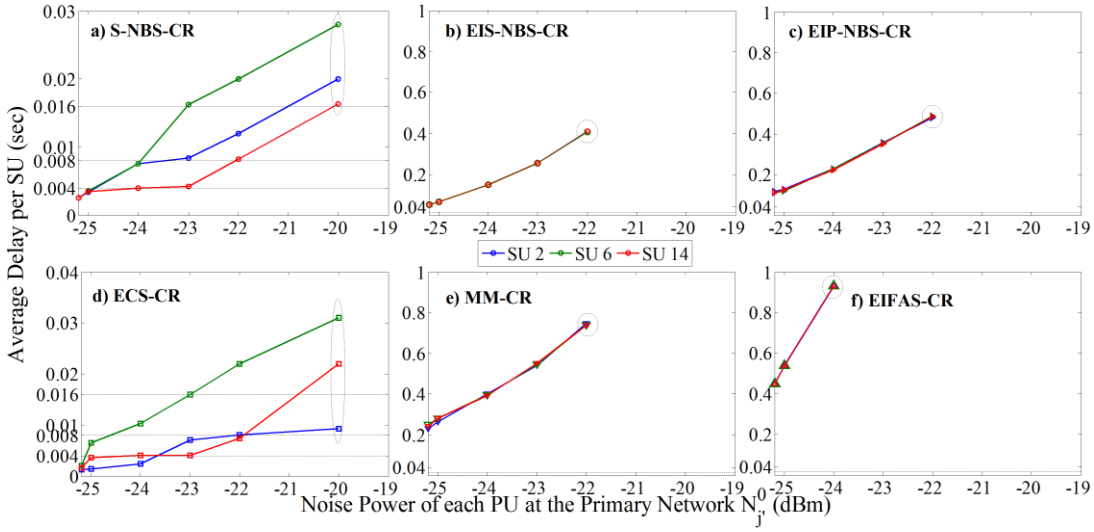

Figure 5.9 - Comparison regarding the impact of the primary users' conditions on the secondary network: average delay per secondary user versus the noise power $N_0^{j'}$ of the j'-th PU.

demands of SUs when the PUs move away from the BS in the primary network for more than 12*m*. Nevertheless, a notable phenomenon in this simulation is that beyond the distance of 140*m*, the resource allocation of all schemes is infeasible. The reason is that at that point the summation of the maximum interference power $P_j^{\max}$ of each SU j, e.g., $\sum_{j=1}^{K} P_j^{\max}$, is that small where the feasibility condition in (5.45) not satisfied and hence, the CR allocation policies are not valid. In other words, beyond the distance of 140*m*, CR scheduling is prohibited in the system because transmission interference between PUs and SUs will definitely occur. Consequently, in Figure 5.8 we show the importance of the introduced feasibility condition (5.45) in the wireless system, in contrary to other studies that do not examine such limitations [37], [42], [43], [149], [175].

Similar observations can be made by examining Figure 5.9. For example, S-NBS-CR and ECS-CR manage to provide good service up to -23*dBm* of noise power $N_0^{j'}$, while for $N_0^{j'} > -20\,dBm$ their resource allocations are infeasible. On the other hand, the error-inconsiderate schemes EIS-SNBS-CR, EPS-NBS-CR, MM-CR and EIFAS-CR cannot

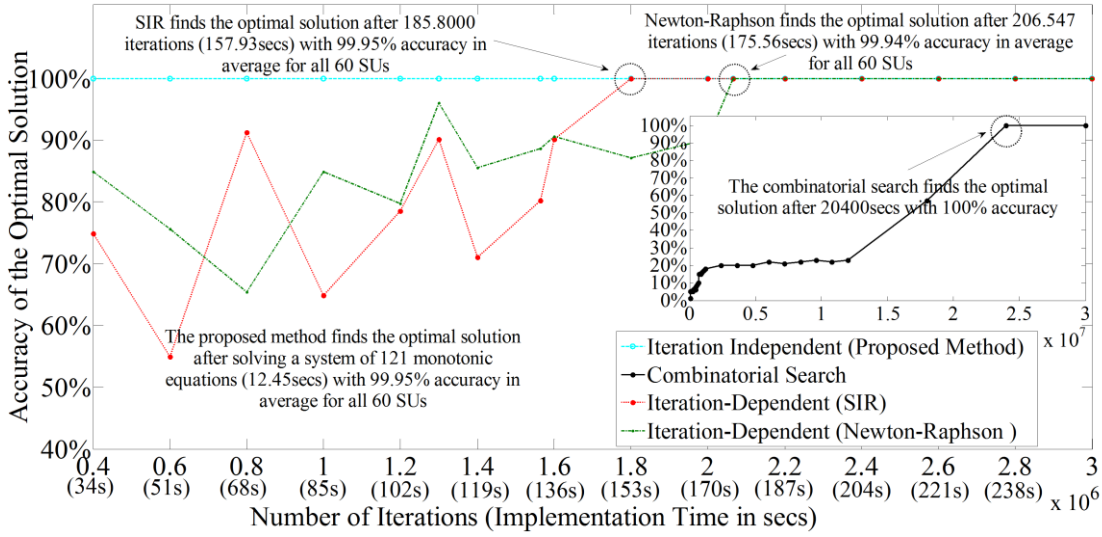

Figure 5.10 - Comparison regarding the implementation efficiency of S-NBS-CR: accuracy of the optimal solution versus number of iterations and implementation time.

provide good QoS to the SUs due to imperfect channel conditions, while their allocations are infeasible for $N_0^{j'} > -22\,dBm$ and $N_0^{j'} > -24\,dBm$ for EIFAS-CR. This simulation also shows that the increase of the noise power $N_0^{j'}$ of the j'-th PU has slightly less effects on the CR system's performance than the increase of the distance between PUs from the primary BS.

Finally, we demonstrate in Figure 5.10 that the introduced S-NBS-CR and also the EIS-NBS-CR, which is proposed in our work [178], [180], achieve 99.95% accurate solutions in average with incomparable lower implementation time than others. More precisely, we simulate a system with 60 SUs and 1024 subcarriers in MatLab and observe that the proposed iteration-independent method obtains the optimal solutions only in 12.45*secs*, while the iteration-dependent schemes ECS-CR, EIP-NBS-CR, MM-CR and EIFAS-CR require 157.93*sec* or 175.56*sec* under using either SIR or Newton-Raphson root-finding mechanisms, respectively[76]. In addition, although the combinatorial search is 100% accurate, its

[76] We remark that our reported measurements have been obtained through using a personal computer with 3.2GHz CPU computational power. Obviously the implementation time of iterative-dependent and iterative-independent schemes can be significantly reduced through using dedicated hardware as e.g., SoC.

implementation time is extremely high, while we have experienced several convergence issues during our simulations.

5.8 Conclusion

In this research part, we proposed an iteration-independent game-theoretic cross-layer scheduling scheme to provide performance enhancements in CR systems with imperfect channel, packet outage and heterogeneous SUs. Relying on the imperfect channel modelling and estimation procedure presented in the first research part of this Thesis, we initially introduced a PBL process to describe each SU's level of satisfaction in terms of effective throughput under channel and packet outage. We show that our PBL process fully complies with the S-NBS of power and subcarrier allocation in contrary to existing approaches that consider only the NBS of power. Furthermore, by adopting the throughput correlation between each SU's delay constraints from the upper layers with its PHY layer parameters presented in the first research part of this Thesis, we established a relationship between each user's minimum requirement to join the S-NBS game and its traffic arrival rate ensuring that way the feasibility of the S-NBS. In addition, we correlated each SU's traffic arrival rate with power-driven regulations for transmission interference cancelation between PUs and SUs. We then formulated a game-theoretic cross-layer optimization problem that targets to maximize the average SUs' satisfaction in terms of throughput, subject to subcarrier, power, QoS and transmission interference cancelation constraints. Through applying subcarrier time-sharing relaxation, we established an important feasibility condition to show the region where our game-theoretic cross-layer optimization problem is convex over a feasible convex set. In continue, we utilized Lagrangian optimization and approached the solution of our cross-layer problem with a different than existed scope that results iteration-independent optimal policies and enhances system's power efficiency. In addition, within our scope we introduced an innovative methodology to provide solutions by means of final formulas to the transcendental algebraic equations that appear during the optimization process due to the recursive origin of the S-NBS problem. We show that the proposed joint optimal game-theoretic adaptive-power and dynamic-subcarrier-allocation policy has actual linear complexity in the number of users and subcarriers and it also performs asymptotically in terms of throughput gain due to multi-

user and multi-carrier diversity exploitations. With simulations we demonstrated that the proposed S-NBS-CR provides scheduling with close to ideal fairness and maintains the system's effective throughput at remarkably high levels under various uncertain channel conditions. Finally, simulation comparisons with relevant approaches witnessed that the proposed game-theoretic scheme achieves the best trade-off between fairness and throughput/power efficiency by simultaneously providing superior QoS support according to heterogeneous SUs requirements and PUs' conditions.

Appendix C

C.1 Equivalency between the Problem (5.18) and the S-NBS Throughput Maximization Problem (5.17) - Proof of *Theorem 5.3*

To prove that the problem (5.18) is equivalent to the S-NBS throughput maximization problem (5.17), it is sufficient to show that the utility function $\mathcal{U}_j$ in (5.19) strictly increases for all $\left(\tilde{s}_{ij}, \tilde{p}_{ij}\right)$, which satisfy that the effective data rate $\tilde{r}_j$ allocated to SU j is larger than the SU j's minimum requirement, e.g., $\tilde{r}_j > u_j^0$. To prove that the utility function $\mathcal{U}_j$ strictly increases, we examine its first derivative over $\tilde{p}_{ij}$, given by

$$\frac{\partial \mathcal{U}_j}{\partial \tilde{p}_{ij}} = \frac{\left(1-\mathcal{P}_{out}\right)\cdot \tilde{s}_{ij} \mathcal{H}_{ij} \left|h_{ij}\right|^2}{\ln 2\left(\tilde{s}_{ij} + \mathcal{H}_{ij}\tilde{p}_{ij}\left|h_{ij}\right|^2\right)\left(\underbrace{\left(1-\mathcal{P}_{out}\right)\cdot \tilde{s}_{ij}\cdot \log_2\left(1+\frac{\mathcal{H}_{ij}\tilde{p}_{ij}\left|h_{ij}\right|^2}{\tilde{s}_{ij}}\right)}_{\tilde{r}_j} - u_j^0\right)}. \tag{5.53}$$

From (5.53), it is straightforward that the first derivative of the utility function $\mathcal{U}_j$ in (5.19) over $\tilde{p}_{ij}$ is positive, e.g., $\partial \mathcal{U}_j / \partial \tilde{p}_{ij} > 0$. Hence, $\mathcal{U}_j$ in (5.19) strictly increases for all $\tilde{p}_{ij} > 0$, which satisfy that $\tilde{r}_j > u_j^0$. Let us now denote the function $\mathcal{F}_{ij}\left(\tilde{s}_{ij}\right)$ to represent the first-order derivative of $\mathcal{U}_j$ in (5.19) over $\tilde{s}_{ij}$, e.g., $\partial \mathcal{U}_j / \partial \tilde{s}_{ij}$, given by

$$\mathcal{F}_{ij}\left(\tilde{s}_{ij}\right) \equiv \frac{\partial \mathcal{U}_j}{\partial \tilde{s}_{ij}} = \left(1-\mathcal{P}_{out}\right)\cdot \left(\frac{\log_2\left(1+\frac{\mathcal{H}_{ij}\tilde{p}_{ij}\left|h_{ij}\right|^2}{\tilde{s}_{ij}}\right) - \frac{\mathcal{H}_{ij}\tilde{p}_{ij}\left|h_{ij}\right|^2}{\ln 2\left(\tilde{s}_{ij} + \mathcal{H}_{ij}\tilde{p}_{ij}\left|h_{ij}\right|^2\right)}}{\underbrace{\left(1-\mathcal{P}_{out}\right)\cdot \tilde{s}_{ij}\cdot \log_2\left(1+\frac{\mathcal{H}_{ij}\tilde{p}_{ij}\left|h_{ij}\right|^2}{\tilde{s}_{ij}}\right)}_{\tilde{r}_j} - u_j^0}\right). \tag{5.54}$$

Recalling that $\tilde{p}_{ij} > 0$, the denominator of the function $\mathcal{F}_{ij}\left(\tilde{s}_{ij}\right)$ in (5.54) is positive for all $\tilde{s}_{ij}$ satisfying $\tilde{r}_j > u_j^0$. Thus, to prove the strictly increasing property of $\mathcal{U}_j$ in (5.19) it is sufficient to show that the numerator of the function $\mathcal{F}\left(\tilde{s}_{ij}\right)$ in (5.54) is also positive for $\tilde{s}_{ij} > \tilde{s}_{ij}^{\min}$, where $\tilde{s}_{ij}^{\min} > 0$ is the unique solution of $\tilde{r}_j = u_j^0$. The numerator of the function $\mathcal{F}_{ij}\left(\tilde{s}_{ij}\right)$ in (5.54) can be represented by the function $\mathcal{T}(a)$ denoted by

$$\mathcal{T}(a) = \frac{\log_2(1+a) - a}{\ln 2 \cdot (1+a)}, \tag{5.55}$$

where the variable a is given by $a = \hbar_{ij}\tilde{p}_{ij}\left|h_{ij}\right|^2 / \tilde{s}_{ij}$ and it is positive, e.g., $a > 0$. It is easy to verify that the first-order derivative of the function $\mathcal{T}(a)$ over a is positive when $a > 0$, i.e.,

$$\frac{\partial \mathcal{T}(a)}{\partial a} = \frac{a}{\ln 2 \cdot (1+a)^2} > 0.$$

Therefore, not only the function $\mathcal{T}(a)$ in (5.55) strictly increases but also we can reduce the numerator of the function $\mathcal{F}_{ij}\left(\tilde{s}_{ij}\right)$ in (5.54) into $\left((1-\mathcal{P}_{out})/\ln 2\right)\cdot\mathcal{T}\left(\hbar_{ij}\tilde{p}_{ij}\left|h_{ij}\right|^2/\tilde{s}_{ij}\right)$ as from (5.55) it stands that $\mathcal{T}(a) > \mathcal{T}(0) = 0$. Thus, the function $\mathcal{F}_{ij}\left(\tilde{s}_{ij}\right)$ in (5.54) is positive, e.g., $\mathcal{F}_{ij}\left(\tilde{s}_{ij}\right) > 0$, as both its nominator and denominator are positive. Consequently the first derivations of the utility function $\mathcal{U}_j$ in (5.19) over $\tilde{p}_{ij}$ and $\tilde{s}_{ij}$ are positive. In conclusion, the utility function $\mathcal{U}_j$ in (5.19) strictly increases for all $\left(\tilde{s}_{ij}, \tilde{p}_{ij}\right)$, which satisfy $\tilde{r}_j > u_j^0$, meaning that the two problems (5.18) and (5.17) are equivalent.

In continue, we prove that the utility function (5.17) is designed based on the S-NBS Theorem matching the metric of proportional fairness of resource sharing [157]. We consider the $K \times 1$ vector $\tilde{\boldsymbol{r}}$ given by

$$\tilde{\boldsymbol{r}} = \left[\left(\tilde{r}_1 - u_1^0\right), ..., \left(\tilde{r}_K - u_K^0\right)\right]^T, \tag{5.56}$$

which expresses the SUs' satisfaction. Then we can define the $K\times 1$ utility vector $\mathcal{U}(\tilde{\boldsymbol{r}})$ with entries the utility function of each SU j, e.g.,

$$\mathcal{U}(\tilde{\boldsymbol{r}})=\prod_{j\in K}\left(\tilde{r}_j-u_j^0\right). \tag{5.57}$$

For the purpose of equilibrium analysis, we set the disagreement points of the utility function $\mathcal{U}_j$ in (5.19) to be equal to zero, e.g., $u_j^0=0$, reducing the utility vector $\mathcal{U}(\tilde{\boldsymbol{r}})$ in (5.57) to

$$\mathcal{U}(\tilde{\boldsymbol{r}})=\prod_{j\in K}\left(\tilde{r}_j\right). \tag{5.58}$$

As we have proven that the two problems (5.18) and (5.17) are equivalent, the utility vector $\mathcal{U}(\tilde{\boldsymbol{r}})$ in (5.58) can be written as

$$\mathcal{U}(\tilde{\boldsymbol{r}})=\sum_{j=1}^{K}\left(\tilde{r}_j\right). \tag{5.59}$$

Moreover, assuming that the optimal allocation index and power are given by $\tilde{s}_{ij}^*$ and $\tilde{p}_{ij}^*$, respectively then we can define the $K\times 1$ vector $\tilde{\boldsymbol{r}}^*$ with entries the optimal effective data rate of each of the K SUs, e.g., $\tilde{\boldsymbol{r}}^*=\left[\tilde{\boldsymbol{r}}_1^*,...,\tilde{\boldsymbol{r}}_K^*\right]^{\mathcal{T}}$. From utility theory [33], a vector of rates, e.g., $\tilde{\boldsymbol{r}}^*$, is said to be proportionally fair if and only if it is feasible and for any other feasible rate vector $\tilde{\boldsymbol{r}}$ it satisfies that $\left(\tilde{\boldsymbol{r}}-\tilde{\boldsymbol{r}}^*\right)/\tilde{\boldsymbol{r}}^*\le 0$ [157]. Hence, we examine the first derivative of the utility vector $\mathcal{U}(\tilde{\boldsymbol{r}})$ in (5.59) at the point $\tilde{\boldsymbol{r}}=\tilde{\boldsymbol{r}}^*$, e.g.,

$$\left(\tilde{\boldsymbol{r}}-\tilde{\boldsymbol{r}}^*\right)\cdot\left.\frac{\partial\mathcal{U}(\tilde{\boldsymbol{r}})}{\partial(\tilde{\boldsymbol{r}})}\right|_{(\tilde{\boldsymbol{r}})=(\tilde{\boldsymbol{r}}^*)}=\left(\frac{\tilde{\boldsymbol{r}}-\tilde{\boldsymbol{r}}^*}{\tilde{\boldsymbol{r}}^*}\right)\le 0. \tag{5.60}$$

From (5.60) we observe that the first derivative of the utility vector $\mathcal{U}(\tilde{\boldsymbol{r}})$ at the point $\tilde{\boldsymbol{r}}=\tilde{\boldsymbol{r}}^*$ is indeed smaller or equal to zero. Consequently, the utility vector $\mathcal{U}(\tilde{\boldsymbol{r}})$ in (5.59) guarantees the proportional fairness condition for spectrum sharing as any movement along any direction $\tilde{\boldsymbol{r}}-\tilde{\boldsymbol{r}}^*$ at the optimum rate vector $\tilde{\boldsymbol{r}}^*$ cannot improve the utility vector $\mathcal{U}(\tilde{\boldsymbol{r}})$. Hence, the optimal allocation index $\tilde{s}_{ij}^*$ and transmitting power $\tilde{p}_{ij}^*$ provide

proportionally fair resource allocation when considered in the utility function $\mathcal{U}_j$ in (5.19). This completes the proof of *Theorem 5.3*. ■

C.2 Definition of the Cost Function of the S-NBS Optimization Problem under Imperfect CSIT and Channel Outage - Proof of *Theorem 5.4*

In this Appendix, we aim to express the cost function of the S-NBS cross-layer optimization problem (5.20) - (5.28) in terms of the outage constraint (5.28), e.g., $\mathcal{P}_{out} = \mathcal{P}_{app}$.

Let us firstly consider the case where the channel is perfect. From the maximum achievable capacity c_{ij} in (5.12) and the time-sharing variables $\tilde{s}_{ij}$ and $\tilde{p}_{ij}$ we can define the time-shared maximum achievable capacity $\tilde{c}_{ij}$ of SU j on subcarrier i under perfect channel conditions as

$$\tilde{c}_{ij} = \log_2\left(1 + \frac{\tilde{p}_{ij}\left|h_{ij}\right|^2}{\tilde{s}_{ij}}\right). \tag{5.61}$$

Considering (5.61) and the outage constraint (5.28), e.g., $\mathcal{P}_{out} = \mathcal{P}_{app}$, the instantaneous effective data rate r_{ij} of SU j on subcarrier i in (5.14) can be written in terms of time-sharing as $\tilde{r}_{ij} = E_{\hat{h}_{ij}}\left[\left(1-\mathcal{P}_{app}\right)\cdot\tilde{c}_{ij}\right]$ and the instantaneous effective data rate $\tilde{r}_j$ of SU j in (5.16) becomes $\tilde{r}_j = \sum_{i=1}^{N_C}\tilde{s}_{ij}\cdot\tilde{r}_{ij} = E_{\hat{h}_{ij}}\left[\sum_{i=1}^{N_C}\left(1-\mathcal{P}_{app}\right)\cdot\tilde{s}_{ij}\cdot\tilde{c}_{ij}\right]$. Hence, as we define that $\mathcal{U} = \sum_{j=1}^{K}\mathcal{U}_j$, from (5.17) the utility function $\mathcal{U}_j$ of SU j in (5.19) can be rewritten in terms of time-shared maximum achievable capacity $\tilde{c}_{ij}$ as

$$\begin{aligned}\mathcal{U}_j &= E\left[\ln\left(\tilde{r}_j - u_j^0\right)\right] \\ &= E\left[\ln\left(\left(\sum_{i=1}^{N_C}\cdot\tilde{s}_{ij}\cdot\tilde{r}_{ij}\right) - u_j^0\right)\right] \\ &= E\left[\ln\left(E_{\hat{h}_{ij}}\left[\sum_{i=1}^{N_C}\left(1-\mathcal{P}_{app}\right)\cdot\tilde{s}_{ij}\cdot\tilde{c}_{ij}\right] - u_j^0\right)\right]\end{aligned} \quad . \tag{5.62}$$

Examining (5.62) and our new definition for the utility function $\mathcal{U}_j$ of SU j in (5.29) it is straightforward that in order to prove *Theorem 5.4* it is sufficient to show that under imperfect channel conditions the capacity $E_{\hat{h}_{ij}}\left(\tilde{c}_{ij}\right)$ as perceived by the system satisfies the outage constraint (5.28), e.g., $\mathcal{P}_{out} = \mathcal{P}_{app}$, if

$$E_{\hat{h}_{ij}}\left[\tilde{c}_{ij}\right] = \log_2\left(1 + \frac{\tilde{h}_{ij}\,\tilde{p}_{ij}\sigma_h^2}{\tilde{s}_{ij}}\cdot\mathbb{F}^{-1}_{\left(\frac{\left|\hat{h}_{ij}\right|^2}{\sigma_h^2}\right)_2}\left(\mathcal{P}_{app}\right)\right). \tag{5.63}$$

From the definition of the target outage probability $\mathcal{P}_{out}$ in Section 4.4.1 and our assumption in (5.63) we can express $\mathcal{P}_{out}$ as follows.

$$\begin{aligned}\mathcal{P}_{out} &= 1 - \Pr\left[E_{\hat{h}_{ij}}\left[\tilde{c}_{ij}\right] \le \tilde{c}_{ij}\,\middle|\,\hat{h}_{ij}\right] \\ &= \Pr\left[\tilde{c}_{ij} \le E_{\hat{h}_{ij}}\left[\tilde{c}_{ij}\right]\middle|\hat{h}_{ij}\right] \\ &= \Pr\left[\log_2\left(1+\frac{\tilde{h}_{ij}\,\tilde{p}_{ij}\left|h_{ij}\right|^2}{\tilde{s}_{ij}}\right) < \log_2\left(1+\frac{\tilde{h}_{ij}\,\tilde{p}_{ij}\sigma_h^2}{\tilde{s}_{ij}}\cdot\mathbb{F}^{-1}_{\left(\frac{\left|\hat{h}_{ij}\right|^2}{\sigma_h^2}\right)_2}\left(\mathcal{P}_{app}\right)\right)\middle|\,\hat{h}_{ij}\right] \\ &= \Pr\left[\left|h_{ij}\right|^2 < \sigma_h^2\cdot\mathbb{F}^{-1}_{\left(\frac{\left|\hat{h}_{ij}\right|^2}{\sigma_h^2}\right)_2}\left(\mathcal{P}_{app}\right)\middle|\,\hat{h}_{ij}\right] \Leftrightarrow\end{aligned}$$

$$\mathcal{P}_{out} = \Pr\left[\frac{\left|h_{ij}\right|^2}{\sigma_h^2} < \mathcal{F}^{-1}_{\left(\frac{\left|\hat{h}_{ij}\right|^2}{\sigma_h^2}\right)_2}\left(\mathcal{P}_{app}\right) \middle| \hat{h}_{ij} \right]. \tag{5.64}$$

We recall that the actual channel realization h_{ij} in (5.64) is CSGC distributed, e.g., $h_{ij} \sim \mathcal{CN}\left(\hat{h}_{ij}, \sigma_h^2\right)$, the term $\left|h_{ij}\right|^2 / \sigma_h^2$ is a non-central random chi-squared variable with two degrees of freedom and non-centrality parameter the term $\left|\hat{h}_{ij}\right|^2 / \sigma_h^2$. Hence, we can define the non-central chi-squared CDF $\mathcal{F}_{(\cdot)}\left(x\right)$ of the random variable x with non-centrality parameter $\left|\hat{h}_{ij}\right|^2 / \sigma_h^2$ and two degrees of freedom, e.g., $\mathcal{F}_{\left(\left|\hat{h}_{ij}\right|^2/\sigma_h^2\right)_2}\left(x\right)$[77] to rewrite equation (5.64) as

$$\begin{aligned}
\mathcal{P}_{out} &= \Pr\left[\frac{\left|h_{ij}\right|^2}{\sigma_h^2} < \mathcal{F}^{-1}_{\left(\frac{\left|\hat{h}_{ij}\right|^2}{\sigma_h^2}\right)_2}\left(\mathcal{P}_{app}\right) \middle| \hat{h}_{ij} \right] \\
&= \mathcal{F}_{\left(\frac{\left|\hat{h}_{ij}\right|^2}{\sigma_h^2}\right)_2}\left[\mathcal{F}^{-1}_{\left(\frac{\left|\hat{h}_{ij}\right|^2}{\sigma_h^2}\right)_2}\left(\mathcal{P}_{app}\right) \right] \quad .^{78} \\
&= \mathcal{P}_{app}
\end{aligned} \tag{5.65}$$

[77] The non-central CDF of x with two degrees of freedom and non-centrality parameter a is given by $\mathcal{F}_{\left(a^a\right)_2}\left(x\right) = 1 - \mathcal{Q}_1\left(\sqrt{x} \cdot \sqrt{a^2}\right)$, where $\mathcal{Q}_1\left(\cdot\right)$ denotes the Marcum Q-function of the first order [59].

[78] Through defining the inverse non-central chi-squared CDF $\mathcal{F}^{-1}_{(\cdot)}\left(\cdot\right)$ of the random variable y, with non-centrality parameter $\left|\hat{h}_{ij}\right|^2 / \sigma_h^2$ and two degrees of freedom e.g., $\mathcal{F}^{-1}_{\left(\left|\hat{h}_{ij}\right|^2/\sigma_h^2\right)_2}\left(y\right)$, we can utilize the property of the CDF [156], which specifies that $\mathcal{F}_{\left(\left|\hat{h}_{ij}\right|^2/\sigma_h^2\right)_2}\left(x\right) = y \Leftrightarrow \mathcal{F}^{-1}_{\left(\left|\hat{h}_{ij}\right|^2/\sigma_h^2\right)_2}\left(y\right) = x$, to compute the equation in (5.65).

From (5.65) we confirm that he capacity $E_{\hat{h}_{ij}}\left[\tilde{c}_{ij}\right]$ as perceived by the system in (5.63) verifies the outage condition (5.28), e.g., $\mathcal{P}_{out}=\mathcal{P}_{app}$. Consequently, from (5.61), (5.62) and (5.65) the utility function $\mathcal{U}_j$ of SU j in (5.19) can indeed be written as

$$\mathcal{U}_j = E\left[\ln\left(E_{\hat{h}_{ij}}\left[\sum_{i=1}^{N_C}\left(1-\mathcal{P}_{app}\right)\cdot\tilde{s}_{ij}\cdot\tilde{c}_{ij}\right]-u_j^0\right)\right]$$

$$= \ln\left(\sum_{i=1}^{N_C}\left(1-\mathcal{P}_{app}\right)\cdot\tilde{s}_{ij}\cdot\log_2\left(1+\frac{\hat{h}_{ij}\tilde{p}_{ij}\sigma_h^2}{\tilde{s}_{ij}}\cdot\mathcal{F}^{-1}_{\left(\frac{|\hat{h}_{ij}|^2}{\sigma_h^2}\right)_2}\left(\mathcal{P}_{app}\right)\right)-u_j^0\right),$$

which resolves (5.29). This completes the proof of *Theorem 5.4*. ■

C.3 Convexity of the S-NBS Optimization Problem – Proof of *Proposition 5.1*

In this Appendix we focus on proofing the convexity of the S-NBS cross-layer optimization problem (5.38) - (5.44) along with the convexity and feasibility of its determined set. To avoid confusion, we separate our proofs into three different topics as below.

1) Convexity of the S-NBS cross-layer optimization problem (5.38) - (5.44). By introducing the subcarrier time-sharing factor $\tilde{s}_{ij}\in(0,1]$ and the continues variable $\tilde{p}_{ij}=\tilde{s}_{ij}p_{ij}$, the cost function in (5.38) has the form $\ln\left(\tilde{r}_{ij}-\left(\tilde{q}_j\left(F,T_j^{\max},\lambda_j\right)-1\right)\right)$, which is a logarithmically concave function over the non-empty and convex set $\left(\tilde{s}_{ij},\tilde{p}_{ij}\right)$ [135] (see *Theorem 4.1* in Section 4.4.2 of Chapter 4 for more details). Thus, the cost function in (5.38) is also concave function over the convex set $\left(\tilde{s}_{ij},\tilde{p}_{ij}\right)$ as any positive linear combination of concave functions is a concave function. In addition, it is straightforward that the subcarrier and power constraints (5.39) - (5.44) are all affine over $\tilde{s}_{ij}$ or $\tilde{p}_{ij}$ and hence, they are convex functions over the convex set $\left(\tilde{s}_{ij},\tilde{p}_{ij}\right)$.

2) Convexity of the determined set of the S-NBS cross-layer optimization problem (5.38) - (5.44). Given the subcarrier time-sharing factor $\tilde{s}_{ij} \in (0,1]$ and the variable $\tilde{p}_{ij} = \tilde{s}_{ij} p_{ij}$, the cost function (5.38) is concave determining a convex set over $(\tilde{s}_{ij}, \tilde{p}_{ij})$ [135]. In addition, each of the constraints (5.39) - (5.44), determines a convex set over $(\tilde{s}_{ij}, \tilde{p}_{ij})$ due to its affinity. Therefore, the set defined by all six constraints (5.39) - (5.44) and the cost function (5.38), is convex over $(\tilde{s}_{ij}, \tilde{p}_{ij})$ as it is well-known that the intersection of convex sets is also convex.

3) Feasibility of the determined set of the S-NBS cross-layer optimization problem (5.38) - (5.44). We recall that the set $(\tilde{s}_{ij}, \tilde{p}_{ij})$ determined by all six constraints (5.39) - (5.44) and the cost function (5.38) on one hand is convex but on the other hand it may not be feasible due to the opposite sign of the inequality of the power constraint (5.43). In other words the convex set $(\tilde{s}_{ij}, \tilde{p}_{ij})$ may exist but it can be the empty set. For this reason we examine the validity of the set $(\tilde{s}_{ij}, \tilde{p}_{ij})$ through a feasibility condition to show when the convex set $(\tilde{s}_{ij}, \tilde{p}_{ij})$ is non-empty or in other words, when the convex optimization problem (5.38) - (5.44) is valid.

Let us consider the case where one SU and multiple subcarriers are involved in our system, e.g., $K = 1$ and $N_C > 1$. Then the power conditions (5.44), (5.43) and (5.42) are written as

$$E\left[\sum_{i=1}^{N_C} \tilde{p}_{i1}\right] \le P_{TOTAL}, \tag{5.66}$$

$$E\left[\sum_{i=1}^{N_C} \tilde{p}_{i1} \left|\hat{h}_{i1}\right|^2\right] \ge P_1^{\min}, \tag{5.67}$$

$$E\left[\sum_{i=1}^{N_C} \tilde{p}_{i1}\right] \le P_1^{\max}. \tag{5.68}$$

Examining equations (5.66), (5.67) and (5.68) we can observe that their conjunction can be written as

$$E\left[\sum_{i=1}^{N_C}\tilde{p}_{i1}\right]\leq \min\left(P_{TOTAL},P_1^{\max}\right). \tag{5.69}$$

In continue we need to prove that using (5.67) and (5.69) we can determine a non-empty set. To prove that we assume that one SU and one subcarrier are involved in our system, e.g., $K=1$ and $N_C=1$. As P_{TOTAL}, $P_j^{\min}$, $P_j^{\max}$ and $\left|\hat{h}_{ij}\right|^2$ are all positive, from equation (5.67) we get

$$E\left[\tilde{p}_{11}\left|\hat{h}_{11}\right|^2\right]\geq P_1^{\min}. \tag{5.70}$$

Similarly, equation (5.69) yields

$$\tilde{p}_{11}\leq \min\left(P_{TOTAL},P_1^{\max}\right). \tag{5.71}$$

From (5.70) and (5.71) we conclude that they determine a non-empty set if

$$E\left[\left|\hat{h}_{11}\right|^2\right]\geq \frac{P_1^{\min}}{\min\left(P_{TOTAL},P_1^{\max}\right)}. \tag{5.72}$$

Furthermore, by assuming that one SU and two subcarriers are involved in our system, e.g., $K=1$ and $N_C=2$, then (5.67) is written as

$$E\left[\tilde{p}_{11}\left|\hat{h}_{11}\right|^2\right]+E\left[\tilde{p}_{12}\left|\hat{h}_{12}\right|^2\right]\geq P_1^{\min}, \tag{5.73}$$

while (5.69) yields that

$$\tilde{p}_{11}+\tilde{p}_{12}\leq \min\left(P_{TOTAL},P_1^{\max}\right). \tag{5.74}$$

From (5.73) and (5.74) we conclude that they determine a non-empty set if

$$\left\{E\left[\left|\hat{h}_{11}\right|^2\right],E\left[\left|\hat{h}_{12}\right|^2\right]\right\}\geq \frac{P_1^{\min}}{\min\left(P_{TOTAL},P_1^{\max}\right)}. \tag{5.75}$$

Consequently, from (5.72) and (5.75) we show that if one SU and multiple subcarrier are involved in our system, e.g., $K=1$ and $N_C>1$, the convex set determined by the power constraints (5.42), (5.43) and (5.44) of the S-NBS cross-layer optimization problem (5.38) - (5.44) is non-empty if

$$\max\left\{E\left[\left|\hat{h}_{ij}\right|^2\right]\right\}\geq \frac{P_j^{\min}}{\min\left(P_{TOTAL},P_j^{\max}\right)}. \tag{5.76}$$

We shall now examine the case where multiple users and multiple subcarriers are involved in our system. Let us consider that $K=2$ and $N_C>1$. Then constraints (5.42), (5.43) and (5.44) of the S-NBS cross-layer optimization problem (5.38) - (5.44) become as below.

$$\sum_{i=1}^{N_C}\tilde{p}_{i1}\le P_{TOTAL},\sum_{i=1}^{N_C}\tilde{p}_{i2}\le P_{TOTAL}, \tag{5.77}$$

$$E\left[\sum_{i=1}^{N_C}\left(\tilde{p}_{i1}\left|\hat{h}_{i1}\right|^2\right)\right]\ge P_1^{\min},E\left[\sum_{i=1}^{N_C}\left(\tilde{p}_{i2}\left|\hat{h}_{i2}\right|^2\right)\right]\ge P_2^{\min}, \tag{5.78}$$

$$\sum_{i=1}^{N_C}\tilde{p}_{i1}\le P_1^{\max},\sum_{i=1}^{N_C}\tilde{p}_{i2}\le P_2^{\max}. \tag{5.79}$$

It is straightforward that (5.78) and (5.79) are just like (5.66) and (5.68) where only one SU and multiple subcarrier were involved in our system, e.g., $K=1$, $N_C>1$. Nevertheless, by also accounting (5.77) it is the same as having two instances of the $K=1$, $N_C>1$ problem. So the conjunctions between (5.77) and (5.79) are now two, e.g.,

$$\sum_{i=1}^{N_C}\tilde{p}_{i1}\le\min\left(P_{TOTAL},P_1^{\max}\right)\text{ and }\sum_{i=1}^{N_C}\tilde{p}_{i2}\le\min\left(P_{TOTAL},P_2^{\max}\right), \tag{5.80}$$

and from (5.80) we can write that

$$E\left[\left|\hat{h}_{11}\right|^2\right]\ge\frac{P_1^{\min}}{\min\left(P_{TOTAL},P_1^{\max}\right)}\text{ and }E\left[\left|\hat{h}_{12}\right|^2\right]\ge\frac{P_2^{\min}}{\min\left(P_{TOTAL},P_2^{\max}\right)}. \tag{5.81}$$

Examining (5.81) we observe that if it is required only one of the two conditions to be true, then the feasibility condition for the convex set to be non-empty it would have been the same as (5.76). However, as we need both the condition in (5.81) to be true we should define our constraint on the minimum maximum of those two conditions, e.g.,

$$\min\left\{\max\left\{E\left[\left|\hat{h}_{i1}\right|^2\right]\right\},\max\left\{E\left[\left|\hat{h}_{i2}\right|^2\right]\right\}\right\}\ge\frac{P_1^{\min}+P_2^{\min}}{\min\left(P_{TOTAL},P_1^{\max}+P_2^{\max}\right)}. \tag{5.82}$$

Generalizing (5.82) for multiple users and subcarrier we derive the necessary condition that ensures that the convex set of the S-NBS cross-layer optimization problem (5.38) - (5.44) is non-empty as

$$\min\left\{\max\left\{E\left[\left|\hat{h}_{ij}\right|^2\right]\right\}\right\} \geq \frac{\sum_{j=1}^{K} P_j^{\min}}{\min\left(P_{TOTAL}, \sum_{j=1}^{K} P_j^{\max}\right)}. \tag{5.83}$$

We remark that, if the power condition $E\left[\frac{1}{N_C}\sum_{j=1}^{K}\sum_{i=1}^{N_C}\tilde{p}_{ij}\right] \leq P_{TOTAL}$ in (5.44) is subsumed by the condition $E\left[\sum_{i=1}^{N_C}\tilde{p}_{ij}\right] \leq P_j^{\max}$ in (5.42), e.g., $P_{TOTAL} >> \sum_{j=1}^{K} P_j^{\max}$, then the condition (5.83) is not only necessary but it is also sufficient. This completes the proof of *Proposition 5.1*. ■

We shall now show that given the feasibility condition (5.83), the power constraint (5.44) on total transmitting power is not redundant to the S-NBS cross-layer optimization problem (5.38) - (5.44). The only case where (5.44) is irrelevant to our problem, is the instance where the summation of the maximum power $P_j^{\max}$ of each PU is smaller than the total available power to the BS, e.g., $\sum_{j=1}^{K} P_j^{\max} < P_{TOTAL}$. Then obviously in that case, the condition (5.44) is not necessary to be included as only the power condition $E\left[\sum_{i=1}^{N_C}\tilde{p}_{ij}\right] \leq P_j^{\max}$ in (5.42) is needed to upper bound the transmitting power. Hence, it is sufficient to show that the feasibility condition is that case is different that our condition defined in *Proposition 5.1*. To derive the feasibility condition that makes constraint (5.44) irrelevant we examine the case where one SU and multiple subcarrier are involved in the system, e.g., $K=1$ and $N_C>1$, which has been previously described in equation (5.76). If we had continued with this rational and upon accounting (5.77), (5.78), (5.79), we should have concluded that for multiple SUs and subcarriers, e.g., $K=2$ and $N_C>1$, the feasibility condition would have been

$$\max\left\{E\left[\left|\hat{h}_{ij}\right|^2\right]\right\} \geq \frac{\sum_{j=1}^{K} P_j^{\min}}{\min\left(P_{TOTAL}, \sum_{j=1}^{K} P_j^{\max}\right)}. \tag{5.84}$$

However, (5.84) makes the power constraint (5.44) on total transmitting power irrelevant to our problem (5.38) - (5.44) as it is straightforward that the transmitting power is upper bounded by (5.42). This completes the proof of *Proposition 5.2*. ■

C.4 Optimal Subcarrier Allocation Index in Compliance with the S-NBS Principle - Proof of *Theorem 5.5*

In this Appendix we determine the optimal subcarrier allocation index $\tilde{s}_{ij}^*$ for SU j on subcarrier i. Let us firstly define the Lagrangian function $\mathcal{L}\left(\tilde{s}_{ij}, \tilde{p}_{ij}, \xi_j, \vartheta, \kappa_i, \iota_j\right)$ of the S-NBS cross-layer optimization problem (5.38) - (5.44) as

$$\mathcal{L}\left(\tilde{s}_{ij}, \tilde{p}_{ij}, \xi_j, \vartheta, \kappa_i, \iota_j\right) =$$

$$\sum_{j=1}^{K} \ln\left(\sum_{i=1}^{N_C}\left(1-\mathcal{P}_{app}\right)\cdot\tilde{s}_{ij}\cdot\log_2\left(1+\frac{h_{ij}\tilde{p}_{ij}\sigma_h^2}{\tilde{s}_{ij}}\cdot\mathbb{F}^{-1}_{\left(\frac{\left|\hat{h}_{ij}\right|^2}{\sigma_h^2}\right)_2}\left(\mathcal{P}_{app}\right)\right)-\left(\tilde{q}_j\left(F, T_j^{\max}, \lambda_j\right)-1\right)\right),$$

$$+\vartheta\left(P_{TOTAL}-\frac{1}{N_F}\left(\sum_{j=1}^{K}\sum_{i=1}^{N_F}\tilde{p}_{ij}\right)\right)-\kappa_i\left(\sum_{j=1}^{K}\tilde{s}_{ij}-1\right)+\xi_j\left(P_j^{\max}-\sum_{i=1}^{N_C}\tilde{p}_{ij}\right)+\iota_j\left(\sum_{i=1}^{N_C}\left(\tilde{p}_{ij}\left|\hat{h}_{ij}\right|^2\right)-P_j^{\min}\right) \tag{5.85}$$

where ξ_j, ϑ, κ_i and ι_j are the LMs related with the power-driven interference cancelation constraint (5.42), the power constraint (5.44), the subcarrier constraint (5.40) and the power-driven QoS constraint (5.43) for SUs, respectively. The necessary and sufficient conditions that satisfy the global optimum solutions of the S-NBS cross-layer optimization problem (5.38) - (5.44), are the KKT conditions defined as follows [135].

$$\left.\frac{\partial \mathcal{L}\left(\tilde{s}_{ij},\tilde{p}_{ij},\xi_j,\vartheta,\kappa_i,\iota_j\right)}{\partial \tilde{p}_{ij}}\right|_{\left(\tilde{s}_{ij},\tilde{p}_{ij},\xi_j,\vartheta,\kappa_i,\iota_j\right)=\left(\tilde{s}_{ij}^*,\tilde{p}_{ij}^*,\xi_j^*,\vartheta^*,\kappa_i^*,\iota_j^*\right)} \begin{cases} <0, \text{ if } \tilde{p}_{ij}^*=0 \\ =0, \text{ if } \tilde{p}_{ij}^*>0 \end{cases}, \quad \forall i,j, \tag{5.86}$$

$$\left.\frac{\partial \mathcal{L}\left(\tilde{s}_{ij},\tilde{p}_{ij},\xi_j,\vartheta,\kappa_i,\iota_j\right)}{\partial \tilde{s}_{ij}}\right|_{\left(\tilde{s}_{ij},\tilde{p}_{ij},\xi_j,\vartheta,\kappa_i,\iota_j\right)=\left(\tilde{s}_{ij}^*,\tilde{p}_{ij}^*,\xi_j^*,\vartheta^*,\kappa_i^*,\iota_j^*\right)} \begin{cases} >0, \text{ if } \tilde{s}_{ij}^*=1 \\ =0, \text{ if } 0<\tilde{s}_{ij}^*<1 \end{cases}, \quad \forall i,j, \tag{5.87}$$

$$\left.\frac{\partial \mathcal{L}\left(\tilde{s}_{ij},\tilde{p}_{ij},\xi_j,\vartheta,\kappa_i,\iota_j\right)}{\partial \xi_j}\right|_{\left(\tilde{s}_{ij},\tilde{p}_{ij},\xi_j,\vartheta,\kappa_i,\iota_j\right)=\left(\tilde{s}_{ij}^*,\tilde{p}_{ij}^*,\xi_j^*,\vartheta^*,\kappa_i^*,\iota_j^*\right)} \begin{cases} >0, \text{ if } \xi_j^*<0 \\ =0, \text{ if } \xi_j^*\geq 0 \end{cases}, \quad \forall j, \tag{5.88}$$

$$\left.\frac{\partial \mathcal{L}\left(\tilde{s}_{ij},\tilde{p}_{ij},\xi_j,\vartheta,\kappa_i,\iota_j\right)}{\partial \vartheta}\right|_{\left(\tilde{s}_{ij},\tilde{p}_{ij},\xi_j,\vartheta,\kappa_i,\iota_j\right)=\left(\tilde{s}_{ij}^*,\tilde{p}_{ij}^*,\xi_j^*,\vartheta^*,\kappa_i^*,\iota_j^*\right)} \begin{cases} >0, \text{ if } \vartheta^*<0 \\ =0, \text{ if } \vartheta^*\geq 0 \end{cases}, \tag{5.89}$$

$$\left.\frac{\partial \mathcal{L}\left(\tilde{s}_{ij},\tilde{p}_{ij},\xi_j,\vartheta,\kappa_i,\iota_j\right)}{\partial \kappa_i}\right|_{\left(\tilde{s}_{ij},\tilde{p}_{ij},\xi_j,\vartheta,\kappa_i,\iota_j\right)=\left(\tilde{s}_{ij}^*,\tilde{p}_{ij}^*,\xi_j^*,\vartheta^*,\kappa_i^*,\iota_j^*\right)} \begin{cases} >0, \text{ if } \kappa_i^*<0 \\ =0, \text{ if } \kappa_i^*\geq 0 \end{cases}, \quad \forall i, \tag{5.90}$$

$$\left.\frac{\partial \mathcal{L}\left(\tilde{s}_{ij},\tilde{p}_{ij},\xi_j,\vartheta,\kappa_i,\iota_j\right)}{\partial \iota_j}\right|_{\left(\tilde{s}_{ij},\tilde{p}_{ij},\xi_j,\vartheta,\kappa_i,\iota_j\right)=\left(\tilde{s}_{ij}^*,\tilde{p}_{ij}^*,\xi_j^*,\vartheta^*,\kappa_i^*,\iota_j^*\right)} \begin{cases} >0, \text{ if } \iota_j^*<0 \\ =0, \text{ if } \iota_j^*\geq 0 \end{cases}, \quad \forall j, \tag{5.91}$$

$$\tilde{p}_{ij}^* \geq 0 \quad \forall i,j, \tag{5.92}$$

$$\xi_j^* \geq 0, \quad \forall j, \tag{5.93}$$

$$\vartheta^* \geq 0, \tag{5.94}$$

$$\kappa_i^* \geq 0, \quad \forall i, \tag{5.95}$$

$$\iota_j^* \geq 0, \quad \forall j, \tag{5.96}$$

$$\sum_{j=1}^{K} \tilde{s}_{ij}^* \leq 1, \tag{5.97}$$

$$\sum_{i=1}^{N_F} \kappa_i^* \left(\sum_{j=1}^{K} \tilde{s}_{ij}^* - 1 \right) \leq 0, \quad \forall j, \tag{5.98}$$

$$P_{TOTAL} - \frac{1}{N_F} \sum_{j=1}^{K} \sum_{i=1}^{N_F} \tilde{p}_{ij}^* \geq 0, \tag{5.99}$$

$$\vartheta^*\left(P_{TOTAL}-\frac{1}{N_F}\sum_{j=1}^{K}\sum_{i=1}^{N_F}\tilde{p}_{ij}^*\right)=0\,, \tag{5.100}$$

$$P_j^{\max}-\sum_{i=1}^{N_C}\tilde{p}_{ij}^*\geq 0\,,\quad \forall j\,, \tag{5.101}$$

$$\xi_j^*\left(P_j^{\max}-\sum_{i=1}^{N_C}\tilde{p}_{ij}^*\right)\geq 0\,,\quad \forall j\,, \tag{5.102}$$

$$\sum_{i=1}^{N_C}\left(\tilde{p}_{ij}\left|\hat{h}_{ij}\right|^2\right)-P_j^{\min}\geq 0\,,\quad \forall j\,, \tag{5.103}$$

$$\iota_j^*\left(\sum_{i=1}^{N_C}\left(\tilde{p}_{ij}\left|\hat{h}_{ij}\right|^2\right)-P_j^{\min}\right).\quad \forall j\,, \tag{5.104}$$

where ξ_j^*, ϑ^*, κ_i^* and ι_j^* are the optimal LMs of ξ_j, ϑ, κ_i and ι_j, respectively. Considering the correlation condition (5.36) and the definition of the function $\mathcal{F}\left(\tilde{s}_{ij}\right)$ in (5.54), the differentiation of the Lagrangian function $\mathcal{L}\left(\tilde{s}_{ij},\tilde{p}_{ij},\xi_j,\vartheta,\kappa_i,\iota_j\right)$ in (5.85) over $\tilde{s}_{ij}$, represented by the KKT condition(5.87), yields that

$$\left.\frac{\partial\mathcal{L}\left(\tilde{s}_{ij},\tilde{p}_{ij},\xi_j,\vartheta,\kappa_i,\iota_j\right)}{\partial\tilde{s}_{ij}}\right|_{\left(\tilde{s}_{ij},\tilde{p}_{ij},\xi_j,\vartheta,\kappa_i,\iota_j\right)=\left(\tilde{s}_{ij}^*,\tilde{p}_{ij}^*,\xi_j^*,\vartheta^*,\kappa_i^*,\iota_j^*\right)} =$$

$$\underbrace{\left(1-\mathcal{P}_{app}\right)\left(\frac{\log_2\left(1+\dfrac{\hbar_{ij}\tilde{p}_{ij}^*\left|h_{ij}\right|^2}{\tilde{s}_{ij}^*}\right)-\dfrac{\hbar_{ij}\tilde{p}_{ij}^*\left|h_{ij}\right|^2}{\ln 2\left(\tilde{s}_{ij}^*+\hbar_{ij}\tilde{p}_{ij}^*\left|h_{ij}\right|^2\right)}}{\left(1-\mathcal{P}_{app}\right)\tilde{s}_{ij}^*\log_2\left(1+\dfrac{\hbar_{ij}\tilde{p}_{ij}^*\left|h_{ij}\right|^2}{\tilde{s}_{ij}^*}\right)-\left(\tilde{q}_j\left(F,T_j^{\max},\lambda_j\right)-1\right)}\right)}_{\mathcal{F}\left(\tilde{s}_{ij}^*\right)}-\kappa_i^*=\mathcal{F}_{ij}\left(\tilde{s}_{ij}^*\right)-\kappa_i^*=0\,. \tag{5.105}$$

From (5.105) we conclude the following relationship between the function $\mathcal{F}\left(\tilde{s}_{ij}^*\right)$ and the optimal LM κ_i^*

$$\mathcal{F}_{ij}\left(\tilde{s}_{ij}^*\right)=\kappa_i^*\,. \tag{5.106}$$

Differentiating the function $\mathcal{F}_{ij}\left(\tilde{s}_{ij}^{*}\right)$ with respect to $\tilde{s}_{ij}^{*}$, it is easy to verify that the derivation is negative, e.g., $\partial\mathcal{F}_{ij}\left(\tilde{s}_{ij}^{*}\right)/\partial\tilde{s}_{ij}^{*}<0$ for all $\tilde{s}_{ij}^{*}>\tilde{s}_{ij}^{\min}$ [79]. Hence, the function $\mathcal{F}_{ij}\left(\tilde{s}_{ij}^{*}\right)$ strictly decreases and its inverse function $\mathcal{F}_{ij}^{-1}\left(\tilde{s}_{ij}^{*}\right)$ exists for $\tilde{s}_{ij}^{*}>0$, e.g.,

$$\tilde{s}_{ij}^{*}=\mathcal{F}_{ij}^{-1}\left(\kappa_{i}^{*}\right). \tag{5.107}$$

Moreover, differentiating the Lagrangian function $\mathcal{L}\left(\tilde{s}_{ij},\tilde{p}_{ij},\xi_{j},\vartheta,\kappa_{i},\iota_{j}\right)$ in (5.85) over κ_{i}^{*}, which corresponds to the KKT condition(5.90), we get that

$$\left.\frac{\partial\mathcal{L}\left(\tilde{s}_{ij},\tilde{p}_{ij},\xi_{j},\vartheta,\kappa_{i},\iota_{j}\right)}{\partial\kappa_{i}}\right|_{\left(\tilde{s}_{ij},\tilde{p}_{ij},\xi_{j},\vartheta,\kappa_{i},\iota_{j}\right)=\left(\tilde{s}_{ij}^{*},\tilde{p}_{ij}^{*},\xi_{j}^{*},\vartheta^{*},\kappa_{i}^{*},\iota_{j}^{*}\right)}=\left(\sum_{j=1}^{K}\tilde{s}_{ij}^{*}\right)-1=0. \tag{5.108}$$

Hence, accounting the relations in (5.107) and (5.108) we conclude that

$$\sum_{j=1}^{K}\mathcal{F}_{ij}^{-1}\left(\kappa_{i}^{*}\right)=1. \tag{5.109}$$

Proposition 5.3 - If the function $\mathcal{X}$ is defined as $\mathcal{X}\equiv\sum_{j=1}^{K}\mathcal{F}_{ij}^{-1}\left(\kappa_{i}^{*}\right)$ then its inverse function $\mathcal{X}^{-1}$ exists for $\mathcal{X}\left(\kappa_{i}^{*}\right)$.

Proof - From the fact that that the derivation of $\mathcal{F}_{ij}\left(\tilde{s}_{ij}^{*}\right)$ over $\tilde{s}_{ij}^{*}$ is negative, e.g., $\partial\mathcal{F}_{ij}\left(\tilde{s}_{ij}^{*}\right)/\partial\tilde{s}_{ij}^{*}<0$ we can compute that the derivation of $\mathcal{X}\left(\kappa_{i}^{*}\right)$ over κ_{i}^{*} is also negative, e.g.,

$$\frac{\partial\mathcal{X}\left(\kappa_{i}^{*}\right)}{\partial\kappa_{i}^{*}}=\frac{\partial\sum_{j=1}^{K}\mathcal{F}_{ij}^{-1}\left(\kappa_{i}^{*}\right)}{\partial\kappa_{i}^{*}}=\sum_{j=1}^{K}\left\{\frac{1}{\frac{\partial\mathcal{F}_{ij}\left(\tilde{s}_{ij}^{*}\right)}{\partial\tilde{s}_{ij}^{*}}}\right\}<0,\ \forall i. \tag{5.110}$$

[79] We recall that $\tilde{s}_{ij}^{\min}>0$ is the unique solution of $\tilde{r}_{j}=\left(\tilde{q}_{j}\left(F,T_{j}^{\max},\lambda_{j}\right)-1\right)$.

Thus, $\mathcal{X}\left(\kappa_i^*\right)$ strictly decreases and its inverse function $\mathcal{X}^{-1}(\cdot)$ does exist. This completes the proof of *Proposition 5.3*. ■

From (5.110) and *Proposition 5.3* we can define the optimal LM κ_i^* as

$$\kappa_i^* = \mathcal{X}^{-1}(1),\ \forall i\,. \tag{5.111}$$

From (5.111) and (5.109) we finally derive the optimal subcarrier allocation index $\tilde{s}_{ij}^*$ as

$$\tilde{s}_{ij}^* = \mathcal{F}_{ij}^{-1}\left(\kappa_i^*\right),\ \forall i, j\,,$$

which resolves equation (5.46) of *Theorem 5.5*. This completes the proof of *Theorem 5.5*. ■

We remark that in equation (5.46) of Theorem 5.5 the chance for the optimal subcarrier allocation index $\tilde{s}_{ij}^*$ to be the same for different SUs happens only with probability 0. This is because the imperfect channel realizations $\left|\hat{h}_{ij}\right|^2$ are i.i.d. for different SUs, e.g., for SUs j and j' it stands that $\left|\hat{h}_{ij}\right|^2 \neq \left|\hat{h}_{ij'}\right|^2$, hence it is ensured that the function $\mathcal{F}_{ij}^{-1}\left(\kappa_i^*\right)$ is also different for different SUs, e.g., $\mathcal{F}_{ij}^{-1}\left(\kappa_i^*\right) \neq \mathcal{F}_{ij'}^{-1}\left(\kappa_i^*\right),\ \forall i, j \neq j'$.

C.5 Optimal Transmitting Power in Compliance with the S-NBS Principle - Proofs of *Theorem 5.6*

In this Appendix we determine the optimal transmitting power allocation $\tilde{p}_{ij}^*$ for SU j on subcarrier i. From the KKT condition (5.86), the differentiation of the Lagrangian function $\mathcal{L}\left(\tilde{s}_{ij}, \tilde{p}_{ij}, \xi_j, \vartheta, \kappa_i, \iota_j\right)$ in (5.85) over $\tilde{p}_{ij}$ yields the optimal channel allocation index $\tilde{p}_{ij}^* > 0$ of SU j on subcarrier i to be global maxima, e.g.,

$$\left.\frac{\partial \mathcal{L}\left(\tilde{s}_{ij}, \tilde{p}_{ij}, \xi_j, \vartheta, \kappa_i, \iota_j\right)}{\partial \tilde{p}_{ij}}\right|_{\left(\tilde{s}_{ij}, \tilde{p}_{ij}, \xi_j, \vartheta, \kappa_i, \iota_j\right) = \left(\tilde{s}_{ij}^*, \tilde{p}_{ij}^*, \xi_j^*, \vartheta^*, \kappa_i^*, \iota_j^*\right)} = 0 \qquad \Leftrightarrow$$

$$\frac{\dfrac{\hbar_{ij}\sigma_h^2\cdot\mathbb{F}^{-1}_{\left(\left|\hat{h}_{ij}\right|^2/\sigma_h^2\right)_2}\left(\mathcal{P}_{app}\right)}{\ln 2\cdot\left(1+\dfrac{\hbar_{ij}\tilde{p}_{ij}^*\sigma_h^2}{\tilde{s}_{ij}^*}\cdot\mathbb{F}^{-1}_{\left(\left|\hat{h}_{ij}\right|^2/\sigma_h^2\right)_2}\left(\mathcal{P}_{app}\right)\right)}}{\tilde{s}_{ij}^*\cdot\log_2\left(1+\dfrac{\hbar_{ij}\tilde{p}_{ij}^*\sigma_h^2}{\tilde{s}_{ij}^*}\cdot\mathbb{F}^{-1}_{\left(\left|\hat{h}_{ij}\right|^2/\sigma_h^2\right)_2}\left(\mathcal{P}_{app}\right)\right)-\dfrac{\left(\tilde{q}_j\left(F,T_j^{\max},\lambda_j\right)-1\right)}{\left(1-\mathcal{P}_{app}\right)}}-\frac{1}{N_F}\vartheta^*-\xi_j^*+\iota_j^*\left|\hat{h}_{ij}\right|^2=0\quad\Leftrightarrow$$

$$\left(\tilde{s}_{ij}^*\cdot\log_2\left(1+\frac{\hbar_{ij}\tilde{p}_{ij}^*\sigma_h^2}{\tilde{s}_{ij}^*}\cdot\mathbb{F}^{-1}_{\left(\left|\hat{h}_{ij}\right|^2/\sigma_h^2\right)_2}\left(\mathcal{P}_{app}\right)\right)-\frac{\left(\tilde{q}_j\left(F,T_j^{\max},\lambda_j\right)-1\right)}{\left(1-\mathcal{P}_{app}\right)}\right)$$

$$\times\left(1+\frac{\hbar_{ij}\tilde{p}_{ij}^*\sigma_h^2}{\tilde{s}_{ij}^*}\cdot\mathbb{F}^{-1}_{\left(\left|\hat{h}_{ij}\right|^2/\sigma_h^2\right)_2}\left(\mathcal{P}_{app}\right)\right)=\frac{\hbar_{ij}\sigma_h^2\cdot\mathbb{F}^{-1}_{\left(\left|\hat{h}_{ij}\right|^2/\sigma_h^2\right)_2}\left(\mathcal{P}_{app}\right)}{\ln 2\cdot\left(\dfrac{1}{N_F}\vartheta^*+\xi_j^*-\iota_j^*\left|\hat{h}_{ij}\right|^2\right)}\cdot \tag{5.112}$$

For notational brevity, let us define the variables $\mathcal{X}_{ij}^*$ and $\mathcal{Z}_{ij}^*$ denoted by

$$\mathcal{X}_{ij}^*=1+\frac{\hbar_{ij}\tilde{p}_{ij}^*\sigma_h^2}{\tilde{s}_{ij}^*}\cdot\mathbb{F}^{-1}_{\left(\left|\hat{h}_{ij}\right|^2/\sigma_h^2\right)_2}\left(\mathcal{P}_{app}\right) \tag{5.113}$$

and

$$\mathcal{Z}_{ij}^*=\frac{\hbar_{ij}\sigma_h^2\cdot\mathbb{F}^{-1}_{\left(\left|\hat{h}_{ij}\right|^2/\sigma_h^2\right)_2}\left(\mathcal{P}_{app}\right)}{\ln 2\cdot\left(\dfrac{1}{N_F}\vartheta^*+\xi_j^*-\iota_j^*\left|\hat{h}_{ij}\right|^2\right)}, \tag{5.114}$$

respectively. Then from (5.113) and (5.114) the equation in (5.112) becomes

$$\mathcal{X}_{ij}^*\left(\tilde{s}_{ij}^*\cdot\log_2\left(\mathcal{X}_{ij}^*\right)-\frac{\left(\tilde{q}_j\left(F,T_j^{\max},\lambda_j\right)-1\right)}{\left(1-\mathcal{P}_{app}\right)}\right)=\mathcal{Z}_{ij}^*\Leftrightarrow$$

$$\tilde{s}_{ij}^*\cdot\log_2\left(\mathcal{X}_{ij}^*\right)^{\mathcal{X}_{ij}^*}=\mathcal{X}_{ij}^*\frac{\left(\tilde{q}_j\left(F,T_j^{\max},\lambda_j\right)-1\right)}{\left(1-\mathcal{P}_{app}\right)}+\mathcal{Z}_{ij}^*. \tag{5.115}$$

It is easy to discriminate that the equation in (5.115) is a transcendental algebraic equation over the variable $\mathcal{X}_{ij}^*$, e.g., it has the form $\log\left(x\right)^x=ax+b$, $a,b>0$. Although other

studies provide numerical or graphical solutions to equations similar to (5.115), we propose the following solution methodology to define $\mathcal{X}_{ij}^{*}$ and hence, the optimal transmitting power $\tilde{\mathcal{P}}_{ij}^{*}$ by means of final formulas.

Let us suppose that the term $\left(\tilde{q}_j\left(F,T_j^{\max},\lambda_j\right)-1\right)/\left(1-\mathcal{P}_{app}\right)$ at the right side of the equation in (5.115) is equal to $\tilde{s}_{ij}^{*}\log_2\left(\mathcal{U}_{ij}^{*}\right)$, e.g.,

$$\frac{\left(\tilde{q}_j\left(F,T_j^{\max},\lambda_j\right)-1\right)}{\left(1-\mathcal{P}_{app}\right)}=\tilde{s}_{ij}^{*}\log_2\left(\mathcal{U}_{ij}^{*}\right), \tag{5.116}$$

with the variable $\mathcal{U}_{ij}^{*}$ to be defined as

$$\mathcal{U}_{ij}^{*}=2^{\frac{\left(\tilde{q}_j\left(F,T_j^{\max},\lambda_j\right)-1\right)}{\tilde{s}_{ij}^{*}\left(1-\mathcal{P}_{app}\right)}}>1. \tag{5.117}$$

Then from (5.116) and (5.117) the equation in (5.115) becomes

$$\tilde{s}_{ij}^{*}\cdot\log_2\left(\mathcal{X}_{ij}^{*}\right)^{\mathcal{X}_{ij}^{*}}=\tilde{s}_{ij}^{*}\log_2\left(\mathcal{U}_{ij}^{*}\right)^{\mathcal{X}_{ij}^{*}}+\mathcal{Z}_{ij}^{*}\Leftrightarrow$$

$$\tilde{s}_{ij}^{*}\cdot\log_2\left(\mathcal{X}_{ij}^{*}\right)^{\mathcal{X}_{ij}^{*}}-\tilde{s}_{ij}^{*}\log_2\left(\mathcal{U}_{ij}^{*}\right)^{\mathcal{X}_{ij}^{*}}=\mathcal{Z}_{ij}^{*}\Leftrightarrow$$

$$\tilde{s}_{ij}^{*}\cdot\log_2\left(\frac{\mathcal{X}_{ij}^{*}}{\mathcal{U}_{ij}^{*}}\right)^{\mathcal{X}_{ij}^{*}}=\mathcal{Z}_{ij}^{*}\quad . \tag{5.118}$$

Multiplying both sides of (5.118) with $1/\mathcal{U}_{ij}^{*}$ it becomes

$$\frac{1}{\mathcal{U}_{ij}^{*}}\tilde{s}_{ij}^{*}\cdot\log_2\left(\frac{\mathcal{X}_{ij}^{*}}{\mathcal{U}_{ij}^{*}}\right)^{\mathcal{X}_{ij}^{*}}=\frac{1}{\mathcal{U}_{ij}^{*}}\mathcal{Z}_{ij}^{*}\Leftrightarrow$$

$$\tilde{s}_{ij}^{*}\cdot\log_2\left(\frac{\mathcal{X}_{ij}^{*}}{\mathcal{U}_{ij}^{*}}\right)^{\frac{\mathcal{X}_{ij}^{*}}{\mathcal{U}_{ij}^{*}}}=\frac{\mathcal{Z}_{ij}^{*}}{\mathcal{U}_{ij}^{*}}. \tag{5.119}$$

Defining the variable $\mathcal{Y}_{ij}^{*}$ as

$$\mathcal{Y}_{ij}^{*}=\frac{\mathcal{X}_{ij}^{*}}{\mathcal{U}_{ij}^{*}}, \tag{5.120}$$

then equation (5.119) becomes

$$\tilde{S}_{ij}^{*}\cdot\log_2\left(\mathcal{Y}_{ij}^{*}\right)^{\mathcal{Y}_{ij}^{*}}=\frac{\mathcal{Z}_{ij}^{*}}{\mathcal{U}_{ij}^{*}}\Leftrightarrow$$

$$\mathcal{Y}_{ij}^{*\mathcal{Y}_{ij}^{*}}=2^{\frac{\mathcal{Z}_{ij}^{*}}{\mathcal{U}_{ij}^{*}\tilde{S}_{ij}^{*}}}. \tag{5.121}$$

To solve the equation (5.121) over $\mathcal{Y}_{ij}^{*}$ we use the Lambert-*W* function's property [158] according to which if $x^x=z$ then $z=\exp\left(W\left(\ln\left(z\right)\right)\right)$ or $z=\ln\left(z\right)/W\left(\ln\left(z\right)\right)$, where $W\left(\cdot\right)$ denotes the Lambert-*W* function. Hence, (5.121) yields that

$$\mathcal{Y}_{ij}^{*}=\exp\left(W\left(\ln\left(2^{\frac{\mathcal{Z}_{ij}^{*}}{\mathcal{U}_{ij}^{*}\tilde{S}_{ij}^{*}}}\right)\right)\right),^{80} \tag{5.122}$$

In continue, with in sequence substitutions of the variables $\mathcal{Y}_{ij}^{*}$, $\mathcal{U}_{ij}^{*}$, $\mathcal{Z}_{ij}^{*}$ and $\mathcal{X}_{ij}^{*}$ as defined in (5.120), (5.117), (5.114) and (5.113), respectively, into equation (5.122), we easily derive the optimal transmitting power $\tilde{\mathcal{P}}_{ij}^{*}$, e.g.,

$$\tilde{\mathcal{P}}_{ij}^{*}=\frac{\tilde{S}_{ij}^{*}}{\mathcal{H}_{ij}\sigma_h^2\cdot\mathbb{F}^{-1}_{\left(\left|\hat{h}_{ij}\right|^2/\sigma_h^2\right)_2}\left(\mathcal{P}_{app}\right)}\left(2^{\frac{\left(\tilde{q}_j\left(F,T_j^{\max},\lambda_j\right)-1\right)}{\tilde{S}_{ij}^{*}\left(1-\mathcal{P}_{app}\right)}}\cdot\exp\left(W\left(\ln\left(2^{\frac{\mathcal{H}_{ij}\sigma_h^2\cdot\mathbb{F}^{-1}_{\left(\left|\hat{h}_{ij}\right|^2/\sigma_h^2\right)_2}\left(\mathcal{P}_{app}\right)}{\ln 2\cdot\tilde{S}_{ij}^{*}\cdot\left(\frac{1}{N_F}\vartheta^{*}+\xi_j^{*}-\iota_j^{*}\left|\hat{h}_{ij}\right|^2\right)\cdot 2^{\frac{\left(\tilde{q}_j\left(F,T_j^{\max},\lambda_j\right)-1\right)}{\tilde{S}_{ij}^{*}\left(1-\mathcal{P}_{app}\right)}}}}\right)\right)\right)-1\right), \tag{5.123}$$

which yields the formula of the optimal transmitting power in (5.47) of *Theorem 5.6*. Finally, it is apparent that the optimal instantaneous transmitting power $\tilde{\mathcal{P}}_{ij}^{*}$ in (5.123) is always larger or equal to zero, e.g., $\tilde{\mathcal{P}}_{ij}^{*}\geq 0$.

[80] We remark that according to Lambert-*W* function's property, equation (5.122) can be also written as $\mathcal{Y}_{ij}^{*}=\ln\left(2^{\mathcal{Z}_{ij}^{*}/\left(\mathcal{U}_{ij}^{*}\tilde{S}_{ij}^{*}\right)}\right)/W\left(\ln\left(2^{\mathcal{Z}_{ij}^{*}/\left(\mathcal{U}_{ij}^{*}\tilde{S}_{ij}^{*}\right)}\right)\right)$.

In conclusion, $\tilde{p}_{ij}^{*}$ in (5.123) indicates the amount of the instantaneous optimal transmitting power on subcarrier i of each SU j. To increase power efficiency, we need to discriminate which users require less power than others and consider them as optimal SUs. This can be achieved by a simple linear search among the N_C subcarriers for the optimum SU j^{*}, given by $j^{*} = \arg\min \tilde{p}_{ij}^{*}$. Our search would be always feasible for the reason that the chance for the optimal instantaneous transmitting power $\tilde{p}_{ij}^{*}$ to be the same for different SUs happens only with probability 0, as the imperfect channel realizations $\left|\hat{h}_{ij}\right|^2$ are i.i.d. This completes the proof of *Theorem 5.6*. ■

Conclusions & Direction for Future Research

This Thesis includes three proposals each one composed of two main components; the cross-layer design and OFDMA. On one hand, the cross-layer design is an important concept for providing high spectral efficiency, QoS and fair resource allocation for integrated service of heterogeneous applications in next-generation wireless networks. On the other hand, OFDMA enhances the spectral efficiency by allowing multiple data transmission from multiple users through properly allocating the subcarriers and power according to the time-varying channel conditions. Although the numerous efforts in this research topic, the source statistics and queueing dynamics are usually ignored in previous designs. In addition, limited works consider heterogeneous users' delay requirements, the channel imperfectness is frequently neglected, while fairness considerations need to be significantly examined and improved. In particular, NBS fairness has been developed by only considering the power allocation excluding the NBS allocation of subcarriers. Above all, real-time operation has not been yet accomplished as current cross-layer designs have been approached with a solution methodology that induces Lagrange multiplier finding algorithms, which require a lot of iterations to converge. Finally, it is evident that most of existing approaches on NBS fair resource allocation provide numerical or even graphical solutions inducing explicit analytical solutions to emerge.

Accounting the abovementioned issues, our first proposal presented in Chapter 3 regards a power-efficient cross-layer scheduling scheme that provides significant performance enhancements in OFDMA systems with imperfect channel, packet outage and heterogeneous users considerations. Initially, we presented the imperfect channel model with its estimation procedure and we introduced an advantageous PBL process, compared to current approaches, to describe the average effective data rate at the PHY layer. Moreover, focusing on higher layers' dynamics we developed an advanced traffic model based on the $M/G/1/\infty/\infty$ queue to express the equivalent throughput at the cross-layer. Our cross-layer optimization problem targets to minimize the average transmitting power subject to cross-layer constraints on subcarrier and power distribution and QoS provision regulations. The proposed optimal policy has low linear complexity and performs asymptotically in terms of throughput gain due to

multi-user and multi-carrier diversity exploitations. In addition, we demonstrated that our proposal has superior scheduling versatility than relevant schemes as it significantly reduces the overall transmitting power and simultaneously it provides ideal QoS to heterogeneous users under very uncertain channel conditions.

Our second proposal, presented in Chapter 4, concerns a game-theoretic cross-layer scheduling scheme that provides performance enhancements in OFDMA systems with imperfect channel, packet outage, heterogeneous QoS and asymmetric users' payoffs. We introduced a PBL process that fully complies with the A-NBS fairness of power and subcarrier allocation in contrary to existing approaches that consider only the NBS of power. Our PBL describes each weighted user's level of satisfaction in terms of effective throughput under channel and packet outage, and it has been utilized as maximization objective in the cross-layer problem. We approached the solution of our cross-layer problem with a different than existed scope that results iteration-independent optimal policies and also enhances system's power efficiency. Within our scope we introduced an innovative methodology to provide solutions by means of final formulas to the transcendental algebraic equations that appear during the optimization process due to the recursive origin of the A-NBS problem. Our proposed solution is the first iteration-independent allocation policy with actual linear complexity in the number of users and subcarriers, which allows our system to perform real-time operation.

Our third proposal, presented in Chapter 5, regards imporoved exploitations of spectrum scarcity utilising the enabling technology of CRs. In particular, we introduced an iteration-independent game-theoretic cross-layer scheduling scheme, which provides performance enhancements in CR systems with imperfect channel, packet outage and heterogeneous SUs. We formulated a PBL process to describe each SU's level of satisfaction in terms of effective throughput under channel and packet outage. Our PBL process fully complies with the S-NBS fairness of power and subcarrier allocation in contrary to existing approaches that consider only the NBS of power. Furthermore, we established an important cross-layer relationship between each SU's traffic arrival rate at higher layers with power-driven system regulations for transmission interference cancelation between PUs and SUs. We then maximized the average SUs' satisfaction in terms of throughput, subject to subcarrier, power, QoS and transmission interference cancelation constraints. We also established an important feasibility condition to show the region where our game-theoretic

cross-layer optimization problem is convex over a feasible convex set. Our optimal solution has been provided by means of final formulas, with actual linear complexity in the number of users and subcarriers favouring that way real-time system operation. We have also shown that our design performs asymptotically in terms of throughput gain due to multi-user and multi-carrier diversity exploitations, providing ideal fairness and maintaining the system's effective throughput at remarkably high levels under various uncertain channel conditions.

In follow, we recommend aspects for future research.

- *Development of the Propoed Schemes for Multi-Cell Networks*: The introduced designs assume single-cell environments. However, our proposals can be extended to multi-cell enviroments, where system's performance can be further increased exploiting the intercell diversity, which is as important as other system diversities such as multi-channel and multi-user diversity discussed in the Thesis.

- *Uplink Phase*: Our proposed cross-layer designs address the downlink phase of OFDMA transmissions. Nevertheless, further investigations on uplink scenarios are of great interest.

- *Multiple-Input-Multiple-Output (MIMO) Technology*: It is widely recognised that MIMO systems with OFDM spectrum access bring substantial improvements in systems' throughput. MIMO-OFDM technology has high spectral efficiency and link reliability offering significant increases in data throughput and link range without additional bandwidth or transmiting power. Hence, our proposals can be further evolved by considering such scenarios.

- *Wireless Mesh Ad-Hoc Networks*: Another worthmentioned aspect is to develop our designs considering Mesh Ad-Hoc network topology. In such case we can propose attractive cross-layer solutions with higher performance and more flexible deployment for fixed and mobile broadband wireless access than the star network topology adopted in this Thesis.

List of Abbreviations

3G LTE	Third Generation Long Term Evolution
ADSL	Asymmetric Digital Subscriber Line
A-NBS	Asymmetric Nash Bargaining Solution
APA	Adaptive Transmitting power allocation
BER	Bit Error Rate
CDF	Cumulative Density Function
CDM	Code Division Multiplexing
CDMA	Code Division Multiple Access
CP	Cyclic Prefix
CPU	Central Processing Unit
CR	Cognitive Radio
CSCG	Circularly Symmetric Complex Gaussian
CSI	Channel State Information
CSIR	Channel State Information at the Receiver
CSIT	Channel State Information at the Transmitter
CSMA	Carrier Sense Multiple Access
DAB	Digital Audio Broadcasting
DFT	Discrete Fourier Transformation
DSA	Dynamic Subcarrier Allocation
DSP	Digital Signal Processor
ECS	Error-Considerate Scheduler
ECS-CR	Error Considerate opportunistic Scheduler for Cognitive Radio systems
EIF	Exponential Integral Function
EIFAS	Error-Inconsiderate Fixed Assignment Scheduler
EIFAS-CR	Error Inconsiderate and Fixed Assignment Scheduler for Cognitive Radio systems
EIOS	Error-Inconsiderate Opportunistic Scheduler
EIOS-CR	Error Inconsiderate Opportunistic Scheduler for Cognitive Radio systems
EIS-NBS-CR	Error Inconsiderate Scheduler Nash Bargaining-based for Cognitive Radio systems
ETSI- BRAN	European Telecommunication Standards Institute Broadband Radio Access Network
FDD	Frequency Division Duplex
FDM	Frequency Division Multiplexing
FDMA	Frequency Division Multiple Access
FFT	Fast Fourier Transformation
FIFO	First In First Out
FIR	Finite Impulse Response
i.i.d	Independent and identically distributed
ICI	Inter Channel Interference

IDFT	Inverse Discrete Fourier Transformation
IEEE	Institute of Electrical & Electronics Engineers
IFFT	Inverse Fast Fourier Transformation
ISI	Inter Symbol Interference
ISI	Inter Symbol Interference
LIFO	Last In First Out
LL	Local Loop
LM	Lagrangian Multipliers
M/D/1	Memoryless/Degenerate Distributed/Single Server
M/G/1	Memoryless/General/Single Server
M/M/1	Memoryless/Markovian/Single Server
MAC	Medium Access Control
M-M	Max-Min
MMAC	Multimedia Mobile Access Communications
MM-CR	Max-Min scheduler for Cognitive Radio systems
MMPP/G/1	Markov Modulated Poisson Process/General/Single Server
MMSE	Minimum Mean Square Error
MSE	Minimum Square Error
NBS	Nash Bargaining Solution
NP	Non Polynomial-time
NPCG	Non Cooperative Power Control Game
OFDM	Orthogonal Frequency Division Multiplexing
OFDMA	Orthogonal Frequency Division Multiple Access
OSI	Open System Interconnection
PARP	Peal-to-Average Power Ratio
PBL	Power-Bit-Loading
PDF	Probability Density Function
PE-AETS	Power-Efficient Adaptive Error-Tolerant Scheduler
PHY	Physical
PR	Priority
PS	Parallel-to-Serial
PSK	Phase Shift Keying
PU	Primary User
QAM	Quadrature Amplitude Modulation
QoS	Quality-of-Service
QSI	Queue State Information
SDM	Space Division Multiplexing
SDMA	Space Division Multiple Access
SINR	Signal-to-Interference-plus-Noise Ratio
SIRO	Service In Random Order
S-NBS	Symmetric Nash Bargaining Solution
S-NBS-CR	Symmetric Nash Bargaining Solution for Cognitive Radio systems
SNR	Signal-to-Noise Ratio
SoC	System on Chip
SP	Serial-to-Parallel
SPT	Shortest Processing Time

SS	Spread Spectrum
SU	Secondary User
SUI	Stanford University Interim
TDD	Time Division Duplex
TDM	Time Division Multiplexing
TDMA	Time Division Multiple Access
VLSI	Very Large Scale Systems
WiFi	Wireless Fidelity
WiMAX	Worldwide Interoperability for Microwave Access

List of Symbols

Symbol	Description	Units
f_j	Utility function of a user or a player j	-
j	Index of a user or player	-
K	Maximum number of users or players or CR users	-
u_j^0	Minimum utility of a user or a player j to join a game	*Bits/sec/Hz*
$\mathbf{f}$	Vector of the utility functions f_j	-
$\mathbf{u^0}$	Vector of the initial utilities u_j^0	-
$\Im$	Set of game strategies in a bargaining game	-
Ψ	Space of the utility vectors $f = (f_1,..., f_K)$	-
Ψ_0	Feasible space of Ψ	-
ψ	Nash bargaining point	-
S	Set-valued function that represents a utility-based bargaining solution	-
G	Representation of the bargaining problem	-
S^{NBS}	Set-valued function that represents a solution in utility-based Nash bargaining games	-
S^{SNBS}	Set-valued function that represents a solution in utility-based symmetric Nash bargaining games	-
J	Subset of indices of users who are able to achieve a performance strictly superior to their initial performance	-
w_j	Weight of a user or a player j	-
S^{ANBS}	Set-valued function that represents a solution in utility-based asymmetric Nash bargaining games	-
ψ^{sym}	Symmetric Nash bargaining point	-
ψ^{asym}	Asymmetric Nash bargaining point	-
i	Subcarrier index	-
N_F	Maximum number of OFDMA subcarriers or channels	-
α	Known positive constant	-
β	Known positive constant	-
δ	A positive and usually small number	-

λ_j	Poisson arrival rate of user or player j	*packets/time slot*
N_F	Maximum number of subcarriers	-
BW	Bandwidth of a channel	*Hz*
t_s	Duration of a time/scheduling slot	*sec*
Θ	Maximum number of paths in a multiple channel	-
Δf_c	Coherent bandwidth of a channel	*Hz*
n	OFDM-block index	-
$\mathbf{y}_j(n)$	Complex-valued vector of the received OFDM symbols of user j at time slot n	-
$\mathbf{x}_j(n)$	Complex-valued vector of the transmitted OFDM symbols of user j at time slot n	-
$y_{ij}(n)$	Received OFDM block of user j on subcarrier i at time slot n	-
$x_{ij}(n)$	Transmitted OFDM block of user j on subcarrier i at time slot n	-
$\mathbf{H}(n)$	Matrix of the channel gain of all users over all subcarriers at time slot n	-
$\mathbf{h}_j(n)$	Vector of the channel gains of user j at time slot n	-
$h_{ij}(n)$	Channel gain of user j on subcarrier i at time slot n	*dB*
θ	Index of the paths in a multipath channel	-
$h_{ij}(n)$	Channel gain of user j on path θ at time slot n	*dB*
$\sigma^2_{j\theta}$	CSCG variance of the channel gain of user j on path θ at time slot n	-
$h_j(n)$	Channel gain of user j at time slot n	*dB*
$\mathbf{M}_h$	Covariance matrix of the channel gain vectors $\mathbf{h}_j(n)$	-
f_d	Doppler frequency	*Hz*
$\mathbf{z}_j(n)$	Vector of CSCG noise of a user j at time slot n	-
$z_{ij}(n)$	CSCG noise of user j on subcarrier i at time slot n	*dB*
σ^2_z	CSCG noise variance	-
N_0	Noise density	-
p_{ij}	Instantaneous transmitting power of PE-AETS from the BS to user j on subcarrier i	*dBm*

$\mathbf{P}$	Transmitting power allocation policy of PE-AETS	-
r_{ij}	Data rate allocated from the BS to user j on subcarrier i of PE-AETS	*bits/sec/Hz*
$\mathbf{D}$	Set of the possible number of information that can be transmitted by a subcarrier	-
D	Maximum number of bits that can be transmitted by a subcarrier	*bits*
$\mathbf{R}$	Data rate allocation policy of PE-AETS	-
$\mathbf{S}$	Subcarrier allocation policy of PE-AETS	-
s_{ij}	Subcarrier allocation index of user j on subcarrier i of PE-AETS	-
P_{TOTAL}	Total available power at the BS	*dBm*
ς	Uplink dedicated pilot symbols for MMSE estimation	-
$\hat{\mathbf{h}}_j$	Vector of the estimated channel gains of user j	-
$\hat{h}_{ij}$	Estimated channel gain of user j on subcarrier i	*dB*
$\mathbf{h}_j$	Vector of the channel gains of user j	-
h_{ij}	Actual channel gain of user j on subcarrier i	*dB*
$\Delta\hat{\mathbf{h}}_j$	Vector of the channel gain errors of user j	-
Δh_{ij}	Channel gain error of user j on subcarrier i	*dB*
Θ_{FR}	Maximum number of OFDM symbols in a frame (used for CSIT update)	-
$\mathbf{h}\left((\rho+\delta)\Theta_{FR}\right)$	MMSE estimator with horizon $(\rho+\delta)\Theta_{FR}$	-
δ	Known positive number	-
ρ	Number of observations during the estimation process	-
$\mathbf{M}_{\Delta h}$	Covariance matrix of channel error	-
$\Delta\hat{\mathbf{h}}_j$	Vector of the channel error for user j	-
σ_h^2	MMSE variance	-
$\mathbf{W}_\Theta$	Truncated unit-norm FFT matrix	-
$\mathbf{y}_\varsigma(\rho)$	Vector of the received pilot symbols ς for ρ observations	-
$\mathbf{\Sigma}$	Matrix of the pilot symbols ς	-
t	Time instance	*sec*
P_t	Uplink transmitting power for the CSIT estimation at time instance t	*dBm*

$\mathbf{M}_y$	Auto-correlation matrix of the received signal vector $\mathbf{y}$	-
$\mathbf{M}_{xy}$	Cross-correlation matrix between the received $\mathbf{y}$ and transmitted signal $\mathbf{x}$	-
$\mathbf{F}$	Optimal filter of the MMSE estimation	-
$\mathbf{M}_x$	Auto-correlation matrix of the transmitted signal vector $\mathbf{x}$	-
$\mathbf{M}_\varsigma$	The $\varsigma \times \varsigma$ matrix with entries to denote the correlation between the received symbols based on the time-varying actual channel gain modelling and the ς pilot symbols	-
$\mathbf{x}_{\mathbf{M}_\varsigma}$	The $\varsigma \times 1$ vector that denotes the correlation between the incoming OFDM symbols on the multiple paths, which is based on the ς pilot symbols and our $(\rho + \delta)\Theta_{FR}$ measurements	-
$T_j^{\max}$	Delay constraint of user j representing its maximum delay tolerance	*time slots*
F	Size of a packet at each user j's queue	*bits*
$\hat{\mathbf{H}}$	Matrix of the estimated channel gain of PE-AETS	-
$\mathbf{Q}$	Vector of the QSI of PE-AETS	-
$(\hat{\mathbf{H}}, \mathbf{Q})$	System state depended on the system dynamics $\hat{\mathbf{H}}$ and $\mathbf{Q}$ of PE-AETS	-
..	Subcarrier allocation policy of PE-AETS at the MAC layer, depended on the system dynamics $\hat{\mathbf{H}}$ and $\mathbf{Q}$	-
$\mathbf{P}[\hat{\mathbf{H}}, \mathbf{Q}]$	Transmitting power allocation policy of PE-AETS at the MAC layer, depended on the system dynamics $\hat{\mathbf{H}}$ and $\mathbf{Q}$	-
$\mathbf{R}[\hat{\mathbf{H}}, \mathbf{Q}]$	Rate allocation policy of PE-AETS at the MAC layer, depended on the system dynamics $\hat{\mathbf{H}}$ and $\mathbf{Q}$	-
$W(x_{ij}; y_{ij} \mid h_{ij})$	Actual instantaneous mutual information between input x_{ij} and output y_{ij} given the actual channel gain h_{ij} of user j on subcarrier i of PE-AETS	-
$P_{out,ij}$	Target data outage probability of user j on subcarrier i of PE-AETS	-
P_{out}	Target data outage probability of PE-AETS	-
$\tilde{r}_{ij}$	Approximated instantaneous effective data rate of user j on subcarrier i of PE-AETS	*bits/sec/Hz*
$\tilde{r}_j$	Approximated effective data rate of user j of PE-AETS	*bits/sec/Hz*

$\tilde{W}\left(x_{ij};y_{ij}\middle\|\hat{h}_{ij}\right)$	Approximated instantaneous mutual information between input x_{ij} and output y_{ij} given the estimated channel gain $\hat{h}_{ij}$ of user j on subcarrier i of PE-AETS	*bits/sec/Hz*
$\mathbf{S}^*\left[\hat{h}_{ij}\right]$	Optimal subcarrier allocation policy of PE-AETS, depended on the estimated channel gain $\hat{h}_{ij}$	-
$\mathbf{P}^*\left[\hat{h}_{ij}\right]$	Optimal transmitting power allocation policy of PE-AETS, depended on the estimated channel gain $\hat{h}_{ij}$	-
$\mathbf{R}^*\left[\hat{h}_{ij}\right]$	Optimal approximated effective data rate allocation policy of PE-AETS, depended on the estimated channel gain $\hat{h}_{ij}$	-
D_j	Delay of user j	*time slot*
P_{app}	Target packet outage probability of PE-AETS	-
$\tilde{q}_j$	Equivalent traffic arrival rate at user j's queue	*bits/sec/Hz*
q_j	Equivalent traffic arrival rate at user j's queue	*bits*
q_{ij}	The number of identically distributed bits of user j on subcarrier i	*bits*
X_j	Service time of user j	*sec*
$B\left(s_{ij},\tilde{p}_{ij}\right)$	Function used for notational brevity for the proof of convexity of PE-AETS optimization problem	-
$\mathcal{H}_{B\left(s_{ij},\tilde{p}_{ij}\right)}$	Hessian matrix of the function $B\left(s_{ij},\tilde{p}_{ij}\right)$	-
$P\left(\xi_j^*,\mu^*\right)$	Function used to represent the optimal KKT condition related with PE-AETS's transmitting power allocation constraint	-
$f_j\left(\xi_j^*,\mu^*\right)$	Function used to represent the optimal KKT condition related with PE-AETS's QoS constraint	-
$\tilde{p}_{ij}$	Instantaneous transmitting power of user j on subcarrier i, derived by subcarrier time-sharing factor $s_{ij}\in(0,1]$ of PE-AETS	*dBm*
$\tilde{p}_{ij}^*$	Optimal instantaneous transmitting power allocation of user j on subcarrier i of PE-AETS	*dBm*
ξ_j	LM of user j related to QoS optimization constraints of PE-AETS	-
μ	Lagrangian multiplier related to power optimization constraints of PE-AETS	-
ν_i	LM of subcarrier i related to subcarrier optimization	-

	constraints of PE-AETS	
ξ_j^*	Optimal LM of user j related to QoS optimization constraints of PE-AETS	-
μ^*	Optimal LM related to power optimization constraints of PE-AETS	-
ν_i^*	Optimal LM of subcarrier i related to subcarrier optimization constraints of PE-AETS	-
β_{ij}, β'_{ij}, β''_{ij}, $\hat{H}_{ij}$	Variables used for notational brevity during PE-AETS's optimization process	-
s_{ij}^*	Optimal subcarrier allocation index of user j on subcarrier i of PE-AETS	-
j^*	Index of the optimal user of PE-AETS	-
$\tilde{r}_{ij}^*$	Optimal approximated instantaneous effective data rate of user j on subcarrier i of PE-AETS	*bits/sec/Hz*
PL_j	Signal path-loss between BS and user j	*dB*
d_0	Reference distance used for PL_j	*meters*
ϖ	Signal path-loss component	-
d_j	Distance between BS and user j used for PL_j	*meters*
$sd_{\sigma_{sd}^2}$	Gaussian random variable for signal shadowing	-
σ_{sd}^2	Deviation of $sd_{\sigma_{sd}^2}$	-
S_1	The $K \times N_F$ feasible set that satisfies all constraints of the A-NBS optimization problem over $\tilde{s}_{ij}$	-
S_2	The $K \times N_F$ feasible set that satisfies all constraints of the A-NBS optimization problem over $\tilde{p}_{ij}$	-
$r_{ij,EIOS}$	Time-shared data rate allocation policy of EIOS	*bits/sec/Hz*
$r_{ij,EIFAS}$	Time-shared data rate allocation policy of EIFAS	*bits/sec/Hz*
$P_{\min,EIOS}$	Minimum required power of EIOS	*dBm*
ΔP	The difference between the average available power to the BS P_{TOTAL} and the minimum required power $P_{\min,EIOS}$ of EIOS	*dBm*

$r_{P_{\min,EIOS}+\Delta P}$	EIOS data rate under power $P_{\min,EIOS}+\Delta P$	*bits/sec/Hz*
$r_{P_{\min,EIOS}}$	EIOS data rate under power $P_{\min,EIOS}$	*bits/sec/Hz*
Δr	The difference between $r_{P_{\min,EIOS}+\Delta P}$ and $r_{P_{\min,EIOS}}$ in EIOS scheduling	*bits/sec/Hz*
$C_{\max}$	Total number of users' classes	-
$P_{\min,EIFAS}$	Minimum required power of EIFAS	*dBm*
$\Delta P'$	The difference between the average available power to the BS P_{TOTAL} and the minimum required power $P_{\min,EIFAS}$ of EIFAS	*dBm*
$r_{P_{\min,EIFAS}+\Delta P'}$	EIFAS data rate under power $P_{\min,EIFAS}+\Delta P'$	*bits/sec/Hz*
$r_{P_{\min,EIFAS}}$	EIFAS data rate under power $P_{\min,EIFAS}$	*bits/sec/Hz*
$\Delta r'$	The difference between $r_{P_{\min,EIFAS}+\Delta P'}$ and $r_{P_{\min,EIFAS}}$ in EIFAS scheduling	*bits/sec/Hz*
w_j	Weight of user j	-
$\mathbb{P}$	Transmitting power allocation policy of the A-NBS scheme	-
p_{ij}	Instantaneous transmitting power of the A-NBS scheme from the BS to user j on subcarrier i	*dBm*
$\mathbb{R}$	Data rate allocation policy of the A-NBS scheme	-
r_{ij}	Data rate allocated from the BS to user j on subcarrier i of the A-NBS scheme	*bits/sec/Hz*
BER_{ij}	Bit-Error-Rate of user j on subcarrier i of the A-NBS scheme	*bits*
SNR_{ij}	Signal-to-Noise Ratio of user j on subcarrier i of the A-NBS scheme	*dB*
$\mathbb{S}$	Subcarrier allocation policy of the A-NBS scheme	-
s_{ij}	Subcarrier allocation index of user j on subcarrier i of the A-NBS scheme	-
$\hat{\mathbb{H}}$	Matrix of the estimated channel gain of the A-NBS scheme	-
$\mathbb{Q}$	Vector of the QSI of the A-NBS scheme	-
$\mathbb{W}$	Vector of users' weights of the A-NBS scheme	-
$\left(\hat{\mathbb{H}},\mathbb{Q},\mathbb{W}\right)$	System state depended on the system dynamics $\hat{\mathbb{H}}$, $\mathbb{Q}$ and $\mathbb{W}$ of the A-NBS scheme	-

$\mathbb{S}\left[\hat{\mathbb{H}},\mathbb{Q},\mathbb{W}\right]$	Subcarrier allocation policy at the MAC layer, depended on the system dynamics $\hat{\mathbb{H}}$, $\mathbb{Q}$ and $\mathbb{W}$ of the A-NBS scheme	-
$\mathbb{P}\left[\hat{\mathbb{H}},\mathbb{Q},\mathbb{W}\right]$	Transmitting power allocation policy at the MAC layer, depended on the system dynamics $\hat{\mathbb{H}}$, $\mathbb{Q}$ and $\mathbb{W}$ of the A-NBS scheme	-
$\mathbb{R}\left[\hat{\mathbb{H}},\mathbb{Q},\mathbb{W}\right]$	Rate allocation policy at the MAC layer, depended on the system dynamics $\hat{\mathbb{H}}$, $\mathbb{Q}$ and $\mathbb{W}$ of the A-NBS scheme	-
c_{ij}	Maximum capacity of subcarrier i allocated to user j of the A-NBS scheme	*bits/sec*
η_{ij}	A variable used for brevity to express the maximum capacity c_{ij} of subcarrier i allocated to user j of the A-NBS scheme	-
$\mathbb{P}_{out,ij}$	Target data outage probability of user j on subcarrier i of the A-NBS scheme	-
$\mathbb{P}_{out}$	Target data outage probability of the A-NBS scheme	-
$\tilde{r}_{ij}$	Instantaneous effective data rate of user j on subcarrier i of the A-NBS scheme	*bits/sec/Hz*
$\tilde{s}_{ij}$	Subcarrier allocation index of user j on subcarrier i of PE-AETS under time sharing considerations	-
$\tilde{p}_{ij}$	Instantaneous transmitting power of user j on subcarrier i, derived by subcarrier time-sharing factor $\tilde{s}_{ij} \in (0,1]$ of PE-AETS	*dBm*
$\tilde{\mathbf{D}}$	Set of the possible number of information that can be transmitted by a subcarrier under time-sharing considerations	-
U_j	Utility function of user j	-
$\mathbb{S}^*\left[\hat{h}_{ij}\right]$	Optimal subcarrier allocation policy of the A-NBS scheme, depended on the estimated channel gain $\hat{h}_{ij}$	-
$\tilde{s}_{ij}^*$	Optimal subcarrier allocation index of user j on subcarrier i of PE-AETS under time-sharing considerations	-
$\mathbb{P}^*\left[\hat{h}_{ij}\right]$	Optimal transmitting power allocation policy of the A-NBS scheme, depended on the estimated channel gain $\hat{h}_{ij}$	-
$\tilde{p}_{ij}^*$	Optimal instantaneous transmitting power allocation of user j on subcarrier i of the A-NBS scheme	*dBm*
$\mathbb{P}_{app}$	Target packet outage probability of the A-NBS scheme	-

$F^{-1}_{\left(\lvert h_{ij}\rvert^2/\sigma_h^2\right)}\left(\mathbb{P}_{app}\right)$	Inverse non-central chi squared CFD of $\mathbb{P}_{app}$ with 2 degrees of freedom and non-centrality parameter $\lvert h_{ij}\rvert^2 / \sigma_h^2$	-
$\tilde{r}_j$		*bits/sec/Hz*
$\Phi_{ij}(\cdot)$	A function that represents the first derivative of the utility function U_j of user j over $\tilde{s}_{ij}^*$	-
$\Xi^{-1}(\cdot)$	The inverse function of $\Xi(\cdot) \equiv \sum_{j=1}^{K} \Phi_{ij}^{-1}(\cdot)$	-
ν_i	LM of subcarrier i related to subcarrier optimization constraints of the A-NBS scheme	-
μ	LM related to power optimization constraints of the A-NBS scheme	-
ξ_j	LM of user j related to QoS optimization constraints of the A-NBS scheme	-
ε	LM related to users' weights optimization constraints of the A-NBS scheme	-
ν_i^*	Optimal LM of subcarrier i related to subcarrier optimization constraints of the A-NBS scheme	-
μ^*	Optimal LM related to power optimization constraints of the A-NBS scheme	-
ξ_j^*	Optimal LM of user j related to QoS optimization constraints of the A-NBS scheme	-
ε^*	Optimal LM related to users' weights optimization constraints of the A-NBS scheme	-
j^*	Index of the optimal user of the A-NBS scheme	-
$\mathbb{R}^*\left[\hat{h}_{ij}\right]$	Optimal effective data rate allocation policy of the A-NBS scheme, depended on the estimated channel gain $\hat{h}_{ij}$	-
$\tilde{r}_{ij}^*$	Optimal instantaneous effective data rate of user j on subcarrier i of the A-NBS scheme	*bits/sec/Hz*
A_{ij}, B_{ij}, C_{ij}, D_{ij}, Y	Variables used for notational brevity to show the iteration-independent nature of the A-NBS scheme	-
FI	Fairness index	-
R_j	Expression of user j's required data rate used to represent	*bits/sec/Hz*

	the FI in the A-NBS scheme	
$R_j^{\min}$	Expression of user j's minimum required data rate used to represent the FI in the A-NBS scheme	*bits/sec/Hz*
$\mathcal{H}_{\tilde{r}_j}$	Hessian matrix of the function $\tilde{r}_j$	-
$\tilde{s}_{ij}^{\min}$	The unique solution of $\tilde{r}_j = u_j^0$	-
τ	A variable used for notational brevity to show the validity of the proposed A-NBS optimization problem given by $\tau = \eta_{ij}\tilde{p}_{ij}\left\|h_{ij}\right\|^2 / \tilde{s}_{ij}$	-
$\mathrm{T}(\tau)$	A function used for notational brevity to show the validity of the proposed A-NBS optimization problem representing the numerator of the function $\Phi_{ij}\left(\tilde{s}_{ij}\right)$	-
$\tilde{\mathbb{r}}$	The $K\times 1$ vector that expresses the users' satisfaction level under A-NBS scheduling	-
$\mathbb{S}_1$	The $K\times N_F$ feasible set that satisfies all constraints of the A-NBS optimization problem over $\tilde{s}_{ij}$	-
$\mathbb{S}_2$	The $K\times N_F$ feasible set that satisfies all constraints of the A-NBS optimization problem over $\tilde{p}_{ij}$	-
y, z, φ_{ij}^*, υ_{ij}^*, ζ_{ij}^*, χ_{ij}^*	Variables used for notational brevity during the optimization process of the A-NBS scheme	-
$r_{ij,MM}$	Time-shared data rate allocation policy of MM	*bits/sec/Hz*
$r_{ij,WMM}$	Time-shared data rate allocation policy of WMM	*bits/sec/Hz*
$P_{\min,MM}$	Minimum required power of MM	*dBm*
$\Delta\mathbb{P}$	The difference between the average available power to the BS P_{TOTAL} and the minimum required power $P_{\min,MM}$ of MM	*dBm*
$r_{P_{\min,MM}+\Delta\mathbb{P}}$	MM data rate under power $P_{\min,MM}+\Delta\mathbb{P}$	*bits/sec/Hz*
$r_{P_{\min,MM}}$	MM data rate under power $P_{\min,MM}$	*bits/sec/Hz*
$\Delta\mathbb{r}$	The difference between $r_{P_{\min,MM}+\Delta\mathbb{P}}$ and $r_{P_{\min,MM}}$ in MM scheduling	*bits/sec/Hz*

$P_{\min,WMM}$	Minimum required power of WMM	*dBm*
$\Delta\mathbb{P}'$	The difference between the average available power to the BS P_{TOTAL} and the minimum required power $P_{\min,WMM}$ of WMM	*dBm*
$r_{P_{\min,WMM}+\Delta\mathbb{P}'}$	WMM data rate under power $P_{\min,WMM}+\Delta\mathbb{P}'$	*bits/sec/Hz*
$r_{P_{\min,WMM}}$	WMM data rate under power $P_{\min,WMM}$	*bits/sec/Hz*
$\Delta\mathbb{r}'$	The difference between $r_{P_{\min,WMM}+\Delta\mathbb{P}'}$ and $r_{P_{\min,WMM}}$ in WMM scheduling	*bits/sec/Hz*
N_C	Number of orthogonal subcarriers in the CR network.	-
$\mathcal{R}$	Data rate allocation policy for S-NBS-CR.	-
r_{ij}	Instantaneous data rate allocated to SU j on subcarrier i	*bits/sec*
$\mathcal{P}$	Power allocation policy for S-NBS-CR	-
p_{ij}	Instantaneous power allocated to SU j on subcarrier i	*dBm*
$\mathcal{BER}_{ij}$	Bit-error-rate of SU j on subcarrier i	
$\mathcal{SNR}_{ij}$	Signal-to-noise ratio of SU j on subcarrier i	*dB*
$\mathcal{D}$	Set of possible information that can be transmitted by a subcarrier in the CR system	-
$\mathcal{D}$	The maximum number of information that can be transmitted by a subcarrier in the CR system	*bits*
$\mathcal{S}$	Subcarrier allocation policy for S-NBS-CR	-
s_{ij}	Subcarrier allocation index of SU j on subcarrier i	-
$\hat{\mathcal{H}}$	Matrix of the estimated channel gain in the CR system	-
$\mathcal{Q}$	Vector of the QSI of the SUs	-
$\mathcal{M}$	Vector of the positions of SUs	-
$\left(\hat{\mathcal{H}},\mathcal{Q},\mathcal{M}\right)$	System state depended on the system dynamics $\hat{\mathcal{H}}$, $\mathcal{Q}$ and $\mathcal{M}$ of S-NBS-CR	-
$\mathcal{S}\left(\hat{\mathcal{H}},\mathcal{Q},\mathcal{M}\right)$	Subcarrier allocation policy at the MAC layer, depended on the system dynamics $\hat{\mathcal{H}}$, $\mathcal{Q}$ and $\mathcal{M}$ of S-NBS-CR	-
$\mathcal{P}\left(\hat{\mathcal{H}},\mathcal{Q},\mathcal{M}\right)$	Power allocation policy at the MAC layer, depended on the system dynamics $\hat{\mathcal{H}}$, $\mathcal{Q}$ and $\mathcal{M}$ of S-NBS-CR	-
$\mathcal{R}\left(\hat{\mathcal{H}},\mathcal{Q},\mathcal{M}\right)$	Rate allocation policy at the MAC layer, depended on the system dynamics $\hat{\mathcal{H}}$, $\mathcal{Q}$ and $\mathcal{M}$ of S-NBS-CR	-

$\gamma_{PU}^{\min}$	Predefined threshold to for protection of the communication of the PUs	*dBm*
$d_{j'}^{BS}$	Distance between BS and j' PU	*m*
$P_{j'}^{PU}$	Transmitting power of the j'-th PU	*dBm*
$d_{jj'}$	Distance between the j-th SU and the j'-th PU	*m*
ρ	Exponent of signal propagation loss in the CR system	-
$N_0^{j'}$	Noise power of the j'-th PU	*dBm*
c_{ij}	Maximum achievable capacity of SU j on subcarrier i	*bits/sec*
$\mathcal{h}_{ij}$	A variable used for brevity to express the maximum capacity c_{ij} of subcarrier i allocated to SU j of S-NBS-CR	-
$\mathcal{P}_{out,ij}$	Target channel outage probability of each subcarrier i allocated to SU j	-
$\mathcal{P}_{out,ij}$	Target channel outage probability of S-NBS-CR	-
$\tilde{r}_{ij}$	Instantaneous data rate allocated to SU j on subcarrier i in terms of time-sharing of S-NBS-CR	*bits/sec*
$\tilde{p}_{ij}$	Instantaneous power allocated to SU j on subcarrier i in terms of time-sharing of S-NBS-CR	*dBm*
$\tilde{s}_{ij}$	Subcarrier allocation index of SU j on subcarrier i in terms of time-sharing of S-NBS-CR	-
$\tilde{\mathcal{D}}$	Set of possible information that can be transmitted by a subcarrier in terms of time-sharing in the CR system	-
$\mathcal{U}$	Utility function of the S-NBS-CR optimization problem	-
$\mathcal{U}_j$	Utility function of SU j	-
$\mathcal{S}^*$	Optimal subcarrier allocation policy for S-NBS-CR	-
$\tilde{s}_{ij}^*$	Optimal subcarrier allocation index of SU j on subcarrier i in terms of time-sharing of S-NBS-CR	*bits/sec*
N_C	Number of orthogonal subcarriers in the CR network.	-
$\mathcal{R}$	Data rate allocation policy for S-NBS-CR.	-
r_{ij}	Instantaneous data rate allocated to SU j on subcarrier i	*bits/sec*
$\mathcal{P}$	Power allocation policy for S-NBS-CR	-
p_{ij}	Instantaneous power allocated to SU j on subcarrier i	*dBm*
$\mathcal{BER}_{ij}$	Bit-error-rate of SU j on subcarrier i	

$\mathcal{SNR}_{ij}$	Signal-to-noise ratio of SU j on subcarrier i	*dB*
$\mathcal{D}$	Set of possible information that can be transmitted by a subcarrier in the CR system	-
$\mathcal{D}$	The maximum number of information that can be transmitted by a subcarrier in the CR system	*bits*
$\mathcal{S}$	Subcarrier allocation policy for S-NBS-CR	-
s_{ij}	Subcarrier allocation index of SU j on subcarrier i	-
$\hat{\mathcal{H}}$	Matrix of the estimated channel gain in the CR system	-
$\mathcal{Q}$	Vector of the QSI of the SUs	-
$\mathcal{M}$	Vector of the positions of SUs	-
$\left(\hat{\mathcal{H}},\mathcal{Q},\mathcal{M}\right)$	System state depended on the system dynamics $\hat{\mathcal{H}}$, $\mathcal{Q}$ and $\mathcal{M}$ of S-NBS-CR	-
$\mathcal{S}\left(\hat{\mathcal{H}},\mathcal{Q},\mathcal{M}\right)$	Subcarrier allocation policy at the MAC layer, depended on the system dynamics $\hat{\mathcal{H}}$, $\mathcal{Q}$ and $\mathcal{M}$ of S-NBS-CR	-
$\mathcal{P}\left(\hat{\mathcal{H}},\mathcal{Q},\mathcal{M}\right)$	Power allocation policy at the MAC layer, depended on the system dynamics $\hat{\mathcal{H}}$, $\mathcal{Q}$ and $\mathcal{M}$ of S-NBS-CR	-
$\mathcal{R}\left(\hat{\mathcal{H}},\mathcal{Q},\mathcal{M}\right)$	Rate allocation policy at the MAC layer, depended on the system dynamics $\hat{\mathcal{H}}$, $\mathcal{Q}$ and $\mathcal{M}$ of S-NBS-CR	-
$\gamma_{PU}^{\min}$	Predefined threshold to for protection of the communication of the PUs	*dBm*
$d_{j'}^{BS}$	Distance between BS and j' PU	*m*
$P_{j'}^{PU}$	Transmitting power of the j'-th PU	*dBm*
$d_{jj'}$	Distance between the j-th SU and the j'-th PU	*m*
ρ	Exponent of signal propagation loss in the CR system	-
$N_0^{j'}$	Noise power of the j'-th PU	*dBm*
$P_j^{\min}$	Minimum power required by the j-th SU to satisfy its minimum QoS requirements	*dBm*
$P_j^{\max}$	Maximum interference power tolerated by the PUs	*dBm*
c_{ij}	Maximum achievable capacity of SU j on subcarrier i	*bits/sec*
$\mathcal{h}_{ij}$	A variable used for brevity to express the maximum capacity c_{ij} of subcarrier i allocated to SU j of S-NBS-CR	-

$\mathcal{P}_{out,ij}$	Target channel outage probability of each subcarrier i allocated to SU j	-
$\mathcal{P}_{out,ij}$	Target channel outage probability of S-NBS-CR	-
$\tilde{r}_{ij}$	Instantaneous data rate allocated to SU j on subcarrier i in terms of time-sharing of S-NBS-CR	*bits/sec*
$\tilde{p}_{ij}$	Instantaneous power allocated to SU j on subcarrier i in terms of time-sharing of S-NBS-CR	*dBm*
$\tilde{s}_{ij}$	Subcarrier allocation index of SU j on subcarrier i in terms of time-sharing of S-NBS-CR	-
$\tilde{\mathcal{D}}$	Set of possible information that can be transmitted by a subcarrier in terms of time-sharing in the CR system	-
$\mathcal{U}$	Utility function of the S-NBS-CR optimization problem	-
$\mathcal{U}_j$	Utility function of SU j	-
$\mathcal{S}^*$	Optimal subcarrier allocation policy for S-NBS-CR	-
$\tilde{s}_{ij}^*$	Optimal subcarrier allocation index of SU j on subcarrier i in terms of time-sharing of S-NBS-CR	*bits/sec*
$\mathcal{P}^*$	Optimal power allocation policy for S-NBS-CR	-
$\tilde{p}_{ij}^*$	Optimal instantaneous power allocated to SU j on subcarrier i in terms of time-sharing of S-NBS-CR	*dBm*
$\mathcal{R}^*$	Optimal data rate allocation policy for S-NBS-CR	-
$\tilde{r}_{ij}^*$	Optimal instantaneous data rate allocated to SU j on subcarrier i in terms of time-sharing of S-NBS-CR	*bits/sec*
$\mathcal{P}_{app}$	Target packet outage probability	-
$\mathcal{F}_{ij}(\cdot)$	A function that represents the first derivative of the utility function $\mathcal{U}_j$ of SU j over $\tilde{s}_{ij}^*$, with its inverse function to be denoted as $\mathcal{F}_{ij}^{-1}(\cdot)$	-
$\mathcal{X}^{-1}(\cdot)$	The inverse function of $\mathcal{X}(\cdot) \equiv \sum_{j=1}^{K} \mathcal{F}_{ij}^{-1}(\cdot)$	-
$\mathcal{J}^*$	Index of the optimal SU	-
ϑ	Lagrangian multiplier related with the total power constraint of the S-NBS-CR optimization problem	-
ξ_j	Lagrangian multiplier related with the transmission interference cancelation constraint of the S-NBS-CR optimization problem	-
ι_j	Lagrangian multiplier related with the minimum QoS of the SUs and the transmission interference cancelation constraint	-

	of the S-NBS-CR optimization problem	
κ_j	Lagrangian multiplier related with the subcarrier allocation constraint of the S-NBS-CR optimization problem	-
ϑ^*	Lagrangian multiplier related with the total power constraint of the S-NBS-CR optimization problem	-
ξ_j^*	Optimal Lagrangian multiplier related with the transmission interference cancelation constraint of the S-NBS-CR optimization problem	-
ι_j^*	Optimal Lagrangian multiplier related with the minimum QoS of the SUs and the transmission interference cancelation constraint of the S-NBS-CR optimization problem	-
κ_j^*	Optimal Lagrangian multiplier related with the subcarrier allocation constraint of the S-NBS-CR optimization problem	-
$\mathcal{A}_{ij}$ $\mathcal{B}_{ij}$ $\mathcal{C}_{ij}$ $\mathcal{D}_{ij}$ $\mathcal{Y}$	Variables used for notational brevity to show the iteration-independent nature of S-NBS-CR	-
a	A variable used for notational brevity to show the validity of the proposed S-NBS-CR optimization problem given by $a = \tilde{n}_{ij}\tilde{p}_{ij}\left\|h_{ij}\right\|^2 / \tilde{s}_{ij}$	-
$\mathcal{T}(a)$	A function used for notational brevity to show the validity of the proposed A-NBS optimization problem representing the numerator of the function $\mathcal{F}_{ij}\left(\tilde{s}_{ij}\right)$	-
$\tilde{\boldsymbol{r}}$	The $K\times 1$ vector that expresses the SU's satisfaction level under S-NBS-CR scheduling	-
$\mathcal{U}(\cdot)$	A function to denote the utility vector with entries the utility functions of each SU in the CR system	-
y_{ij}^* z_{ij}^* u_{ij}^* y_{ij}^* x_{ij}^*	Variables used for notational brevity during the optimization process of the S-NBS-CR scheme	-

List of Notations

Notation	Description
$U(\cdot)$	Utility-based optimization objective of a function.
$\cdot'$	A different element of a variable or a function.
$\cdot^*$	The optimal of a variable.
$\cdot^{NBS}$	Variable or function in Nash bargaining games.
$\cdot^{SNBS}$	Variable or function in symmetric Nash bargaining games.
$\cdot^{ANBS}$	Variable or function in asymmetric Nash bargaining games.
$(\cdot)^{\mathcal{T}}$	Matrix or vector transpose.
$\mathbb{R}$	Set of real numbers.
$\lfloor \cdot \rfloor$	The floor of a quantity
$[\cdot]^{\mathcal{T}}$	Matrix or vector transpose
$diag(\cdot)$	Diagonal matrix
$\mathcal{J}$	Imaginary part of a number
$\{\cdot\}$	Set of numbers/variables
$E[\cdot]$	Expected value of a variable or a function
$[\cdot]^{\mathcal{H}}$	Matrix or vector Hermitian transpose
$I_0(\cdot)$	Zero-order Bessel function
$\mathbf{I}_{(\cdot)}$	Identity matrix
$\mathcal{CN}(\cdot)$	CSCG distribution
$\mathcal{N}(\cdot)$	Gaussian distribution
$\lvert\cdot\rvert^2$	Absolute value squared of a complex number
$[\cdot]^{\dagger}$	Matrix or vector conjugate transpose
$(x\|y)$	x given y
$\Pr(\cdot)$	Probability
$p(\cdot)$	Probability density function

$Q(\cdot)$	Complementary Gaussian CDF
$E_i(\cdot)$	Exponential integral function
$(\cdot)^{-1}$	Inverse of function or variable
$frac(\cdot)$	Fraction of a variable or function
$(x)^+$	Means the maximum between 0 and x, e.g., $\max(0,x)$
$\mathcal{O}(\cdot)$	Big-*O* notation
$\mathcal{L}(\cdot)$	Lagrangian function
$1_{(\cdot)}$	Indicator function
$W(\cdot)$	Lambert-*W* function

References

[1] *Digital cellular telecommunications system (GSM) Specifications (3GPP TS 01.01 v.8.1.0)*, 1999.

[2] *IEEE. Std 802.11a: Wireless LAN Medium Access Control (MAC) and Physical Layer (PHY) Specifications*, 1999.

[3] A. Rajaniemi, "HIPERLAN Overview," 1999.

[4] H. Ekström et al., "Technical Solutions for the 3G Long-Term Evolution," vol. 44, p. 38–45, March 2006.

[5] *IEEE 802.16e, IEEE Standard for Local and Metropolitan Area Networks, Air Interface for Fixed Broadband Wireless Access Systems, Amendment 2: Physical and Medium Access Control Layers for Combined Fixed and Mobile Operation in Licensed Bands and Corrigend*, February 2006.

[6] M. Kuran and T. Tugcu, "A Survey on Emerging Broadband Wireless Access Technologies," *Elsevier Computer Networks*, vol. 51, pp. 3013-3046.

[7] Q. Zhang, W. Zhu, and Y.Q. Zhang, "End-to-End QoS for Video Delivery Over Wireless Internet," vol. 93, pp. 123-134, 2005.

[8] R. Iyengar, P. Iyer, and B. Sikdar, "Delay Analysis of 802.16 Based Last Mile Wireless Networks," *IEEE GLOBECOM*, pp. 3123-3127, November 2005.

[9] D. Niyato and E. Hossain, "Queue-Aware Uplink Bandwidth Allocation for Polling Services in 802.16 Broadband Wireless Networks," *IEEE GLOBECOM*, pp. 3702-3706, November 2005.

[10] G. Song, Y. Li, L.J. Cimini, and Jr. Zheng, "Joint Channel-Aware and Queue-Aware Data Scheduling in Multiple Shared Wireless Channels," *IEEE Wireless Communication & Networking Conference*, pp. 1939-1944, March 2004.

[11] ALTERA, *WiMAX OFDMA Ranging*., August 2006.

[12] Q. Zhao and B. M. Sadler, "A Survey of Dynamic Spectrum Access," *IEEE Signal Processing Magazine*, vol. 24, no. 3, pp. 79-89, May 2007.

[13] G. Kullarni, S. Adlakha, and M. Srivastava, "Subcarrier Allocation and Bit Loading Algorithms for OFDMA-based Wireless Networks," *IEEE Transactions on Mobile Computing*, vol. 4, no. 6, December 2005.

[14] C. Y. Wong, R. S. Cheng, K. B. Letaief, and R. D. Murch, "Multiuser OFDM with Adaptive Subcarrier, Bit, and Power Allocation," *IEEE Jounral on Selected Areas of Communications*, vol. 17, no. 10, pp. 1747-1758, October 1999.

[15] A. Leke and J. M. Cioffi, "Multicarrier Systems with Imperfect Channel Knowledge," *IEEE International Symposium on PIMRC*, vol. 2, p. 549–553, September 1998.

[16] Y. Yao and G. B. Giannakis, "Rate Maximizing Power Allocation in OFDM based on Partial Channel Knowledge," *IEEE Transactions on Wireless Communications*, vol. 4, no. 3, pp. 1073-1083, May 2005.

[17] D. J. Love and R. W. Heath, "OFDM Power Loading Using Limited Feedback," *IEEE Transactions. on Wireless Communications*, vol. 54, no. 5, pp. 1773-1780, September 2005.

[18] S. Javidi and T. Kittipiyakul, "Subcarrier Allocation in OFDMA Systems: Beyond Water-Filling," *Asilomar Conference on Signals, Systems, and Computers*, vol. 1, pp. 334-338, November 2004.

[19] V. Srivastava and M. Motani, "Cross-Layer Design: a Survey and the Road Ahead," *IEEE Communications Magazine*, vol. 43, no. 12, pp. 112- 119, December 2005.

[20] Y. Zhang and K. B. Letaief, "Adaptive Resource Allocation and Scheduling for Multiuser Packet-Based OFDM Networks," *IEEE International Conference on Communications*, vol. 5, pp. 2949-2953, June 2004.

[21] G. Song and Y. (G.) Li, "Cross-layer Optimization for OFDM Wireless Network–Part I: Theoretical Framework," *IEEE Transactions on Wireless Communications*, vol. 4, no. 2, pp. 614-624, March 2005.

[22] J. Shen, N. Yi, A. Liu, and H. Xiang, "Opportunistic Scheduling for Heterogeneous Services in Downlink OFDMA System," *IEEE International Conference on Communications and Mobile Computing*, vol. 1, pp. 260-264, 2009.

[23] M. Tao, Y. C. Zhang, and F. Liang, "Resource Allocation for Delay Differentiated Traffic in Multiuser OFDM Systems," *IEEE Transactions on Wireless Communications*, vol. 7, no. 6, pp. 2190-2201, June 2008.

[24] N. Mokari, M. R. Javan, and K. Navaie, "Cross-Layer Resource Allocation in OFDMA Systems for Heterogeneous Traffic With Imperfect CSI," *IEEE Transactions on Vehicular Technology*, vol. 59, no. 2, pp. 1011-1017, February 2010.

[25] G. Zhang, "Subcarrier and Bit Allocation for Real-Time Services in Multiuser OFDM Systems," *IEEE International Conference on Communications*, vol. 5, pp. 2985-2989, June 2004.

[26] N. B. Shroff and R. Srikant X. Lin, "A Tutorial on Cross-Layer Optimization in Wireless Networks," *IEEE Journal on Selected Areas of Communications*, vol. 24, no. 8, pp. 1452-1463, August 2006.

[27] E. Yeh, "Multi-access and Fading in Communication Networks," Department of Electrical Engineering and Computer Science, MIT, Ph.D. Thesis 2001.

[28] M. Andrews, K. Kumaran, K. Ramanan, A. Stolyar, and P. Whiting, "Providing Quality of Service over a Shared Wireless Link," *IEEE Communications Magazine*, pp. 150-154, February 2001.

[29] A. Ya. Khinchin, *Mathematical Foundations of Information Theory*, Inc. Dover Publications, Ed. New York, USA: Dover Publications, 1957.

[30] A. S. Alfa, *Queueing Theory for Telecommunications - Discrete Time Modelling of a Single Node System*: Springer, 2010.

[31] H. Luo, J. Cheng, and S. Lu, "Self-Coordinating Localized Fair Queueing in Wireless Ad-Hoc Networks," *IEEE Transactions on Mobile Computing*, vol. 3, no. 1, p. 86–98, March 2004.

[32] H. T. Cheng and W. Zhuang, "An Optimization Framework for Balancing Throughput and Fairness in Wi reless Networks with QoS Support," *EEE Transactions on Wireless Communications*, vol. 7, no. 2, pp. 584 - 593, February 2008.

[33] P.C. Fishburn, *Nonlinear Preference and Utility Theory*. Baltimore, Maryland, USA: Johns Hopkins University Press, 1988.

[34] X. Wang and Q. Zhu, "Power Control For Cognitive Radio Base On Game Theory," *International Conference in Wireless Communication Networks and Mobile Computing*, p. 1256–1259, 2007.

[35] Z. Han and K. J. R. Liu, "Noncooperative Power-Control Game and Throughput Game Over Wireless Networks," *IEEE Transaction on Communications*, vol. 53, p. 1625–1629, October 2005.

[36] Z. Han, Z. Ji, and K. J. R. Liu, "Non-cooperative Resource Competition Game By Virtual Referee In Multi-Cell OFDMA Networks," *IEEE Journal on Selected Areas of Communications, Special Issue on Non-cooperative Behaviour in Networking*, vol. 53, p. 1079–1090, August 2007.

[37] J.E. Suris, L.A. DaSilva, Z. Han, A. B. MacKenzie, and R.S. Komali, "Asymptotic Optimality for Distributed Spectrum Sharing using Bargaining Solutions," *IEEE Transactions on Wireless Communications*, vol. 8, no. 10, pp. 5225-5237, October 2009.

[38] W. Saad, Z. Han, M. Debbah, A. Hjørungnes, and T. Başar, "Coalitional Game Theory for Communication Networks: A Tutorial," *IEEE Signal Processing Magazine, Special Issue on Game Theory in Signal Processing and Communications*, vol. 26, no. 5, pp. 77 - 97.

[39] A. Attar, M. R. Nakhai, and A. H. Aghvami, "Cognitive Radio Game for Secondary Spectrum Access Problem," *IEEE Transactions on Wireless Communications*, vol. 8,

no. 4, p. 2121–2131, April 2009.

[40] J. Nash, "The Bargaining Problem," *Econometrica*, vol. 8, no. 2, p. 155–162, April 1950.

[41] D. Fudenberg and J. Tirole, *Game Theory*. Cambridge, UK: MIT Press, 1991.

[42] Y.-E Lin, K.-H. Liu, and H.-Y. Hsieh, "Design of Power Control Protocols for Spectrum Sharing In Cognitive Radio Networks: A Game Theoretic Perspective," *IEEE International Conference on Communications*, May 2010.

[43] C.-G. Yang, J.-D. Li, and Z. Tian, "Optimal Power Control for Cognitive Radio Networks Under Coupled Interference Constraints: A Cooperative Game-Theoretic Perspective," *IEEE Transactions on Vehicular Technology*, vol. 59, no. 4, pp. 1696 - 1706, May 2010.

[44] D. Andrica, *Number Theory: Structures, Examples and Problems*, 1st ed. Germany: Birkhäuser Boston, 2009.

[45] W. H. Press, S. A. Teukolsky, W. T. Vetterling, and B. P. Flannery, *Numerical Recipies - The Art of Scientific Computing*, 3rd ed. Cambridge, United Kingdom: Cambridge University Press, 2007.

[46] J. Scheffel and C. Hakansson, "Solution of Systems of Nonlinear Equations – A Semi-Implicit Approach," *Applied Numerical Mathematics*, vol. 59, no. 10, pp. 2430-2443, 2009.

[47] P. Gibbons, *A Primer in Game Theory*.: Prentice Hall, 1992.

[48] J. Mitola, *Cognitive Radio: An Integrated Agent Architecture for Software Defined Radio*. Stockholm, Sweden: Royal Institute of Technology, 2000.

[49] S. Haykin, "Cognitive Radio: Brain-empowered Wireless Communications," *IEEE Journal on Selected Areas of Communications*, vol. 23, no. 2, pp. 201-220, February 2005.

[50] H. Xu and B. Li, "Efficient Resource Allocation with Flexible Channel Cooperation in OFDMA Cognitive Radio Networks," in *IEEE Infocom*, San Diego, CA, USA, March 2010.

[51] Z. Ji and K. J. R. Liu, "Dynamic Spectrum Sharing: A Game Theoretical Overview," *IEEE Communications Magazine*, vol. 45, no. 5, pp. 88-95, May 2007.

[52] J. Huang, R. Berry, and M. L. Honig, "Distributed Interference Compensation for Wireless Networks," *IEEE Journal on Selected Areas of Communications*, vol. 24, no. 5, p. 1074–1084, May 2006.

[53] S. Koskie and Z. Gajic, "A Nash Game Algorithm for SIR-based Powercontrol in 3G Wireless CDMA Networks," *IEEE/ACM Transactions on Networking*, vol. 13, no. 5,

p. 1017–1026, October 2005.

[54] A. B. MacKenzie and S. B. Wicker, "Game Theory in Communications: Motivation, Explanation, and Application to Power Control," in *IEEE Global Telecommunications Conference*, 2001, p. 821–826.

[55] Q. Qu, L. B. Milstein, and D. R. Vaman, "Cognitive Radio based Multi-user Resource Allocation in Mobile Ad-hoc Networks using Multi-carrier CDMA," *IEEE Journal on Selected Areas of Communications*, vol. 26, no. 1, pp. 70-82, January 2008.

[56] D. Hui and V. K. N. Lau, "Delay-Sensitive Cross-Layer Designs for OFDMA Systems with Outdated CSIT," *IEEE Transactions on Wireless Communications*, vol. 8, no. 7, pp. 3484-3491, July 2009.

[57] S. Ye, R. Blum, and L. Cimini, "Adaptive Modulation for Variable Rate OFDM Systems with Imperfect Channel Information," ," *IEEE Vehicular Technology Conference*, vol. 2, p. 767–771, May 2002.

[58] P. Xia, S. Zhou, and Giannakis G. B., "Adaptive MIMO-OFDM Based on Partial Channel State Information," *IEEE Transactions on Signal Processing*, vol. 52, pp. 202-213, January 2004.

[59] D. Bertsekas and R.G. Gallager, *Data Networks*, 2nd ed.: Prentice Hall, 1992.

[60] J. H. Jang and K. B. Lee, "Transmit Power Adaptation for Multiuser OFDM Systems," *IEEE Journal on Selected Areas of Communications*, vol. 21, no. 2, pp. 171-178, February 2003.

[61] R. Gallager, *Information Theory and Reliable Communication*. New York: Wiley, 1968.

[62] I.E. Telatar and R. Gallager, "Combining Queuing Theory with Information Theory for Multiaccess," *IEEE Journal on Selected Areas of Communications*, vol. 13, no. 6, pp. 963-969, 1995.

[63] I. E. Telatar, *Multiple Access Information Theory and Job Scheduling*., 1995.

[64] E. Gelenbe and I. Mitrani, *Analysis and Synthesis of Computer Systems*. New York: Academic Press, 1980.

[65] P. Parag, S. Bhashyam, and R. Aravind, "A Subcarrier Allocation Algorithm for OFDMA using Buffer and Channel State Information," in *IEEE Vehicular Technology Conference*, 2005, pp. 622-625.

[66] E. M. Yeh and A. S. Cohen, "Information Theory, Queueing, and Resource Allocation in Multi-user Fading Communications," in *Conference on Information Sciences and Systems*, 2004.

[67] S. Kittipiyakul and T. Javidi, "Resource Allocation in OFDMA: How Load-Balancing Maximizes Throughput When Water-Filling Fails," Technical Report UWEETR-

2004-0007, 2004.

[68] J.W. Lee, R.R. Mazumdar, and N.B. Shroff, "Downlink Power Allocation for Multi-Class Wireless Systems," *IEEE ACM Transactions on Networking*, vol. 13, no. 4, pp. 854-867, August 2005.

[69] Q. Liu, S. Zhou, and G. B. Giannakis, "Cross-Layer Combining of Adaptive Modulation and Coding with Truncated ARQ Over Wireless Links," *IEEE Transactions on Wireless Communications*, vol. 3, no. 5, p. 1746–55, September 2004.

[70] L.T.H. Lee, C.-J. Chang, Y.-S. Chen, and S. Shen, "A Utility-Approached Radio Resource Allocation Algorithm for Downlink in OFDMA Cellular Systems," in *IEEE Conference on Vehicular Technology-Spring*, Dallas, 2005, pp. 1798-1802.

[71] T. K. Chee, C.-C. Lim, and J. Choi, "A Cooperative Game Theoretic Framework for Resource Allocation in OFDMA Systems," in *IEEE International Conference on Communication Systems*, Singapore, 2006, pp. 1-5.

[72] Z. Han, Z. Ji, and K J.R Liu, "Fair Multiuser Channel Allocation for OFDMA Networks Using Nash Bargaining Solutions and Coalitions," *IEEE Transactions on Communications*, vol. 53, no. 8, pp. 1366-1376, August 2005.

[73] H. Yin and H. Liu, "An Efficient Multiuser Loading Algorithm for OFDM-based Broadband Wireless Systems," in *IEEE Globecom*, San Francisco, 2000, pp. 103-107.

[74] J. Holtzman, "Asymptotic Analysis of Proportional Fair Algorithm," in *12th IEEE International Symposium on Personal, Indoor and Mobile Radio Communications*, San Diego, 2001, pp. 33-37.

[75] Y. Fukui, N. Yamagaki, H. Tode, and K. Murakam, "Packet Transfer Scheduling Scheme with Throughput Compensated Considering Wireless Conditions," in *12th International Conference on Computer Communications and Networks*, 2003, pp. 11-16.

[76] H. Zhu and K.R. Liu, "Throughput Maximization using Adaptive Modulation in Wireless Networks with Fairness Constraint," in *IEEE Wireless Communications and Networking Conference* , New Orleans, 2003, pp. 243-246.

[77] K. Khawam and D. Kofman, "Opportunistic Weighted Fair Queueing," in *IEEE Vehicular Technology Conference*, Montreal, 2006, pp. 1-5.

[78] G. Song and Y. Li, "Adaptive Resource Allocation Based on Utility Optimization in OFDM," in *IEEE Globcom*, San Francisco, 2003, pp. 586-590.

[79] W.-H. Kuo and W. Liao, "Utility-Based Optimal Resource Allocation in Wireless Networks," in *IEEE Globecom*, St. Louis, 2005, pp. 3508-3512.

[80] C. Curescu and S.-N. Tehrani, "Time-Aware Utility-Based Resource Allocation in Wireless Networks," *IEEE Transactions on Parallel and Distributed Systems*, vol. 16,

no. 7, pp. 624-636, July 2005.

[81] G. Song and Y. Li, "Utility-Based Resource Allocation and Scheduling in OFDM-based Wireless Broadband Networks," *IEEE, Communications Magazine*, vol. 43, no. 12, pp. 127-134, December 2005.

[82] R. Mazumdar, L.G. Mason, and C. Douligeris, "Fairness in Network Optimal Flow Control: Optimality of Product Forms," *IEEE Transactions on Communications*, vol. 39, no. 5, pp. 775-782, May 1991.

[83] H. Yaiche, R.R. Mazumdar, and C. Rosenberg, "A Game Theoretic Framework for Bandwidth Allocation and Pricing in Broadband Networks," *IEEE/ACM Transactions on Networking*, vol. 8, no. 5, pp. 667-678, October 2000.

[84] C. C. Zarakovitis, Q. Ni, I. G. Nikolaros, and O. Tyce, "A Novel Game-Theoretic Cross-Layer Design for OFDMA Broadband Wireless Networks," in *IEEE International Conference on Communications*, Cape Town, 2010, pp. 23-27.

[85] S. Shakkottai, T.S. Rappaport, and P.C. Karlsson, "Cross-Layer Design for Wireless Networks," *IEEE Communications Magazine*, vol. 41, no. 10, p. 74–80, October 2003.

[86] Z. Ji, Y. Yang, J. Zhou, M. Takai, and R. Bagrodia, "Exploiting Medium Access Diversity in Rate Adaptive Wireless LANs," in *ACM Annual International Symposium in Mobile Computing and Netwirking*, Philadelphia, October 2004.

[87] L. Tong, V. Naware, and P. Venkitasubramaniam, "Signal Processing in Random Access," *IEEE Transactions in Sigal Processing*, vol. 21, no. 5, p. 29–39, September 2004.

[88] V. Kawadia and P.R. Kumar, "A Cautionary Perspective on Cross-layer Design," *IEEE Transactions on Wireless Communications*, vol. 12, no. 1, pp. 3-11, February 2005.

[89] V. T. Raisinghani and S. Iyer, "Cross-Layer Design Optimizations in Wireless Protocol Stacks," *IEEE Transactions on Computer Communications*, vol. 27, p. 720–724, 2004.

[90] R. Rom and M. Sidi, *Multiple access protocols*.: Springer-Verlag, 1989.

[91] N. Abramson, "The ALOHA System - Another Alternative for Computer Communications," in *Fall Joint Computer Conference.*, 1970.

[92] A. S. Tanenbaum, *Computer Networks*, Prentice Hall, Ed. New Jersey, 2003.

[93] A. F. Molisch, *Wireless Communications*.: Wiley, 2011.

[94] H. Rohling and R. Grunheid, "Performance Comparison of Diferent Multiple Access Schemes for the Downlink of an OFDM Communication System," in *IEEE Vehicular*

Technology Conference, 1997, pp. 1365-1369.

[95] J. Chuang and N. Sollenberger, "Beyond 3G: Wideband Wireless Data Access based on OFDM and Dynamic Packet Assignment," *IEEE Communications Magazine*, p. 78–87, july 2000.

[96] "ETSI EN 300 401 Radio Broadcasting Systems; Digital Audio Broadcasting (DAB) to Mobile, Portable and Fxed Receivers," 2001.

[97] "Digital Video Broadcasting (DVB): Architectural Framework for the Delivery of DVB-Services over IP-based Networks," ETSI TR 102 033, 2002.

[98] "Transmission and Multiplexing (TM); Access Transmission Systems on Metallic Access Cables; Asymmetric Digital Subscriber Line (ADSL) - European Specific Requirements," ETSI TS 101 388, 2002.

[99] R. V. Nee and R. Prasad, *OFDM for Wireless Multimedia Communications*.: Artech House, 2000.

[100] S. Weinstein and P. Ebert, "Data Transmission by Frequency-Division Multiplexing using the Discrete Fourier Transformation," *IEEE Transactions on Communications*, vol. 19, p. 628–634, October 1971.

[101] W. Y. Zou and Y. Wu, "COFDM: An Overview," *IEEE Transactions on Broadcasting*, vol. 41, no. 1, p. 1 – 8, March 1995.

[102] R. Laroia, S. Uppala, and J. Li, "Designing a Mobile Broadband Wireless Access Network," *IEEE Signal Processing Magazine*, pp. 78-87, July 2000.

[103] A. J. Goldsmith and S. G. Chua, "Variable Rate Variable Power M-QAM for Fading Channel," *IEEE Transactions on Communications*, vol. 45, pp. 1218-1230, October 1997.

[104] S. Nanda, K. Balachandran, and S. Kumat, "Adaptation Techniques in Wireless Packet Data Services," *IEEE Communications Magazine*, pp. 54-64, January 2000.

[105] D. Tse and S. Hanly, "Multi-Access Fading Channels: Part I: Polymatroid Structure, Optimal Resource Allocation and Throughput Capacities," *IEEE Transactions on Information Theory*, vol. 47, pp. 2796-2815, November 1998.

[106] L. Li and A. J. Goldsmith, "Optimal Resource Allocation for Fading Broadcast Channels - Part I: Ergodic Capacity," *IEEE Transactions on Information Theory*, vol. 47, pp. 1083-1102, March 2001.

[107] A. J. Goldsmith and M. Effros, "The Capacity Region of Broadcast Channels with Inter Symbol Interference and Colored Gaussian Noise," *IEEE Transactions on Information Theory*, vol. 47, pp. 219-240, January 2001.

[108] W. Yu and J. M. Cioffi, "FDMA Capacity of Gaussian Multiple Access Channels with

ISI," *IEEE Transactions on Communications*, vol. 50, pp. 102-111, January 2002.

[109] W. Rhee and M. Cioffi, "Increase in Capacity of Multiuser OFDM System using Dynamic Subcarrier Allocation," in *IEEE Conference on Vehicular Technology*, 2000, pp. 1085-1089.

[110] D. Kivanc, G. Li, and H. Liu, "Computationally Efficient Bandwidth Allocation and Power Control for OFDMA," *IEEE Transactions on Wireless Communications*, vol. 2, pp. 1150-1158, November 2003.

[111] M. Ergen, S. Coleri, and P. Varaiya, "QoS Aware Adaptive Resource Allocation Techniques for Fair Scheduling in OFDMA based Broadband Wireless Access Systems," *IEEE Transactions on Broadcasting*, vol. 49, no. 4, December 2003.

[112] K. Seong, M. Mohseni, and M. Cio, "Optimal Resource Allocation for OFDMA Downlink Systems," in *IEEE International Symposioum on Information Theory*, 2006, pp. 1394 - 1398.

[113] F. Brah, L. Vandendorpe, and J. Louveaux, "Constrained Resource Allocation in OFDMA Downlink Systems with Partial CSIT," , 2008, p. IEEE International Conference in Communications.

[114] S. Gault, W. Hachem, and P. Ciblat, "Performance Analysis of an OFDMA Transmission System in a multi-cell Environment," *IEEE Transactions on Communications*, vol. 55, no. 12, pp. 2143 - 2159, December 2005.

[115] J. Brehmer, C. Guthy, and W. Utschick, "An Effcient Approximation of the OFDMA Outage Probability Region," in *IEEE Workshop on Signal Processing Advances in Wireless Communications*, 2006.

[116] M. Pischella and J. C. Belfiore, "Distributed Resource Allocation in MIMO OFDmA Systems with Statistical CSIT," in *IEEE Workshop on Signal Processing Advances in Wireless Communications*, 2008.

[117] M. J. Osborne and A. Rubinstein, *A Course in Game Theory*.: MIT Press, 1994.

[118] J Neumann and O. Morgenster, *Theory of Games and Economic Behavior*. New Jersey: Princeton University Press, 1944.

[119] M.S. Bazaraa, H. D. Sherali, and C. M. Shetty, *Nonlinear Programming: Theory and Algorithms*, 2nd ed.: John Wiley & Sons, 1993.

[120] D. Bertsimas and J. N. Tsitsiklis, *Introduction to Linear Optimization*.: Athena Scientific, 1997.

[121] D. G Luenberger, *Optimization by Vector Space Methods*.: John Wiley & Sons, 1969.

[122] O. Mangasarian, *Nonlinear Programming*.: Society for Industrial and Applied Mathematics, 1994.

[123] R. T. Rockafellar, *Convex Analysis*.: Princeton University Press, 1970.

[124] J. V. Tiel, *Convex Analysis: An Introductory Text*.: John Wiley & Sons, 1984.

[125] J.-B. Hiriart-Urruty and C. Lemarechal, *Fundamentals of Convex Analysis*, 12th ed.: Springer.

[126] M. Grotschel, L. Lovasz, and A. Schrijver, *Geometric Algorithms and Combinatorial Optimization*.: Springer, 1988.

[127] G. Strang, *Linear Algebra and its Applications*.: Academic Press, 1980.

[128] G. Golub and C. F. V. Loan, *Matrix Computations*, 2nd ed.: Johns Hopkins University Press, 1989.

[129] J. W. Demmel, *Applied Numerical Linear Algebra*.: Society for Industrial and Applied Mathematics, 1997.

[130] R. A. Horn and C. A. Johnson, *Matrix Analysis*.: Cambridge University Press, 1985.

[131] A. Leke and J. M. Cioffi, "Multicarrier Systems with Imperfect Channel Knowledge," in *IEEE International Symposium on PIMRC*, vol. 2, September 1998, p. 549–553.

[132] R. Negi and J. Cioffi, "Delay-constrained Capacity with Causal Feedback," *IEEE Transactions on Information Theory*, vol. 48, no. 9, p. 2478–2494, September 2002.

[133] A. K. Karmokar, D. V. Djonin, and V. K. Bhargava, "Delay-aware Power Adaptive for Incremental Redundancy Hybrid ARQ over Fading Channels with Memory," in *IEEE International Conference on Communications*, vol. 9, June 2006, pp. 4315 - 4320.

[134] S. C. Yang, *OFDMA System Analysis and Design*.: Artech House, 2010.

[135] S. Boyd and L. Vandenberghe, *Convex Optimization*. Cambridge, United Kingdom: Cambridge University Press, 2004.

[136] C. E. Shannon, *The Mathematical Theory of Communication*. Urbana, Illinois US: University of Illinois Press, 1949.

[137] P W.C Chan and R S Cheng, "Optimal Power Allocation in zero-forcing MIMO-OFDM Downlink with Multiuser Diversity," in *IST Mobile & Wireless Communications*, Dresden, 2005.

[138] Yui Ming Tsang and R.S. Cheng, "Optimal Resource Allocation in SDMA/MIMO/OFDM Systems under QoS and Power Constraints," in *IEEE Wireless Communications and Networking Conference, WCNC*, Atlanta, 2004, pp. 1595-1600.

[139] Zukang Shen, J.G. Andrews, and B.L. Evans, "Adaptive Resource Allocation in Multiuser OFDM Systems With Proportional Rate Constraints," *IEEE Transactions on Wireless Communications*, vol. 4, no. 6, pp. 2726-2737, November 2005.

[140] Cheong Yui Wong, R.S. Cheng, K.B. Lataief, and R.D. Murch, "Multiuser OFDM with Adaptive Subcarrier, Bit, and Power Allocation," *IEEE Journal on elected Areas in Communications*, vol. 17, no. 10, pp. 1747-1758, October 1999.

[141] C. C. Zarakovitis, I. G. Nikolaros, D. Skordoulis, M. G. Hadjinicolaou, and Qiang Ni, "A Comparative Study on Iterative Methods Regarding Cross-Layer Optimization for OFDMA Systems," in *IEEE Computer and Information Technology International Conference*, Bradford, United Kingdom, 2010, pp. 420-425.

[142] G. Song, Y. Li, J. Leonard, J. Cimini, and H. Zheng, "Joint Channel-Aware and Queue-Aware Data Scheduling in Multiple Shared Wireless Channels," in *IEEE Wireless Communications and Networking Conference*, vol. 3, March 2004, p. 1939–1944.

[143] J. N. Daigle, *Queuing Theory with Applications to Packet Telecommunication*.: Springer, 2004.

[144] V. Erceg, K. V. S. Hari, M. S. Smith, and D. S. Baum, "Channel Models for Fixed Wireless Applications," *Contribution to IEEE 802.16.3*, July 2001.

[145] W. C. Jakes, *Microwave Mobile Communications*. New York: Wiley.

[146] T. Cover and J. Thomas, *Elements of Information Theory*.: Wiley, 1991.

[147] L. H. Ozarow, S. Shamai, and A. D. Wyner, "Information-Theoretic Considerations for Cellular Mobile Radio," *IEEE Transactions on Vehicular Technology*, vol. 43, p. 359–378, May 1994.

[148] C. C. Zarakovitis, Q. Ni, and D. E. Skordoulis, "Cross-Layer Design for Single-Cell OFDMA Systems with Heterogeneous QoS and Partial CSIT," in *IEEE Wireless Communications and Networking Conference*, Budapest, 2009.

[149] A Attar, M. R. Nakhai, and A. H. Aghvami, "Cognitive Radio Game for Secondary Spectrum Access Problem," *IEEE Transactions on Wireless Communications*, vol. 4, no. 8, p. 2121–2131, April 2009.

[150] Y. Fukui, N. Yamagaki, H. Tode, and Murakami. K., "Packet Transfer Scheduling Scheme with Throughput Compensated Considering Wireless Conditions," in *IEEE International Conference on Computer Communications and Networks*, 2003, pp. 11-16.

[151] E. Hahne, "Round-Robin Scheduling for Max-Min Fairness in Data Networks," *IEEE Journal on Selected Areas in Communications*, vol. 9, no. 7, pp. 1024-1039, September 1991.

[152] L. Tassiulas and S. Sarkar, "Maxmin Fair Scheduling in Wireless Networks," in *IEEE InfoCom*, New York, 2002, pp. 763-772.

[153] E. Zehavi, A. Leshem, R. Levanda, and Z. Han, "Weighted Max-Min Resource Allocation for Frequency Selective Channels," *Journal on Networking and Internet*

Architecture, 2010.

[154] P. Marbach, "Priority Service and Max-Min Fairness," *IEEE/ACM Transactions on Networking*, vol. 11, no. 5, pp. 733- 746, October 2003.

[155] M. Allalouf and Y. Shavitt, "Centralized and Distributed Algorithms for Routing and Weighted Max-Min Fair Bandwidth Allocation," *IEEE/ACM Transactions on Networking*, vol. 16, no. 5, pp. 1015-1024, October 2008.

[156] S. T. Chung and A. Goldsmith, "Degrees of Freedom in Adaptive Modulation: A Unified View," *IEEE Transactions on Communications*, vol. 49, no. 9, pp. 1561-1571, September 2001.

[157] F. P. Kelly, A. Maulloo, and D. Tan, "Rate Control in Communication Networks: Shadow Prices, Proportional Fairness and Stability," *Journal of Operational Research Society*, vol. 49, p. 237–252, 1998.

[158] R. M. Corless, G. H. Gonnet, D. E. G. Hare, D. J. Jeffrey, and D. E. Knuth, "On the Lambert W Function," *Advanced Computing Mathematics*, pp. 329-359, 1999.

[159] Q Zhao and B.M. Sadler, "A Survey of Dynamic Spectrum Access," *IEEE Signal Processing Magazine*, vol. 24, no. 3, pp. 79-89, May 2007.

[160] P. Zhou, W. Yuan, W. Liu, and W. Cheng, "Joint Power and Rate Control in Cognitive Radio Networks: A Game-Theoretical Approach," in *IEEE International Conference in Communications*, 2008, p. 3296–3301.

[161] A. T. Hoang and Y. C. Liang, "Maximizing Sspectrum Utilization of Cognitive Radio Networks using Channel Allocation and Power Control," in *IEEE Conference on Vehicular Technology*, 2006, p. 1202–1206.

[162] Y Chen, G. G. Yu, Z. Zhang, H. H. Chen, and P. L. Qiu, "On Cognitive Radio Networks with Opportunistic Power Control Strategies in Fading Channels," *IEEE Transactions on Wireless Communications*, vol. 7, no. 7, p. 2752–2761, July 2008.

[163] G. Bansal, M. Hossain, and V. Bhargava, "Optimal and Suboptimal Power Allocation Schemes for OFDM-based Cognitive Radio Systems," *IEEE Journal on Wireless Communications*, vol. 7, no. 11, p. 4710–4718, November 2008.

[164] T. Qin and C. Leung, "Fair Adaptive Resource Allocation for Multiuser OFDM Cognitive Radio Systems," in *International Conference CHINACOM*, 2007, pp. 115-119.

[165] P. Wang, M. Zhao, L. Xiao, S. Zhou, and J. Wang, "Power Allocation in OFDM-based Cognitive Radio Systems," in *IEEE Globecom*, 2007, p. 4061–4065.

[166] A. T. Hoang and Y. C. Liang, "Downlink Channel Assignment and Power Control for Cognitive Networks," *IEEE Transactions in Wireless Communications*, vol. 7, no. 8, p. 3106–3117, August 2008.

[167] P. Cheng, Z. Zhang, H. H. Chen, and P. Qiu, "Optimal Distributed Joint Frequency, Rate and Power Allocation in Cognitive OFDMA Systems," *IET Journal in Communications*, vol. 2, no. 6, p. 815–826, July 2008.

[168] W. Yu and R. Lui, "Dual Methods for Nonconvex Spectrum Optimization of Multicarrier Systems," *IEEE Transactions in Communications*, vol. 7, no. 8, pp. 1310-1322, July 2006.

[169] Z. Hasan, E. Hossain, C. Despins, and V. K. Bhargava, "Power Allocation for Cognitive Radios based on Primary User Activity in an OFDM System," in *IEEE Globecom*, 2008, pp. 1-6.

[170] D. T. Ngo, C. T. llambura, and H. H. Nguyen, "Resource Allocation f or OFDMA-Based Cognitive Radio Multicast Networks with Primary User Activity Consideration," *IEEE Transactions on Vehicular Technology*, vol. 59, no. 4, pp. 1669-1679, May 2010.

[171] P. Mitran, N. Devroye, and V. Tarokh, "On Compound Channels with Side Information at the Transmitter," *IEEE Trasnactions in Information Theory*, vol. 52, pp. 1745-1755, April 2006.

[172] D. Huang, C. Miao, and C. Leung, "Resource Allocation of MU-OFDM based Cognitive Radio Systems Under Partial Channel Stat," *Computing Research Repository*, August 2008.

[173] S. Koskie and Z. Gajic, "A Nash Game Algorithm for SIR-based Power Control in 3G Wireless CDMA Networks," *ACM/IEEE Transactions in Networking*, vol. 13, no. 5, p. 1017–1026, Otober 2007.

[174] M. Rasti, A. R. Sharafat, and B. Seyfe, "Pareto-Efficient and Goal-Driven Power Control in Wireless Networks: A Game-Theoretic Approach with a Novel Pricing Scheme," *ACM/IEEE Transactions in Networking*, vol. 17, no. 2, pp. 556-569, April 2009.

[175] H. Zhu, Z. Ji, and K. J. R. Liu, "Fair Multiuser Channel Allocation for OFDMA Networks using Nash Bargaining Solution and Coalitions," *IEEE Transactions in Communications*, vol. 53, no. 8, p. 1366–1376, August 2005.

[176] N. Qiang and C. C. Zarakovitis, "Nash Bargaining Game Theoretic Scheduling for Joint Channel & Power Allocation in Cognitive Radio Systems," *IEEE Journal on Selected Areas in Communications*, p. Accepted for publication.

[177] National Research Council - Committee on the Future of the Global Positioning, *The Global Positioning System: A Shared National Asset : Recommendations for Technical Improvements and Enhancements*, National Academy of Public Administration U.S, Ed. U.S.A: National Academies Press, 1995.

[178] K. L. Du, M. N. S. Swamy, and Qiang N., "A Dynamic Spectrum Access Scheme for Cognitive Radio Networks," in *Canadian Conference on Electrical and Computer*

Engineering, 2009, pp. 450 - 454.

[179] T. P. Coleman and M. Médard, "A Distributed Scheme for Achieving Energy-Delay Tradeoffs with Multiple Service Classes over a Dynamically Varying Network," *IEEE Journal on Selected Areas in Communications*, vol. 22, no. 5, pp. 929-941, 2004.

[180] N. Qiang and C. C. Zarakovitis, "Nash Bargaining Game Theoretic Scheduling forJoint Channel and Power Allocation in Cognitive Radio Systems," *IEEE Journal on Selected Areas of Communications - Special Issue Game Theory*, 2011.

[181] R. Berry and R. Gallager, "Communication Over Fading Channels with Delay Constraints," *IEEE Transactions on Information Theory*, vol. 48, no. 5, pp. 1135-1149, May 2002.

[182] W. H. Press, S. A. Teukolsky, W. T. Vetterling, and B. P. Flannery, *Numerical Recipies - The Art of Scientific Computing*, 3rd ed.: Cambridge University Press, 2007.

[183] Federal Communications, "Communication Spectrum Policy Task Force," *Rep. ET Docket*, pp. 2-135, November 2002.

[184] N. Devroye, P. Mitran, and V. Tarokh, "Achievable Rates in Cognitive Radio Channels," *IEEE Transaction in Information Theory*, vol. 52, pp. 1813-1827, May 2006.